

TECHNISCHE UNIVERSITÄT MÜNCHEN

Lehrstuhl für Mikrobielle Ökologie

Analysis of *Bacillus cereus* virulence factors *in vitro* and *in vivo*

Viktoria Magdalena Doll

Vollständiger Abdruck der von der Fakultät Wissenschaftszentrum Weihenstephan für Ernährung, Landnutzung und Umwelt der Technischen Universität München zur Erlangung des akademischen Grades eines

Doktors der Naturwissenschaften

genehmigten Dissertation.

Vorsitzender: Univ.-Prof. Dr. Dr. h.c. J. Bauer

Prüfer der Dissertation:

1. Univ.-Prof. Dr. S. Scherer
2. Priv.-Doz. Dr. R. Vogelmann
(Universität Heidelberg)
3. Univ.-Prof. Dr. M. Ehling-Schulz
(Veterinärmedizinische Universität Wien/Österreich)

Die Dissertation wurde am 15.02.2012 bei der Technischen Universität München eingereicht und durch die Fakultät Wissenschaftszentrum Weihenstephan für Ernährung, Landnutzung und Umwelt am 10.05.2012 angenommen.

Science never solves a problem without creating ten more.

George Bernard Shaw

TABLE OF CONTENTS

TABLE OF CONTENTS	I
ABBREVIATIONS AND SYMBOLS	V
LIST OF FIGURES	VII
LIST OF TABLES	IX
SUMMARY	X
ZUSAMMENFASSUNG	XI
1. INTRODUCTION	1
1.1 Foodborne illness	1
1.2. The <i>Bacillus cereus</i> group.....	2
1.3. <i>B. cereus</i> ecology	3
1.4. Pathogenicity of <i>B. cereus</i>.....	4
1.4.1 <i>Local and systemic non-gastrointestinal-tract infections.....</i>	<i>4</i>
1.4.2 <i>B. cereus emetic syndrome.....</i>	<i>5</i>
1.4.3 <i>B. cereus diarrheal syndrome</i>	<i>6</i>
1.5. Regulation of virulence gene expression	7
1.5.1 <i>The emetic toxin cereulide</i>	<i>8</i>
1.5.2 <i>Non-emetic virulence factors and the PlcR regulon.....</i>	<i>9</i>
1.6. Host-pathogen interaction.....	11
1.7. Interaction of <i>B. cereus</i> and the intestinal epithelium.....	12
1.8. Research objective.....	14
2. MATERIALS AND METHODS	15
2.1. Materials	15
2.1.1 <i>Bacterial media and buffers</i>	<i>15</i>
2.1.2 <i>Chemicals, materials and cell culture equipment.....</i>	<i>16</i>
2.2. Microbiological methods	18
2.2.1 <i>Bacterial strains and growth conditions</i>	<i>18</i>
2.2.2 <i>Preparation of bacterial supernatant.....</i>	<i>20</i>
2.2.3 <i>Production of <i>B. cereus</i> spores.....</i>	<i>20</i>
2.3. Cell culture	21
2.4. Molecular biological methods	21
2.4.1 <i>DNA isolation</i>	<i>21</i>
2.4.2 <i>RNA isolation and reverse transcription.....</i>	<i>21</i>
2.4.3 <i>Standard PCR.....</i>	<i>22</i>

2.4.4	DNA sequencing	23
2.4.5	Enzymatic DNA modifications/cloning	23
2.5.	Genetic modification of bacteria	24
2.5.1	Transformation	24
2.5.2	Heterogramic conjugation	24
2.5.3	Mutagenesis of <i>B. cereus</i>	25
2.5.3.1	Construction of <i>B. cereus</i> strain expressing GFP	25
2.5.3.2	Construction of <i>B. cereus</i> strain overexpressing SMase	25
2.5.3.3	Construction of <i>B. cereus</i> deletion mutants	27
2.5.3.4	Complementation of deletion mutants	27
2.6.	Biochemical methods	28
2.6.1	Protein analysis.....	28
2.6.1.1	Protein separation using gelfiltration.....	28
2.6.1.2	Identification of a cytotoxic secreted <i>B. cereus</i> protein.....	28
2.6.1.3	Identification of a growth promoting secreted <i>B. cereus</i> protein.....	28
2.6.1.4	SDS-PAGE and Western Blot.....	29
2.6.2	Enzymatic assays	29
2.6.2.1	SMase activity assay	29
2.6.2.2	Caspase-3 activity assay	30
2.7.	Bacterial adhesion.....	30
2.8.	Cytotoxicity assay (Ampel assay).....	31
2.9.	Detection of dead epithelial cells by flow cytometric analysis.....	31
2.10.	Immunofluorescence staining.....	31
2.10.1	Anti- <i>B. cereus</i> antibody production.....	31
2.10.2	Visualization of adherent <i>B. cereus</i>	32
2.10.3	Detection of apoptosis induction in Ptk6 cells.....	32
2.11.	Analysis of differential protein expression - <i>B. cereus</i> wt and $\Delta plcR$	32
2.11.1	Protein sample preparation for 2-D DIGE analysis.....	32
2.11.2	Two-dimensional gel electrophoresis (2-D DIGE).....	33
2.11.3	MALDI-TOF-MS/MS protein identification.....	35
2.12.	Insect infection experiments.....	36
2.13.	Software and statistical analysis	37
3.	RESULTS.....	38
3.1.	<i>B. cereus</i> cytotoxic effects towards IECs and pathogenicity	38
3.1.1	<i>B. cereus</i> cytotoxicity towards intestinal epithelial cells.....	38
3.1.2	<i>B. cereus</i> adhesion capacity to intestinal epithelial cells	40
3.1.3	Cytotoxicity is mediated by a secreted, PlcR-regulated factor.....	41
3.1.4	Identification of sphingomyelinase (SMase) from cytotoxic bacterial supernatant ..	42

3.1.5	<i>SMase expression in B. cereus ΔplcR</i>	44
3.1.5.1	<i>SMase expression restores B. cereus cytotoxicity in vitro and pathogenicity in vivo</i>	44
3.1.5.2	<i>SMase expression induces apoptosis in polarized IEC via caspase-3 activation</i>	47
3.1.6	<i>B. cereus sphingomyelinase deletion mutants</i>	50
3.1.6.1	<i>Construction of sph deletion mutants and complemented strains</i>	50
3.1.6.2	<i>Phenotypic characterization</i>	52
3.1.6.3	<i>Growth characterization</i>	54
3.1.6.4	<i>SMase expression and activity</i>	57
3.1.7	<i>Contribution of SMase to B. cereus cytotoxicity in vitro</i>	59
3.1.8	<i>Contribution of SMase to B. cereus pathogenicity in vivo</i>	60
3.2.	<i>B. cereus growth characterization</i>	63
3.2.1	<i>Growth deficit of the ΔplcR mutant can be rescued by bacterial and host factors</i> ..	64
3.2.2	<i>InhA2 is involved in B. cereus growth regulation</i>	66
3.2.2.1	<i>Identification of InhA proteins as possible growth promoting factors</i>	66
3.2.2.2	<i>InhA2 stimulates B. cereus growth</i>	69
3.2.3	<i>Identification of B. cereus proteome changes induced by host epithelial cells</i>	72
4.	DISCUSSION	79
4.1.	<i>B. cereus virulence mechanisms</i>	79
4.1.1	<i>Toxin secretion upstages bacterial adhesion to host cells</i>	79
4.1.2	<i>PlcR-mediated cytotoxicity towards intestinal epithelial cells</i>	80
4.1.3	<i>B. cereus Sphingomyelinase – reassessment of a virulence factor</i>	81
4.1.3.1	<i>Co-transcription of plc and sph</i>	81
4.1.3.2	<i>SMase expression in ΔplcR rescued B. cereus virulence</i>	82
4.1.3.3	<i>SMase induced apoptosis in IEC</i>	83
4.1.3.4	<i>Influence of SMase to B. cereus virulence in vitro</i>	84
4.1.3.5	<i>Influence of SMase on in vivo pathogenicity</i>	85
4.2.	<i>Intrinsic and extrinsic factors influence B. cereus growth</i>	87
4.2.1	<i>The PlcR-dependent metalloprotease InhA2 is involved in growth regulation</i>	87
4.2.2	<i>Influence of IEC-derived factors on B. cereus ΔplcR proteome and growth</i>	92
4.2.2.1	<i>Regulation of proteins involved in amino acid and protein biosynthesis</i>	93
4.2.2.2	<i>Downregulation of proteins involved in TCA cycle and purine biosynthesis</i>	94
4.2.2.3	<i>Regulation of secreted proteins</i>	96
4.2.2.4	<i>Upregulation of the metalloproteases InhA3 and NprB</i>	97
4.3.	<i>Conclusion and perspectives</i>	101
5.	REFERENCES	103
6.	PUBLICATIONS	121
7.	APPENDIX	122
7.1.	<i>B. cereus strains used in cytotoxicity screening</i>	122

TABLE OF CONTENTS

7.2. Vectors and Plasmids	123
7.3. Oligonucleotide primers	124
7.4. MALDI-TOF mass spectrometric protein identification	126
8. DANKSAGUNG	128
CURRICULUM VITAE	129

ABBREVIATIONS AND SYMBOLS

Δ	Gene deletion <i>via</i> allelic replacement
2-D	Two-dimensional
aa	Amino acids
AMP	Adenosine monophosphate
APS	Ammonium persulfate
BCAA	Branched-chain amino acid
BSA	Bovine serum albumin
CFU	Colony forming unit
dH ₂ O	distilled water
ddH ₂ O	double distilled water
DEPC H ₂ O	Diethylpyrocarbonate treated water
DIGE	Differential gel electrophoresis
DMEM	Dulbecco's Modified Eagle's Medium
DPBS	Dulbecco's Phosphate buffered saline
DTT	Dithiothreitol
EDTA	2, 2', 2'', 2'''-(Ethane-1,2-diyldinitrilo)tetraacetic acid
FI	Fluorescence intensity
FPLC	Fast protein liquid chromatography
GFP	Green fluorescent protein
GMP	Guanosine monophosphate
IB	Immuno blot
IEC	Intestinal epithelial cell
IF	Immunofluorescence
IMP	Inosine monophosphate
InhA	Immune inhibitor A
LB	Luria Bertani
LD ₅₀	Lethal dose (50% dead animals)
MALDI	Matrix-assisted Laser Desorption/Ionization
MOI	Multiplicity of infection
MS	Mass spectrometry
MSM	Minimal sporulation medium
MYP	Mannitol-egg yolk-polymyxin
NprB	Neutral protease B
OD	Optical density
PAGE	Polyacrylamide gel electrophoresis
PBS	Phosphate buffered saline
PC-Plc	Phosphatidylcholine-specific phospholipase C

ABBREVIATIONS AND SYMBOLS

PI	Propidium iodide
PI-Plc	Phosphatidylinositol-specific phospholipase C
Plc	Phospholipase C
PlcR	Phospholipase C regulator
PMF	Peptide mass fingerprinting
RPMI	Roswell Park Memorial Institute (cell culture medium)
SDS	Sodium dodecyl sulfate
SMase	Sphingomyelinase
<i>sph</i>	Sphingomyelinase gene
TAE	Tris/Acetate/EDTA
TCA	Tricarboxylic acid
TEMED	<i>N,N,N',N'</i> -tetramethyl-ethane-1,2-diamine
TOF	Time of flight
v/v	Volume per volume
w/v	Weight per volume
wt	<i>wild-type</i>

LIST OF FIGURES

Figure 1: Environmental niches and transmission routes of the foodborne human pathogen <i>Bacillus cereus</i>	4
Figure 2: Current scheme of the regulation of virulence gene expression in emetic <i>B. cereus</i> ... 9	
Figure 3: Scheme of the PlcR regulon organization in <i>B. cereus</i>	10
Figure 4: Respective images of <i>B. cereus</i> treated Ptk6 cell monolayer	39
Figure 5: Attachment of <i>Bacillus cereus</i> to IECs.....	40
Figure 6: Immuno blot detection of <i>nheABC</i> operon expression	42
Figure 7: Protein separation of <i>B. cereus</i> NVH 0075-95 $\Delta nheBC$ supernatant via gel filtration	43
Figure 8: Protein fractions obtained from gel filtration were tested on Ptk6 cells for cytotoxicity and analysed by SDS-PAGE	44
Figure 9: Immuno blot detection of <i>sph</i> expression in <i>B. cereus</i> F4810/72 wt and mutant supernatants	44
Figure 10: Transient <i>sph</i> expression by $\Delta plcR$ <i>sph/PcspA</i> rescued cytotoxic effects on Ptk6 cells	45
Figure 11: The great wax moth <i>Galleria mellonella</i> as <i>in vivo</i> insect model	45
Figure 12: Survival of <i>G. mellonella</i> injected with <i>B. cereus</i> F4810/72 <i>wild-type</i> , mutant strains, <i>E. coli</i> DH10B and controls	46
Figure 13: Growth of <i>B. cereus</i> F4810/72 wt and mutant strains in <i>G. mellonella</i> larvae	47
Figure 14: SMase induced IEC apoptosis is visualized by Annexin V staining of translocated phosphatidylserine	48
Figure 15: <i>B. cereus</i> SMase induced apoptosis in IECs	49
Figure 16: <i>B. cereus</i> SMase induces IEC apoptosis via caspase-3 activation	50
Figure 17: Genetic organization of the chromosomal <i>plc-sph</i> gene cluster	51
Figure 18: Co-transcription analysis of the <i>plc-sph</i> gene cluster	52
Figure 19: Characterisation of <i>B. cereus</i> wt and mutant haemolytic activity	53
Figure 20: Characterisation of <i>B. cereus</i> wt and mutant lecithinase (Plc) activity	54
Figure 21: Growth of <i>B. cereus wild-type</i> compared to their deletion mutants	55
Figure 22: Growth of <i>B. cereus wild-type</i> and deletion mutants compared to complemented strains	56
Figure 23: Characterisation of <i>sph</i> deletion mutants, complemented and parental strains on protein level	57
Figure 24: Sphingomyelin-hydrolysing activity of concentrated bacterial supernatants measured by Amplex® Red Sphingomyelinase Assay Kit (Invitrogen)	58
Figure 25: Flow cytometric analysis of cytotoxic effects of <i>B. cereus</i> supernatant on intestinal epithelial cells	60
Figure 26: Survival of <i>G. mellonella</i> larvae injected with <i>B. cereus</i> F4810/72 (A) and <i>B. cereus</i> NVH 0075-95 (B) <i>wild-type</i> and isogenic mutant strains at 15 °C	61

Figure 27: Growth of <i>B. cereus</i> wt and mutant strains in <i>G. mellonella</i> larvae	62
Figure 28: Growth kinetics of <i>B. cereus</i> F4810/72 <i>wild-type</i> and $\Delta plcR$ in LB medium compared to unsupplemented cell culture medium	64
Figure 29: Growth rescue of <i>B. cereus</i> F4810/72 $\Delta plcR$ in unsupplemented cell culture medium by conditioning with <i>wild-type Bacillus</i>	65
Figure 30: Growth rescue of <i>B. cereus</i> F4810/72 $\Delta plcR$ in unsupplemented cell culture medium by conditioning with IEC or co-cultivation	66
Figure 31: Protein separation of <i>B. cereus</i> F4810/72 supernatant via gel filtration	67
Figure 32: SDS-PAGE analysis of growth promoting gel filtration fractions	68
Figure 33: SDS-PAGE analysis of bacterial supernatant for InhA2 expression	69
Figure 34: Rescue of <i>B. cereus</i> $\Delta plcR$ growth deficit by InhA2	71
Figure 35: 2-D DIGE analysis of differentially expressed proteins in the cytosolic proteome of <i>B. cereus</i> F4810/72 <i>wild-type</i> or $\Delta plcR$	73
Figure 36: Representative silver stained 2-D gel	78
Figure 37: Genetic organization of the metalloprotease and haemolysin gene cluster of <i>B. cereus</i> AH187 (F4810/72) in comparison to <i>V. cholerae</i> O1	91
Figure 38: Genetic organization of the <i>pur</i> operon of <i>B. cereus</i> F4810/72 encoding genes involved in purine biosynthesis	95
Figure 39: Organization of the genomic regions directly upstream of three different <i>B. cereus</i> F4810/72 neutral protease genes	100

LIST OF TABLES

Table 1: Bacterial media used in this study	15
Table 2: Buffers used in this study	16
Table 3: Antibodies used in this study	17
Table 4: Bacterial strains regularly used in this study	19
Table 5: <i>B. cereus</i> mutant strains generated or used in this study	26
Table 6: Labelling scheme for 2-D DIGE experiments	34
Table 7: Cytotoxic effect of different <i>B. cereus</i> strains on Ptk6 cells	39
Table 8: Cytotoxic effect of sterile <i>B. cereus</i> supernatants on Ptk6 cells	41
Table 9: Cytotoxic effect of sterile supernatant of <i>B. cereus wild-type</i> and mutant strains	59
Table 10: Detailed gene and protein sequence information of the three immune inhibitor proteins A of <i>B. cereus</i> ATCC 14579 and <i>B. cereus</i> F4810/72	68
Table 11: Number of total and differentially regulated protein spots in <i>B. cereus</i> F4810/72 <i>wild-type</i> and $\Delta plcR$ based on 2-D DIGE analysis	74
Table 12: Differentially expressed proteins of <i>B. cereus</i> F4810/72 $\Delta plcR$ in Ptk6 conditioned medium compared to unsupplemented RPMI medium revealed by 2-D DIGE analysis	76
Table A1: <i>B. cereus</i> strains used in cytotoxicity and adhesion screening including their toxin profiles	122
Table A2: Vectors and plasmids used in this study	123
Table A3: Oligonucleotide primers used in this study	124
Table A4: Detailed statistical analysis of differentially expressed proteins of <i>B. cereus</i> F4810/72 $\Delta plcR$ in Ptk6 conditioned medium compared to unsupplemented RPMI medium	126

SUMMARY

Bacillus cereus causes food poisoning and severe non-gastrointestinal-tract infections. While the emetic type of *B. cereus* foodborne disease is clearly attributed to one single toxin, cereulide, non-emetic *B. cereus* expresses a whole arsenal of enterotoxins and degradative enzymes that contribute to diarrhoea and serious clinical manifestations. Non-haemolytic enterotoxin (Nhe), which is present in all known *B. cereus* strains, is considered to be one of the main virulence factors, although there is increasing evidence that other single toxins and enzymes play a role for disease initiation.

In a screen for additional cytotoxic factors in an *in vitro* model for polarized colon epithelial cells *B. cereus* sphingomyelinase (SMase) was identified via liquid chromatography and mass spectrometry from bacterial supernatant. This study revealed SMase as a strong inducer of epithelial cell death via apoptosis involving caspase-3 activation. Gene inactivation and complementation of *sph* (*sphingomyelinase gene*) and *nheBC* in *B. cereus* F4810/72 and NVH 0075-95 demonstrated that SMase is a key player in *B. cereus* cytotoxicity *in vitro* and pathogenicity *in vivo*, both in emetic and diarrheal strains. While SMase and Nhe synergistically induced *B. cereus* cytotoxicity *in vitro*, only SMase but not Nhe contributed significantly to the mortality rate of larvae in the insect model *Galleria mellonella*. These results indicate that SMase as a key virulence factor of *B. cereus* has been far underestimated. It is expected that the presented results help to improve the still limited understanding of *B. cereus* pathogenesis in non-gastrointestinal-tract infections.

Furthermore, this work provides important insights into the complex intrinsic and extrinsic regulatory mechanisms that control or alter *B. cereus* growth and gene expression in response to host epithelium and environment. The PlcR-regulated protein immune inhibitor A2 was identified as essential secreted factor promoting growth of *B. cereus* F4810/72 in nutrient-poor medium. Additionally, the proteome of a growth-deficient *plcR* mutant was analysed for differential protein expression induced by intestinal epithelial cell factors. An initial 2-D DIGE approach revealed a significant impact of host-derived factors on bacterial core metabolic pathways, such as purine, amino acid and protein biosynthesis. Moreover, strong upregulation of two extracellular zinc metalloproteases, namely InhA3 and NprB, in host-conditioned medium stresses the pivotal role of bacterial proteases in nutrient acquisition and cell signalling essential for growth stimulation. The presented study draws a first important picture on the complexity of *B. cereus* protein expression and growth regulation under nutrient-limiting conditions and provides evidence that *B. cereus* benefits from the mammalian host intestinal epithelium via external proliferation stimuli.

ZUSAMMENFASSUNG

Bacillus cereus kann Lebensmittelvergiftungen und schwere nicht-gastrointestinale Infektionen verursachen. Während das Toxin Cereulid eindeutig die emetische Form der Lebensmittel-assoziierten Erkrankung hervorruft, wird von nicht-emetischen *B. cereus* Stämmen ein ganzes Arsenal an Enterotoxinen und Enzymen produziert, die zu Durchfall und ernsthaften systemischen Erkrankungen beitragen. Da das nicht-haemolytische Enterotoxin (Nhe) von allen bislang bekannten *B. cereus* Stämmen kodiert wird, gilt es als einer der Hauptvirulenzfaktoren, obwohl sich die Hinweise mehren, dass auch andere Toxine und weniger bekannte Enzyme eine Rolle bei der Krankheitsentstehung spielen.

Unter Verwendung eines *in vitro* Modells für polarisierte Kolonepithelzellen zum Screening nach weiteren zytotoxischen Faktoren wurde die *B. cereus* Sphingomyelinase (SMase) aus bakteriellem Überstand mittels Flüssigchromatographie und Massenspektrometrie identifiziert. Es wurde gezeigt, dass SMase die Caspase-3 Aktivität von Epithelzellen erhöht und somit zu apoptotischem Zelltod führt. Durch Mutagenese der *sphingomyelinase (sph)* und *nheBC* Gene in *B. cereus* F4810/72 und NVH 0075-95 wurde untersucht, welchen Beitrag SMase zur *in vitro* Zytotoxizität und *in vivo* Pathogenität, sowohl in emetischen, als auch in Durchfall auslösenden *B. cereus* Stämmen leistet. Dabei stellte sich heraus, dass SMase bislang als Schlüsselfaktor der *B. cereus* Virulenz unterschätzt wurde. Im Gegensatz zur synergistisch-zytotoxischen Aktivität von SMase und Nhe *in vitro*, ist SMase im *in vivo* Insekten-Modell *Galleria mellonella* alleine (ohne Nhe) ausreichend, um Larvenmortalität zu vermitteln. Die vorliegende Arbeit trägt somit zum besseren Verständnis der Pathogenität von *B. cereus* bei Infektionen außerhalb des Gastrointestinaltrakts bei.

Darüber hinaus konnte ein Einblick in die komplexen intrinsischen und extrinsischen Mechanismen gewonnen werden, die in Reaktion auf Umwelt und Wirtsfaktoren Wachstum und Genexpression in *B. cereus* regulieren und verändern. Aus dem *B. cereus* F4810/72 Wildtyp-Sekretom konnte der PlcR regulierte Immuninhibitor A2 als essentieller Wachstumsfaktor in nährstoffarmem Medium identifiziert werden. Da auch intestinale Epithelzellen das *B. cereus* Wachstum förderten, wurde zusätzlich das Proteom einer wachstumsdefizienten *plcR* Mutante auf veränderte Proteinexpression nach Behandlung mit Wirtsfaktoren analysiert. Erste differentielle Proteomstudien zeigten, dass epitheliale Faktoren einen signifikanten Einfluss auf den bakteriellen Primärstoffwechsel, einschließlich der Purin-, Aminosäure- und Proteinbiosynthese haben. Zudem konnte eine verstärkte Expression der beiden sekretierten Metalloproteasen InhA3 und NprB in Wirtszell-konditioniertem Medium nachgewiesen werden. Dies lässt auf eine Schlüsselfunktion von mikrobiellen Proteasen bei der Beschaffung von Nährstoffen und der Wachstumsinitiierung schließen. Ferner verdeutlichen die Ergebnisse dieser Studie die Komplexität des regulatorischen Netzwerks, das die gezielte Expression von Proteinen und die Vermehrung von *B. cereus* unter nährstoff-limitierenden Bedingungen steuert. Es konnte der Nachweis erbracht werden, dass *B. cereus* von externen Stimuli des Säugerepithels profitieren kann, indem das Wachstum des Pathogens angeregt wird.

1. INTRODUCTION

1.1 Foodborne illness

Foodborne illness is generally characterised as acute gastroenteritis accompanied by abdominal pain, watery diarrhoea, and cramps or vomiting. Disease can be evoked by ingestion of bacterial or viral pathogens (toxicoinfection) as well as bacterial toxins preformed in food or water (intoxication). The Centers for Disease Control and Prevention reported a doubling of foodborne outbreaks in the United States between 1991 and 2000 that can be attributed both to enhanced reporting systems but also increasing incidence of food poisoning (Widdowson *et al.* 2005). Meanwhile it is estimated that in the United States 9.4 million cases of foodborne illness lead to 55,961 hospitalizations and 1,351 deaths each year (Scallan *et al.* 2011). These data indicate the immense importance of food safety interventions and preventions in order to keep health costs affordable. While in the United States Norovirus infections played the major role, the European Food Safety Authority (EFSA) recorded the bacterial pathogens *Campylobacter* spp. and nontyphoidal *Salmonella* spp. as the most common etiological agents for foodborne outbreaks followed by viruses (13.1%) and bacterial toxins (9.8%) (Anonymous 2010). Intoxications arise most often from food contaminated with *Staphylococcus aureus*, *Clostridium* spp. or *Bacillus* spp. Interestingly, the incidence of foodborne outbreaks caused by *Bacillus* toxins increased noticeable in recent years (Anonymous 2009). In the European Union food authorities reported that *Bacillus cereus* toxins caused 45 verified foodborne outbreaks in 2008 entailing 1132 cases of human illness and 41 hospitalizations (Anonymous 2010). *B. cereus* causes two types of foodborne gastrointestinal disease (emetic and diarrheal) that are associated with a variety of different kinds of food (reviewed in (Stenfors Arnesen *et al.* 2008)). It was first recognised and classified as the causative agent of foodborne diarrheal gastroenteritis in 1950 (Hauge 1955). This type of illness has often been connected with the consumption of protein-rich foods, vegetables, meat and milk products (Kramer and Gilbert 1989; Meer *et al.* 1991). In contrast, starch-rich foods (fried and cooked rice and pasta) have been identified most commonly as source of emetic intoxication (Kramer and Gilbert 1989; Schoeni and Wong 2005). Although surveillance systems and detection methods have been improved over the years, *B. cereus* foodborne disease is most probably under-estimated in many countries as a consequence of several facts. *B. cereus* causes mostly mild and self-limiting disease that is barely diagnosed and only occasionally recorded as case reporting is not mandatory (Stenfors Arnesen *et al.* 2008). Furthermore, the symptom resemblance of bacterial intoxications hamper the differentiation between *B. cereus* and *S. aureus* caused emetic disease (Ehling-Schulz *et al.* 2006). Additionally, *B. cereus* diarrheal disease mimics *C. perfringens* food intoxication symptoms (Stenfors Arnesen *et al.* 2008). Recently developed specific molecular methods for *B. cereus* detection and identification could facilitate diagnosis in

public health facilities when adapted and standardised for routine testing (Ehling-Schulz *et al.* 2006b; Fricker *et al.* 2007).

1.2. The *Bacillus cereus* group

The *Bacillus cereus* (*sensu lato*) group represents a genetically highly related subgroup within the genus *Bacillus*. Six species are included in this group, namely *Bacillus weihenstephanensis*, *Bacillus mycoides*, *Bacillus pseudomycoides*, *Bacillus anthracis*, *Bacillus thuringiensis* and *Bacillus cereus* (*sensu stricto*) (Gordon *et al.* 1973; Priest and Alexander 1988; Lechner *et al.* 1998; Nakamura 1998). At least the latter three species are classified as opportunistic or pathogenic bacteria. All six species are Gram-positive, facultative anaerobic rods, which can form spores that are metabolically inactive and present an alternative form of life to endure harsh environmental conditions. Once *Bacillus* spores are exposed to organic matter, be it in soil, food or after ingestion into the mammalian or invertebrate host intestinal system, nutrient availability is sensed and induces germination. After infecting a susceptible host, *B. anthracis* and *B. thuringiensis* can enter a pathogenic life cycle with extensive vegetative growth to the stationary phase and subsequent sporulation (Jensen *et al.* 2003). However, so far no comparable life cycle has been demonstrated for the human pathogen *B. cereus*.

Despite their distinct phenotypic traits and different pathological effects, the species definition became subject of discussion during the last decades. Based on chromosomal gene content, gene synteny and 16S rRNA similarity it has been proposed that the *Bacillus cereus* group strains comprise one species (Helgason *et al.* 2000; Kolstø *et al.* 2009; Ehling-Schulz 2011). In particular, *B. anthracis*, *B. cereus* and *B. thuringiensis* are closely related and share more than 99% 16S rRNA sequence similarity (Ash *et al.* 1991). Nevertheless, traditionally defined characteristic phenotypic traits are still used to distinguish the *B. cereus* group members. Interestingly, many of these discriminating determinants are encoded by plasmid-located genes. Therefore, horizontal transfer of mobile genetic elements between the *B. cereus* group members is facilitated and may result in a dramatic alteration of phenotypes. Especially, *B. cereus* strains harbouring pXO1- and pXO2-like plasmids have already been identified and hold responsible for an anthrax-like disease (Hoffmaster *et al.* 2004; Klee *et al.* 2006). As a result it has been proposed to designate these strains *B. cereus* var. *anthracis* (Kolstø *et al.* 2009).

The non-pathogenic members of the *B. cereus* group *B. mycoides* and *B. pseudomycoides* can be distinguished from other species by their characteristic rhizoidal colony morphology on solid medium. They form two distinct genetic groups that cluster closely to *B. cereus*, but can be separated from each other based on fatty acid composition (Nakamura 1998; Di Franco *et al.* 2002). *B. weihenstephanensis* is a food spoiling organism mainly characterized by its psychrotolerant growth below 7 °C, but not at 43 °C and specific sequence differences in the cold shock protein A (*cspA*) gene (Lechner *et al.* 1998).

B. thuringiensis is commonly known as insect pathogen producing parasporal crystal inclusions. Synthesis of these insecticidal δ -endotoxins is encoded by plasmid-located *cry* genes. The

crystal toxins are widely used as bioinsecticides to protect crop against insect infestations (Betz *et al.* 2000; Aronson and Shai 2001; Berry *et al.* 2002).

B. anthracis is the most pathogenic species of the *B. cereus* group causing the fatal human and animal disease anthrax and has therefore gained special attention as bioterrorism weapon (Jernigan *et al.* 2002). The main virulence determinants of *B. anthracis* are the anthrax toxins controlled by the regulator AtxA and the antiphagocytic poly- γ -glutamic capsule which are encoded by genes located on the two virulence plasmids pXO1 and pXO2 (Mock and Fouet 2001).

Similarly to *B. weihenstephanensis*, *B. cereus* is known as food spoilage, but also food poisoning organism. Noteworthy, the toxicity spectrum of *B. cereus* ranges from strains used in probiotic formulas for human (Hong *et al.* 2005) to extremely toxic strains responsible for foodborne lethal outbreaks (Mahler *et al.* 1997; Lund *et al.* 2000). As an opportunistic pathogen, *B. cereus* is increasingly associated with foodborne gastrointestinal diseases (emesis and diarrhoea) (see Ch. 1.1.), but also non-gastrointestinal pathologies (reviewed in (Stenfors Arnesen *et al.* 2008) and (Bottone 2010)). While the gene determinants of the emetic syndrome are encoded on pXO1-like mega plasmids (Ehling-Schulz *et al.* 2006a), most of the *B. cereus* virulence factors and enterotoxins associated with the diarrheal type of disease are chromosomally encoded.

1.3. *B. cereus* ecology

Bacillus cereus can be found in a wide range of environments (Figure 1) including soil, sediment, dust and on plants (Kramer and Gilbert 1989; Kotiranta *et al.* 2000). During a saprophytic life cycle spores can even germinate in soil and exhibit vegetative growth (Vilain *et al.* 2006). From this habitat bacterial cells or spores easily accompany plants to the food processing area and are transmitted to ingredients and other foods, such as meat products, via cross-contamination (Johnson 1984; Kramer and Gilbert 1989). Since *B. cereus* spores are highly resistant to low pH, high temperatures used for conservation (heating, pasteurization) and chemical preservation procedures (Setlow 2006), especially mass catering and industrial food processing facilities bare a risk for contamination, if not adequately sanitized (Stenfors Arnesen *et al.* 2008; Abee *et al.* 2011; Ehling-Schulz *et al.* 2011).

Once ingested, spore germination is triggered in the host environment (Abee *et al.* 2011). Recent genome-wide analysis revealed numerous genes involved in invasion, colonization and propagation within the mammalian as well as the insect gut (Ivanova *et al.* 2003; Jensen *et al.* 2003; Read *et al.* 2003; Huang *et al.* 2005). This points to a more symbiotic or parasitic life cycle in addition to the saprophytic niche of *B. cereus* due to specialization on protein metabolism (Ivanova *et al.* 2003; Read *et al.* 2003). Accordingly, *B. cereus* has also been isolated from the faeces of healthy adults (Ghosh 1978), suggesting *B. cereus* as a part of human intestinal flora.

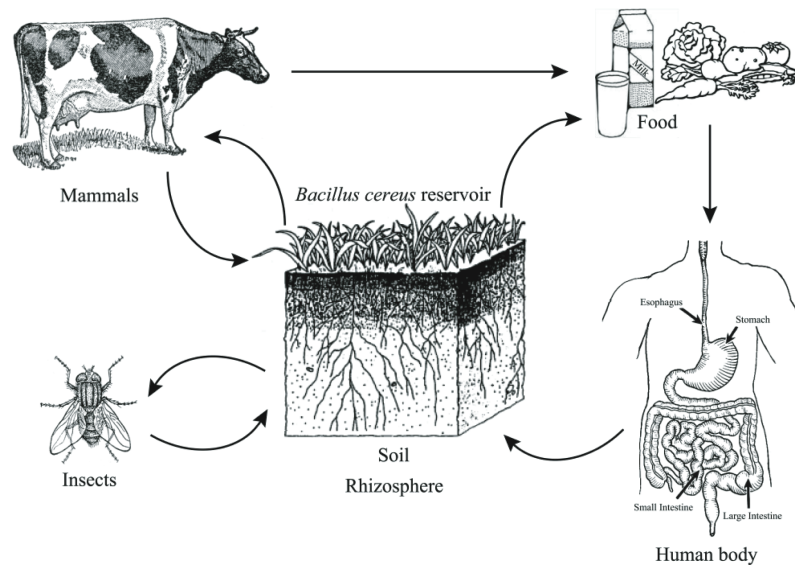


Figure 1: Environmental niches and transmission routes of the foodborne human pathogen *Bacillus cereus*. Spores and/or vegetative cells can be isolated from a variety of habitats including soil, plant rhizosphere, insect and mammalian gut. Reproduced from Mols, 2009 (Mols 2009, PhD Thesis), published in Mols and Abee, 2011 (Mols and Abee 2011).

Based on the potential adaptation to the gastrointestinal environment a probiotic effect has been proposed for some *B. cereus* strains although all strains harbour the genes for at least one enterotoxin (Nhe) associated with diarrhoea (Duc *et al.* 2004; Hong *et al.* 2005).

1.4. Pathogenicity of *B. cereus*

1.4.1 Local and systemic non-gastrointestinal-tract infections

Besides the specific niches of *B. cereus* as benign organism, *B. cereus* is most commonly connected to mostly mild gastroenteric pathologies of short duration, provoked by toxin production (Stenfors Arnesen *et al.* 2008). However, *B. cereus* has also been recognised as the etiological agent for a variety of rare, but often fatal non-gastrointestinal local and systemic infections (Bottone 2010). Due to a premature or impaired epithelial barrier lining the gut, neonates, elderly and immunocompromised individuals are at special risk to suffer from *B. cereus* infections, which mainly result from postoperative and posttraumatic wound contaminations (Bottone 2010). Cases of fulminant bacteraemia (Hilliard *et al.* 2003), meningitis (Turnbull *et al.* 1979; Barrie *et al.* 1992; Lebessi *et al.* 2009), pneumonia (Avashia *et al.* 2007), severe ocular infections (keratitis, endophthalmitis) (Drobniewski 1993; Callegan *et al.* 2002; Callegan *et al.* 2007), endocarditis (Craig *et al.* 1974) and cutaneous infections have been reported. Severe and lethal *B. cereus* infections are commonly connected to contaminated hospital linen, colonized indwelling catheters and nosocomial transmission (Hernaiz *et al.* 2003; Kuroki *et al.* 2009; Sasahara *et al.* 2011). All these pathologies are characterised by massive tissue degradation/destruction as a result of unspecific cytolytic and tissue-reactive enzyme activity (Bottone 2010). A role for the different *B. cereus* haemolysins, the collagenase,

cereolysin O and the three phospholipases sphingomyelinase (SMase), phosphatidylcholine-specific phospholipase C (PC-Plc) and phosphatidylinositol-specific phospholipase C (PI-Plc) has been suggested (Drobniewski 1993; Beecher *et al.* 2000; Beecher and Wong 2000). In many pathogenic bacteria phospholipase C is recognised as virulence factor contributing to tissue damage by degranulation of human neutrophils (Wazny *et al.* 1990; Titball 1993). In addition, recent studies focussed on haemolysin II (HlyII) and secreted proteases like the neutral protease and immune inhibitor metalloproteases (InhA1, InhA2 and InhA3) as novel contributors to *B. cereus* pathogenicity (Chung *et al.* 2006; Cadot *et al.* 2010; Chung *et al.* 2011). Results indicate that *B. cereus* likely uses several virulence factors concomitantly to enhance tissue degradation and circumvent host defence mechanisms (Cadot *et al.* 2010; Guillemet *et al.* 2010).

1.4.2 *B. cereus* emetic syndrome

However, the majority of *B. cereus* caused diseases affects the gastrointestinal tract resulting either in diarrhoea or emesis. The emetic syndrome is an intoxication with the emetic toxin cereulide, which is preformed in food during vegetative *B. cereus* growth. Ingestion of 8-10 µg per kg body weight results in abdominal cramps, nausea and vomiting within 0.5 – 6 hours and symptoms can last up to 24 hours (Stenfors Arnesen *et al.* 2008). Cereulide is a cyclic dodecadepsipeptide toxin that is synthesized enzymatically by a nonribosomal peptide synthetase (NRPS) from three repeats of alternating α-amino and α-hydroxy acid monomers (D-O-Leu—D-Ala—L-O-Val—L-Val)₃ (Agata *et al.* 1994; Ehling-Schulz *et al.* 2005). All genes involved in cereulide biosynthesis constitute the *ces* gene cluster located on a pXO1-like mega plasmid (pBCE, also referred to as pCER270) (Ehling-Schulz *et al.* 2006). The 24 kb cereulide biosynthetic gene cluster encodes for seven enzymes, amongst them CesA and CesB that constitute the core NRPS modules. Since cereulide is very small (1.2 kDa), extremely stable and resistant to a broad range of pH (2-11), digestive enzymes and heat (150 °C), it can not be removed by filtration and can overcome reheating of food, the gastric passage and proteolytic degradation in the intestine (Shinagawa *et al.* 1996; Granum and Lund 1997; Rajkovic *et al.* 2008). It is therefore of great importance to inhibit outgrowth of emetic *B. cereus* in food and subsequent cereulide production. Although detailed mechanisms by which emetic *B. cereus* evokes its symptoms in humans have not been determined, stimulation of the vagus afferent nerve by cereulide binding to the 5-HT₃ receptor caused vomiting in the animal model *Suncus murinus* (Agata *et al.* 1995). Like the antibiotic valinomycin, cereulide acts as a potassium ionophore leading to membrane depolarization in mitochondria and uncoupling of ATP synthesis (Mikkola *et al.* 1999; Kawamura-Sato *et al.* 2005; Andersson *et al.* 2007). The inhibition of mitochondrial activity was presumably the reason for several fatal cases of liver failure associated with *B. cereus* food poisoning (Mahler *et al.* 1997; Dierick *et al.* 2005; Shiota *et al.* 2010).

1.4.3 *B. cereus* diarrheal syndrome

In contrast, only one lethal case of foodborne diarrheal outbreak has been reported (Lund *et al.* 2000). The diarrheal syndrome is characterised by abdominal pain and watery (occasionally bloody) diarrhoea starting 8-16 hours after consumption of food contaminated with a total of 10^5 - 10^8 vegetative *B. cereus* cells or spores (Stenfors Arnesen *et al.* 2008). The long incubation time is typical for a toxicoinfection, where heat-labile enterotoxins have to be produced and secreted during vegetative growth of bacteria in the small intestine (Clavel *et al.* 2004). Duration of illness can vary between 12-24 hours and is usually self-limiting. Although *B. cereus* produces a large number of secreted enzymes and cytotoxins that might contribute, currently only the haemolysin BL (Hbl), cytotoxin K (CytK) and nonhaemolytic enterotoxin (Nhe) are considered the enterotoxins causative for diarrheal disease (Beecher and Macmillan 1991; Lund and Granum 1996; Lund *et al.* 2000). The related three-component toxins Hbl and Nhe are composed of three single proteins each that build up a functional unit. All three proteins are therefore necessary for full biological activity (Beecher *et al.* 1995; Lindbäck *et al.* 2004). The single component protein toxin cytotoxin K (CytK) has been isolated from a foodborne outbreak leading to necrotic enteritis and three deaths (Lund *et al.* 2000). Nevertheless, during the last years several other enzymes and toxins have been discussed to play a role for *B. cereus* diarrheal disease. Amongst these proteins were the enterotoxin FM (EntFM) (Asano *et al.* 1997; Tran *et al.* 2010), enterotoxin T (BceT) (Agata *et al.* 1995), the haemolysins II and III (Baida and Kuzmin 1995; Baida *et al.* 1999), proteases like InhA2 (Fedhila *et al.* 2003), phospholipases C (Kuppe *et al.* 1989) and cereolysin O (Kreft *et al.* 1983). Proteases and phospholipases can enzymatically degrade host cell membranes, other tissue components and protective host enzymes to counteract the host immune system (Miyoshi and Shinoda 2000; Chung *et al.* 2006; Guillemet *et al.* 2010; Chung *et al.* 2011).

Both CytK and haemolysin II (HlyII) are members of the family of β -barrel pore-forming toxins including also α -haemolysin of *S. aureus* (Gouaux 1998; Baida *et al.* 1999; Lund *et al.* 2000). Hbl is composed of the proteins B, L1 and L2, which are encoded in an operon comprising the genes *hblA*, *hblD* and *hblC* (Heinrichs *et al.* 1993; Ryan *et al.* 1997; Lindbäck *et al.* 1999). Turnbull *et al.* identified Hbl from *B. cereus* strain F837/76 isolated from a postoperative wound (Turnbull *et al.* 1979). The haemolytic and dermonecrotic activity of Hbl as well as cytotoxic activity towards Vero cells has been demonstrated (Beecher and Wong 1994; Lund and Granum 1997; Beecher and Wong 2000). The non-haemolytic enterotoxin Nhe consists of the three proteins NheA, NheB and NheC. Similar to Hbl, the corresponding *nhe* genes are organized in the *nheABC* operon (Granum *et al.* 1999). Nhe was first purified from the *hbl*-negative *B. cereus* strain NVH 0075-95 that caused a large foodborne outbreak in Norway in 1995 (Lund and Granum 1996). Despite its misleading designation Nhe exhibits haemolytic activity towards erythrocytes from different mammalian species (Fagerlund *et al.* 2008). Maximal enterotoxic activity requires a defined ratio of NheA, NheB and NheC (10:10:1) and a specific binding order (Lindbäck *et al.* 2004). Recently, Lindbäck *et al.* proposed the following model for

Nhe mode of action: Initial attachment of NheC and NheB to the cell surface, heterooligomer formation accompanied by conformational changes and subsequent binding of NheA resulting in pore formation (Lindbäck *et al.* 2010).

Pore formation is a common mechanism of *B. cereus* enterotoxins that cause diarrhoea due to osmotic lysis of the intestinal epithelial cells (Finlay and Falkow 1997). Transmembrane pore formation after assembly of a membrane-attacking complex has been shown for Hbl (Beecher and Wong 1997). Furthermore, CytK as well as Nhe are able to form pores in synthetic phospholipid membrane or lipid bilayers, respectively (Hardy *et al.* 2001; Fagerlund *et al.* 2008). These findings render it unlikely that specific host cell receptors are required for toxin binding and cell lysis.

Considering enterotoxin gene abundance, the *hbl* operon, as well as *cytK* can solely be found in a distinct group of *B. cereus* strains, usually only present in less than 50% of randomly chosen strains (Ehling-Schulz *et al.* 2005; Ehling-Schulz *et al.* 2006b; Moravek *et al.* 2006). However, clinical and food-associated isolates show higher frequencies of *cytK* and *hblACD* (Guinebretière *et al.* 2002). In contrast, all strains analysed so far tested positive for Nhe genes (Ngamwongsatit *et al.* 2008). This is one reason why Nhe is currently assumed to be the major diarrheal toxin of *B. cereus*. In line with this cytotoxicity of *B. cereus* culture supernatants strongly correlated with the concentration of Nhe therein (Moravek *et al.* 2006). Furthermore, cytotoxicity was neutralized using an Nhe-specific antibody and mutation of *nheB* and *nheC* abolished cytotoxic activity of *B. cereus* NVH 0075-95 (Dietrich *et al.* 2005; Fagerlund *et al.* 2008). However, the most dominant toxin may vary dependent on *B. cereus* strain and protein expression level. For instance, enterotoxigenic activity of *B. cereus* ATCC 14579 could be markedly reduced by *hbl* operon inactivation (Lindbäck *et al.* 1999). Probably, gastroenteritis results from a cooperative or even synergistic teamwork of several *Bacillus cereus* toxins (Callegan *et al.* 2003; Fedhila *et al.* 2003).

1.5. Regulation of virulence gene expression

In general, it has long been observed that *B. cereus* cytotoxicity levels vary substantially depending on the individual strain, but also on multiple environmental factors such as temperature, pH, glucose concentration and oxygen tension (Glatz and Goepfert 1976; Spira and Silverman 1979; Sutherland and Limond 1993). Especially, for the diarrheal disease, presence or absence of single toxin genes alone can not fully explain the virulence of a specific *B. cereus* strain (Stenfors Arnesen *et al.* 2008). On the contrary, the pathogenicity seems more likely to be determined by individual protein expression levels and strain-specific differences in toxin expression regulation. Since production and transport of toxins and degradative enzymes require a considerable amount of energy, bacteria have developed sophisticated regulatory circuits to sense their environment and tightly control and coordinate virulence factor expression accordingly. Gram-positive bacteria monitor population density utilizing a quorum-sensing system and in parallel sense the quality and abundance of available nutrients (Lazazzera 2000).

A whole set of global regulators is employed by *Bacillus subtilis* and *Bacillus cereus* to integrate metabolic environmental information and achieve coordinated transcription activation or shut-off (Phillips and Strauch 2002; Lücking *et al.* 2009). To facilitate the process, genes that encode for functional groups of proteins, like enterotoxins, frequently belong to the same regulon (Finlay and Falkow 1997). During lag phase and early exponential growth of *Bacilli* several transition-state regulators (AbrB, CodY, SinR) are active and prevent redundant expression of proteins and functions needed for sporulation initiation and stationary phase but not during vegetative growth (Phillips and Strauch 2002). Besides typical stationary phase processes such as motility, competence and production of degradative enzymes and proteases, also the cereulide synthetase (*ces*) cluster is subject to a tight transition-state regulation (Lücking *et al.* 2009). The *ces* operon is transcribed during the exponential phase of growth (Dommel *et al.* 2011).

1.5.1 The emetic toxin cereulide

The *B. subtilis* global regulator CodY has been shown to sense environmental levels of GTP and branched-chain amino acids and to repress cereulide production until mid-exponential phase correspondingly (Ratnayake-Lecamwasam *et al.* 2001; Shivers and Sonenshein 2004). Deletion of *codY* in the emetic *B. cereus* F4810/72 strongly increased *cesA* mRNA synthesis and total cereulide accumulation (Frenzel 2011, PhD Thesis). Furthermore, CodY seems to play a contradictory role in virulence regulation in other gram-positive bacteria. While repression of virulence gene expression by CodY has been demonstrated in *Clostridium difficile* and *Staphylococcus aureus* (Dineen *et al.* 2007; Majerczyk *et al.* 2008; Majerczyk *et al.* 2010), CodY was found to act as a positive regulator in *Listeria monocytogenes* and *Bacillus anthracis* (Bennett *et al.* 2007; van Schaik *et al.* 2009).

Very recent work on emetic *B. cereus* cereulide synthetase expression has identified major involvement of the two global regulators AbrB and Spo0A in a precisely timed circuit comparable to regulation mechanisms in *B. subtilis* (Figure 2) (Lücking *et al.* 2009). In the *B. cereus* relative *B. subtilis* the global transition state regulator AbrB is active and autoregulated during lag and early exponential phase (Strauch *et al.* 1989). AbrB protein levels over an effective threshold ensure direct transcriptional repression of the *ces* synthetase genes (Phillips and Strauch 2002). In addition, AbrB is a repressor of *sigH* gene expression encoding for the alternative sigma factor A (σ^H), that drives transcription of late *spo0A* and sporulation specific genes (Strauch 1995; Britton *et al.* 2002). As a response to nutrient deprivation at the onset of transition state the primary *Bacillus* sigma factor of RNA polymerase (σ^A) initiates early expression of the sporulation master regulator Spo0A. Upon a complex regulatory phosphorelay cascade Spo0A is phosphorylated to form the active transcription factor Spo0A~P (Strauch and Hoch 1993; Jiang *et al.* 2000). Spo0A~P represses *abrB* transcription and decreasing AbrB concentrations lift its repressive effect on cereulide synthesis (Figure 2) (Lücking *et al.* 2009). In turn Spo0A~P can activate genes required for sporulation. Furthermore, Lücking *et al.* demonstrated that the major virulence regulator PlcR is not involved in production of the emetic toxin cereulide,

indicating two completely different regulation circuits for enterotoxin versus cereulide production (Lücking *et al.* 2009).

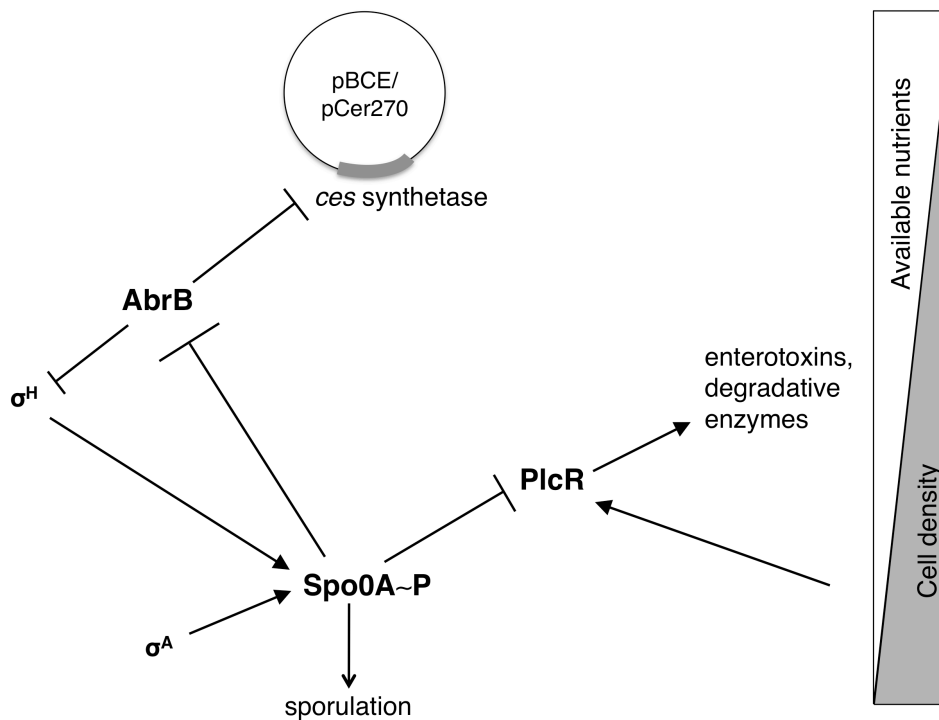


Figure 2: Current scheme of the regulation of virulence gene expression in emetic *B. cereus*. The figure was adapted from (Lücking 2009, PhD Thesis).

1.5.2 Non-emetic virulence factors and the PlcR regulon

In contrast to emetic toxin expression, most of *B. cereus* virulence factors associated with diarrhoea and non-gastrointestinal infections are members of the PlcR regulon. The pleiotropic transcriptional regulator PlcR (Phospholipase C Regulator) is part of the PapR-PlcR quorum-sensing system that activates virulence gene transcription during transition state in response to increasing cell density (Lereclus *et al.* 1996; Agaisse *et al.* 1999) (see Figure 3). PlcR belongs to the RNPP (named after the corresponding receptor proteins Rap, Npr, PlcR and PrgX) superfamily of gram-positive quorum sensors that bind directly to their autoinducer peptide inside the cell (Declerck *et al.* 2007). The autoinducer PapR is secreted as an inactive propeptide (48 aa) that is processed to the active heptapeptide by an extracellular protease (neutral protease B, NprB) (Gominet *et al.* 2001; Slamti and Lereclus 2002; Pomerantsev *et al.* 2009). After reimport of the mature PapR via an oligopeptide permease system (Opp), the autoinducer peptide PapR interacts with the PlcR protein (34 kDa) (Slamti and Lereclus 2002) (Fig. 3). This interaction triggers oligomerization of PlcR dimers into a right-handed spiral (Declerck *et al.* 2007), which may facilitate DNA binding of PlcR activating positive autoregulation of *plcR* and target gene transcription.

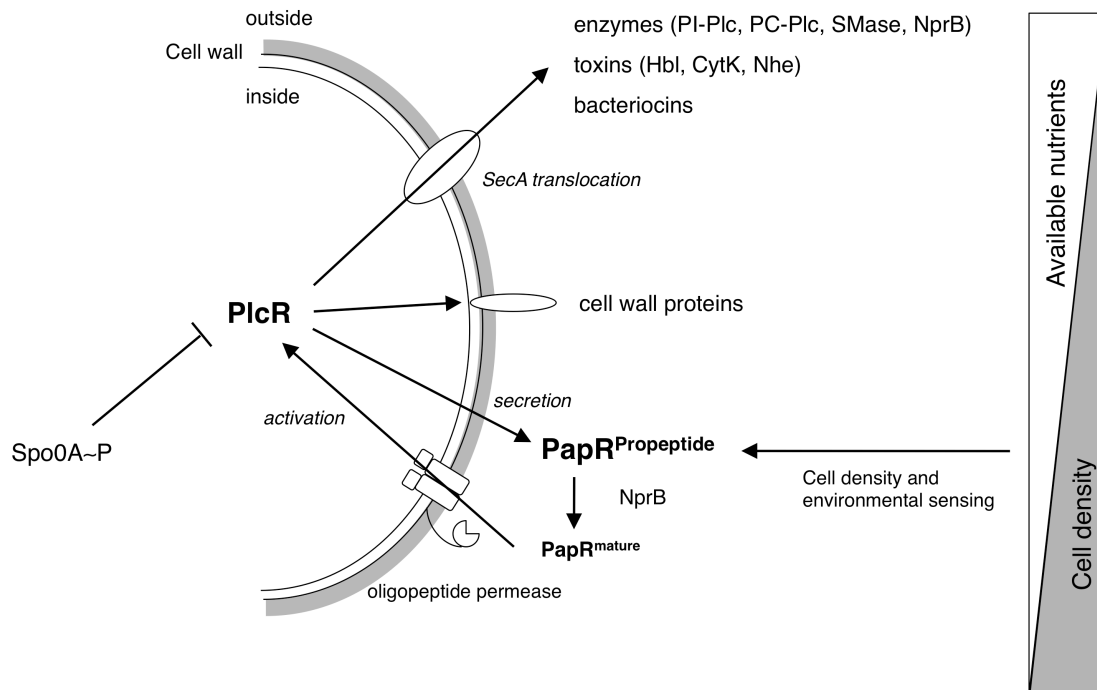


Figure 3: Scheme of the PlcR regulon organization in *B. cereus*. PlcR positively regulates the transcription of many genes coding for extracellular or cell wall located proteins. A detailed description of the PlcR-PapR quorum sensing system is outlined in the text. The figure was adapted from (Gohar *et al.* 2008).

Upon binding to a conserved DNA motif (PlcR-box) upstream of target genes PlcR activates the expression of about 45 different proteins, 90% of which are secreted or cell-wall associated (Gohar *et al.* 2002). The PlcR regulon comprises the enterotoxin genes for Nhe, Hbl, CytK and cereolysin O, as well as degradative enzymes such as the three phospholipases C (PI-Plc, PC-Plc, SMase) and the immune inhibitor A2 protease (InhA2) (Gohar *et al.* 2002). Secretion of Nhe, Hbl and CytK is mediated via the Sec translocation pathway (Fagerlund *et al.* 2010). Deletion of *plcR* decreased the amount of secreted proteins by 50% compared to wild-type (Gohar *et al.* 2002) and strongly reduced virulence of *B. thuringiensis* and *B. cereus* against epithelial cells, insect larvae, mice and rabbit retinal tissue (Salamitou *et al.* 2000; Callegan *et al.* 2003; Ramarao and Lereclus 2006). Although these data emphasize the significance of PlcR, *B. cereus* virulence is not completely abolished in the *plcR* deletion mutant, indicating additional regulatory mechanisms and/or PlcR-independent factors that contribute to virulence.

One of the few virulence factors that are not a member of the PlcR regulon is haemolysin II (HlyII), which seems to be negatively regulated by the HlyIIR transcriptional regulator (Budarina *et al.* 2004; Gohar *et al.* 2005). Expression of *hlyII* is further predicted to be controlled by the ferric uptake regulator Fur, that represses transcription of genes involved in iron uptake and metabolism when sufficient iron levels are present. Reduced virulence of *B. cereus* after *fur* deletion suggests a close link between virulence and iron metabolism (Harvie *et al.* 2005).

Interestingly, in *B. anthracis* the PlcR regulon is inactive because a nonsense mutation in the *plcR* gene resulted in a truncated inactive PlcR protein (Agaisse *et al.* 1999; Gohar *et al.* 2005).

This might be the result of a counterselection of the PlcR regulon in *B. anthracis* due to incompatibility between the major anthrax toxin regulator AtxA and PlcR (Mignot *et al.* 2001).

Unlike AbrB, PlcR is a transcriptional activator of transition state factors. Under nutrient-limiting conditions protein expression is terminated by Spo0A~P repressing *plcR* transcription in the stationary phase (Figure 2 and 3) (Lereclus *et al.* 2000). Hence, PlcR activity needs at least two conditions to be fulfilled: 1) sufficient nutrient state of the cell that ensures low concentrations of Spo0A~P allowing *plcR* transcription and 2) a cell density high enough to initiate the quorum-sensing mechanism. This also presents first evidence for a close link between *B. cereus* cytotoxic activity and the bacterial metabolic state.

In line with this Hbl and Nhe expression has been found to be regulated by the nutritional state and the oxidoreduction potential of the cell in addition to PlcR control. Noteworthy, anaerobic, highly reducing fermentative conditions as they are found in the small intestine (Moriarty-Craige and Jones 2004), have been shown to favour Nhe and Hbl production (Duport *et al.* 2004; Zigha *et al.* 2006). Enterotoxin and protease expression might present a mean of exploiting residual nutrient resources.

Further evidence for a tight connection between *B. cereus* metabolism, redox status and virulence is presented by the contribution of the two-component system ResDE and the transcriptional regulator Fnr to enterotoxin expression. Both regulatory systems primarily modulate the metabolism responding to oxygen availability and redox conditions. A contribution to toxin expression regulation has been demonstrated for Nhe and Hbl (Duport *et al.* 2006; Zigha *et al.* 2007). Moreover, in non-emetic *B. cereus* catabolite repression involving the carbon catabolite-control protein (CcpA), as well as motility has been discussed to play a role in virulence regulation independent of PlcR. (Callegan *et al.* 2003; Duport *et al.* 2004; Ouhib *et al.* 2006; Ghelardi *et al.* 2007; van der Voort *et al.* 2008). In summary, virulence factor expression in *B. cereus* is a very complex regulatory network that integrates a vast number of environmental, nutritional and intrinsic signals leading to an elaborate adaptation of gene transcription to the metabolic status of the cell. With regard to *B. cereus* safety risk assessment, understanding virulence gene regulations constitutes an essential step for deciphering *B. cereus* pathogenicity.

1.6. Host-pathogen interaction

Interaction with enteric epithelial cells is necessary for successful bacterial colonization and is a major part of the virulence of intestinal pathogens. In healthy individuals, enteric epithelial cells constitute the first physical barrier fending off microbial invasion. Direct intimate cell-cell association mediated by adherens and tight junctions is essential for epithelial adhesion and barrier function (Niessen 2007). In polarized epithelial cells the junctions (apical-junctional complex, AJC) are composed of a complex set of transmembrane and scaffolding proteins, like claudin, occludin and ZO proteins at the tight junctions and E-cadherin and catenins at the adherens junction (Vogelmann *et al.* 2004), which maintain cell-cell contact. The epithelial lining

also limits contact of gut microbes and foodborne pathogens with the underlying host immune system. But the intestinal epithelium is not only a physical barrier preventing microorganisms from entering host tissue, hence the blood and lymphoid circulation. Epithelial cells seem to actively interact and communicate with pathogens via contacts resulting from adherence of bacteria to the host epithelium. Thereby, epithelial cells participate as immune sensors of microbial pathogens and commensal organisms (Sartor 2008).

Due to monitoring of and discrimination between commensal and pathogenic bacteria, intestinal cells clear most of host-pathogen interactions unnoticed, making inflammation a rare event (Merrell and Falkow 2004). However, impaired barrier function in neonates, immunocompromised or elderly hosts may support development of severe enteric disease. Defective or entirely open barrier junctions facilitate invasion of non-invasive pathogens, hence exposing the underlying host tissue and extracellular matrix to direct pathogen contact (Westerlund and Korhonen 1993). Independent of barrier function, adhesion of foodborne pathogens to host epithelial cells is believed to play a significant role in overcoming barrier and disease formation. The resulting tight contacts between bacterial and intestinal cells may prevent clearance of bacteria and enable host colonization (Finlay and Falkow 1997). Furthermore, direct pathogen-host contact often triggers host cell signalling pathway activation. Bacterial spores, which can be found in contaminated food or water, can adhere to the intestinal epithelium facilitating germination and intensive growth of vegetative cells inducing bacterial virulence gene expression in a quorum-sensing dependent manner (Andersson *et al.* 1998; Gohar *et al.* 2008). Invasion may allow pathogens to escape the host immune system, while attachment of pathogens to intestinal epithelial cells may lead to a locally high concentration of bacterial secreted toxins that can exponentiate the cytotoxic effect and is important for the severity of symptoms (Finlay and Falkow 1997).

1.7. Interaction of *B. cereus* and the intestinal epithelium

For the foodborne opportunistic pathogen *B. cereus*, production of several toxins is well established (see Ch. 1.4.), while little is known about adherence of *B. cereus* to the intestinal epithelium as a first step for successfully conquering of the epithelial barrier.

Adherence of *B. cereus* spores and vegetative cells has only been investigated in a few experiments using different epithelial cell lines as *in vitro* model system. Generally, *B. cereus* spores demonstrated higher adhesion capacities than vegetative cells (Andersson *et al.* 1998), which has been attributed to the markedly higher hydrophobicity of the spore surface. This is in line with various reports that indicate a strong correlation between bacterial surface hydrophobicity and adhesion to different surface structures including mammalian cells as well as their ability to cause infections (Nesbitt *et al.* 1982; Wibawan *et al.* 1992; Doyle 2000). Especially S-layer proteins and attached molecules mediate effective binding to extracellular matrix proteins such as collagen, laminin and fibronectin, but also to mucin (Kotiranta *et al.* 1998; Sánchez *et al.* 2009). Interestingly, vegetative cells of different *Bacillus* species strongly

differed in their hydrophobicity causing distinct differences in the respective adhesion capacity to respiratory (A459) and macrophage (J774) cell lines. While *B. anthracis* and *B. thuringiensis* significantly adhered to the host cells, almost no adhesion could be detected for *B. cereus* and *B. subtilis* vegetative cells (Thwaite *et al.* 2009). In addition, discrimination between *B. cereus* strains of varying sources or toxigenic profiles was possible based on their adhesion capacity to HeLa cells. More than 60% of *B. cereus* strains isolated from dental cavities and diarrhoea-associated strains were tested positive for adhesion, while emetic strains were poorly adherent (Auger *et al.* 2009). Spores of several enterotoxigenic *B. cereus* strains adhered to monolayers of polarized human epithelial Caco-2 and HeLa cells, but differences in adhesion could be seen between various strains. In addition, adhesion efficiency was very low (~ 1 %) in strains that were able to adhere (Andersson *et al.* 1998; Wijnands *et al.* 2007). Moreover, Wijnands *et al.* reported that the presence of Caco-2 cells in contrast to HeLa cells triggered germination of spores (Wijnands *et al.* 2007). This suggests differences in the potential to induce bacterial cell signalling depending on the tissue the host cells originate from.

Since the number of adhering bacterial cells directly correlated with the number of applied cells, the mechanism of adhesion was proposed to be nonspecific rather than mediated by certain adhesin molecules (Wijnands *et al.* 2007). However, during the last years contribution of several cell surface associated *B. cereus* proteins such as the cell wall peptidase CwpFM (EntFM) and exosporium components to adhesion has been implicate (Faille *et al.* 2010; Tran *et al.* 2010). Furthermore, proteins involved in motility and flagellum assembly have been shown to participate in *B. cereus* adhesion to epithelial cells. Mutation of the *flhA* gene, which encodes for a component of the flagellum apparatus, significantly reduced the adhesion capacity of *B. cereus* and *B. thuringiensis* to Caco-2 and HeLa cells (Ramarao and Lereclus 2006).

Similar to spores, vegetative *B. cereus* cells exhibited strain-dependent adhesion to the human epithelial cell line Caco-2 and internalization into these non-phagocytic cells could be observed (Minnaard *et al.* 2004). Since attachment commonly precedes toxin expression and secretion, *B. cereus* adhesion was found to be accompanied by disruption of the infected epithelium. With progressing infection duration *B. cereus* and *B. thuringiensis* strains caused cytotoxicity toward epithelial cells and adhesion was followed by cell damage due to F-actin disassembly *in vitro* (Minnaard *et al.* 2004; Ramarao and Lereclus 2006). This indicates that bacterial adhesion to epithelial cells can initiate signal cascades in the host cells leading to rearrangement of cellular structures. A second study supporting this hypothesis showed that expression of tight junctional proteins ZO-1 and occludin decreased resulting in junction leakage after *B. cereus* infection of retinal pigment epithelium (RPE) cell monolayers. *B. cereus* infection resulted in disruption of the epithelial barrier and increased barrier permeability (Moyer *et al.* 2008). Taken together, interaction of *B. cereus* and the host epithelium *in vivo* must be a very complex, fine-tuned balance between bacterial attachment and induction of enterotoxin expression in order to prevent host cell damage through pore-formation long enough to establish *B. cereus* colonization.

1.8. Research objective

The opportunistic human pathogen, *B. cereus* is increasingly associated with foodborne gastroenteritis (emesis and diarrhoea) as well as severe non-gastrointestinal pathologies. The broad spectrum of *B. cereus* associated disease might reflect the very diverse toxigenic potential of different strains comprised in the *B. cereus* species. *B. cereus* pathogenicity ranges from highly toxic strains to such used in probiotic formulas for human. However, the underlying virulence contributors and regulation mechanisms responsible for these diversity are poorly understood rendering *B. cereus* an extremely interesting study subject.

While the emetic type of *B. cereus* foodborne disease is clearly attributed to one single toxin, cereulide, *B. cereus* expresses a whole arsenal of enterotoxins and degradative enzymes that contribute to diarrhoea and systemic infections. Most studies focussed on the three enterotoxins CytK, Hbl and Nhe, which are assumed to be the etiological agents for diarrheal disease, although there is increasing evidence that other single toxins and enzymes contribute to disease initiation. Nevertheless, synergistic effects of *B. cereus* single virulence factors are poorly understood. Furthermore, little is known about the interaction of *B. cereus* with the host intestinal epithelial cells and its consequences for pathogenesis.

The objectives of this thesis were to (i) assess the direct bacterial-host cell interaction using a murine intestinal epithelial cell (IEC) culture model, (ii) examine the role of *B. cereus* known toxins for epithelial cell physiology and (iii) identify a novel, less characterised contributor to *B. cereus* virulence *in vitro* as well as (v) characterise its *in vivo* role with respect to *B. cereus* pathogenicity.

To gain insight into the intrinsic and extrinsic regulatory mechanisms that control or alter *B. cereus* growth and gene expression in response to host epithelium, central aims of this thesis were to (iv) identify an intrinsic PlcR-regulated factor that enables *B. cereus* growth under nutrient-limiting conditions and (v) determine if and how *B. cereus* can benefit metabolically from host intestinal epithelial cells via differential protein expression.

2. MATERIALS AND METHODS

2.1. Materials

2.1.1 Bacterial media and buffers

Table 1: Bacterial media used in this study

Media	Composition	Media	Composition
LB	10 g/l Peptone from casein 5 g/l Yeast extract 10 g/l NaCl	MYP	10 g/l Casein peptone 10 g/l D-mannitol 1 g/l Meat extract 10 g/l NaCl 0.013 mg/l Polymyxin B 0.025 g/l Phenol red 50 ml/l Egg-yolk emulsion
MSM	8 g/l Bacto nutrient broth (Oxoid)	SOC	20 g/l Tryptone 5 g/l Yeast extract 10 mM NaCl 2.5 mM KCl 10 mM MgCl ₂ 10 mM MgSO ₄ 20 mM D-glucose
Trace elements	1 M MgCl ₂ x 6 H ₂ O 1 M Ca(NO ₃) ₂ x 4 H ₂ O 12.5 mM ZnCl ₂ 2.5 mM CuCl ₂ 0.001 mM FeSO ₄ 2.5 mM CoCl ₂ x 6 H ₂ O 2.5 mM Na ₂ MoO ₄ x 2 H ₂ O		
Nitrogen and sulfur source	5 mM (NH ₄) ₂ SO ₄ 0.066 mM MnSO ₄ x H ₂ O 10 mM Maltose		

All cell culture media were purchased from Invitrogen.

Table 2: Buffers used in this study

Buffer	Composition	Buffer	Composition
1x TAE	40 mM Tris 20 mM Acetic acid 1 mM EDTA pH 8.0	PBS-EDTA	1x DPBS, sterile 0.1 mM EDTA pH 7.4 at 20 °C
Permeabilization and Blocking Buffer for IF	PBS 3% BSA 1% Saponin 0.1% Triton X-100 0.05% Sodium Azide	PBS-Trypsin-EDTA	1x DPBS, sterile 0.07% Trypsin 0.1 mM EDTA pH 7.4 at 20 °C

Table 2 - continued

Buffer	Composition	Buffer	Composition
2D-DIGE lysis buffer	7 m Urea 2 M Thiourea 4% (w/v) CHAPS	4x SDS Sample Buffer	0.8% SDS 160 mM Tris, pH 6.8 30% Glycerol
Caspase 3 Assay Buffer	50 mM HEPES 100 mM NaCl 0.1% CHAPS 0.1 mM EDTA 10 mM DTT 10% Glycerol pH 7.4 at 20 °C	Ringer's solution	2.25 g/l NaCl 0.105 g/l KCl 0.12 g/l CaCl ₂ 0.05 g/l NaHCO ₃ pH 7.0 at 20 °C
Cell Lysis Buffer for Caspase 3 Assay	50 mM HEPES 100 mM NaCl 0.1% CHAPS 0.1 mM EDTA 0.1 mM DTT pH 7.4 at 20 °C	SDS-Running buffer	192 mM Glycine 25 mM Tris 0.1% SDS
Collagen solution	dilute 1:10 Rat-tail collagen (extracted from rat-tails, kindly provided by R. Vogelmann) in 1:1000 Acetic acid	Spore washing buffer	2 mM KH ₂ PO ₄ 8 mM K ₂ HPO ₄ pH 7.4
Fixative - 2% paraformaldehyde	<u>Solution A - 100mM sodium phosphate, pH 7.4:</u> 1 M dibasic Na-phosphate pH 9 - 2430µl 1 M monobasic Na-phosphate pH 4.1 - 570µl dH ₂ O - 27ml <u>Solution B - 8% paraformaldehyde pH 7.4</u> Solution A and B are combined 3:1	Transfer buffer	25 mM Tris 192 mM Glycine 20% v/v Methanol
		Washing Buffer for IF	PBS 3% BSA 1% Saponin 0.05% Na Azide

2.1.2 Chemicals, materials and cell culture equipment

All chemicals were purchased from AppliChem, Biochrom, Bio-Rad, Carl Roth GmbH, Invitrogen, LI-COR, Merck, Serva and Sigma-Aldrich. Cell culture consumables were obtained from BD Biosciences or Greiner Bio-One.

Detailed information about all antibodies used for Western blot analysis or immunofluorescence staining are listed in Table 3.

Table 3: Antibodies used in this study

Antibody	Concentration	Source
Mouse anti-ZO1	IF 1:200 IB 1:1000	Zymed Laboratories, Invitrogen, (USA)
Alexa Fluor 488 phalloidin	IF 1:500	Molecular Probes, Invitrogen, (USA)
Alexa Fluor 594 phalloidin	IF 1:200	Molecular Probes, Invitrogen, (USA)
Alexa Fluor 647 phalloidin	IF 1:50	Molecular Probes, Invitrogen, (USA)
Alexa Fluor 488 Goat anti-Mouse	IF 1:200	Molecular Probes, Invitrogen, (USA)
Alexa Fluor 546 Goat anti-Mouse	IF 1:200	Molecular Probes, Invitrogen, (USA)
Alexa Fluor 594 Goat anti-Mouse	IF 1:200	Molecular Probes, Invitrogen, (USA)
Goat anti-Mouse IgG Dye Light 649	IF 1:200	Pierce Biotechnology, (USA)
Alexa Fluor 488 Goat anti-Rabbit	IF 1:200	Molecular Probes, Invitrogen, (USA)
Alexa Fluor 546 Goat anti-Rabbit	IF 1:200	Molecular Probes, Invitrogen, (USA)
Alexa Fluor 594 Goat anti-Rabbit	IF 1:200	Molecular Probes, Invitrogen, (USA)
Alexa Fluor 647 Goat anti-Rabbit	IF 1:200	Molecular Probes, Invitrogen, (USA)
Alexa Fluor 680 Goat anti-Mouse	IB 1:30,000	Molecular Probes, Invitrogen, (USA)
Alexa Fluor 680 Goat anti-Rabbit	IB 1:30,000	Molecular Probes, Invitrogen, (USA)
Anti-Rabbit IgG IRDye 800	IB 1:30,000	Rockland, (USA)
Anti-Mouse IgG IRDye 800	IB 1:30,000	Rockland, (USA)
Alexa Fluor 546 Goat anti-chicken	IF 1:200	Pierce Biotechnology, (USA)
Mouse anti-NheA	IB	Kind Gift from R. Dietrich, E. Märtlbauer (Germany)
Mouse anti-NheB	IB	
Mouse anti-NheC	IB	
Chicken anti- <i>B. cereus</i>	IF 1:10 - 1:100	AvesLab, (USA)
Rabbit anti-BcSMase	IB 1:1000	Kind Gift from M. Oda, J. Sakurai (Japan)

IF: Immunofluorescence; IB: Immuno blot

2.2. Microbiological methods

2.2.1 Bacterial strains and growth conditions

All *B. cereus* wild-type and isogenic mutant strains were grown routinely on Luria-Bertani (LB) agar plates or in LB broth at 30 °C or 37 °C. For phenotypic characterisation of deletion mutants the selective plating media MYP agar (mannitol-egg yolk-polymyxin agar, Oxoid) and Columbia agar (with 5% sheep blood) was used. *E. coli* TOP10, DH10B and the non-methylating strain INV110 were used as general cloning strains and *E. coli* JM83/pRK24 served as the donor strain in conjugation experiments. The non-pathogenic *E. coli* DH10B was used as a control for insect infection experiments. All *E. coli* strains were grown in LB broth or on LB plates at 37 °C. When required, appropriate antibiotics were added to the media: 100 µg/ml ampicillin, 100 µg/ml spectinomycin, 50 µg/ml polymyxin B, 50 µg/ml kanamycin, 3 µg/ml erythromycin, 5 µg/ml chloramphenicol. All strains regularly used in this study are listed in Table 4. For bacterial adhesion assay and the cytotoxicity screening an additional strain set including various enterotoxin profiles was used. These strains are specified in Table A1 in the Appendix 7.1.

For growth curves growth of bacteria in liquid medium was monitored by measuring the optical density at 600nm (OD₆₀₀) using a UV/Vis spectrophotometer (Perkin-Elmer, Bio-Rad). For OD₆₀₀ values exceeding 1 the liquid culture samples were diluted 1:10. Spore formation was observed using a phase contrast microscopy (Olympus). Where indicated, colony forming units (CFU)/ml were determined additionally by plating serial dilutions on LB agar plates. In general, growth curves were done in shaking flasks or in 100-well plates in the Bioscreen C system (iLF bioserve).

The *sph* null mutant and the *nhe sph* double null mutant were phenotypically characterised. Small amounts of bacterial material were applied to different selective and differential solid media plates and incubated at 30 °C and 37 °C over night. Columbia agar (with 5% sheep blood) was used to detect haemolysis. The *B. cereus* selective MYP agar (mannitol egg yolk polymyxin agar) (Mossel *et al.* 1967) was used to confirm phospholipase C activity. *B. cereus* is able to grow on polymyxin, which selectively kills Gram-negative bacteria, but is unable to ferment mannitol. Therefore, *B. cereus* typically forms pink coloured colonies on MYP agar. Because of *B. cereus* phosphatidylcholinespecific phospholipase C (PC-Plc) and phosphatidylinositol-specific phospholipase C (PI-Plc) lecithinase activity the rough and dry colonies are surrounded by a zone of precipitation resulting from the hydrolysis of egg-yolk. Colony morphology of *sph* null mutants was compared to wild-type strains, other isogenic mutants and complemented mutant strains.

Table 4: Bacterial strains regularly used in this study

Strain	Description	Reference or source ^a
<i>E. coli</i>		
TOP10	general cloning strain	Invitrogen
DH10B	non-entomopathogenic strain used for insect infection experiments and cloning	Durfee <i>et al.</i> , 2008
INV110	methylase-deficient cloning strain	Invitrogen
JM83/pRK24	donor strain for conjugation; Tra ⁺ Mob ⁺ Amp ^r	Trieu-Cuot <i>et al.</i> , 1987
ColD	Colicin D producer for heterogramic conjugation	Institute Pasteur
ColE3	Colicin E3 producer for heterogramic conjugation	Institute Pasteur
<i>B. cereus</i>		
F4810/72 (AH187)	emetic reference strain	Turnbull <i>et al.</i> , 1979
NVH 0075-95	<i>nhe</i> reference strain	Lund and Granum, 1996
NVH 0230-00	diarrhoeal food poisoning (Norway)	NVH
NVH 0861-00	diarrhoeal food poisoning (Norway)	NVH
NVH 0391-98	<i>cytK</i> reference strain, diarrhoeal food poisoning (France)	Lund <i>et al.</i> , 2000
F837/76	<i>hbl</i> reference strain, isolate from surgical wound (UK)	Beecher and Macmillan, 1990
F3605/73	emetic food poisoning (UK)	F
F4430/73	diarrhoeal food poisoning (Belgium)	F
INRA I21	cooked food (France)	INRA
RIVM BC67	human faeces, emetic food poisoning	RIVM
WSBC 10030	pasteurized milk (Germany)	Prüss <i>et al.</i> , 1999;
WSBC 10035	pasteurized milk (Germany)	Prüss <i>et al.</i> , 1999;
var. <i>toyoi</i>	probiotic used in piglet feeding (Germany)	Toyocerin [®]
IP 5832	probiotic used in human (France)	Hoa <i>et al.</i> , 2000

^a source of strains: F, Central Public Health Laboratory Service, London, United Kingdom; INRA, Institut National de Recherche Agronomique, Avignon, France; NVH, The Norwegian School of Veterinary Science, Oslo, Norway; RIVM, Rijksinstituut voor Volksgezondheid en Milieu, Bilthoven, Netherlands; WSBC, Weihenstephan Bacillus cereus Collection, Weihenstephan, Germany

2.2.2 Preparation of bacterial supernatant

Bacterial supernatants were harvested for cytotoxicity tests. Therefore, 100 ml LB was inoculated with approximately 10^3 CFU/ml from an overnight pre-culture (14 - 16 hours) and cultures were incubated in 250 ml flasks with rotary shaking (150 rpm) at 37 °C for 8 hours. The cultures were centrifuged at 4400 rpm for 20 min (RT) and sterile supernatants were obtained after sterile filtration (0.2 μ m). When required, bacterial supernatants were concentrated 17 - to 30 - fold at 4 °C using Amicon® centrifugal filter devices (10 KDa, Millipore). For the identification of growth promoting *B. cereus* factors 500 ml RPMI1640 (Invitrogen) was inoculated with approximately 10^3 CFU/ml from an overnight pre-culture (14 - 16 hours) and cultures were incubated in 1 l flasks with rotary shaking (150 rpm) at 37 °C for 8 hours.

Sterile bacterial supernatant were harvested as described above. To concentrate the large volume of 1 l up to 12-fold a Minimate™ Tangential Flow Filtration Capsules (10 KDa, Pall) was used. Further 10-fold concentration was carried out using the Amicon® centrifugal filter devices (10 KDa, Millipore). Supernatants were frozen in liquid nitrogen and stored at -80 °C.

2.2.3 Production of *B. cereus* spores

As bacterial spore surfaces differ markedly from the surface structures of vegetative bacterial cells, it seems likely that spores exhibit divergent adhesion characteristics than vegetative cells. For this reason, spores of various *B. cereus* strains were produced and isolated. Pre-cultures in 3 ml LB medium were inoculated with a single colony from LB agar plates and incubated at 30 °C (150 rpm) over night. Fresh minimal sporulation medium (MSM) (pH 7.6) containing trace elements (1 M MgCl₂ x 6 H₂O, 1 M Ca(NO₃)₂ x 4 H₂O, 12.5 mM ZnCl₂, 2.5 mM CuCl₂, 2.5 mM CoCl₂ x 6 H₂O, 2.5 mM Na₂MoO₄ x 2 H₂O), 5 mM (NH₄)₂SO₄ and 0,066 mM MnSO₄ x H₂O as nitrogen and sulphur source, 1 mM FeSO₄ and 1 M maltose in bacto nutrient broth (Oxoid) was prepared immediately before spore preparation.

B. cereus precultures were diluted (1:200) in 50 ml MSM in 500 ml baffled shaking flasks and incubated at 24 °C shaking (150 rpm) for 2 – 3 days. Sporulation was monitored by phase contrast microscopy (Olympus). Once more than 80% of cells were free spores, spores were harvested (7 min, 4000 rpm at 4 °C), resuspended in precooled phosphate washing buffer (2 mM KH₂PO₄, 8 mM K₂HPO₄, pH 7.4) by vigorous vortexing. After 6 washing steps (7 min., 4000 rpm at 4 °C), the spore suspension was stored at 4 °C. Spores were washed three times and once on the two consecutive days. Thereafter, washing was carried out once a week at 4000 rpm until vegetative cells were gone completely followed by washing at 7000 rpm. Prior to experiments, spore suspensions were washed once. For the determination of the spore concentration, suspensions were heated to 80 °C for 15 min. to kill residual vegetative cells. Serial dilutions of heat-treated and untreated samples were plated on LB agar plates. After incubation at 30 °C over night CFU were counted.

2.3. Cell culture

The *Ptk6* null epithelial cell line (Ptk6) from mouse colonic mucosa was cultured in RPMI 1640 (Invitrogen) supplemented with 5% fetal bovine serum (FBS), 1% insulin (1 $\mu\text{g}/\text{ml}$) - transferrin-selenium (Invitrogen) and 10 U/ml recombinant murine INF- γ (Invitrogen) at 33 °C/5% CO² atmosphere as described (Whitehead et al. 2008). The human epithelial colonic adenocarcinoma cell line Caco-2 was cultured in DMEM/F-12 (Invitrogen) supplemented with 10% fetal bovine serum. Cells were splitted at 90 – 100% confluence.

Therefore, cells were washed once with PBS-EDTA, PBS-Trypsin-EDTA was added and incubated until cells detach from cell culture dish. Trypsin activity was blocked by adding medium containing FBS, cells were harvested by centrifugation at 1200 rpm for 4 min, resuspended in fresh culture medium and seeded on new culture dishes. For cytotoxicity testing 1×10^6 cells were seeded into 6-well plates and grown until confluence. Immunofluorescence staining was done with polarized Ptk6 monolayers on rat tail collagen coated coverslips (12 mm) or on transwell filters (12-mm well, 0.4 μm pore size, collagen coated polycarbonate membrane, Corning). Two days prior to the experiments, 5×10^5 cells were seeded onto coverslips or transwell filters containing 0.5 ml culture medium in the upper and 1.5 ml culture medium in the lower compartment. Culture medium was changed every second day.

2.4. Molecular biological methods

2.4.1 DNA isolation

B. cereus genomic DNA was isolated from liquid overnight cultures using the Puregene Yeast and Bacteria kit (Gentra) or the DNeasy[®] Blood & Tissue Kit (QIAGEN) according to the manufacturer's protocol. The protocols were slightly modified to isolate DNA of Gram⁺ bacteria. Therefore, bacterial pellets were incubated with enzymatic lysis buffer containing 20 mg/ml lysozyme prior to proteinase K digestion.

Plasmid isolation from *E. coli* strains was done with the QIAprep Spin Miniprep Kit (QIAGEN), the GeneElute[™] Plasmid Miniprep kit (Sigma-Aldrich) or the HiPure Plasmid Filter MidiPrep Kit (Invitrogen, Germany) for larger plasmid amounts. For subsequent experiments DNA concentrations of chromosomal DNA, plasmid preparation or PCR products were determined as the absorbance at 260 nm and 280 nm using a ND-1000 spectrophotometer (NanoDrop, Peqlab).

2.4.2 RNA isolation and reverse transcription

During *B. cereus* growth in liquid cultures at different OD₆₀₀ (representing different growth phases) 1 ml samples were taken, cells were harvested (13200 rpm, 1 min) and pellets were frozen immediately in liquid nitrogen. For RNA isolation cells were thawed on ice and broken up in a RiboLyser homogenizer (Hybaid) using 0.1 mm zirconia/silica-beads (Carl Roth GmbH). Total RNA was isolated with 1 ml TRIzol reagent (Invitrogen, Germany) and the remaining DNA was removed by treating 5 μg RNA with 10 U RQ1 DNase (Promega) for 45 min at 37 °C. RNA

was extracted with chloroform and precipitated with sodium acetate (pH 5.2) and ethanol. The resulting RNA pellet was washed twice with 70% ethanol, dried and resuspended in DEPC ddH₂O. RNA concentration was measured as absorbance at 260 nm and 280 nm at the ND-1000 spectrophotometer (NanoDrop, peqlab) and purity was analysed by agarose gel electrophoresis. To ensure complete DNA removal standard PCR with extracted RNA as template and 16S rDNA universal primers (Martineau *et al.* 1996) as well as the target primers was performed. For cDNA synthesis 1 µg total RNA was mixed with RNase/DNase-free H₂O and the qScript cDNA Supermix containing reaction buffer, qScript reverse transcriptase, random primers and oligo(dT) primers (Quanta). The mixture was incubated at 25 °C for 5 min, 30 min at 42 °C and 5 min at 85 °C. A PCR reaction using the RT reaction (1:10 diluted) as template and *inplc_for/in sph_rev* primers was used to check for cotranscription of *plc* and *sph* genes.

2.4.3 Standard PCR

For standard cloning PCR Platinum® *Taq* DNA Polymerase (Invitrogen), PCR Platinum® *Taq* DNA Polymerase High Fidelity (Invitrogen) or Thermo-Start *Taq* DNA Polymerase (ABgene) was used in 50 µl reactions. Test PCR reactions were performed with Platinum® *Taq* DNA Polymerase (Invitrogen). PCR reactions contained appropriate amounts of MgCl₂/MgSO₄, dNTPs, forward and reverse primer, 10-100 ng DNA template and 1 U DNA polymerase in the respective reaction buffer as specified below. The reaction started with a 15 min denaturation step at 95 °C, followed by 35 – 40 cycles of amplification (95 °C for 30 sec, primer annealing temperature for 45 sec, 72 °C for 1 min/kb) and ended with a final elongation step at 72 °C for 10 min. For colony PCR cell material of a bacterial colony was transferred into 50 µl ddH₂O, boiled at 100 °C for 10 min and pelleted (13200 rpm, 5 min). 2 µl of the supernatant was used as template for PCR reaction.

Thermo-Start Taq PCR

36.9 µl	ddH ₂ O				
5 µl	10 x buffer				
0.8 mM	each dNTP				
1.5 mM	MgCl ₂				
50 pmol	forward primer				
50 pmol	reverse primer				
1 U	Thermo-Start Taq DNA Polymerase				
		35 cycles	}		
				95 °C	15 min
				95 °C	30 sec
				Tm - 5 °C	45 sec
			72 °C	1 min/kb	
			72 °C	4 min	
			8/15 °C	∞	

<u>Platinum[®] Taq PCR</u>		<u>Programm:</u>	
36.8 μ l	ddH ₂ O	94 °C	5 min
5 μ l	10 x buffer	35 cycles {	94 °C 30 sec
0.2 mM	each dNTP		Tm - 5 °C 45 sec
2 mM	MgCl ₂		72 °C 1 min/kb
25 pmol	forward primer	72 °C	10 min
25 pmol	reverse primer	4 °C	∞
1 U	Platinum [®] Taq DNA Polymerase		

<u>Platinum[®] Taq High Fidelity PCR</u>		<u>Programm:</u>	
36.8 μ l	ddH ₂ O	94 °C	5 min
5 μ l	10 x buffer	35 cycles {	94 °C 30 sec
0.2 mM	each dNTP		Tm - 5 °C 45 sec
2 mM	MgSO ₄		72 °C 1 min/kb
25 pmol	forward primer	72 °C	10 min
25 pmol	reverse primer	4 °C	∞
1 U	Platinum [®] Taq DNA Polymerase High Fidelity		

2.4.4 DNA sequencing

After isolation and purification plasmids and PCR products were sequenced by GATC (Konstanz). PCR products were either subcloned into the pCR2.1 vector using the TOPO TA cloning kit (Invitrogen) or sequenced directly after purification.

2.4.5 Enzymatic DNA modifications/cloning

Prior to restriction digest, PCR amplicons were purified using the QIAquick PCR Purification Kit (Qiagen). Generally, 0.5 – 1 μ g plasmid DNA or PCR amplicon were digested by 1-5 U restriction enzyme (NEB or Fermentas) in specific reaction buffer under enzyme specific conditions. Final reaction volumes ranged from 10 - 40 μ l. To avoid plasmid re-ligation, digested vectors were treated with 45 U Antarctic phosphatase for 1 hr at 37 °C to dephosphorylate vector ends.

Subsequent agarose gel electrophoresis using 0.8 – 1.5% agarose gels in TAE-buffer (at 80 – 120 mV) confirmed successful DNA digest. DNA fragment size was estimated by comparison to 100 bp and 1 kb DNA marker (NEB). Target DNA fragments were excised from agarose gel, extracted using the QIAquick Gel Extraction Kit (Qiagen) and eluted in ddH₂O. The digested fragments were ligated with a molar ratio of vector and insert of 1:1 - 1:6 (up to 0.2 μ g total DNA) in a 20 μ l reaction volume of 5x ligation buffer and 0.2 U T4 DNA ligase (Invitrogen) at 14 °C overnight.

2.5. Genetic modification of bacteria

2.5.1 Transformation

Competent *E. coli* DH10B, TOP10 and INV110 were purchased from Invitrogen. Calcium chloride chemically competent *E. coli* JM83/pRK24 were prepared and transformed according to a standard protocol (Sambrook and Russell, 2001). In general, for heat shock transformation chemically competent cells were thawed on ice, 5 ng of vector DNA (1 μ l ligation reaction) were added followed by incubation for 30 min on ice. Subsequent heat shock was carried out at 42 °C for 30 – 45 sec and cells were placed on ice immediately. After addition of 250 μ l SOC medium, cells were incubated shaking at 37 °C for 1 hr. Recovered cells were plated on LB agar plates with the appropriate antibiotics and colonies were visible after 24 h. *E. coli* DH10B/TOP10 were used for standard transformation of ligation reactions. For high transformation efficiency in *B. cereus* plasmids were transformed into the non-methylating *E. coli* strain INV110, reisolated and desalted prior to electroporation into *B. cereus*. To prepare electro-competent *B. cereus* cells, *B. cereus* was grown in LB medium containing 2% glycine until an OD₆₀₀ of 0.4 – 0.7. Cells were harvested (3500 g, 10 min, 4 °C) and consecutively washed in ddH₂O supplemented with 2.5, 5 and 10% glycerol. After the third washing step, cells were resuspended in ddH₂O containing 10% glycerol and frozen in liquid nitrogen.

Electroporation of competent *B. cereus* was performed in a 0.4 cm cuvette using the BioRad Gene Pulser. Therefore, 1 μ g of DNA was added to 100 μ l of competent cells and pulsed (2.0 kV, 25 μ F, 200 W, 4.6 - 4.8 ms). Immediately after pulsing, the cells were diluted in LB medium, incubated at 30 °C for 2 – 3 h and plated on LB agar plates containing appropriate antibiotics. Colonies were visible after 24 – 48 hours at 30 °C.

2.5.2 Heterogramic conjugation

Alternatively to eletroporation, recombinant plasmid can be transferred from the cloning host *E. coli* to the Gram⁺ recipient *B. cereus* by conjugation. For this purpose, the *E. coli* strain JM83/pRK24 harbouring the DNA mobilization IncP plasmid pRK24 (Thomas and Smith 1987) was transformed with the target construct integrated into the conjugative suicide vector pAT113 (Trieu-Cuot *et al.* 1991). *E. coli* (50 ml) and *B. cereus* (5 ml) cultures were grown in parallel in LB medium until OD₆₀₀ 0.5. Then, *E. coli* cells were harvested, washed once in LB medium and mixed with *B. cereus* culture for the mating process. After cell pelleting, the bacterial mixture was resuspended in 1 ml LB medium, applied to two Millipore HA 0.45 μ m filter membranes on a LB agar plate and incubated at 37 °C overnight. Bacterial cells were scraped off the filters, resuspended in 3 ml medium containing the bacteriocins colicin D and E and plated onto LB agar plates with polymyxin B and appropriate additional antibiotics to select for *B. cereus* transconjugants while eliminating *E. coli*. Tranconjugants could be detected after 24 - 48 h at 30 °C.

2.5.3 Mutagenesis of *B. cereus*

Unfortunately, there is no genome sequence of *B. cereus* NVH 0075-95 available so far. Therefore, target gene sequences were searched using the annotated genome sequence of *B. cereus* F4810/72 (NC_011658). Target gene sequences of *B. cereus* F4810/72 were blasted and aligned to the gene sequences found from *B. cereus* E33L (NC_006274), AH820 (NC_011773), Q1 (NC_011969) and ATCC14579 (NC_004722) using ClustalW2 on the EMBL-EBI server (<http://www.ebi.ac.uk/Tools/msa/clustalw2/>). Conserved sequence regions were used for oligonucleotide primer design. *InhA2* and *inhA3* were identified by alignment of gene sequences from the *B. cereus* type strain ATCC 14579 (NC_004722) (Guillemet *et al.* 2010) with the genome sequence of *B. cereus* F4810/72. Detailed information about the vectors and oligonucleotides used for mutagenesis is provided in Table A2 and A3 in the Appendix (7.2 and 7.3). All generated genetically modified *B. cereus* strains are listed in Table 5.

2.5.3.1 Construction of *B. cereus* strain expressing GFP

A *B. cereus* F4810/72 $\Delta plcR$ mutant constitutively expressing *gfp* was generated to enable the detection of vegetative bacterial cell directly via fluorescence microscopy. Therefore, the gram-negative/gram-positive shuttle vector pHT315 (Arantes and Lereclus 1991) was used harbouring the *gfp* gene under the control of the *aph3A* gene promoter. The pHT315/*gfp*/*Paph3A* (Arantes and Lereclus 1991) construct was electroporated into electrocompetent *B. cereus* F4810/72 $\Delta plcR$ cells and positive mutants were selected on LB agar plates containing erythromycin. The resulting mutant strain was named F4810/72 $\Delta plcR$ pHT315/*gfp*/*Paph3A*.

2.5.3.2 Construction of *B. cereus* strain overexpressing SMase

For SMase protein overexpression the shuttle vector pAD123/*PcspA*, harbouring the cold shock inducible promoter of *cspA*, was used. The promoterless *sph* gene was amplified by PCR using the primers *sph_Sac_F*/*sph_Hind_R* (Table A3, Appendix 7.3.). Restriction digest of the product and ligation between the *SacI* and *HindIII* site of pAD/*PcspA* resulted in pAD/*sph*/*PcspA*. After isolation from non-methylating *E. coli* INV110, the plasmid was electroporated into *B. cereus* F4810/72 $\Delta plcR$, giving *B. cereus* F4810/72 $\Delta plcR$ pAD/*sph*/*PcspA*.

To overexpress *sph* under the control of the cold inducible *cspA* promoter the strain was incubated in LB media at 15 °C for 2 – 4 days. As a control the parental strain *B. cereus* F4810/72 $\Delta plcR$ and the wild type strain *B. cereus* F4810/72 were grown in parallel under same conditions.

For the overexpression of *InhA2*, the shuttle vector pWH1520 (a kind gift of W. Hillen, University of Erlangen) was used containing a xylose inducible promoter (Rygus and Hillen, 1991). The *InhA2* overexpressing *B. cereus* strains *B. cereus* F4810/72 $\Delta plcR$ pWH $inhA2$ and *B. cereus* F4810/72 pWH $inhA2$ were constructed and kindly provided by Elrike Frenzel. Therefore, the promoterless *inhA2* gene was amplified from *B. cereus* F4810/72 genomic DNA by PCR using the primers *inhA2_Sma_F2*/*inhA2_Kpn_R* (Table A3, Appendix 7.3.). pWH1520 was digested

with *SpeI* and *KpnI* and the 5' overhang was filled up using Klenow fragment. Restriction digest of the PCR product with *SmaI/KpnI* and ligation between the blunt end and the *KpnI* site of pWH1520 resulted in pWHinhA2. After isolation from non-methylating *E. coli* INV110, the plasmid was electroporated into *B. cereus* F4810/72 $\Delta plcR$ and *B. cereus* F4810/72, giving rise to *B. cereus* F4810/72 $\Delta plcR$ pWHinhA2 and *B. cereus* F4810/72 pWHinhA2, respectively. *InhA2* expression was induced by addition of 0.1% xylose in LB media or RPMI 1640.

Table 5: *B. cereus* mutant strains generated or used in this study

Strain	Description	Reference or source
<i>B. cereus</i>		
F4810/72 $\Delta plcR$	<i>plcR</i> deletion mutant of F4810/72; <i>Spc</i> ^r	Lücking <i>et al.</i> , 2009
F4810/72 $\Delta plcR$ pAD/ <i>sph</i> / <i>PcspA</i>	F4810/72 $\Delta plcR$ harbouring pAD/ <i>sph</i> / <i>PcspA</i> ; <i>Spc</i> ^r <i>Cm</i> ^r	This study
F4810/72 $\Delta plcR$ pHT315/ <i>gfp</i> / <i>Paph3A</i>	F4810/72 $\Delta plcR$ harbouring pHT315/ <i>gfp</i> / <i>Paph3A</i> ; <i>Spc</i> ^r <i>Erm</i> ^r	This study
F4810/72 Δsph	<i>sph</i> deletion mutant of F4810/72; <i>Cm</i> ^r	This study
NVH 0075-95 $\Delta nheBC$ (NVH 1173)	<i>nheB</i> truncation and <i>nheC</i> deletion mutant of NVH 0075-95; <i>Spc</i> ^r	Fagerlund <i>et al.</i> , 2008
NVH 0075-95 Δsph	<i>sph</i> deletion mutant of NVH 0075-95; <i>Cm</i> ^r	This study
NVH 0075-95 $\Delta nheBC\Delta sph$	<i>nheB</i> truncation, <i>nheC</i> deletion and <i>sph</i> deletion mutant of NVH 0075-95; <i>Spc</i> ^r <i>Cm</i> ^r	This study
F4810/72 Δsph com <i>Pplc</i>	F4810/72 Δsph complemented with pAD/ <i>sph</i> / <i>Pplc</i> /tet; <i>Cm</i> ^r Tet ^r	This study
F4810/72 Δsph com <i>Psph</i>	F4810/72 Δsph complemented with pAD/ <i>sph</i> / <i>Psph</i> /tet; <i>Cm</i> ^r Tet ^r	This study
NVH 0075-95 $\Delta nheBC\Delta sph$ com <i>Pplc</i>	NVH 0075-95 $\Delta nheBC\Delta sph$ complemented with pAD/ <i>sph</i> / <i>Pplc</i> /tet; <i>Cm</i> ^r <i>Spc</i> ^r Tet ^r	This study
NVH 0075-95 $\Delta nheBC\Delta sph$ com <i>Psph</i>	NVH 0075-95 $\Delta nheBC\Delta sph$ complemented with pAD/ <i>sph</i> / <i>Psph</i> /tet; <i>Cm</i> ^r <i>Spc</i> ^r Tet ^r	This study
F4810/72 pWHinhA2	F4810/72 harbouring pWHinhA2; Tet ^r	Frenzel, unpublished
F4810/72 $\Delta plcR$ pWHinhA2	F4810/72 $\Delta plcR$ harbouring pWHinhA2; <i>Spc</i> ^r Tet ^r	Frenzel, unpublished

2.5.3.3 Construction of *B. cereus* deletion mutants

Construction of *sph* null mutants was done basically as described previously (Lücking *et al.* 2009). A TOPO pCR 2.1 vector construct was cloned which carried the chloramphenicol resistance cassette flanked by 1.0 – 1.5 kb *B. cereus* DNA fragments, representing the upstream and downstream sequences of the *sph* (*sphingomyelinase*) gene. A chloramphenicol resistance gene cassette (Cm) was amplified by PCR using the primer pair Cm_F/Cm_R_Not and the pAD123 vector as template. The Cm cassette was inserted into the *EcoRI/NotI* restriction site of the TOPO pCR 2.1 vector giving rise to pCR 2.1/cm. Subsequently, 1.0 – 1.5 kb flanking regions of the *sph* gene were amplified by PCR using the primers *sph_up_Sac_F/sph_up_Spe_R* and *sph_down_Xho_F/sph_down_Xba_R* listed in Table A2 (Appendix 7.2). Restriction digest of the PCR products and ligation of the upstream fragment between the *SacI/SpeI* and the downstream fragment between the *XhoI/XbaI* sites of TOPO pCR 2.1/cm resulted in the vector pCR 2.1 Δ *sph/cm*. Correct sequence of inserts was controlled by PCR, restriction analysis and sequencing. After excision of the *sph* upstream/cm/downstream region from pCR 2.1 Δ *sph/cm* using *SacI* and *XbaI*, the construct was inserted into the multiple cloning site of the conjugative suicide vector pAT113, giving rise to pAT113 Δ *sph/cm*. The conjugative plasmid pAT113 Δ *sph/cm* was transformed into the conjugation donor strain *E. coli* JM83/pRK24. This strain was used to transfer the plasmid into *B. cereus* F4810/72, *B. cereus* NVH 0075-95 and *B. cereus* NVH 0075-95 Δ *nheBC* carrying out the heterogramic conjugation procedure as described before (see 2.13.). All plasmids constructed and used in this study are listed in Table A2 in the Appendix 7.2.

Transconjugants were screened for chloramphenicol resistance and erythromycin sensitivity. PCR and sequencing confirmed gene deletion by integration of the resistance cassette resulting from a double crossover recombination event. The *sph* null single and double mutants were named *B. cereus* F4810/72 Δ *sph*, NVH 0075-95 Δ *sph* and NVH 0075-95 Δ *nheBC* Δ *sph*, respectively.

2.5.3.4 Complementation of deletion mutants

To complement the *sph* deletion mutants, plasmids were constructed using the pAD/*sph*/*PcspA* backbone and two different promoter regions. The tetracycline resistance cassette was PCR amplified from the shuttle vector pWH1520 (a kind gift of W. Hillen, University of Erlangen) using the primer pair TetR_for_Nsil and TetR_rev_Nsil and introduced into the *Nsil* restriction site of the *sph* expression vector pAD/*sph*/*PcspA*. The resulting plasmid was named pAD/*sph*/*PcspA/tet*. PCR amplification of the genomic DNA of *B. cereus* using the primer pair Pplc_for/Pplc_rev resulted in a 538 bp fragment of the putative promoter region upstream of the *plc-sph* operon (see Figure 17, Pplc*). This PCR product was cloned into the *EcoRI-SacI* restriction site of the shuttle vector pAD/*sph*/*PcspA/tet*, releasing *PcspA* and yielding pAD/*sph*/*Pplc/tet*. Additionally, the *sph* gene including a 499 bp upstream region (putative dysfunctional promoter region P*sph** directly in front of the *sph* start codon, see Fig. 17) was PCR amplified using the primer pair Psph1_for/*sph*_Hind_R. After restriction digest the PCR

product was inserted into the *EcoRI-HindIII* site of pAD/*sph/PcspA*/tet giving rise to a plasmid named pAD/*sph/Psph*/tet while releasing *sph/PcspA*. These two plasmids were electroporated into the *sph* single and double mutant strains as described previously (Ehling-Schulz *et al.* 2005). PCR analysis with Tet^r-specific primers confirmed the introduction of the plasmids into the *sph* deletion mutants giving rise to the complemented strains *B. cereus* F4810/72 Δ *sph* comP*plc*, F4810/72 Δ *sph* comP*spH*, *B. cereus* NVH 0075-95 Δ *nheBC* Δ *sph* comP*plc* and NVH 0075-95 Δ *nheBC* Δ *sph* comP*spH*.

2.6. Biochemical methods

2.6.1 Protein analysis

2.6.1.1 Protein separation using gel filtration

Concentrated bacterial supernatants (see Ch. 2.2.2) of *B. cereus* NVH 0075-95 Δ *nheBC* and *B. cereus* F4810/72 were dialysed against PBS (pH 7.4) and total protein concentration was determined using a BCA protein assay (Thermo Scientific Pierce) with BSA as a standard. About 1 – 2 mg of total bacterial secreted proteins were fractionated according to their molecular weight by gel filtration using a Superdex-75 10/300 GL column in a ÄKTA Purifier system (GE) with a flow rate of 0.2 ml/min in PBS (pH 7.4). Proteins were detected by their absorbance at 280 nm.

2.6.1.2 Identification of a cytotoxic secreted *B. cereus* protein

Gel filtration fractions of *B. cereus* NVH 0075-95 Δ *nheBC* supernatant were tested for their cytotoxic activity in Ptk6 cell monolayers. To identify candidate proteins within the active fractions, samples were analysed by 12% SDS-PAGE under reducing conditions according to Laemmli (Laemmli 1970), followed by Coomassie staining using IRDye® Blue Protein Stain (LI-COR) and silver staining modified from Blum *et al.* (Blum *et al.* 1987). Two silver stained protein bands were sent to NextGen Sciences (AnnArbor, USA) to be analysed by LC/MS/MS on a ThermoFisher LTQ Orbitrap XL mass spectrometer after tryptic digestion of the proteins. Protein identifications were accepted according to NextGen Science's guidelines (greater than 90,0% probability, at least 2 identified peptides). Probabilities of the protein hits were assigned by the Protein Prophet algorithm (Nesvizhskii *et al.* 2003).

2.6.1.3 Identification of a growth promoting secreted *B. cereus* protein

Gel filtration fractions of *B. cereus* F4810/72 supernatant were tested for their growth promoting activity on *B. cereus* F4810/72 Δ *plcR*. Therefore, 0.5 ml of each fraction in round bottom tubes were inoculated 1:10000 with *B. cereus* F4810/72 Δ *plcR* from an overnight pre-culture (14 - 16 hours) and incubated with rotary shaking (150 rpm) at 37 °C for 8 hours. Bacterial growth was analysed by plating serial dilutions on LB agar plates and counting CFUs. Inoculated *B. cereus* F4810/72 wild-type supernatant and PBS (pH 7.4) served as a positive and negative control, respectively. Fractions with the highest growth of *B. cereus* F4810/72 Δ *plcR* were analysed by

14% SDS-PAGE under reducing conditions according to Laemmli (Laemmli 1970), followed by silver staining modified from Blum et al. (Blum *et al.* 1987). Three silver stained candidate protein bands were sent to Proteome Factory AG (Berlin, Germany) for protein identification by nanoLC-ESI-MS/MS.

2.6.1.4 SDS-PAGE and Western Blot

Bacterial pellets and supernatant at different growth phases were used for protein separation and detection. For SMase detection via immunoblotting concentrated bacterial supernatants were used. Protein samples were boiled in SDS sample buffer containing dithiothreitol (final concentration, 50 mM) for 10 min and were analysed by 14% SDS-PAGE under reducing conditions according to Laemmli (Laemmli 1970). For detection of total protein SDS gels were Coomassie stained using IRDye® Blue Protein Stain (LI-COR) or silver stained according to the protocol modified from Blum et al. (Blum *et al.* 1987). SMase protein was detected by Western blot. For this purpose, proteins were transferred to an Immobilon-FL 0.45-m polyvinylidene fluoride membrane (Millipore). After blocking the proteins with LI-COR blocking buffer (LI-COR) in PBS (1:1) for 1 h at room temperature, staining with primary antibody (1:1000) and fluorescence-labelled secondary antibody (1:30,000), diluted in T-PBS (PBS + 0.1% Tween 20), was carried out for 1 h at room temperature each. The membranes were scanned with the Odyssey infrared imaging system (LI-COR) at 680 nm wavelength. The primary antibody against *B. cereus* SMase (rabbit polyclonal) was a kind gift of Dr. Masataka Oda (Oda *et al.* 2010). Alexa-Fluor680 goat anti-rabbit was purchased from Invitrogen.

2.6.2 Enzymatic assays

2.6.2.1 SMase activity assay

The activity of *B. cereus* sphingomyelinase was measured using an Amplex® Red Sphingomyelinase Assay Kit (Molecular Probes) basically as described previously (Nishiwaki *et al.* 2004). Concentrated bacterial supernatants were dialysed against 100 mM Tris/HCl buffer (pH 7.5). For the assay, 5 μ l 100 mM Tris/HCl buffer (pH 7.5) containing 2% Triton X-100 and different concentrations of the sphingomyelin substrate (200, 500, 1000, 2000, 3000 and 4000 μ M) were added into each well of a 96-well microplate (μ Clear® 655096, Greiner), followed by 45 μ l 100 mM Tris/HCl buffer (pH 7.5) containing 100 μ M Amplex red reagent, 10 mM MgCl₂, 2 U/ml horseradish peroxidase, 0.2 U/ml choline oxidase and 8 U/ml alkaline phosphatase. To start the enzymatic reaction 50 μ l of concentrated supernatant was added and the reaction mixture was incubated for 30 min at 37 °C. Using a microplate reader (FLUOstar OPTIMA, BMG Labtech) fluorescence was measured at 590 nm, with excitation at 560 nm. The fluorescence intensity data was corrected for background fluorescence and plotted using Microsoft Excel. SMase activity with 200 μ M sphingomyelin substrate is expressed as relative SMase activity compared to lowest sphingomyelin concentration (10 μ M).

2.6.2.2 Caspase-3 activity assay

To detect caspase-3 activity in cells undergoing apoptosis, Ptk6 cell monolayers were treated with bacterial supernatant, 1 U/ml SMase (S9396, Sigma-Aldrich), mock or 0.1 μ M staurosporine as a positive control at 37 °C. After 24 hours, cells were harvested, washed once with 1x DPBS (Invitrogen) and lysed in 50 μ l cell lysis buffer (see 2.2) for 5 min on ice. Centrifugation (10.000 x g, 10 min, 4 °C) released the total cell proteins in the supernatant. In the caspase-3 activity assay, 2 x 19 μ l sample were used for duplicates. To 80 μ l of prewarmed assay buffer (see 2.2) 19 μ l of protein sample was added into each well of a 96-well plate (Microtest™ 96, BD). Then the assay was started by adding 1 μ l of caspase-3 substrate (200 mM, Calbiochem) and measuring absorbance at 405 nm in a microplate reader (MultiskanEX, Thermo Labsystems) immediately. The plate was kept in the dark at 37 °C and absorbance was measured every 30 min. Absorbance at 405 nm was corrected against an assay buffer control and normalized to the sample protein concentration detected using a BCA protein assay (Thermo Scientific Pierce) with BSA as standard. Caspase-3 activity represented by absorbance at 405 nm was plotted over time using Microsoft Excel.

2.7. Bacterial adhesion

The adhesion capacity of vegetative cells and spores of different *B. cereus* strains to intestinal epithelial cells (Ptk6, Caco-2) was tested.

For counting of attached bacteria/spores, intestinal epithelial cells were seeded in 6-well plates (1 x 10⁶ cell/well) and grown until confluence (2 – 3 days) resulting in approximately 2 x 10⁶ cells/well. Epithelial cell monolayers were washed twice with DPBS and treated with 3 ml cell culture medium containing 10⁷ (MOI 10) to 10⁸ spores (MOI 100) or 10⁶ (MOI 1) to 10⁷ (MOI 10) exponentially growing vegetative *B. cereus* cells. To determine absolute multiplicity of infection retrospectively, a 100 μ l sample was taken from the cell supernatant, was serially diluted and plated on LB agar. Epithelial cells were incubated at 37 °C for 30 min. and 1 hr, respectively.

After infection, epithelial cells were washed three times with DPBS to remove unspecifically adhering *B. cereus*. Epithelial cells and attaching bacteria or spores were scratched off the cell culture plate into 1 ml ddH₂O using a cell scraper. To determine the number of adherent spores or vegetative bacteria, serial dilutions of cell-bacteria suspensions were plated on LB agar plates and incubated at 37 °C. Bacterial colonies were counted and numbers of adherent spores or vegetative bacteria were calculated by extrapolation.

To visualize adherent *B. cereus* cells, Ptk6 cells were seeded onto rat-tail collagen coated coverslips or on transwell filters (12-mm well, 0.4 μ m pore size, collagen coated polycarbonate membrane, Corning) two days prior to infection experiments. For subconfluent Ptk6 cells 0.5 x 10⁵ cells/well and for confluent polarized monolayer 5 x 10⁵ cells/well were seeded resulting in approximately 1 x 10⁵ and 1 x 10⁶ cells at the time of infection, respectively. Infection with exponentially growing *B. cereus* was carried out as described above using a MOI between 1-100. After 0.5 to 4 h infection epithelial cells were washed twice with DPBS, fixed with 2%

paraformaldehyde in 100 mM sodium phosphate buffer, pH 7.4 and strained for adhering bacteria according to the protocol depicted in Ch. 2.10.2.

2.8. Cytotoxicity assay (Ampel assay)

Ptk6 cell monolayers (6-well plates; 2×10^6 cells/well) were washed twice with DPBS and treated with either vegetative bacteria at an MOI of 1 (2×10^6 bacteria) or sterile bacterial supernatant at 37 °C/5% CO² atmosphere. Cell morphology changes and cell detachment was monitored over time using light microscopy.

2.9. Detection of dead epithelial cells by flow cytometric analysis

For flow cytometric analysis, Ptk6 cells were treated with bacterial supernatant diluted in RPMI 1640 for 4 h. Cells were trypsinized and approximately 1×10^6 cells per condition were stained according to the manufacturer's protocol using the Annexin V Apoptosis Detection Kit APC (eBioscience). Propidium iodide was added to detect the amount of total dead cells. Cells were assayed using a Gallios flow cytometer (Beckman Coulter). Resulting data were analysed with FlowJo flow cytometry analysis software (Version 8.8.4).

2.10. Immunofluorescence staining

2.10.1 Anti-B. cereus antibody production

Since there is no anti-*B. cereus* antibody commercially available that could be used for immunofluorescence staining of *B. cereus*, vegetative *B. cereus* cells were prepared and inactivated for polyclonal antibody production in chicken. *B. cereus* NVH 0230-00 was used for antibody production as this strain presents a typical diarrhoea-associated strain harbouring all genes for Nhe, Hbl and CytK. For the production of a sufficient amount of pure vegetative cells, 100 ml LB medium was supplemented with 2% glucose to repress spore formation and inoculated 1:25 from an over night preculture of *B. cereus* NVH 0230-00. The liquid culture was grown at 37 °C, 150 rpm for 24 h. *B. cereus* cells were harvested by centrifugation (7 min., 4000 rpm, RT) and resuspended in 12.5 ml of 2% glutaraldehyde to fix and inactivate bacterial cells. After 2 h at room temperature glutaraldehyde was removed and cells were washed three times in PBS (pH 7.4) to completely remove fixation agent. To test for the complete inactivation of *B. cereus* cells, a small volume of the bacterial suspension was plated onto LB agar and incubated at 37 °C over night. Finally, inactivated *B. cereus* cells were harvested (3 min., 13200 rpm, RT) and pellet was dried using the Concentrator 5301 system (Eppendorf). Bacterial pellets were sent to Aves Labs, Inc. (Tigard, USA) for immunisation of two hens. Chickens were injected with a mixture (1:1) of antigen solution and adjuvant. Immune anti-*B. cereus* antibodies were collected from eggs after the fourth injection. To reduce unspecific binding of the polyclonal antibody to epithelial cells, the antibody solution was preincubated with Ptk6 cells prior to application for fluorescence staining.

2.10.2 Visualization of adherent *B. cereus*

After fixation with 2% paraformaldehyde in 100 mM sodium phosphate buffer, pH 7.4, *B. cereus* infected cells were washed three times with PBS and filters/coverlips were transferred into a humidified chamber. Cells were permeabilized in PBS containing 3% bovine serum albumin, 1% saponin, 0.1% Triton X-100 for 10 min at room temperature and stained with primary antibodies (anti-*B. cereus*, anti-ZO-1) in PBS (3% bovine serum albumin, 1% saponin). After 1 – 4 h incubation at room temperature, cells were washed three times with PBS (3% bovine serum albumin, 1% saponin) and incubated with secondary antibodies (1:200; Alexa Fluor 594/647-coupled phalloidin, Alexa Fluor 488-coupled goat anti-chicken IgG, DAPI; Invitrogen) in PBS (3% bovine serum albumin, 1% saponin) for 1 h, room temperature in the dark. Prior to mounting cells were washed three times with PBS containing 3% bovine serum albumin and 1% saponin and once with pure PBS. Coverlips and filter membranes were mounted onto microscope glass slides using VECTASHIELD® Mounting Medium with DAPI (Vector Lab., Inc.). The samples were imaged with a confocal microscope (Leica SP5), and z-stacks were projected onto three-dimensional reconstructions by using Volocity 4.1 software (PerkinElmer Life Sciences). The figures were assembled with Photoshop CS (Adobe Systems). Detailed information of all antibodies used in this study is provided in Table 3 (Ch. 2.1.2).

2.10.3 Detection of apoptosis induction in Ptk6 cells

For detection of apoptosis induction via confocal immunofluorescence microscopy, cells were stained using Alexa Fluor 594-coupled annexinV, Alexa Fluor 647-coupled phalloidin, SYTOX® Green and DAPI (Invitrogen). Ptk6 cell monolayers on collagen coated coverslips or filters were treated with bacterial supernatants diluted in RPMI 1640 (Invitrogen) and 0.1 μ M staurosporine as a positive control. After incubation for 3 h at 37 °C, cells were washed once with ice cold DPBS and incubated in annexinV binding buffer (10 mM HEPES, 140 mM NaCl, 2.5 mM CaCl₂, pH 7.4) containing Alexa Fluor 594-coupled annexinV (1:20) and SYTOX® Green (1:1000) for 15 min at room temperature. Cells were washed three times with annexinV binding buffer, fixed with 2% paraformaldehyde in 100 mM sodium phosphate buffer, pH 7.4, and were permeabilized in PBS (3% bovine serum albumin, 1% saponin, 0.1% Triton X-100) for 10 min at room temperature. Then cells were stained with phalloidin and DAPI. The samples were imaged with a confocal microscope (Leica SP5), and z-stacks were projected onto three-dimensional reconstructions by using Volocity 4.1 software (PerkinElmer Life Sciences). For each condition three different representative microscopic fields (including about 600 cells) were imaged and annexinV⁺/SYTOX® Green⁻ as well as total cell numbers were counted using ImageJ software.

2.11. Analysis of differential protein expression - *B. cereus* wt and Δ plcR

2.11.1 Protein sample preparation for 2-D DIGE analysis

Ptk6 conditioned RPMI medium was obtained by washing confluent Ptk6 cells twice with DPBS followed by incubation in 15 cm cell culture dishes with unsupplemented RPMI medium (without

FBS, Interferon gamma and Insulin-Transferrin-Selenium A mix) for 24 h. Ptk6 supernatant (conditioned RPMI medium) was harvested and sterile filtrated (0.2 μm) directly before the experiment. To detect differentially expressed proteins in *B. cereus wild-type* and ΔplcR when incubated in unsupplemented RPMI medium compared to Ptk6 conditioned RPMI medium, 100 ml LB medium was inoculated 1:100000 from an over night preculture of *B. cereus* F4810/72 *wild-type* and ΔplcR and bacteria were grown until mid-exponential growth phase at 37 °C and 170 rpm. Identical growth of *wild-type* and mutant was assured by determining CFUs/ml. After 6 h bacterial cells were harvested by centrifugation (4000 rpm, 10 min, 4 °C), washed once with PBS and resuspended either in 100 ml unsupplemented RPMI medium or in Ptk6 conditioned medium. For protein expression bacteria were incubated in shaking flasks for 2 h at 37 °C, 170 rpm. Finally, bacterial cells were harvested at 6000 rpm (15 min, room temperature), pellets were washed twice with 10 mM TrisHCl buffer (1 mM EDTA, 1 mM Pefabloc; pH 7.5) at 4 °C and stored at -80 °C. After sterile filtration (0.2 μm) of the supernatant secreted proteins (*B. cereus* secretome) were precipitated using ice cold trichloro acetic acid (10% w/v) at 4 °C over night. Proteins were harvested (10000 rpm, 1 h at 4 °C) and washed four times with acetone containing 0.2% DTT (13200 rpm, 15 min at 4 °C). Protein pellets were dried over night at 4 °C before they were resuspended in 200 μl DIGE lysis buffer (see 2.2) and stored at -80 °C until use. Ptk6 conditioned RPMI medium only was treated in parallel and served as a control (condition C).

To extract the cytosolic protein fraction the washed bacterial cell pellet was directly dissolved in DIGE lysis buffer and cells were disrupted by three passages through a chilled French Press at 140 mPa. Repeated centrifugation at 15000 rpm for 30 min at 4 °C separated the soluble protein extract from remaining cell debris. The resulting supernatant contained the soluble cytosolic protein fraction. After determination of total protein concentration of secreted and cytosolic protein fractions using 2-D Quant kit (GE Healthcare) aliquot samples were stored at -80 °C until further analysis.

The protein samples comprised three biological replicates per treatment (unsupplemented RPMI medium or Ptk6 conditioned RPMI medium) and genotype (*B. cereus* F4810/72 *wild-type* vs. ΔplcR).

2.11.2 Two-dimensional gel electrophoresis (2-D DIGE)

Protein extracts were analysed by Dr. Tom Grunert (Institute of Functional Microbiology, Department of Pathobiology, University of Veterinary Medicine Vienna, 1210 Vienna, Austria) using fluorescence two-dimensional (2-D) difference gel electrophoresis (DIGE) and MALDI-TOF/MS(MS). Protein identification was done conjointly by Viktoria Doll and Dr. Tom Grunert at the Proteomic Core Facility of the University of Veterinary Medicine. DIGE labelling, 2-D electrophoretic separation and statistical analysis were carried out as described previously (Radwan *et al.* 2008).

In brief, protein samples were labelled with CyDye DIGE™ fluorescent dyes (GE Healthcare Life Sciences) according to the manufacturing's protocol. The experiment compared four different

conditions namely: A: *B. cereus* F4810/72 $\Delta plcR$ incubated in unsupplemented RPMI medium, B: *B. cereus* F4810/72 $\Delta plcR$ incubated in Ptk6 conditioned medium, D: *B. cereus* F4810/72 *wild-type* incubated in unsupplemented RPMI medium and E: *B. cereus* F4810/72 *wild-type* incubated in Ptk6 conditioned medium. Comparisons of A/B and D/E together represent the treatment effect (unsuppl. RPMI medium vs. Ptk6 conditioned medium), while comparing A/D and B/E should show the genotypic differences (*wild-type* vs. $\Delta plcR$). The experiment included three biological replicates per condition (A, B, D, E), resulting in 12 samples of secreted proteins and 12 samples of cytosolic proteins. Further analysis however focussed on the cytosolic proteome.

Table 6 describes the labelling scheme. For an internal standard, equimolar amounts of all 12 samples were pooled and 25 μg of the mixture was incubated with 200 pmol Cy2 dye for 30 min kept in the dark on ice. The samples were prepared by incubating 25 μg of protein with 200 pmol Cy3 or Cy5.

Table 6: Labelling scheme for 2-D DIGE experiments^a

Gel #	Cy2 (Internal standard)	Cy3	Cy5
1	Equimolar mix (A1-3; B1-3; D1-3; E1-3)	B2	D1
2	Equimolar mix (A1-3; B1-3; D1-3; E1-3)	A1	B3
3	Equimolar mix (A1-3; B1-3; D1-3; E1-3)	D3	E1
4	Equimolar mix (A1-3; B1-3; D1-3; E1-3)	D2	A3
5	Equimolar mix (A1-3; B1-3; D1-3; E1-3)	E3	A2
6	Equimolar mix (A1-3; B1-3; D1-3; E1-3)	E2	B1

^aEach gel was loaded with a total of 75 μg labelled protein comprising 1) 25 μg of the Cy2 labelled internal standard (containing an equimolar protein mix obtained from three biological replicates of *B. cereus* F4810/72 $\Delta plcR$ in unsupplemented RPMI medium (samples A1-3), $\Delta plcR$ in Ptk6 conditioned medium (samples B1-3), *wild-type* in unsupplemented RPMI medium (samples D1-3), and *wild-type* in Ptk6 conditioned medium (samples E1-3) and 2) 25 μg of each sample-specific protein labelled with Cy3 or Cy5. Direct comparison of the protein patterns of two conditions was possible after co-separation and dual-channel analysis.

In the first dimension proteins were separated on 18 cm IPG Dry strips with a linear pH gradient of pH 4-7 using the IPGphor III system (all GE Healthcare). On each gel strip, a total of 75 μg of protein (25 μg internal standard mix and 25 μg of each of the two samples to be compared (Cy3/Cy5)) were co-separated.

For the second dimension isocratic SDS-PAGE (25.5 x 20.5 cm gels, 10% T) according to Laemmli (Laemmli 1970) was performed using an Ettan Dalt Six electrophoresis chamber (GE Healthcare). The fluorescence gel images were acquired on a Typhoon 9400 scanner (GE Healthcare). The DeCyder software (Version 5.02, GE Healthcare) was used for protein spot detection, spot matching, quantification and normalization. Additionally, to avoid false positives, image analysis including spot matching and spot quality were checked manually for all proteins of interest. To obtain a master gel automated matching of all spots per gel was carried out and

the six gel images of each condition were fused for spot detection. Thereafter, spot mask was overlaid on the individual gel scans (Cy2, Cy3, or Cy5) to compute individual spot volume ratios. The volume of a specific spot was calculated in relation to the volume of the corresponding pooled Cy2 protein spot (internal standard). As the main interest was to detect host (Ptk6)-induced differences in protein expression of $\Delta plcR$ that might explain growth rescue, primarily $\Delta plcR$ samples A (treated with unsupplemented RPMI) and B (treated with Ptk6 conditioned medium) were compared. When spot volume changed more than 1.3-fold, spots were selected for protein identification.

2.11.3 MALDI-TOF-MS/MS protein identification

Protein identification of differentially expressed spots was carried out by Matrix-Assisted-Laser-Desorption/Ionization – Time-Of-Flight- (Tandem) Mass-Spectrometry (MALDI-TOF-MS(MS)). For mass spectrometry (MS)-compatible spot detection, protein gels were stained with a modified acidic silver nitrate staining protocol adapted from Heukoven by Miller and Gemeiner (Miller and Gemeiner 1992). Spots of up to six gels were excised manually from semipreparative 2-DE-gels (loading 150 μ g protein) and pooled to have sufficient protein concentration for MS analysis. Prior to protein identification, spot destaining (Gharahdaghi *et al.* 1999), in-gel tryptic digestion (Shevchenko *et al.* 1996) and sample purification using Zip-Tip $_{\mu}$ -C18 (Millipore) pipette tips were conducted as described before (Radwan *et al.* 2008). In brief, destaining of the protein spots was achieved by oxidation of the silver with sodium thiosulfate and potassium ferricyanide followed by two washing steps with 50% EtOH, 40% ddH₂O, 10% AcOH, dehydrating with acetonitrile and drying of the gel pieces in a vacuum centrifuge. Gel pieces were rehydrated in 50 mM ammonium bicarbonate containing 12.4 ng/ μ l trypsin (Trypsin Gold, MS grade, Promega) at 4 °C for 30 min. Excessive trypsin solution was removed and in-gel digestion was performed over night at 37 °C in 50 mM ammonium bicarbonate. The supernatant containing digested peptides was treated twice with 66% acetonitrile, 33% 0.1% TFA and dried in a vacuum centrifuge. Peptides were resolved in 0.1% TFA before they were prepared for MS analysis by using Zip-Tip $_{\mu}$ -C18 pipette tips. Samples were analysed on a MALDI-TOF instrument (Ultraflex II, Bruker Daltonics) applying peptide mass fingerprinting (PMF) as described earlier (Grunert *et al.* 2011). All settings for external instrument calibration were applied as described elsewhere (Radwan *et al.* 2008). Mass spectra were reassessed for typical ions of trypsin autolysis products, blank gel artefacts, keratin and matrix clusters as described previously (Radwan *et al.* 2008). The resulting monoisotopic list of m/z values was submitted to the search engine MASCOT (Matrix Science) (Perkins *et al.* 1999), revision 2.3, searching the databases UniProtKB/Swiss-Prot and NCBI. Search parameters were: taxonomy: *Bacillus cereus*; mass accuracy: 100 ppm; fixed modification: carbamidomethylation; variable modifications: methionine oxidation and acetylation at the protein N-terminal end, missed cleavages: one. For unambiguous protein identification at least two peptides resulting from the PMF were selected for fragment ion analysis experiments. MS/MS database search parameters based on these experiments were identical to PMF experiments, except for product ion

tolerance (+/- 1.0 Da). A protein was considered as identified, if the scores of at least two database searches clearly exceeded the algorithm's significance threshold ($p < 0.05$) for PMF data and for MS/MS data.

2.12. Insect infection experiments

The pathogenic potential of *B. cereus* F4810/72 wt, *B. cereus* NVH 0075-95 wt and isogenic mutants was assessed with the greater wax-moth *Galleria mellonella* as model organism, essentially as described previously (Salamitou *et al.* 2000; Mukherjee *et al.* 2010). *G. mellonella* larvae were purchased from Kerf (Unna, Germany) and kept at 15 °C. 30 last-instar *G. mellonella* larvae per condition, weighting 200 – 400 mg were kept in groups of 10 larvae per box at 15 °C. Bacterial strains were grown over night in LB medium at 30 °C or 37 °C, respectively. The non-pathogenic *E. coli* DH10B was used for infection of the control groups.

To estimate the mean lethal dose (LD₅₀) of sphingomyelinase and the influence of temperature on its activity, *G. mellonella* larvae were injected with different concentrations (0.05, 0.1, 0.5, 1.0, 2.5, 5 µg) of purified SMase (S9396, Sigma-Aldrich) and incubated at 15 °C or 37 °C, respectively. Using the log-probit analysis method according to Miller and Tainter (1944) simplified by Randhawa (2009) (Randhawa 2009) LD₅₀ values were calculated with SigmaPlot 8.0 as mean values of two independent experiments.

SMase overexpression was induced by growing bacillal strains for 2 days in LB medium at 15 °C. 5 µl suspensions of vegetative bacteria were injected intraheamocoelic into the base of the last left proleg of last-instar larvae using a 0.025 ml syringe (#80230, Hamilton) and a 0.31 mm needle (#7803-07, Hamilton). For pathogenicity assessment of *sph* overexpressing strain I injected $0.6 - 1.1 \times 10^6$ CFU/larva for *B. cereus* F4810/72 wt, $\Delta plcR$, $\Delta plcR$ pAD/*sph*/P*cspA* and about 3.4×10^6 CFU/larva for *E. coli* DH10B, respectively.

To achieve a more precise and strong separation of pathogenicity of *sph* null mutants compared to *wild-types*, $1.2 - 2.2 \times 10^5$ vegetative bacteria/larva for *B. cereus* F4810/72 wt, $\Delta plcR$, Δsph , *B. cereus* NVH 0075-95 wt, $\Delta nheBC$, Δsph , $\Delta nheBC\Delta sph$ and about 7.0×10^5 CFU/larva for *E. coli* DH10B were injected, respectively. Doses (CFU) were determined for all strains by plating serial dilutions of the inocula on appropriate media.

The number of viable and killed *G. mellonella* larvae was determined daily over 7 days at 15 °C. Larvae were considered dead if they failed to respond to stimulation with a forceps. All tests were run at least in triplicates.

To determine bacterial growth within *G. mellonella* larvae, for each time point, indicated in the diagrams, 5 larvae of each condition (different injected bacterial strains) were homogenized individually and serial dilutions of the homogenate were plated on LB agar plates for determination of CFU per larva. Larvae were surface-cleaned with 70% EtOH prior to homogenizing them in 1 ml Ringer's solution in a RiboLyser (Hybaid) using 10 glass beads (Ø 3 mm) per tube (2 x 6.5 m/s, 20 sec). Bacterial growth monitoring was done in two independent experiments.

2.13. Software and statistical analysis

Mean values and standard errors (S.E.) were calculated from at least three independent experiments each. For statistical analysis, 2-tailed Student's *t* test was used, where applicable, to determine statistically significant differences as indicated in figure legends (Microsoft Excel, GraphPad Prism, Graph Pad Software). Raw data of the insect experiments were analysed using the GraphPad Prism (version 5.0) computer program and plotted by the Kaplan-Meier method. The curves were compared using a log rank test, which generates a *P* value testing the null hypothesis that the survival curves are identical. *P* values of 0.05 or less were considered significantly different from the null hypothesis. Protein and gene sequences were compared using the BLAST algorithm (NCBI) and BLASTP analysis was applied to identify homologous proteins. Multiple sequence alignments were carried out using ClustalW2 on the EMBL-EBI server (<http://www.ebi.ac.uk/Tools/msa/clustalw2/>). Signal peptide prediction was done on the SignalP 3.0 server ((Bendtsen *et al.* 2004); <http://www.cbs.dtu.dk/services/SignalP-3.0/>) using both neural networks and hidden Markov models trained for Gram-positive bacteria. To identify potential PlcR-binding boxes within the *B. cereus* F4810/72 genome sequence comprehensive xBASE 2.0 database search ((Chaudhuri *et al.* 2008); <http://xbase.bham.ac.uk>) was applied using the pattern search tool and two PlcR target sequences published previously (Gohar *et al.* 2008).

3. RESULTS

3.1. *B. cereus* cytotoxic effects towards IECs and pathogenicity

3.1.1 *B. cereus* cytotoxicity towards intestinal epithelial cells

Since *B. cereus* pathogenic potential ranges from probiotic strains to such associated with lethal outbreaks, a broad strain set (see Table A1, Appendix 7.1) was selected for detailed analysis of the role of cytotoxicity factors in *B. cereus* infection. To narrow down *B. cereus* virulence to single cytotoxic factors *in vitro* this strain set comprised strains with varying toxin gene profiles, food isolates, strains associated with diarrheal and emetic food poisoning, as well as wound isolates and two strains used in probiotic formulas. In total, 14 different *B. cereus* strains and two isogenic mutant strains were screened for their cell cytotoxicity towards polarized intestinal epithelial cells (IECs). Colon epithelial cells derived from Ptk6 null mice served as a cell culture model for polarized IEC. Infection of Ptk6 IEC with various *B. cereus* strains at an MOI of 1 caused rapid cell death with a complete detachment of cells from the tissue culture plate within 4 h (Table 7). Although the beginning of cellular rounding and detachment (see Figure 4) varied between 2 and 4 h there was not a gross difference between strains tested.

Even the two *B. cereus* strains isolated from two different probiotic formulas used in humans and piglet feeding, *B. cereus* var. *toyoi* and IP5832, revealed comparable cytotoxicity to *B. cereus* NVH 0391-98 isolated from a foodborne outbreak associated with high patient mortality (Lund *et al.* 2000) or the *nhe* reference strain *B. cereus* NVH 0075-95 (Table 7).

In the *in vitro* assay cytotoxicity was highly similar for all strains tested, except for a mutant strain deleted in the global virulence regulator gene *plcR*. As expected, cytotoxicity of *B. cereus* F4810/72 $\Delta plcR$ was completely abolished for more than 15 h indicating the involvement of PlcR regulated proteins.

For many pathogens, bacterial adherence to the host epithelium is a prerequisite to initiate infection and mediate cytotoxicity. Therefore, the question arose, if *B. cereus* adhesion to intestinal epithelial cells might play a role for the observed cytotoxic effect and variations in adhesion capacity between the different *B. cereus* strains could be detected.

Table 7: Cytotoxic effect of different *B. cereus* strains on Ptk6 cells. Intestinal epithelial cells (Ptk6) were treated with 14 different *B. cereus* strains and two isogenic mutants, morphological changes were monitored over time using light microscopy. At a low multiplicity of infection (MOI) of one bacterium per Ptk6 cell, all strains tested caused epithelial cell rounding and detachment within 2 – 4 hours after infection except for a *plcR* deletion mutant. Intact monolayer (green), cell rounding (yellow) and 100% cell detachment (red) are indicated.

Time [h]	<i>Bacillus cereus</i>																
	F481072	F481072 Δ <i>plcR</i>	NVH 0075-95	NVH (0075-95 Δ <i>trfheBC</i>)	NVH 0230-00	NVH 0861-00	NVH 0391-98	F83776	F360573	F443073	INRA I21	RIVM BC67	WSBC 10030	WSBC 10035	var. <i>toyoi</i>	IP 5832	
0	intact IEC monolayer	intact IEC monolayer	intact IEC monolayer	intact IEC monolayer	intact IEC monolayer	intact IEC monolayer	intact IEC monolayer	intact IEC monolayer	intact IEC monolayer	intact IEC monolayer	intact IEC monolayer	intact IEC monolayer	intact IEC monolayer	intact IEC monolayer	intact IEC monolayer	intact IEC monolayer	intact IEC monolayer
1.0	intact IEC monolayer	intact IEC monolayer	intact IEC monolayer	intact IEC monolayer	intact IEC monolayer	intact IEC monolayer	intact IEC monolayer	intact IEC monolayer	intact IEC monolayer	intact IEC monolayer	intact IEC monolayer	intact IEC monolayer	intact IEC monolayer	intact IEC monolayer	intact IEC monolayer	intact IEC monolayer	intact IEC monolayer
1.5	intact IEC monolayer	intact IEC monolayer	intact IEC monolayer	intact IEC monolayer	intact IEC monolayer	intact IEC monolayer	intact IEC monolayer	intact IEC monolayer	intact IEC monolayer	intact IEC monolayer	intact IEC monolayer	intact IEC monolayer	intact IEC monolayer	intact IEC monolayer	intact IEC monolayer	intact IEC monolayer	intact IEC monolayer
2.0	intact IEC monolayer	intact IEC monolayer	cell rounding	cell rounding	cell rounding	cell rounding	cell rounding	cell rounding	cell rounding	cell rounding	cell rounding	cell rounding	cell rounding	cell rounding	cell rounding	cell rounding	cell rounding
2.5	intact IEC monolayer	intact IEC monolayer	cell rounding	cell rounding	cell rounding	cell rounding	cell rounding	cell rounding	cell rounding	cell rounding	cell rounding	cell rounding	cell rounding	cell rounding	cell rounding	cell rounding	cell rounding
3.0	intact IEC monolayer	intact IEC monolayer	cell rounding	cell rounding	cell rounding	cell rounding	cell rounding	cell rounding	cell rounding	cell rounding	cell rounding	cell rounding	cell rounding	cell rounding	cell rounding	cell rounding	cell rounding
4.0	100% cell detachment	100% cell detachment	100% cell detachment	100% cell detachment	100% cell detachment	100% cell detachment	100% cell detachment	100% cell detachment	100% cell detachment	100% cell detachment	100% cell detachment	100% cell detachment	100% cell detachment	100% cell detachment	100% cell detachment	100% cell detachment	100% cell detachment

intact IEC monolayer

cell rounding

100% cell detachment

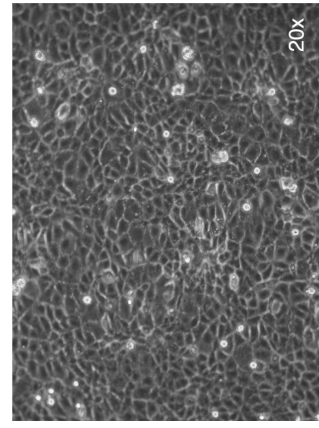
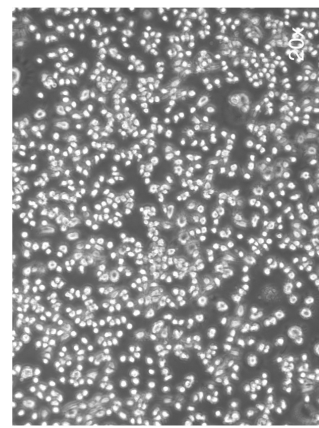
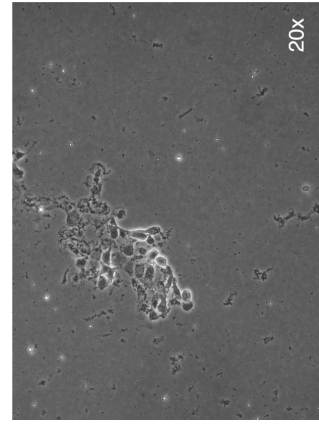


Figure 4: Representative images of *B. cereus* treated Ptk6 cell monolayers are shown (20-fold magnification).

3.1.2 *B. cereus* adhesion capacity to intestinal epithelial cells

The adhesion capacity of a subset of *B. cereus* strains (marked with an asterisk in Table A1, Appendix 7.1) harbouring different toxin profiles was investigated by CFU determination (Ch. 2.7) and fluorescence microscopy (Ch. 2.10.2). Different MOIs (1-100) and infection times (0.5 – 2 h) were tested. In general, only marginal differences between spores and vegetative cells and no correlation between the virulence gene profile of different bacterial strains and their adhesion capacity could be observed. Adhesion of spores and vegetative bacterial cells to Caco-2 and Ptk6 cells was very low. Counting CFUs the adhesion capacity of spores ranged from 0.016 - 0.438 adherent spores per Caco-2 cell and 0.067 – 0.897 adherent spores per Ptk6 cell for an MOI of 6 and 0.5 h of infection. For vegetative bacteria the adhesion capacity was even lower, with respect to the five-fold higher MOI of 30 used, ranging from 0.025 – 0.857 bacteria per Caco-2 cell and 0.026 – 0.413 per Ptk6 cell. There was no difference detectable between *B. cereus* adhesion capacity to subconfluent and confluent epithelial cells.

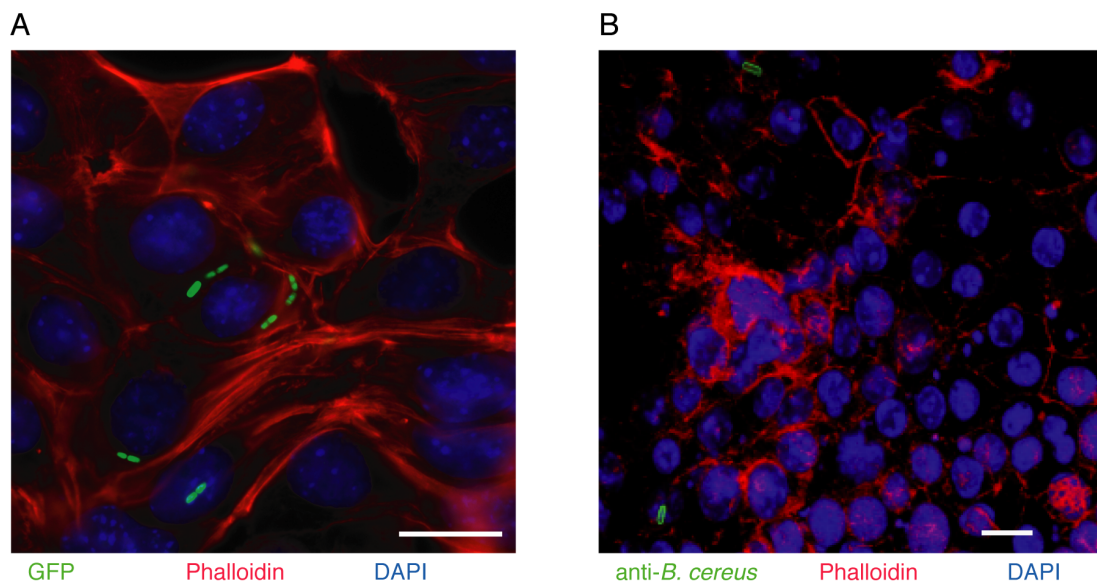


Figure 5: Attachment of *Bacillus cereus* to IECs. **A:** vegetative *B. cereus* $\Delta plcR$ pHT315/*gfp*/*Paph3A* adhere to subconfluent Ptk6 cells after infection with a MOI of 100 for 4 h. Bacteria transiently expressing *gfp* stained in green. **B:** Spores of *B. cereus* NVH 0230-00 poorly adhered to subconfluent Ptk6 cells when infecting for 2 h (MOI1). *B. cereus* were stained using an α -*B. cereus* antibody. Actin was stained using phalloidin (red), DNA/cell nuclei were stained using DAPI (blue). White bar (10 μ m).

In Figure 5 exemplary pictures of vegetative bacteria and spores adhering to Ptk6 cells are shown. Using low MOIs of the different *B. cereus* strains did not result in microscopically detectable amounts of adherent bacteria, while higher MOIs caused cytotoxicity towards epithelial cells (compare Ch. 3.1.1). Only due to its strongly reduced cytotoxicity (see Ch. 3.1.1), a *plcR* deletion mutant could be tested using the maximal bacterial concentration and an incubation time of 4 h. To directly visualize vegetative *B. cereus* cells a $\Delta plcR$ pHT315/*gfp*/*Paph3A* mutant was used which constitutively expressed *gfp* and was therefore detectable by fluorescence microscopy. Very few $\Delta plcR$ pHT315/*gfp*/*Paph3A* vegetative

bacteria adhered to subconfluent Ptk6 cells with respect to the high MOI of 100 and the long incubation (Figure 5A). Figure 5B shows sporadic adhering *B. cereus* NVH 0230-00 spores. For this assay a lower MOI of 1 and shorter incubation time of 2 h had to be applied since spore germination within the time of infection and expression of enterotoxins caused fast destruction of the epithelial cells. *B. cereus* spores were stained using an α -*B. cereus* antibody, epithelial cell actin was stained using phalloidin (red) and eukaryotic cell nuclei stained blue using DAPI. When testing higher MOIs and longer incubation times in order to increase the number of adherent spores or vegetative bacterial cells, the experiments emerged to be unfeasible, as bacteria of all strains except for the *B. cereus* F4810/72 *plcR* mutant started to disrupt epithelial monolayers and killed the epithelial cells (Figure 5).

These results indicated that bacterial adherence to epithelial cells is low and hence plays only a minor role for *B. cereus* virulence and cytotoxicity. Thus, the question remained how *B. cereus* cytotoxicity is mediated.

3.1.3 Cytotoxicity is mediated by a secreted, *PlcR*-regulated factor

To investigate if *B. cereus* cytotoxicity even does without direct cell-cell contact, sterile bacterial secretomes were tested on Ptk6 epithelial cell monolayer. In fact, cellular cytotoxicity was mediated by a secreted *B. cereus* factor as rapid rounding and detachment of IEC was induced by bacterial supernatants alone (Table 8) without any bacteria-cell contact needed. Again *plcR* deletion completely abolished cytotoxicity of *B. cereus* supernatant suggesting *PlcR* regulated proteins as cytotoxic mediators.

Time [h]	<i>Bacillus cereus</i>			
	F4810/72	F4810/72 Δ <i>plcR</i>	NVH 0075-95	NVH 0075-95 Δ <i>nheBC</i>
0	Green	Green	Green	Green
0.5	Orange	Green	Orange	Yellow
1.0	Red	Green	Red	Yellow
2.0	Red	Green	Red	Orange
3.0	Red	Green	Red	Orange
4.0	Red	Green	Red	Orange
5.0	Red	Green	Red	Orange
6.0	Red	Green	Red	Red

Table 8: Cytotoxic effect of sterile *B. cereus* supernatants on Ptk6 cells. Intestinal epithelial cells (Ptk6) were treated with *B. cereus* F4810/72 and NVH 0075-95 wild-type and isogenic mutant strains. Morphological changes of Ptk6 cells were monitored over time using light microscopy. All diluted supernatants (1:2) caused almost immediate epithelial cell rounding and detachment except for the Δ *plcR* deletion mutant that was abolished in its cytotoxicity. Intact monolayer (green), cell rounding < 50% (yellow), cell rounding > 50% (orange) and 100% cell detachment (red) are indicated.

Common to all *B. cereus* strains tested is the presence of the *nhe* operon genes *nheA*, *nheB* and *nheC* (Table A1, Appendix 7.1). A *B. cereus* NVH 0075-95 Δ *nheBC* mutant (kindly provided by Simon P. Hardy) lacking a functional Nhe complex due to *nheB* truncation and *nheC* gene

deletion caused a delay of onset of cellular rounding by 1 h compared to *wild-type*, but IEC still detached completely after 4 h (Table 7). Similarly, bacterial supernatant of the $\Delta nheBC$ mutant caused also a delay of cellular detachment with an early onset of cellular rounding after 0.5 h compared to *wild-type* (Table 8).

Western blot analysis was used to exclude a possible contamination of *B. cereus* NVH 0075-95 $\Delta nheBC$ mutant with the *wild-type* strain explaining the remaining cytotoxicity. Figure 6 shows the immuno blot detection of the three Nhe subunits in *B. cereus* NVH 0075-95 *wild-type* and $\Delta nheBC$ mutant using monoclonal antibodies reacting with NheA or NheB and a polyclonal antiserum against NheC (kindly provided by Dr. R. Dietrich and Prof. Dr. E. Märklbauer). Only the *wild-type* strain expressed all three *nhe* genes, while the $\Delta nheBC$ mutant lacked NheB and NheC. Without these two subunits NheA cannot form a functional enterotoxin complex (Lindbäck *et al.* 2004).

These data indicated that additional extracellular proteins contribute to IEC cytotoxicity.

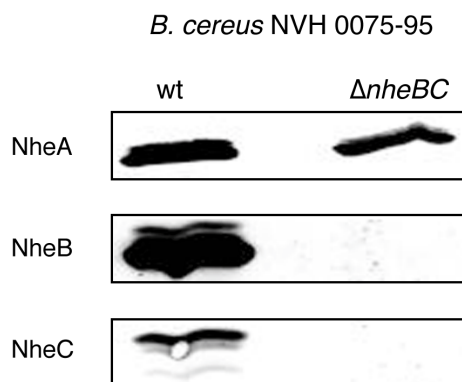


Figure 6: Immuno blot detection of *nheABC* operon expression. Western blot analysis of Nhe expression by *B. cereus* NVH 0075-95 *wild-type* and $\Delta nheBC$ mutant (Fagerlund *et al.* 2008) confirmed the absence of NheB and NheC proteins in the bacterial supernatant of $\Delta nheBC$ after *nheB* truncation and *nheC* gene deletion. Monoclonal antibodies α -NheA, α -NheB and polyclonal α -NheC (Dietrich *et al.* 2005) were kindly provided by Dr. R. Dietrich and Prof. Dr. E. Märklbauer. Identical amounts of total protein preparation were subjected to SDS-PAGE.

3.1.4 Identification of sphingomyelinase (SMase) from cytotoxic bacterial supernatant

As *B. cereus* NVH 0075-95 does not express enterotoxins Hbl and CytK, the *B. cereus* NVH 0075-95 $\Delta nheBC$ supernatant could be used to screen for a factor that causes remaining cytotoxicity of *B. cereus* NVH 0075-95 $\Delta nheBC$. Using Fast protein liquid chromatography (FPLC) proteins contained in the bacterial supernatant were separated according to their size on a Superdex-75 10/300 GL gel filtration column (Figure 7). Fractions 11-18 contained most of the extracellular bacterial proteins. IEC cytotoxicity was confined to three fractions by infecting polarized epithelial monolayer with each of the fractions of the bacterial supernatant of *B. cereus* NVH 0075-95 $\Delta nheBC$. Only fractions 12-14 conveyed complete epithelial cell detachment. SDS gel electrophoresis analysis of fractions 8-14, as well as unfractionated supernatant is demonstrated in Figure 8.

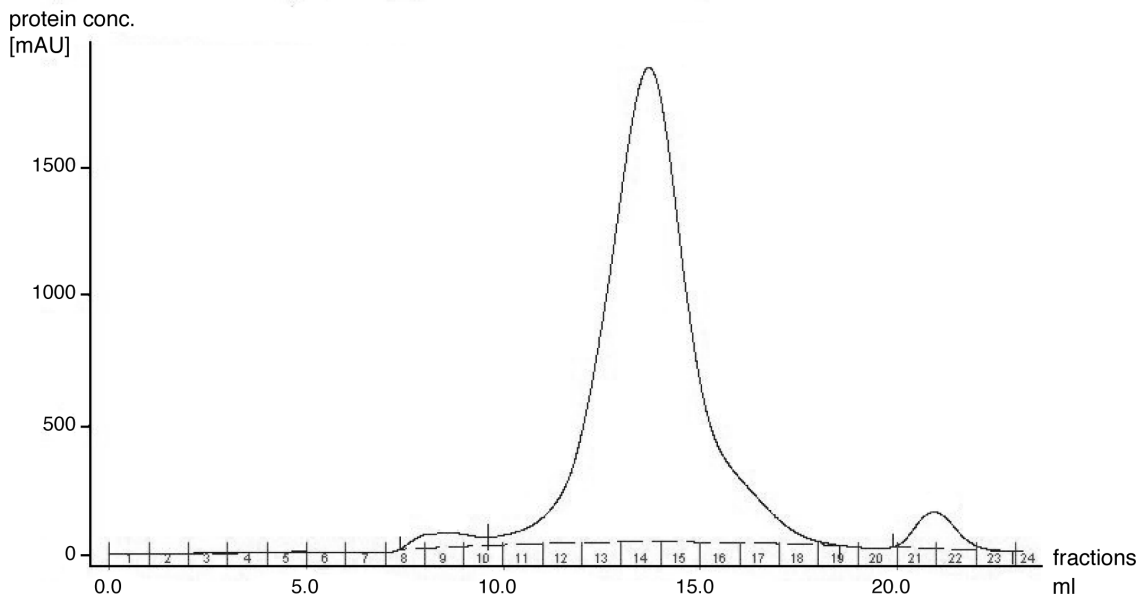


Figure 7: Protein separation of *B. cereus* NVH 0075-95 $\Delta nheBC$ supernatant via gel filtration. Chromatogram of fractionated bacterial proteins is shown (fraction1-24). Numbering of 1 ml fractions is indicated.

Comparison of proteins contained in the cytotoxic fractions 12-14 with unfractionated mutant and *wild-type* *B. cereus* supernatants revealed a 34 kDa and a 25 kDa protein band (indicated in Figure 8 by red asterisk) that were absent in the non-cytotoxic supernatant of *B. cereus* F4810/72 $\Delta plcR$ mutant (Figure 8B).

Protein identification of the two silver stained protein bands was carried out by NextGen Sciences (AnnArbor, USA) using LC/MS/MS on a ThermoFisher LTQ Orbitrap XL mass spectrometer. Mass spectrometry analysis of the 34 kDa protein identified sphingomyelin phosphodiesterase (sphingomyelinase) of *B. cereus* (gil217958262) by two unique peptide sequences, (K)DHANPSFVENK(V) and (K)VQYVFANGCGPDNLSNK(G), and a sequence coverage of 74%. The 25 kDa protein band was identified as hybrid cereolysin AB (gil39422) with a molecular mass of 67 kDa, indeed both samples contained peptides unique for the 3'-terminal part of hybrid cereolysin AB.

Hybrid cereolysin AB is the designation chosen by Gilmore *et al.*, 1989 for the functional unit of a phospholipase C (5'-terminal region) and a sphingomyelinase (3'-terminal region) proposed to work together as a haemolytic determinant of *B. cereus* (Gilmore *et al.* 1989).

This result suggests that the 25 kDa protein might be a degradation/dissociation product of the larger cereolysin AB complex comprising major parts of sphingomyelinase. Therefore, further work focussed on *B. cereus* sphingomyelinase (SMase), a 333 amino acid protein (37 kDa) that is secreted as a 34 kDa protein after signal peptide cleavage (27 aa). Interestingly, the *sph* gene is present in all *B. cereus* strains tested in the cytotoxicity assay as assessed by PCR amplification (data not shown).

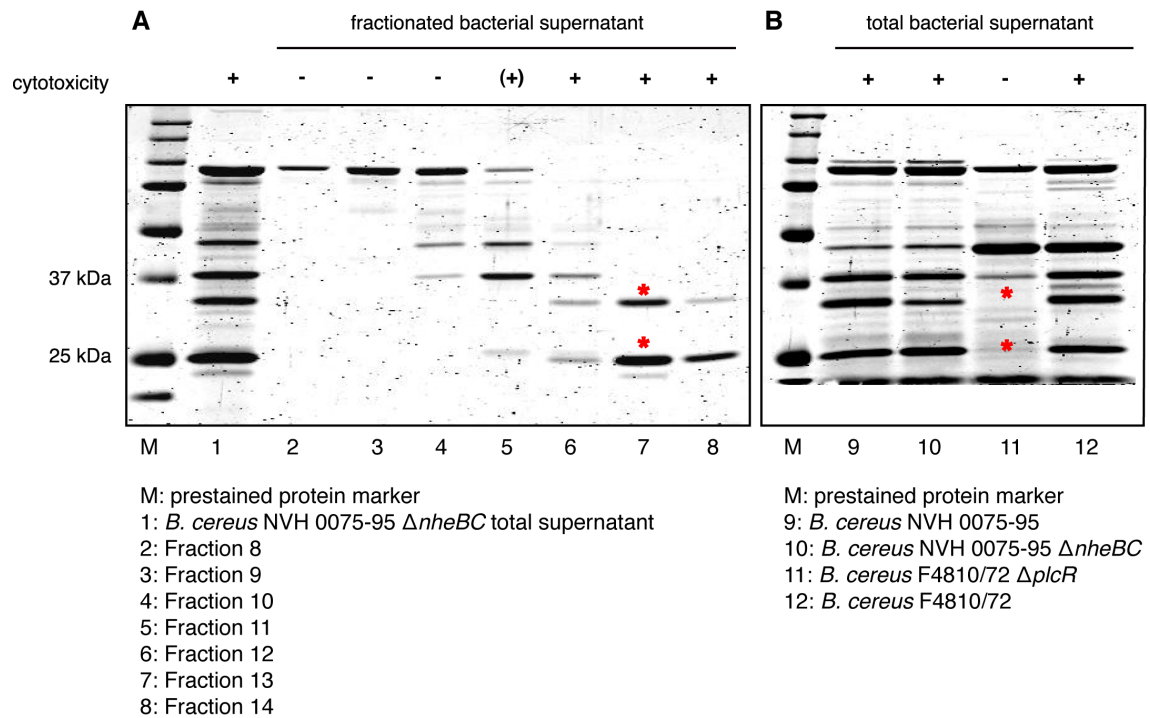


Figure 8: Protein fractions obtained from gel filtration were analysed by SDS-PAGE. **A:** Gel filtration fractions 12–14 which transferred cytotoxicity to Ptk6 cells contained two distinct proteins at 34 kDa and 25 kDa (red asterisk). **B:** Comparison to total extracellular proteins of *wild-type* and mutant *B. cereus* strains confirmed absence of the two potential cytotoxic proteins (red asterisk) in supernatant of the avirulent $\Delta plcR$ strain. Prestained protein marker (M).

3.1.5 SMase expression in *B. cereus* $\Delta plcR$

In order to test if *B. cereus* SMase can rescue IEC cytotoxicity, the *sph* gene was transiently expressed in *B. cereus* F4810/72 $\Delta plcR$ under the control of an inducible cold shock protein A promoter (*PcspA*) (*B. cereus* F4810/72 $\Delta plcR$ pAD/*sph*/*PcspA*) (Figure 9).

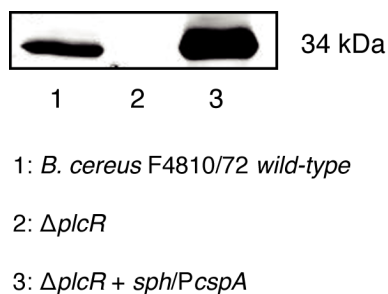


Figure 9: Immuno blot detection of *sph* expression in *B. cereus* F4810/72 wt and mutant supernatants. Western blot analysis of bacterial supernatants using a polyclonal anti-SMase antibody (1:1000) confirmed SMase production and secretion by *B. cereus* $\Delta plcR$ *sph/PcspA*.

3.1.5.1 SMase expression restores *B. cereus* cytotoxicity *in vitro* and pathogenicity *in vivo*

Incubation of polarized Ptk6 epithelial cells with the bacterial supernatant of the SMase expressing $\Delta plcR$ mutant strain restored some of *B. cereus* F4810/72 *wild-type* cytotoxicity *in vitro* after 1.5 h (Figure 10). Cell rounding continued until complete detachment of IEC after 2.5 -

3 h in *wild-type* and the *sph* expressing mutant in contrast to $\Delta plcR$. These data hint to an active role of sphingomyelinase in intestinal epithelial cell cytotoxicity.

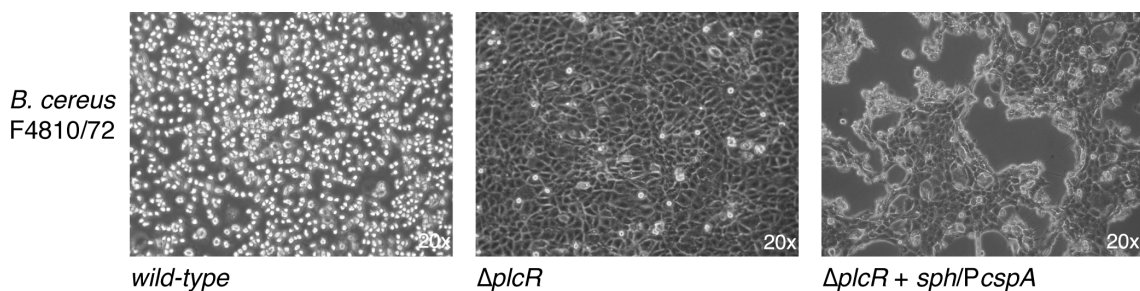


Figure 10: Transient *sph* expression by $\Delta plcR$ *sph/PcspA* rescued cytotoxic effects on Ptk6 cells. Supernatant of *B. cereus* F4810/72 *wild-type* caused 100% cell rounding and single cell detachment of Ptk6 cells within 1.5 h, while supernatant of $\Delta plcR$ mutant did not affect Ptk6 cell morphology. Representative light microscopic images of Ptk6 cell monolayer are shown (20-fold magnification).

Next, to further assess *B. cereus* entomopathogenic properties and the contribution of SMase to *B. cereus* pathogenesis the lepidopteran insect model host *Galleria mellonella* was used.

The greater wax moth larva *G. mellonella* (Figure 11) is a commonly used model organism to investigate toxicity of bacterial toxins or pathogenicity of different bacterial mutant strains. After injection of toxins or bacterial suspensions into the haemocoel, larvae often develop paresis, followed by progressing paralysis up to death of the larvae. Injection of viable bacteria is usually accompanied by a successive deposition of melanin on the microbe within the haemolymph resulting in a brownish to black colouring of the dying larva. Figure 11B demonstrates a sequence of the melanisation process starting from the living larva injected with *B. cereus* F4810/72 *wild-type* bacteria into the last left proleg up to the dead black larva.

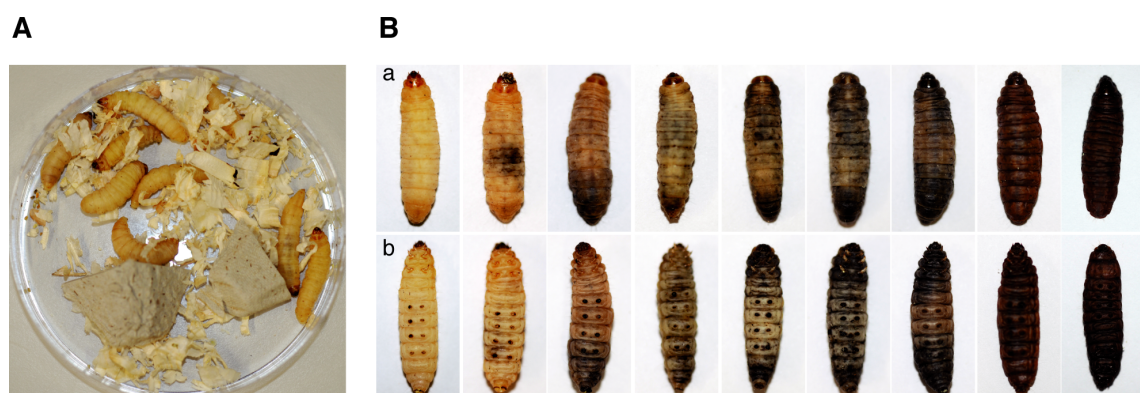


Figure 11: The great wax moth *Galleria mellonella* as *in vivo* insect model. **A:** For injection experiments larvae were kept in groups of 10 at 15 °C or 37 °C. **B:** Different steps in the process of melanisation following the intrahaemocoelic injection of *B. cereus* F4810/72 *wild-type*. Back view (a) and ventral view (b) of the same larva are indicated.

Since the experiments had to be carried out at 15 °C to induce *sph* expression, but SMase enzyme activity is optimal at 37 °C, a preexperiment was performed to determine the temperature dependency of SMase insecticidal activity. Five different concentrations ranging

from 0.05 to 5 μg of purified SMase (S9396, Sigma-Aldrich) in PBS were injected in five *G. mellonella* larvae per condition. Larvae were incubated at 15 °C or 37 °C and mortality was recorded after 24 h. The experiment was done twice and mean LD₅₀ values of SMase at 15 °C and 37 °C were calculated using log-probit analysis (Randhawa 2009). SMase LD₅₀ was $0.711 \pm 0.345 \mu\text{g}$ at 15 °C and with $0.501 \pm 0.185 \mu\text{g}$ only slightly higher at 37 °C. There was no significant difference between the two tested temperatures ($P=0.529$).

Therefore, all subsequent experiments were carried out at 15 °C for optimal induction of *sph* expression.

G. mellonella larvae were injected with *B. cereus* F4810/72 *wild-type*, ΔplcR or ΔplcR pAD/*sph*/P*cspA*. Larvae injected with *E. coli*, LB medium or untreated served as a control. Survival of larvae was monitored over three days (Figure 12). All untreated larvae and those injected with *E. coli* or LB medium survived during the experiment. *B. cereus* F4810/72 *wild-type* caused a mortality of more than 50% of *G. mellonella* larvae within 26 hours.

Infection of larvae with the ΔplcR mutant showed a significant delay of overall mortality compared to *wild-type* ($P<0.0001$). Expression of *sph* in the ΔplcR mutant strain (ΔplcR pAD/*sph*/P*cspA*) restored larvae mortality compared to *wild-type* ($P=0.7904$).

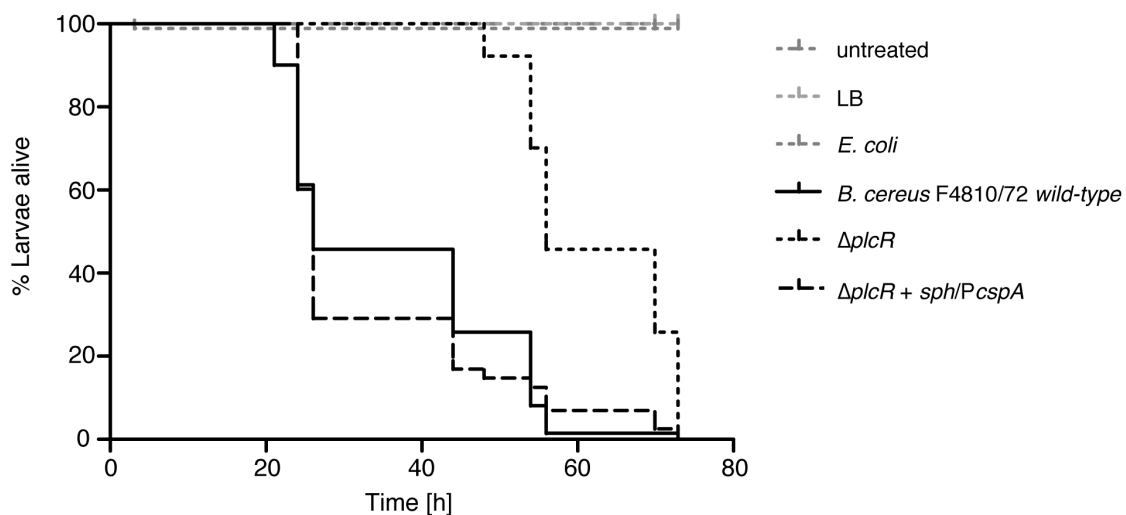


Figure 12: Survival of *G. mellonella* injected with *B. cereus* F4810/72 *wild-type*, mutant strains, *E. coli* DH10B and controls. Larvae injected with *E. coli*, LB medium or untreated served as controls (grey lines). Survival of *G. mellonella* larvae injected with ΔplcR mutant (black dotted line) was significantly longer than when injecting *B. cereus* *wild-type* (black line) or *sph* expressing ΔplcR strain (black dashed line) ($P<0.0001$ each). The Kaplan-Meier plot is based on three independent experiments ($n = 90$ animals per curve).

Differences in bacterial growth did not account for the observed effects as bacterial growth of *wild-type* and mutant strains were similar in *G. mellonella* larvae (Figure 13). These data suggest that SMase activity plays an important role in *B. cereus* mediated IEC cytotoxicity *in vitro* and pathogenicity *in vivo*.

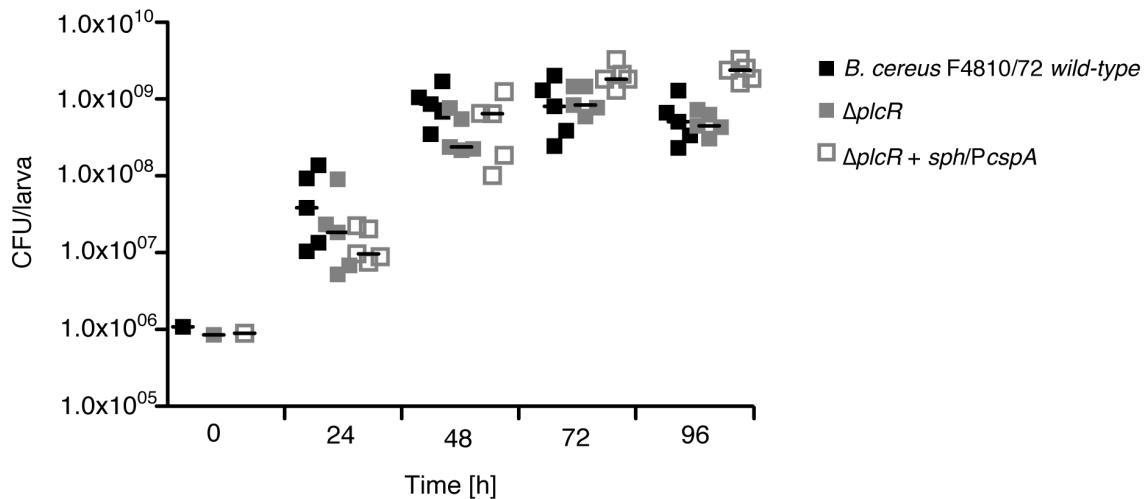


Figure 13: Growth of *B. cereus* F4810/72 wt and mutant strains in *G. mellonella* larvae. To define growth of *B. cereus* in *G. mellonella* larvae, the bacterial counts (CFU/larvae) in infected larvae were determined during the survival experiment. At time points indicated serial dilutions of homogenates of 5 larvae were plated individually. The resulting mean values are indicated as black bars.

3.1.5.2 SMase expression induces apoptosis in polarized IEC via caspase-3 activation

In mammalian cells endogenous sphingomyelinase activity is essentially involved in cleavage of cell membrane phospholipids releasing ceramide. Ceramide is an important signalling molecule in eukaryotic cells triggering signalling cascades and controlling cell development, proliferation and apoptosis. The fact that *B. cereus* SMase mimics the action of mammalian neutral SMase (Ago *et al.* 2006) led to the hypothesis that inappropriate apoptosis induction in epithelial cells might be the mechanism how *B. cereus* SMase causes cytotoxicity in intestinal epithelial cells. Therefore, the capacity of exogenously added *B. cereus* SMase to induce apoptosis was examined. An early event in cells undergoing apoptosis is the translocation of phosphatidylserine from the inner to the outer leaflet of the plasma membrane (van Engeland *et al.* 1998). On apoptotic cells this exposed phosphatidylserine can then be stained using annexin V, a phospholipid-binding protein with high affinity to phosphatidylserine (Andree *et al.* 1990). Polarized Ptk6 cells were stained after incubation with bacterial supernatant for annexin V (apoptosis) and SYTOX[®] Green. SYTOX[®] is a nucleic acid stain, which enters only cells with a defective plasma membrane, hence staining late-apoptotic and necrotic cells. Figure 14 illustrates representative images of Ptk6 cells treated with bacterial supernatant for 1 h. *B. cereus* F1048/72 wild-type supernatant caused strong epithelial cell rounding and single cell detachment within 1 h of treatment. Many rounded cells stained positive for annexin V and SYTOX[®] Green, indicative for necrotic cells dying from destruction of cell membrane integrity and pore-formation by enterotoxins. In contrast, when incubated with $\Delta plcR$ supernatant only very few cells died. When treated with *B. cereus* F4810/72 $\Delta plcR$ pAD/sph/PcspA supernatant, containing SMase in the context of $\Delta plcR$ secretome many Ptk6 cells entered the apoptotic pathway and stained annexin V positive while lacking a SYTOX[®] Green signal and wild-type induced rounded cell morphology. Additionally, double positive stained (annexin V⁺, SYTOX[®]

Green⁺) IECs could be detected. This might also indicate late-apoptotic cells, characterised by externalization of phosphatidylserine and leaking cell membranes.

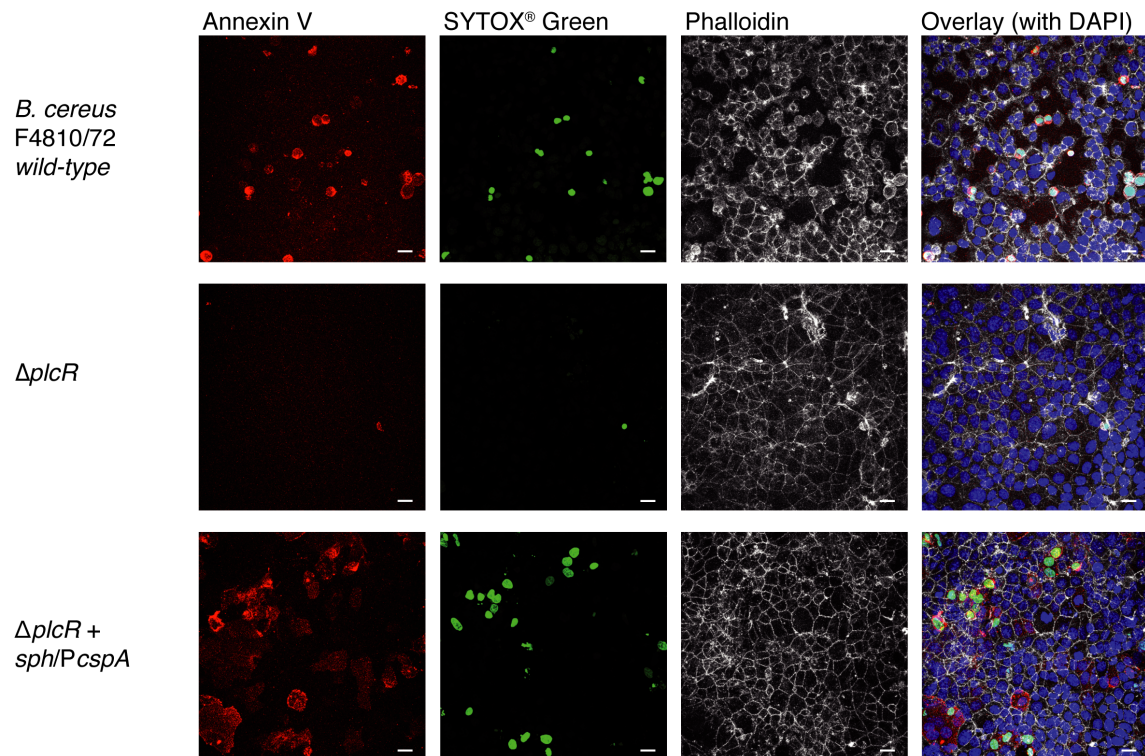


Figure 14: SMase induced IEC apoptosis is visualized by Annexin V staining of translocated phosphatidylserine. Polarized Ptk6 cells were treated with bacterial supernatants (1:4 diluted in RPMI) of *B. cereus* F4810/72 *wild-type* (upper panel), $\Delta plcR$ (middle panel) and $\Delta plcR + sph/PcspA$ (lower panel) for 1 h and late apoptotic/necrotic (green + red) and apoptotic (only red) IECs were visualized by fluorescence microscopy (Scale bars, 10 μ m). Phalloidin and DAPI was used to stain IEC actin (grey) and nuclei (blue), respectively.

To quantify IEC apoptosis induction by *B. cereus* SMase, Ptk6 cells were treated with bacterial supernatants of $\Delta plcR$ containing or lacking SMase. After three hours cells were again stained for externalized phosphatidylserine characterizing apoptosis and imaged with a confocal microscope (Leica SP5). For each condition three different representative microscopic fields (including about 600 cells) were imaged and annexinV⁺/SYTOX[®] Green⁻ as well as total cell numbers were counted to calculate % apoptotic cells. Three hours after treatment with *B. cereus* F4810/72 $\Delta plcR$ supernatant 0.28% \pm 0.22 of Ptk6 cells were apoptotic similar to untreated control (0.31% \pm 0.15) (Figure 15). Staurosporine, a kinase inhibitor that induces cellular apoptosis via caspase-3 served as a positive control. Treatment of Ptk6 cells with 0.1 μ M of staurosporine induced apoptosis in 1.83% \pm 0.89. Supernatant of the SMase expressing *B. cereus* F4810/72 $\Delta plcR$ pAD/*sph/PcspA* mutant strain increased the apoptotic rate significantly to 4.87% \pm 1.36 ($P=0.016$) (Figure 15).

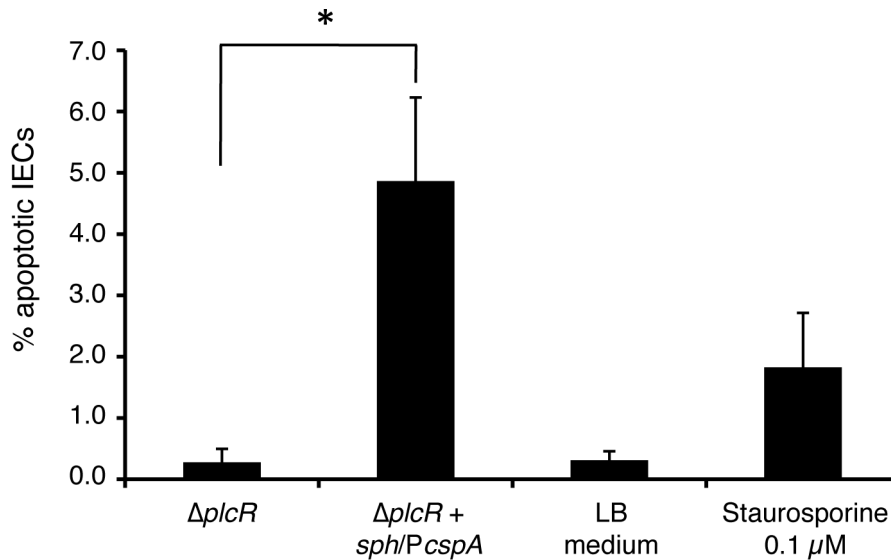


Figure 15: *B. cereus* SMase induced apoptosis in IECs. Ptk6 cells were treated with bacterial supernatant of *B. cereus* F4810/72 $\Delta plcR$ or $\Delta plcR$ *sph/PcspA* (producing SMase) for three hours followed by immunofluorescence staining for phosphatidylserine translocation using Alexa Fluor 594-coupled annexinV. The samples were imaged with a confocal microscope (Leica SP5). For each condition three different representative microscopic fields (including about 600 cells) were imaged and % apoptotic cells were calculated. The graph shows mean values + SEM (n = 4); * $P < 0.05$.

In a second assay for caspase-3 activation, the apoptotic pathway activated by *B. cereus* SMase was further investigated. Caspase-3 activation is a relatively late event in apoptotic cells and is involved in the intrinsic (mitochondrial) as well as in the extrinsic (Fas receptor) pathway (Salvesen 2002). Activation of both pathways initiates a caspase cascade resulting in the cleavage of procaspase-3 by caspase 8 or caspase 9 thereby activating caspase-3 causing DNA fragmentation and typical morphological changes (Porter and Jänicke 1999; Harrington *et al.* 2008).

Ptk6 cell monolayers were treated with bacterial supernatant, 1 U/ml SMase (S9396, Sigma-Aldrich), LB medium (1:2 in RPMI) as a negative control or 0.1 μM staurosporine as a positive control at 37 °C. After 24 hours, cells were lysed, total proteins isolated and caspase-3 activity was measured using a colorimetric caspase-3 substrate (200 mM, Calbiochem). Enzymatic substrate conversion resulting in absorbance at 405 nm was normalized to the sample protein concentration and plotted against time. The curve slope was used as a good measure of enzyme activity. 0.1 μM staurosporine treatment for 24 h resulted in strong caspase-3 activation (data not shown). A representative out of three independent experiments is shown in Figure 16. Incubation of Ptk6 cells with bacterial supernatant of *B. cereus* F4810/72 $\Delta plcR$ pAD/*sph/PcspA* showed 4-fold caspase-3 activation compared to *B. cereus* F4810/72 $\Delta plcR$ (Figure 16). To confirm that this effect was due to SMase activity in the supernatant, cells were incubated with purified *B. cereus* SMase (1 U/ml, Sigma-Aldrich) in $\Delta plcR$ supernatant and assayed as described above. Caspase-3 activation via SMase activity in the supernatant of *B. cereus* F4810/72 $\Delta plcR$ pAD/*sph/PcspA* was similar to 1 U/ml of recombinant SMase in bacterial

supernatant of *B. cereus* F4810/72 $\Delta plcR$ (Figure 16). These data suggest that SMase induces apoptosis of polarized epithelial cells in a caspase-3 dependent manner.

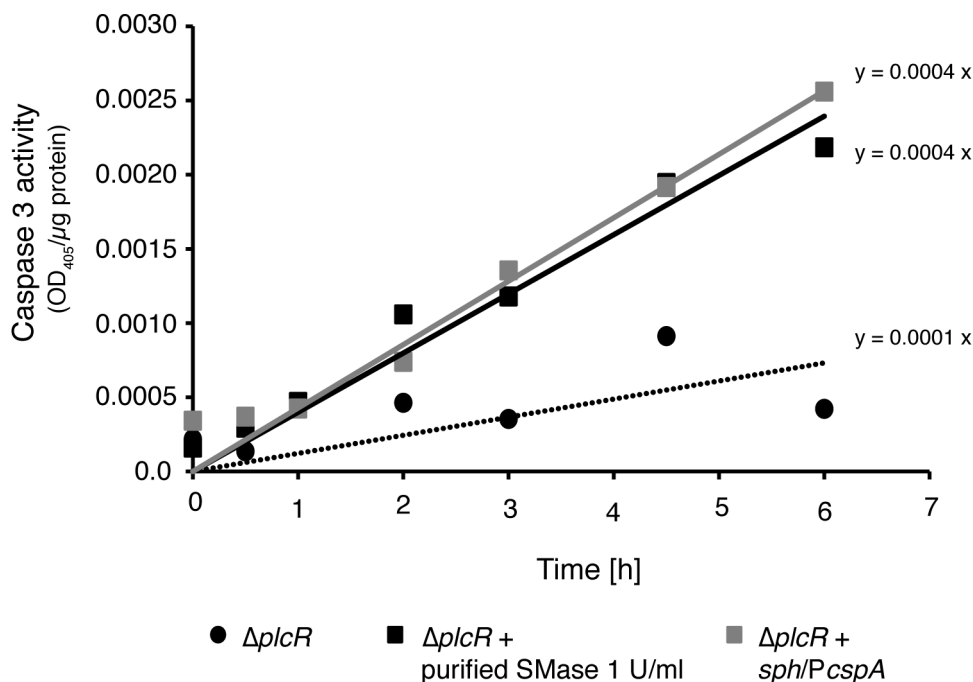


Figure 16: *B. cereus* SMase induced IEC apoptosis via caspase-3 activation. Ptk6 cells were treated with diluted $\Delta plcR$ supernatant with or without expressed or purified (1 U/ml, Sigma-Aldrich) SMase for 24 h. Resulting caspase-3 activity in Ptk6 cells is plotted over time and slope is indicated. One representative of three independent experiments is shown.

3.1.6 *B. cereus* sphingomyelinase deletion mutants

3.1.6.1 Construction of sph deletion mutants and complemented strains

In this work *B. cereus* SMase was identified as a secreted factor conveying cytotoxicity in polarized epithelial cells *in vitro* in addition to Nhe. To address the question to which extent SMase contributes to cellular cytotoxicity *in vitro*, *sph* deletion mutants were constructed in the emetic *B. cereus* F4810/72 *wild-type* strain and the diarrheal *B. cereus* NVH 0075-95 *wild-type* and $\Delta nheBC$ mutant strain by chromosomal replacement of the *sph* gene sequence with a chloramphenicol resistance cassette via double homologous recombination. The *sph* deletion mutants were named *B. cereus* F4810/72 Δsph , *B. cereus* NVH 0075-95 Δsph and *B. cereus* NVH 0075-95 $\Delta nheBC\Delta sph$, respectively. Complete gene replacement was verified by PCR (data not shown).

For complementation of *sph* deletion mutants, SMase protein expression should be reconstituted under its own promoter in the Δsph strains.

However, at that point it was unclear how *sph* transcription is regulated. The *plc-sph* gene cluster is commonly termed as operon (cereolysin AB operon) suggesting a co-transcription of both genes from an operon promoter. Nevertheless, two independent putative promoter regions

including all characteristic conserved promoter elements like RNA-polymerase-binding and recognition sites (-35, -10 region) and a potential ribosome-binding site (RBS) have been described for *plc* and *sph* (Yamada *et al.* 1988; Pomerantsev *et al.* 2009). One putative *sph* promoter region directly upstream of the *sph* start codon (*Psph**) and the additional putative operon promoter region upstream of the 5' adjacent *plc* gene (*Pplc**) were depicted by the authors and are presented in Figure 17.

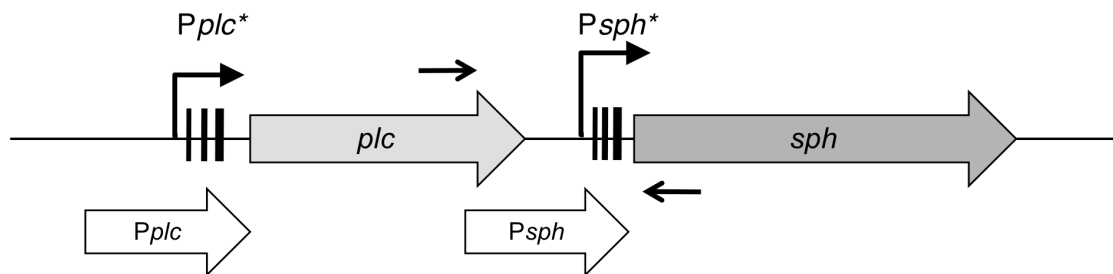


Figure 17: Genetic organization of the chromosomal *plc* – *sph* gene cluster. The operon comprises a phosphatidylcholine-specific phospholipase C (*plc*) and a sphingomyelinase (*sph*) gene. *Pplc** refers to a putative promoter region of the *plc-sph* operon, while *Psph** refers to a putative promoter region directly upstream of the *sph* start codon as described by (Yamada *et al.* 1988; Pomerantsev *et al.* 2009). Three black bars in the promoter regions represent the identified -35, -10 boxes and the ribosome-binding site. *Pplc* designates a 538-bp fragment spanning the operon promoter region *Pplc**, while the intergenic region is covered by *Psph* (499bp). The positions of *inplc_for* and *insph_rev* primer binding for co-transcription analysis are indicated by two small black arrows.

In order to investigate, if the *sph* gene is co-transcribed with *plc* from the putative operon promoter region *Pplc** or from its own promoter region *Psph**, transcriptional analysis was carried out. For the analysis of the *plc-sph* gene cluster, the primer pair *inplc_for/in sph_rev* (Table A3, Appendix 7.3), marked in Figure 17 as small black arrows, was used for reverse transcriptase PCR amplification, with the forward primer in the *plc* and backward primer in the *sph* gene. RNA was isolated from *B. cereus* F4810/72 *wild-type* and Δ *plcR*, translated into cDNA and a PCR product of the expect size (537 bp), spanning the intergenic region between *plc* and *sph* could be amplified from *wild-type* throughout the logarithmic growth phase (OD 1, 4, 7), but was absent during transition and stationary phase (OD 10, 14). None of the Δ *plcR* samples yielded a PCR amplicon (Figure 18). These results demonstrate that PlcR regulated *sph* expression is driven by the operon promoter region *Pplc** and the *plc-sph* operon is co-transcribed as one mRNA transcript.

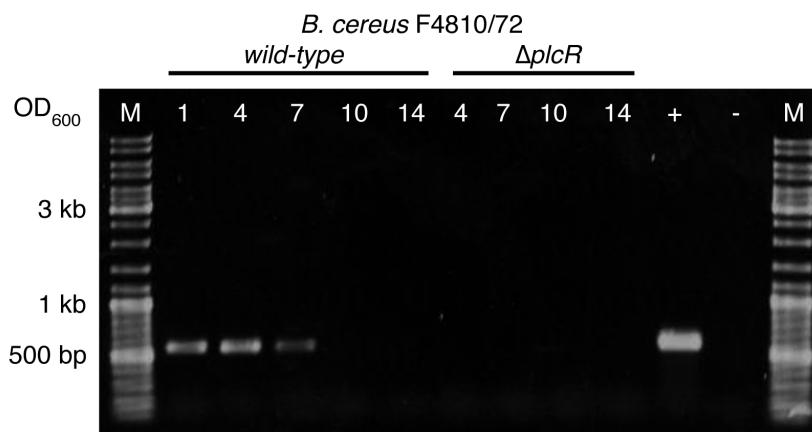


Figure 18: Co-transcription analysis of the *plc-sph* gene cluster. The *inplc_for/inpsph_rev* primer pair was used to amplify a 537 bp reverse transcriptase PCR product (indicative for *plc-sph* co-transcription) from bacterial RNA harvested at different growth phases (respective OD_{600} is indicated). Genomic DNA of *B. cereus* F4810/72 *wild-type* (+) and d_0H_2O (-) served as positive or negative control, respectively. DNA marker (M).

To verify co-transcription results in the presented experimental setting, two plasmids were constructed for complementation of *sph* deletion mutants. A 538 bp fragment (*Pplc*) covering the 5' upstream region of *plc* including the putative operon promoter region *Pplc** and a second construct comprising a 499 bp region (*Psph*) directly in front of the *sph* start codon including the putative *sph* promoter region *Psph** (Figure 17) were amplified by PCR. Each of the promoter regions *Pplc* (spanning *Pplc**) and *Psph* (spanning *Psph**) was inserted into a pAD expression vector in front of the promoterless *sph* gene giving rise to two complementation vectors pAD/*sph/Pplc/tet* and pAD/*sph/Psph/tet*. These non-integrative vectors convey additional tetracycline resistance to *B. cereus*. Both vectors were introduced into *B. cereus* Δsph mutants by electroporation resulting in the complemented strains *B. cereus* F4810/72 Δsph com*Pplc*, *B. cereus* F4810/72 Δsph com*Psph*, *B. cereus* NVH 0075-95 $\Delta nheBC\Delta sph$ com*Pplc* and *B. cereus* NVH 0075-95 $\Delta nheBC\Delta sph$ com*Psph*. Characterization of *sph* deletion mutants and complemented strains with respect to phenotype, growth and cytotoxicity was performed as outlined below.

3.1.6.2 Phenotypic characterization

Columbia agar plates (5% sheep blood) were used to test *B. cereus* induced haemolysis. Since *B. cereus* F4810/72 and NVH 0075-95 do not harbour genes encoding for haemolysin BL or HlyII, their haemolytic phenotype on sheep blood agar must be attributed to other enzymes. In *B. cereus* F4810/72 *sph* deletion abolished most but not all haemolysis (Figure 19). In the *nheBC* mutant *B. cereus* NVH 0075-95 $\Delta nheBC$ the haemolysis zone was markedly reduced in clearance albeit not in diameter compared to *wild-type*. The additional *sph* deletion resembled a $\Delta plcR$ -like, haemolytic-negative phenotype in *B. cereus* NVH 0075-95 $\Delta nheBC\Delta sph$. These findings show that the haemolytic phenotype of Hbl^- , $HlyII^-$ *B. cereus* strains is caused by the synergistic effect of *Nhe* and *SMase*. Complementation of *sph* deletion using *Psph* as the promoter region driving *sph* gene expression failed to reconstitute the haemolytic activity of

SMase in *B. cereus* F4810/72 Δsph comP*sph* and NVH 0075-95 $\Delta nheBC\Delta sph$ comP*sph* (Figure 19). In contrast, complementation of the *sph* null mutants by *B. cereus* F4810/72 Δsph comP*plc* and *B. cereus* NVH 0074-95 $\Delta nheBC\Delta sph$ comP*plc* reconstituted phenotypic characteristics of the respective strains (*B. cereus* F4810/72 and NVH 0075-95 $\Delta nheBC$) (Figure 19) as well as SMase protein expression and secretion (Figure 23) and SMase activity (Figure 24). These data phenotypically demonstrate that under the conditions applied *sph* transcription was driven from the putative operon promoter region P*plc** and therefore confirm the transcription analysis results (see Ch. 3.5.1). Since only promoter region P*plc* is able to complement *sph* expression, following experiments were executed using solely *B. cereus* F4810/72 Δsph comP*plc* and *B. cereus* NVH 0074-95 $\Delta nheBC\Delta sph$ comP*plc*.

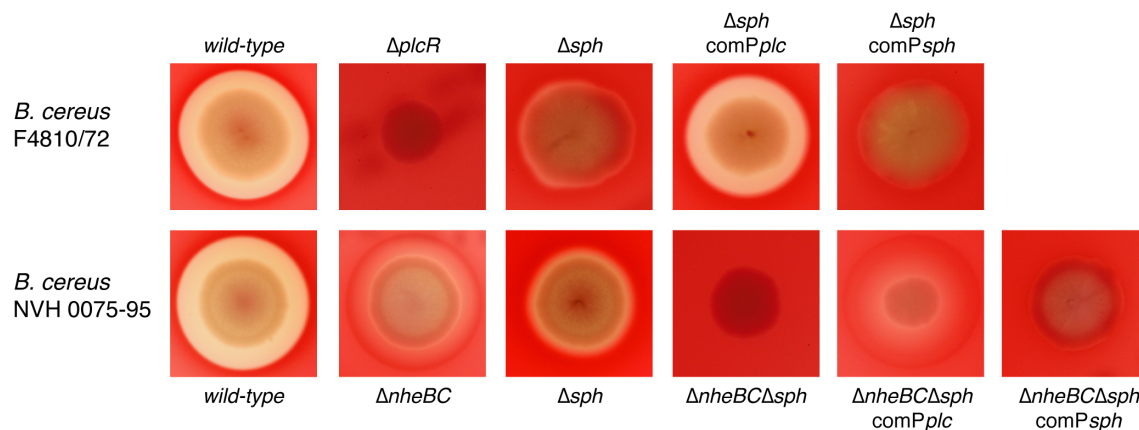


Figure 19: Characterisation of *B. cereus* wt and mutant haemolytic activity. *B. cereus* F4810/72 (upper panel) and *B. cereus* NVH 0075-95 (lower panel) *wild-type*, isogenic mutants and complemented strains were tested for haemolysis on Columbia agar (5% sheep blood) at 37 °C.

In order to confirm a functional intact neighbouring *plc* gene encoding the lecithinase Plc after *sph* gene deletion by homologous recombination, bacteria were grown on mannitol-egg yolk-polymyxin (MYP) agar plates (Figure 20). Lecithinase (Plc) activity indicated by egg-yolk precipitation zones was detected for all Δsph mutants, the $\Delta nheBC$ mutant and the *wild-type* strains. Only the $\Delta plcR$ mutant was lecithinase- and haemolytic-negative. The phenotypic data suggest haemolytic synergy of SMase and Nhe. Results demonstrate that in HbI⁻ *B. cereus* strains both, SMase as well as Nhe activity, are necessary for *B. cereus* entire haemolytic capacity.

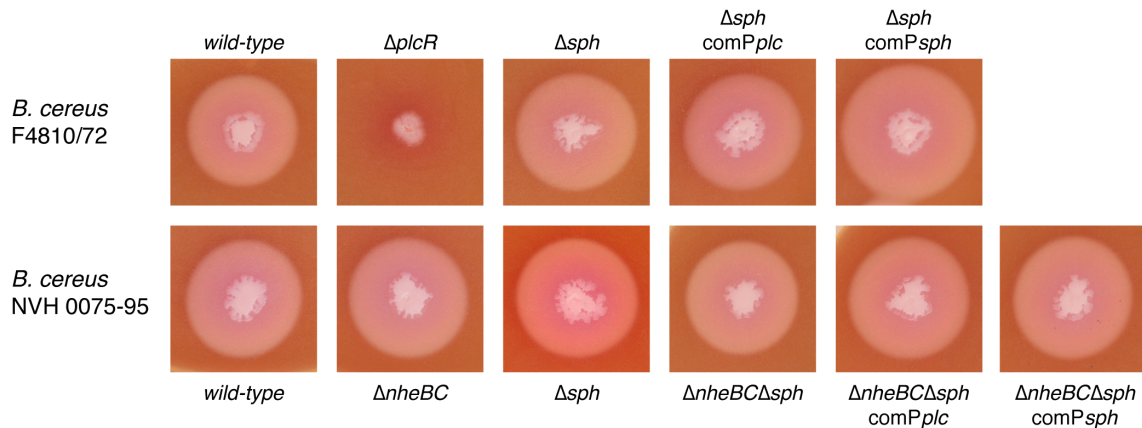


Figure 20: Characterisation of *B. cereus* wt and mutant lecithinase (Plc) activity. *B. cereus* F4810/72 (upper panel) and *B. cereus* NVH 0075-95 (lower panel) *wild-type*, isogenic mutants and complemented strains were grown on MYP (mannitol-egg yolk-polymyxin) agar. Lecithinase activity is indicated by egg-yolk precipitation zones.

3.1.6.3 Growth characterization

All constructed *B. cereus* deletion mutants were characterised for their growth in LB medium at 37 °C and continuous shaking (150 rpm) by OD₆₀₀ measurement (data not shown) and additional plating of serial dilutions for CFU determination. Both methods revealed similar growth curves, although CFU counting indicates the onset of logarithmic growth phase after 3 hours (Figure 21), while bacterial density (OD₆₀₀) increase is not measurable until 5 hours after inoculation (data not shown). The growth kinetics in LB medium displayed similar growth rates for all *B. cereus* *wild-type* and isogenic mutant strains (Figure 21A and B) when grown without antibiotic pressure. Addition of chloramphenicol to the *B. cereus* Δsph cultures delayed the entry of the logarithmic growth phase for 7-8 hours (data not shown). All strains grew to a maximum bacterial density of approximately 1×10^9 CFU/ml within 8 hours. Subsequently, bacterial density slightly decreased 4 hours after entering stationary phase and remained stable over 12 hours. The $\Delta plcR$ mutant showed a more pronounced decrease in cell density during stationary phase compared to *wild-type* and Δsph (Figure 21A).

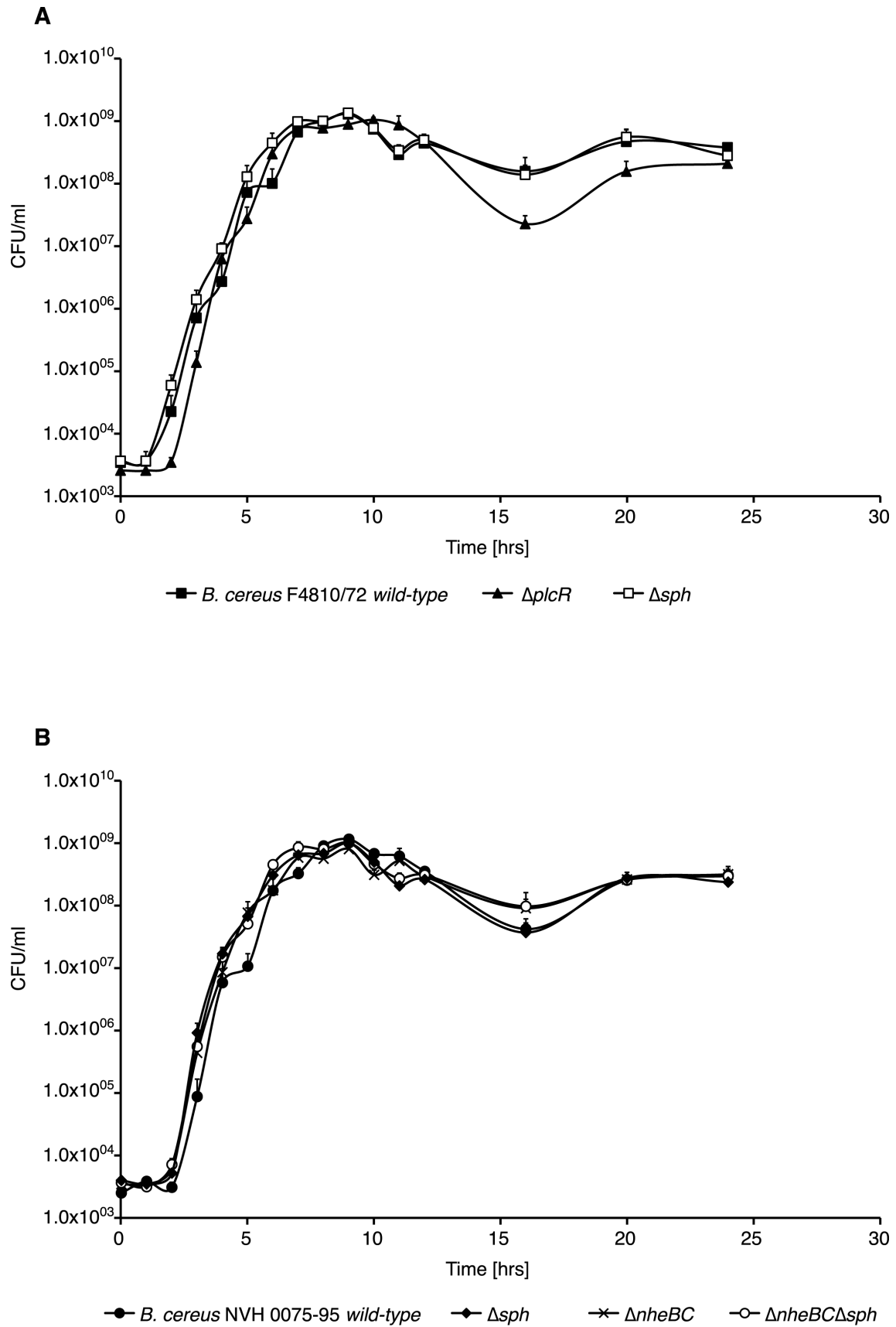


Figure 21: Growth of *B. cereus* wild-type compared to their deletion mutants. Kinetics of **A:** *B. cereus* F4810/72, $\Delta plcR$ and Δsph and **B:** *B. cereus* NVH 0075-95 wild-type, $\Delta nheBC$, Δsph , $\Delta nheBC\Delta sph$ growth in LB at 37 °C and 150 rpm (shaking flasks). Growth curves represent mean values + SEM of three independent experiments.

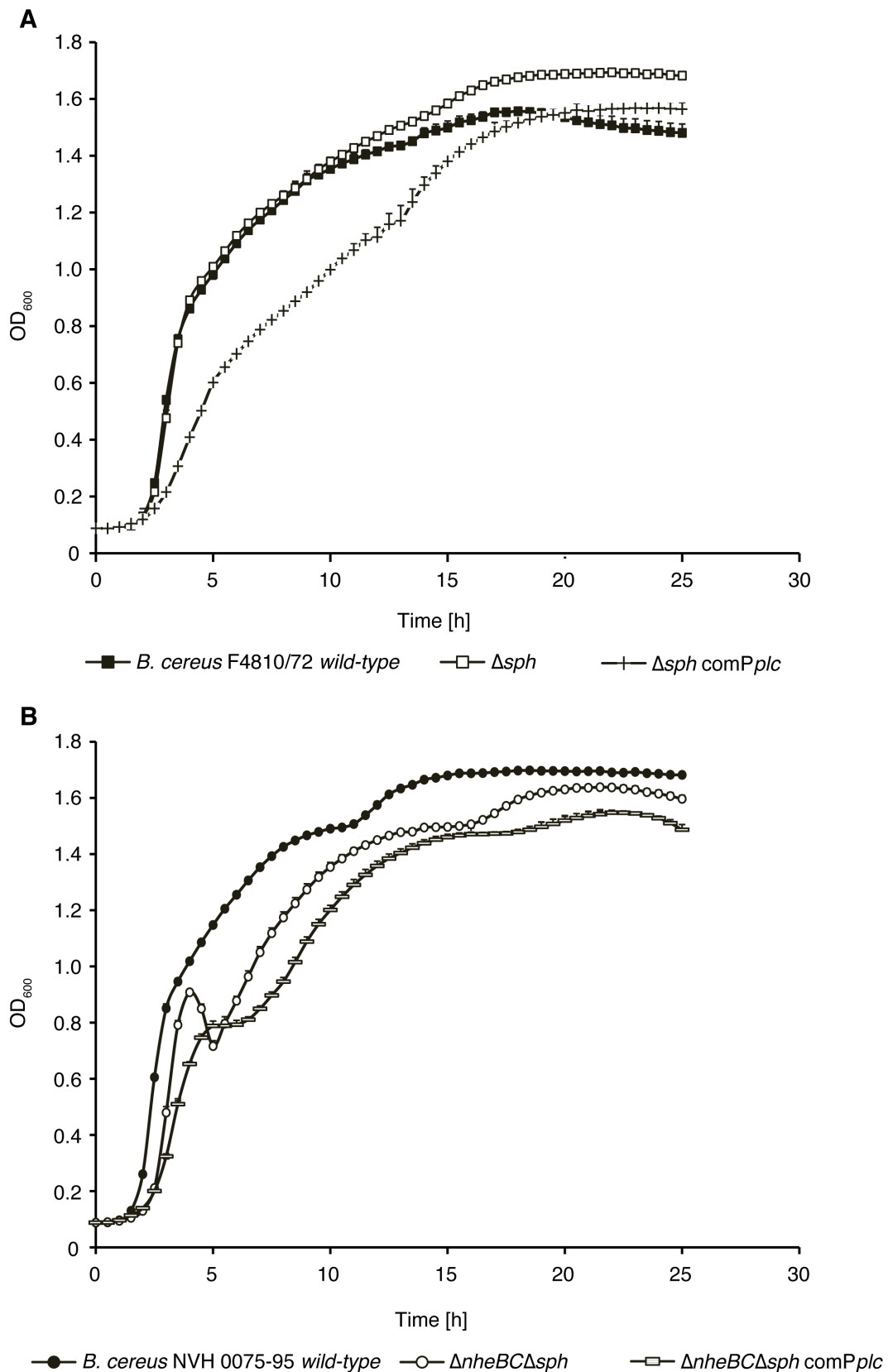


Figure 22: Growth of *B. cereus* wild-type and deletion mutants compared to their complemented strains. Kinetics of **A:** *B. cereus* F4810/72 wild-type, Δsph , Δsph comPplc and **B:** *B. cereus* NVH 0075-95 wild-type, $\Delta nheBC\Delta sph$ and $\Delta nheBC\Delta sph$ comPplc growth in 200 μ l LB at 37 °C and 60 rpm (100-well plate, Bioscreen C). Growth curves present mean values + SEM of five technical replicates of one representative experiment (n=3).

Additionally, growth kinetics of complemented strains were compared to *wild-type* and deletion mutants. In a Bioscreen C system growth in LB medium containing the appropriated antibiotics was monitored by OD₆₀₀ measurement in 100-well plates. Plates were inoculated with approximately 1 x 10⁶ CFU/ml and incubated at 37 °C with continuous shaking. As illustrated in Figure 22A, growth kinetics of *B. cereus* F4810/72 *wild-type* and Δsph were similar, while Δsph comP*plc* paralleled onset of logarithmic growth phase, but grew slower to the same maximal bacterial density.

B. cereus NVH 0075-95 $\Delta nheBC\Delta sph$ and its complemented strain $\Delta nheBC\Delta sph$ comP*plc* revealed comparable growth kinetics (Figure 22B). However they started the logarithmic growth phase with a 0.5 – 1 h delay and grew to a slightly lower maximum OD₆₀₀ than *B. cereus* NVH 0075-95 *wild-type*. Most probably, differences in growth must be attributed to the selective pressure through the use of chloramphenicol and tetracycline.

3.1.6.4 SMase expression and activity

To confirm absence of *sph* expression and secretion in *sph* deletion mutants concentrated bacterial supernatants of deletion mutants, complemented and parental strains were analysed by immuno blotting. Secreted SMase could be detected by western blot in *B. cereus* F4810/72, *B. cereus* NVH 0075-95 *wild-type* and $\Delta nheBC$ supernatant as a distinct protein band (34 kDa) of almost equal intensity (Figure 23). *Sph* deletion resulted in a complete loss of SMase protein expression in *B. cereus* F4810/72 Δsph , *B. cereus* NVH 0075-95 Δsph and $\Delta nheBC\Delta sph$. Complementation of the *sph* deletion using P*plc* as driving promoter showed high levels of SMase protein secreted by Δsph comP*plc* and $\Delta nheBC\Delta sph$ comP*plc* exceeding *wild-type* levels.

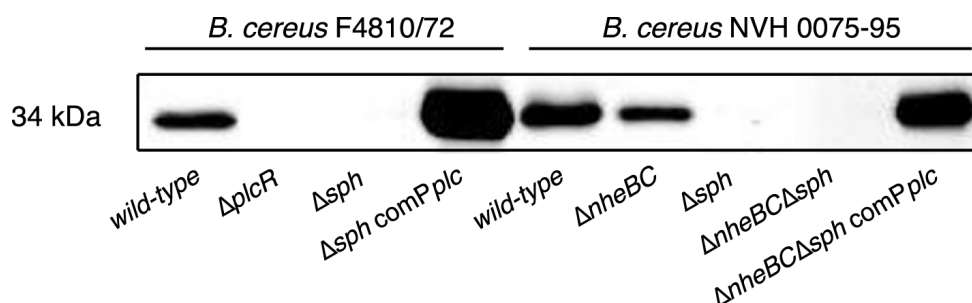


Figure 23: Characterization of *sph* deletion mutants, complemented and parental strains on protein level. Western blot analysis of bacterial supernatants using a polyclonal anti-SMase antibody (1:1000).

Since protein levels not always equal actual enzyme activity, concentrated supernatant samples were analysed in a SMase activity assay as described by Nishiwaki *et al.*, 2004 (Nishiwaki *et al.* 2004). SMase activity was measured as fluorescence intensity (FI) for different substrate concentrations (10 – 200 μ M sphingomyelin) and relative enzyme activity (200 μ M sphingomyelin) is illustrated in Figure 24. Both *wild-type* strains and the $\Delta nheBC$ mutant clearly showed SMase activity with 2.23 ± 0.30 -, 2.14 ± 0.23 - and 1.93 ± 0.16 – fold increases in FI at 200 μ M sphingomyelin compared to the lowest substrate concentration (10 μ M) (Figure 24). In contrast, all *sph* deletion mutants did not exhibit SMase activity as indicated by significantly less changes of FI comparable to mock control (LB dialysed against assay buffer). Deletion of *plcR* resulted in a strong decrease of SMase activity, even if not completely to mock level. Complementation using *Pplc* driven *sph* expression resulted in significantly increased SMase activity of Δsph com*Pplc* ($P=0.002$) and $\Delta nheBC\Delta sph$ com*Pplc* ($P=0.001$) (1.41 ± 0.04 - and 1.35 ± 0.03 -fold FI change, respectively), however lagging behind *wild-type* levels (Figure 24).

These results clearly approve the complete loss of SMase protein and enzyme activity by *sph* gene deletion that can be reconstituted by *sph* expression driven from the *Pplc* operon promoter region.

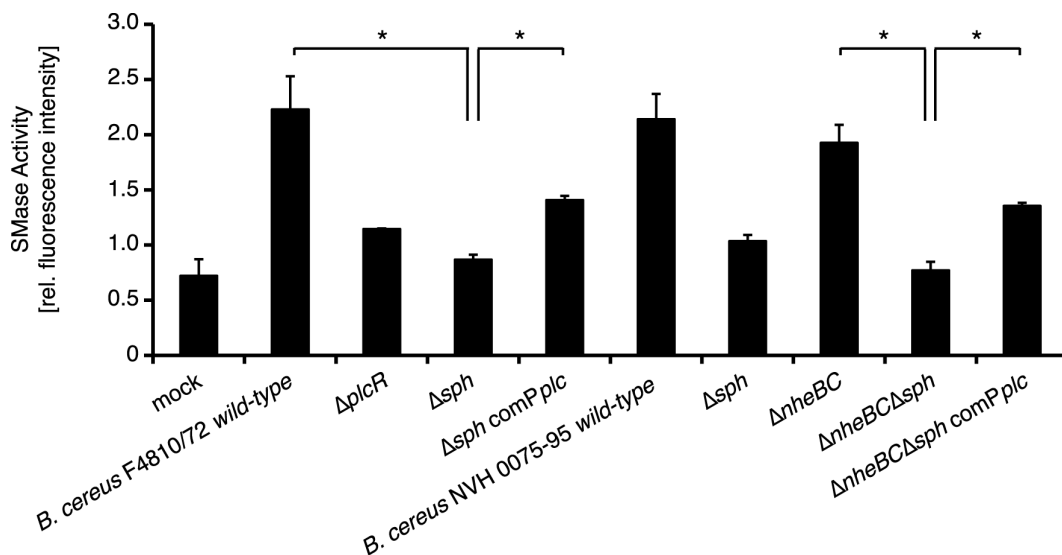


Figure 24: Sphingomyelin-hydrolysing activity of concentrated bacterial supernatants measured by Amplex[®] Red Sphingomyelinase Assay Kit (Invitrogen). The relative enzyme activity with 200 μ M sphingomyelin at 37 °C was calculated and data plotted represent the mean \pm SEM ($n = 3$). *Sph* deletion completely abolished SMase activity of *B. cereus* F4810/72 Δsph , *B. cereus* NVH 0075-95 Δsph and $\Delta nheBC\Delta sph$ compared to *wild-type* and $\Delta nheBC$; * $P \leq 0.01$.

3.1.7 Contribution of SMase to *B. cereus* cytotoxicity *in vitro*

Analysis of the *sph* deletion mutants in the initial screen for colon epithelial cell cytotoxicity, which is based on the morphological characteristics cell rounding and detachment revealed that the contribution of SMase as a single factor to *B. cereus* cytotoxicity was small compared to *wild-type*. However, in combination with *nheBC* deletion *sph* knockout had a much bigger effect on IEC cytotoxicity (Table 9).

Time [h]	<i>Bacillus cereus</i>				
	F4810/72	F4810/72 Δsph	NVH 0075-95	NVH 0075-95 $\Delta nheBC$	NVH 0075-95 $\Delta nheBC$ Δsph
0	Green	Green	Green	Green	Green
0.5	Orange	Orange	Orange	Yellow	Yellow
1.0	Red	Orange	Red	Yellow	Yellow
2.0	Red	Red	Red	Orange	Yellow
3.0	Red	Red	Red	Orange	Yellow
4.0	Red	Red	Red	Orange	Yellow
5.0	Red	Red	Red	Orange	Yellow
6.0	Red	Red	Red	Red	Yellow

Table 9: Cytotoxic effect of sterile supernatant of *B. cereus wild-type* and mutant strains. Ptk6 cells were treated with *B. cereus* F4810/72 and NVH 0075-95 *wild-type* and isogenic mutant strains. Morphological changes of Ptk6 cells were monitored over time using light microscopy. Intact monolayer (green), cell rounding < 50% (yellow), cell rounding > 50% (orange) and 100% cell detachment (red) are indicated.

In order to quantify the influence of SMase on cell cytotoxicity, polarized IEC were incubated for 4 h with bacterial supernatant of the different *B. cereus wild-type* and mutant strains. After staining with Propidium iodide (PI), cells were analysed via flow cytometry. *B. cereus* F4810/72 $\Delta plcR$ supernatant treated IECs had 16.6% \pm 0.9 PI positive cells and were not significantly different to mock treated IECs (11.4% \pm 0.2) (Figure 25). Treatment of epithelial cells with supernatant of the *B. cereus* NVH0075-95 $\Delta nheBC$ mutant strain resulted in 87.5% \pm 1.6 PI positive cells, which was significantly reduced to 30.6% \pm 4.6 after the additional *sph* deletion in *B. cereus* NVH 0075-95 $\Delta nheBC\Delta sph$ ($P < 0.0001$). *Sph* deletion in NVH 0075-95 had a very small effect on *B. cereus* cytotoxicity (95.6% \pm 7.8 PI positive cells) similar to the results of the earlier screening (Table 9). Since the supernatants of *B. cereus* F4810/72, NVH 0075-95 *wild-type* and *B. cereus* F4810/72 Δsph completely detached IEC as a cellular sheet, it was impossible to isolate single cells for flow cytometry analysis with these strains and cytotoxicity was therefore set 100% (Figure 25). The effect of *sph* deletion on Ptk6 cytotoxicity was rescued in the SMase complemented strain *B. cereus* NVH 0075-95 $\Delta nheBC\Delta sph$ *comPplc*. Treatment with $\Delta nheBC\Delta sph$ *comPplc* supernatant resulted in 85.7% \pm 2.7 PI positive cells similar to *B. cereus* NVH 0075-95 $\Delta nheBC$. These results show that SMase has a synergistic effect to Nhe induced cytotoxicity toward polarized epithelial cells *in vitro*.

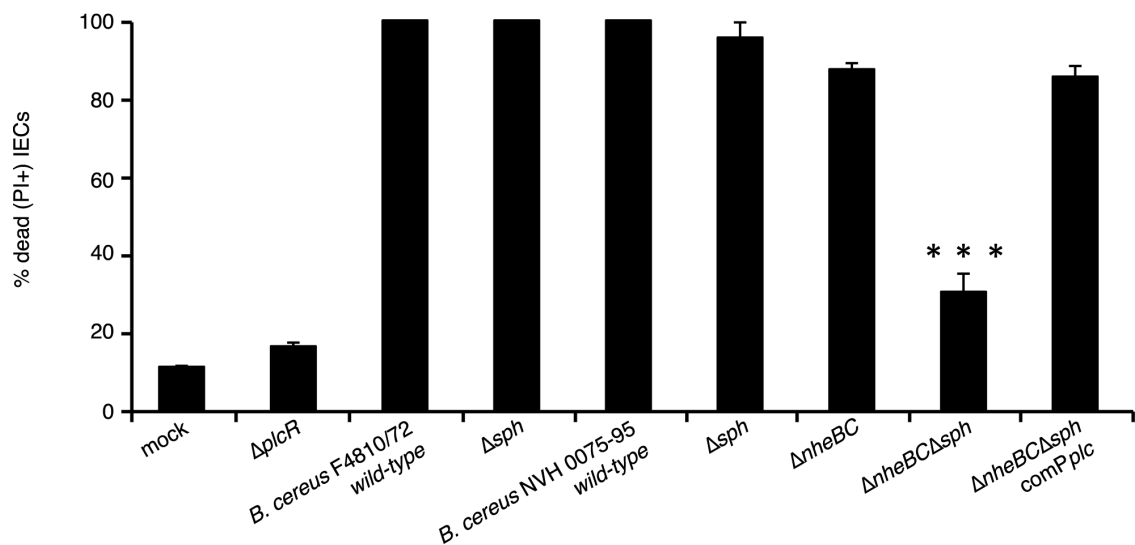


Figure 25: Flow cytometric analysis of cytotoxic effects of *B. cereus* supernatant on intestinal epithelial cells. Ptk6 cells were treated with bacterial supernatant stained with Propidium iodide (PI). *Sph* deletion in addition to *Nhe* inactivation significantly reduced cytotoxicity compared to *Nhe* inactivation alone ($***P < 0.0001$). Cytotoxicity was restored in *B. cereus* $\Delta nheBC\Delta sph$ comPplc. % dead cells (total PI positive cells) were determined from dot plot analysis. Data plotted represent mean values \pm SEM (n = 4).

3.1.8 Contribution of SMase to *B. cereus* pathogenicity in vivo

Additionally, the role of SMase for *B. cereus* entomopathogenic activity was assessed *in vivo*. *G. mellonella* larvae were injected with $1-2 \times 10^5$ CFU/larva *B. cereus* F4810/72 wild-type, $\Delta plcR$, Δsph , *B. cereus* NVH 0075-95 wild-type, $\Delta nheBC$ and $\Delta nheBC\Delta sph$ mutant strains as well as *E. coli* DH10B (7×10^5 CFU/larva) as mock control. Survival of larvae was monitored over seven days and Kaplan-Meier survival curves are shown in Figure 26.

Larvae injected with mock control survived the monitoring period in $81.5\% \pm 3.9$. *PlcR* deletion significantly reduced *B. cereus* F4810/72 pathogenicity compared to wild-type when larvae were infected intrahaemocoelical ($P < 0.0001$). After seven days $56.9\% \pm 4.3$ of larvae injected with $\Delta plcR$ survived (Figure 26A). Mortality rate of *B. cereus* F4810/72 (Figure 26A) and NVH 0075-95 wild-type (Figure 26B) injected *G. mellonella* larvae was $> 50\%$ after 3 and $> 85\%$ after 7 days. Surprisingly, the survival curve of *B. cereus* NVH 0075-95 $\Delta nheBC$ injected larvae was not different to wild-type suggesting that *Nhe* contributes little to larvae mortality (Figure 26B). Deletion of *sph* alone (Δsph) or in combination with *nheBC* ($\Delta nheBC\Delta sph$) significantly reduced *G. mellonella* mortality to $42.3\% \pm 4.3$ and $33.1\% \pm 4.1$ after 3 and $76.9\% \pm 3.7$ after 7 days, respectively ($P < 0.0001$ and $P = 0.0002$). In line with the observation with wild-type *B. cereus* strains, *Nhe* did not contribute to *B. cereus* induced larvae death (Figure 26B).

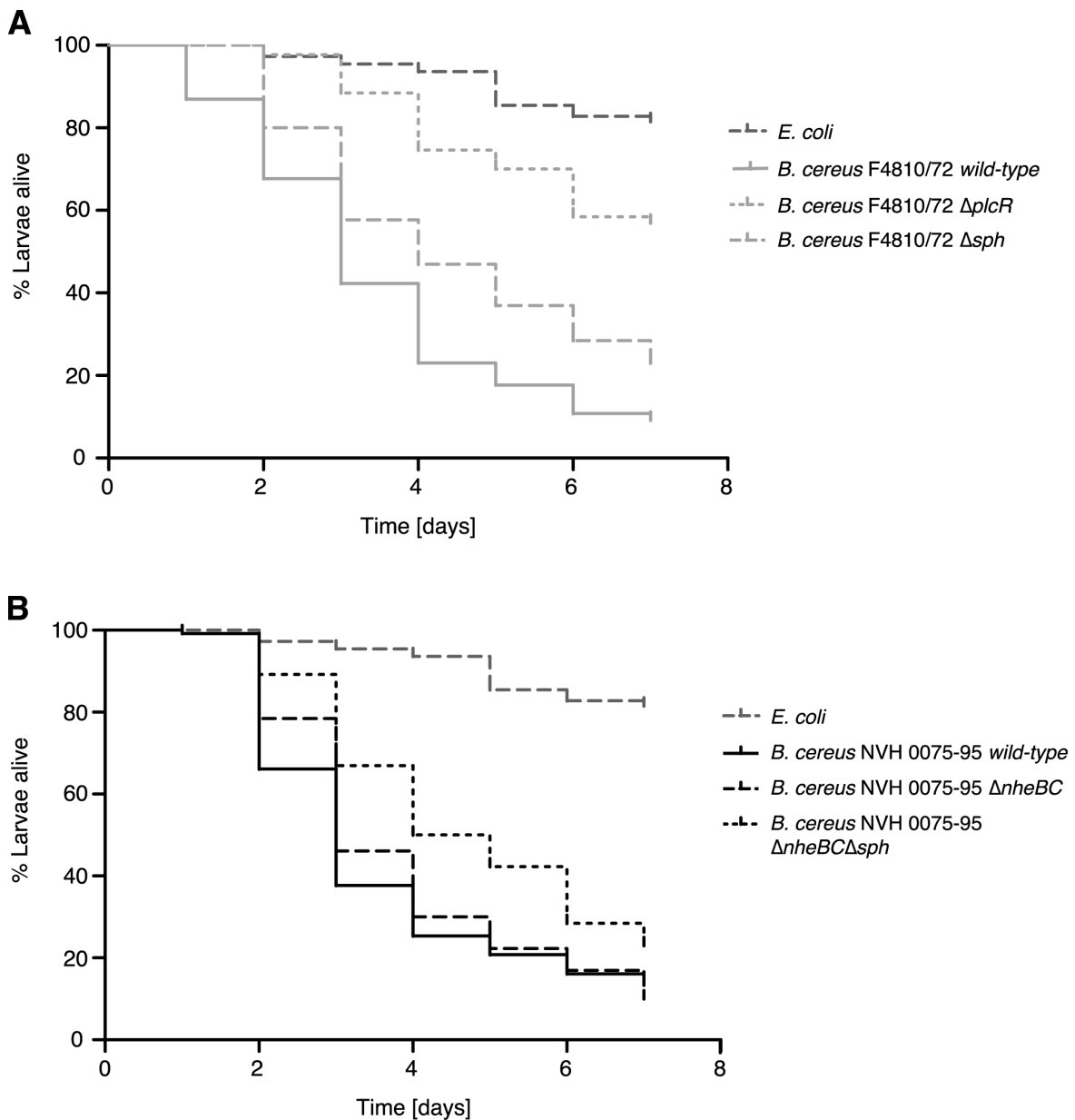


Figure 26: Survival of *G. mellonella* larvae injected with *B. cereus* F4810/72. **(A)** and *B. cereus* NVH 0075-95 **(B)** *wild-type* and isogenic mutant strains at 15 °C. Larvae injected with *E. coli* DH10B served as controls (dark grey dotted line). Survival curves of larvae injected with *sph* deletion mutants significantly differed from *wild-type* injected larvae. The *plcR* deletion mutant **(A)** was strongly reduced in its entomopathogenic potential, while deletion of *nheBC* **(B)** had no significant effect on *B. cereus* pathogenicity. The Kaplan-Meier plots are based on four independent experiments ($n \geq 110$ animals per curve).

The observed differences in larvae mortality were not due to differences in bacterial growth of the various *B. cereus* strains *in vivo* (Figure 27). Bacterial counts increased within the first three days of infection for all strains tested. All *wild-type* and isogenic mutant strains showed similar growth kinetics reaching a constant maximal bacterial count of $0.25 - 3 \times 10^9$ CFU/larva at day three after injection. While bacterial growth increased five-fold within the first four hours of infection for all strains, 24 and 48 h after injection bacterial count within individual larva was very heterogeneous for all bacterial strains (Figure 27A and B). As bacterial growth precedes larvae mortality, data indicates that bacterial intralarval growth is a prerequisite for larvae death.

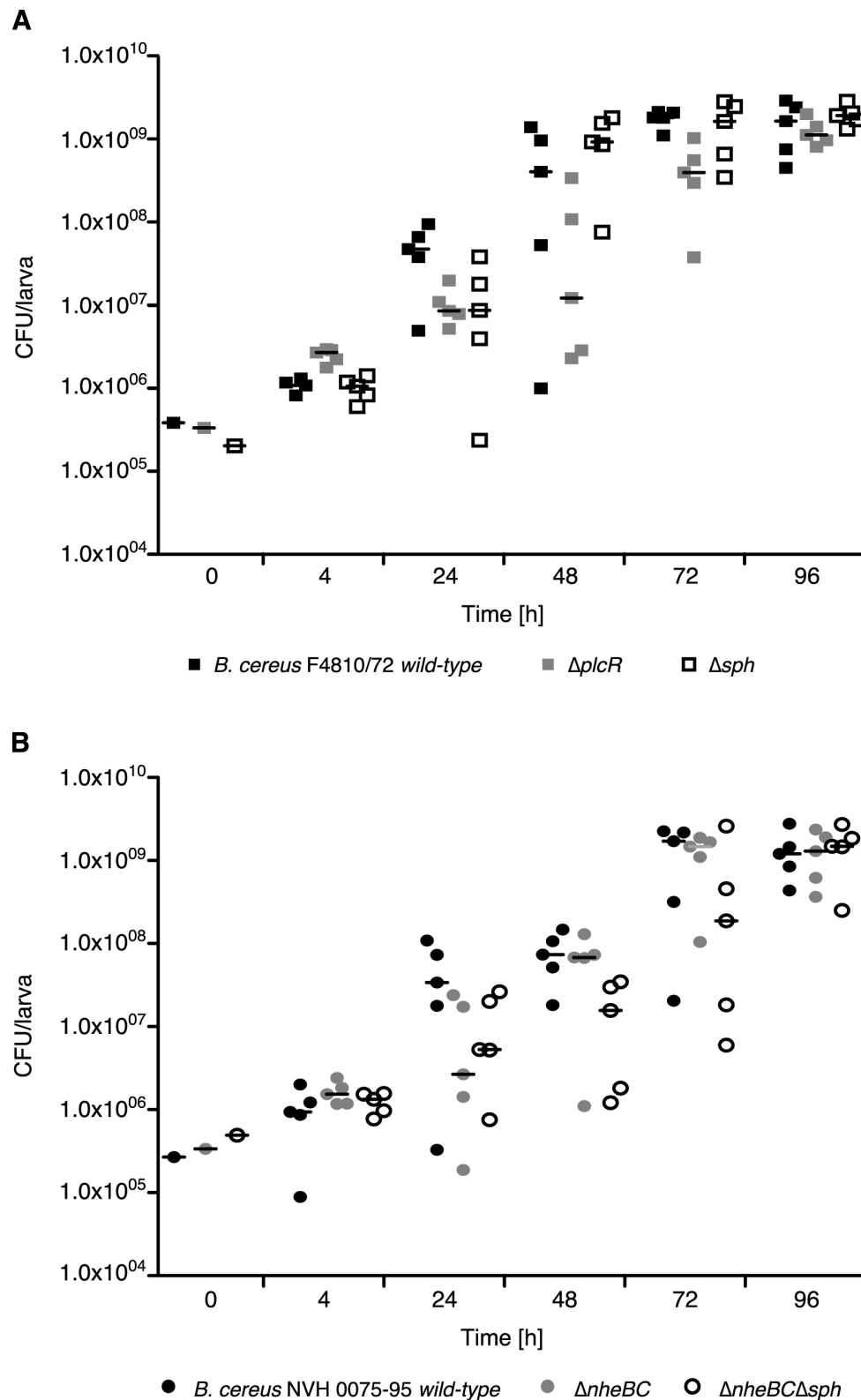


Figure 27: Growth of *B. cereus* wt and mutant strains in *G. mellonella* larvae. To define growth kinetics of *B. cereus* in *G. mellonella* larvae, the bacterial counts (CFU/larva) at several time points after infection with (A) *B. cereus* F4810/72 wild-type, $\Delta plcR$, Δsph and (B) NVH0075-95 wild-type, $\Delta nheBC$ and $\Delta nheBC\Delta sph$ were determined. At time points indicated serial dilutions of homogenates of 5 larvae were plated individually. Resulting mean values are indicated as black bars. Representative results of one of two independent experiments are shown.

3.2. *B. cereus* growth characterization

The previous chapters focussed on the influence of *B. cereus* on epithelial cell survival *in vitro* and insect larvae coping with *B. cereus* infection *in vivo*. Thereby the enzyme activity of single protein toxins, as Nhe and SMase, as well as master transcriptional regulators of the pathogen side took center stage. On the other hand it is undeniable that the epithelial cells as first host defence line against bacterial pathogens play an essential role in the decision process between infection clearance or disease initiation. Therefore, it is of vital importance to characterise not only the direct host-pathogen interaction, but also the effect of secreted molecules of both interaction partners. To gain insights into the reactions of the pathogen to host derived microenvironmental changes and in particular host driven bacterial gene regulation can help to decipher the complex host-pathogen interaction network. Detailed analysis of the initial steps of *B. cereus* colonizing the gastrointestinal tract of a host may lead to the identification of target molecules or mechanisms for drug development. Since *B. cereus* is a common contaminant in the food processing chain novel therapeutics should aim to successfully inhibit *B. cereus* spore outgrowth and colonization of the host.

Initially, growth of the emetic type strain *B. cereus* F4810/72 and its isogenic $\Delta plcR$ mutant was investigated under more 'gut-like' conditions than the standard cultivation in shaking flasks. Different growth media and supplements were inoculated in cell culture dishes with 1×10^3 CFU/ml and incubation was carried out at 37 °C without agitation. Bacterial growth was monitored over eight hours by plating serial dilution on LB agar. Growth of *B. cereus* in standard LB medium was compared to cell culture medium RPMI 1640 (Invitrogen) used for Ptk6 cultivation, containing 5% FBS, Insulin-Transferrin-Selenium A and interferon γ as supplements. When this fully supplemented cell culture medium was used similar growth kinetics to LB medium were achieved (data not shown). Since FBS is a very rich, but more or less undefined source of nutrients, it was not unexpected to promote bacterial growth. To have a defined nutrient source applicable for cell culture pure unsupplemented (unsuppl.) RPMI 1640 medium was used which is, according to the ingredient list of RPMI 1640, almost identical to the commonly used bacterial minimal medium (MOD). While growth of *B. cereus* F4810/72 *wild-type* and $\Delta plcR$ mutant was identical in LB medium (Figure 28), the lag phase of *wild-type B. cereus* was extended to 3.5 hours in unsuppl. cell culture medium compared to 2 hours in LB. Surprisingly, *plcR* deletion completely inhibited bacterial growth in unsuppl. cell culture medium (Figure 28). This growth deficit of $\Delta plcR$ mutant was also observed in minimal medium when grown in shaking flasks (data not shown). In RPMI 1640 bacterial counts of the $\Delta plcR$ mutant decreased one order of magnitude 2 hours after inoculation and remained constant over the monitored period. However, there were no hints that RPMI 1640 mortifies *B. cereus* $\Delta plcR$. Growth deficit of $\Delta plcR$ mutant observed in cell culture dishes could also be reproduced in two independent experiments carried out in shaking flasks (data not shown). The result suggests the essential involvement of PlcR in stimulating bacterial growth initiation in unelaborated medium.

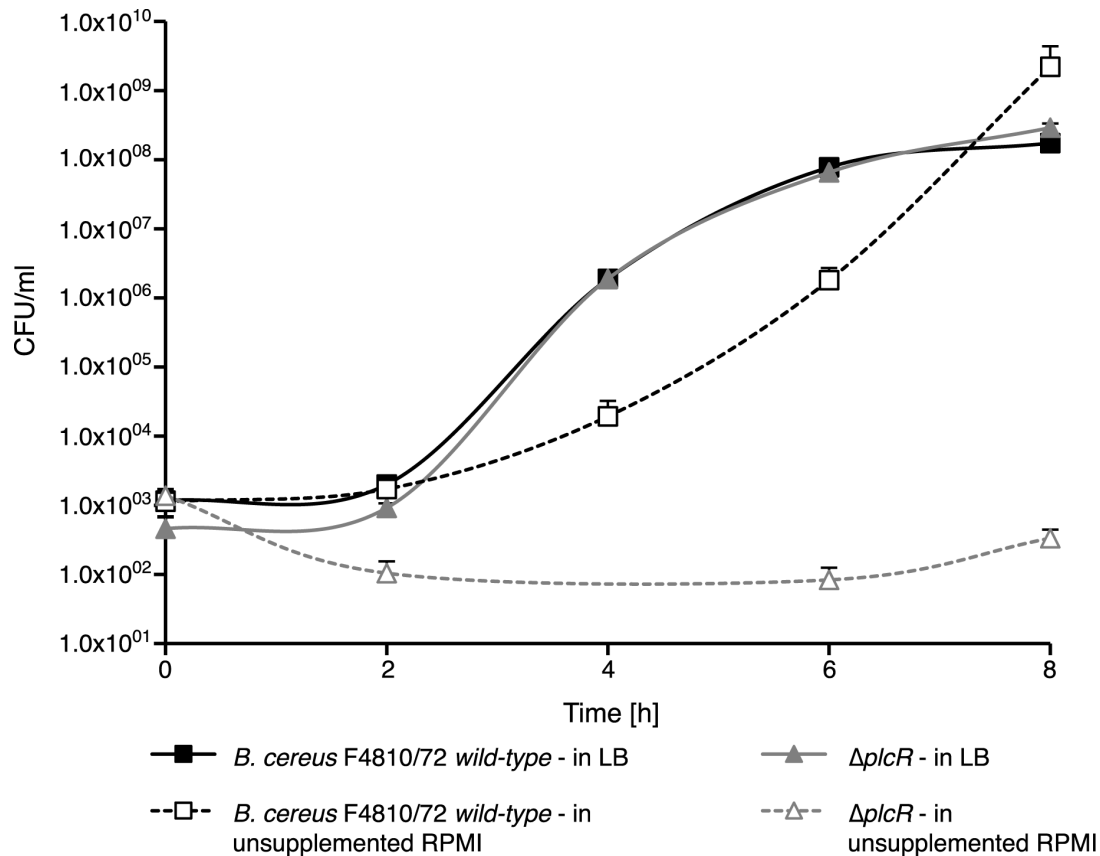


Figure 28: Growth kinetics of *B. cereus* F4810/72 wild-type and $\Delta plcR$ in LB medium compared to unsupplemented cell culture medium. 25 ml of the respective medium in cell culture dishes were inoculated with 1×10^3 CFU/ml. Bacterial growth at 37 °C without agitation was monitored by plating serial dilutions at time points indicated. Growth curves represent mean values + SEM ($n \geq 3$).

3.2.1 Growth deficit of the $\Delta plcR$ mutant can be rescued by bacterial and host factors

PlcR-regulated growth stimulation can be mediated by cytosolic *B. cereus* active compounds or by extracellular proteins. To test if the latter contribute to *B. cereus* growth regulation, wild-type *B. cereus* F4810/72 has been grown in unsuppl. medium for 8 h thus enabling the secretion of potential growth promoting factors into the supernatant. If so, the generated sterile ($0.2 \mu\text{m}$) medium conditioned by bacteria (cbRPMI) should be able to stimulate growth of the *plcR* deletion mutant.

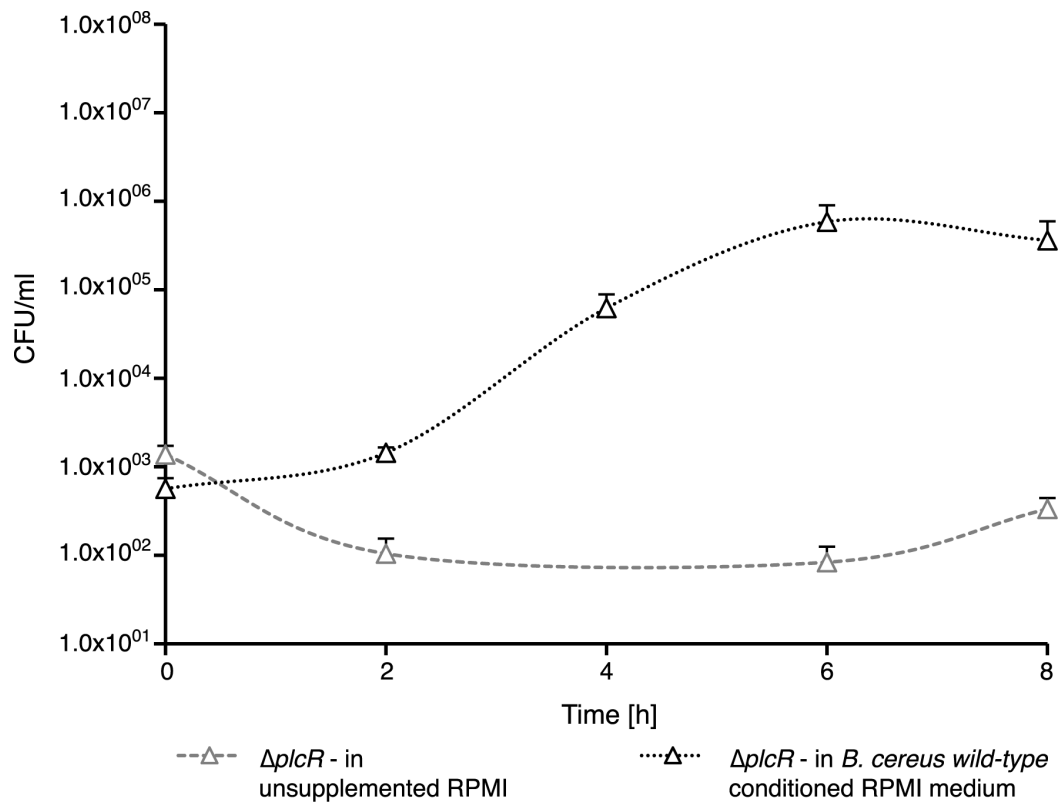


Figure 29: Growth rescue of *B. cereus* F4810/72 $\Delta plcR$ in unsupplemented cell culture medium by conditioning with *wild-type Bacillus. B. cereus wild-type* has been grown in unsuppl. RPMI1640 for 8 h and conditioned medium was harvested by sterile filtration ($0.2 \mu\text{m}$). Growth of $\Delta plcR$ is significantly induced when using preconditioned medium (black dotted line) compared to unsupplemented cell culture medium (grey dashed line). Bacterial growth at 37°C without agitation was monitored by plating serial dilutions at time points indicated. Growth curves represent mean values + SEM (n=3).

In fact, cbRPMI rescued $\Delta plcR$ growth to a significant level compared to unsuppl. medium (Figure 29). As illustrated in Figure 29 *wild-type* conditioned medium stimulated $\Delta plcR$ growth over 2.5 orders of magnitude to a maximal bacterial count of 0.6×10^6 CFU/ml 6 h after inoculation. Since afterwards bacterial count remains stable, even slightly decreasing after 8 h, data suggest that growth promoting factors contained in cbRPMI either were consumed by $\Delta plcR$ or were degraded during the incubation period. Thus, *plcR* deletion mutants lacking nutrients or growth stimulus slow down and stop growth.

Not only *B. cereus* derived factors were able to rescue $\Delta plcR$ growth in unsupplemented medium. Co-cultivation of intestinal epithelial monolayers with the bacterial mutant strain restored bacterial growth to a maximal bacterial count of 0.8×10^6 CFU/ml 8 h after inoculation (Figure 30). Incubation of *B. cereus* $\Delta plcR$ in sterile ($0.2 \mu\text{m}$) RPMI medium preconditioned with Ptk6 cells for 24 h (chRPMI) revealed growth stimulation within 2 - 3 h (Figure 30), indicating a role for Ptk6 secreted growth promoting compounds rather than stimulation mediated through direct contact. Early onset of $\Delta plcR$ growth and decrease of bacterial counts after 8 h in chRPMI (Figure 30) similar to growth kinetics in cbRPMI (Figure 30) hints to the degradation/consumption of preformed growth promoting factors during bacterial growth.

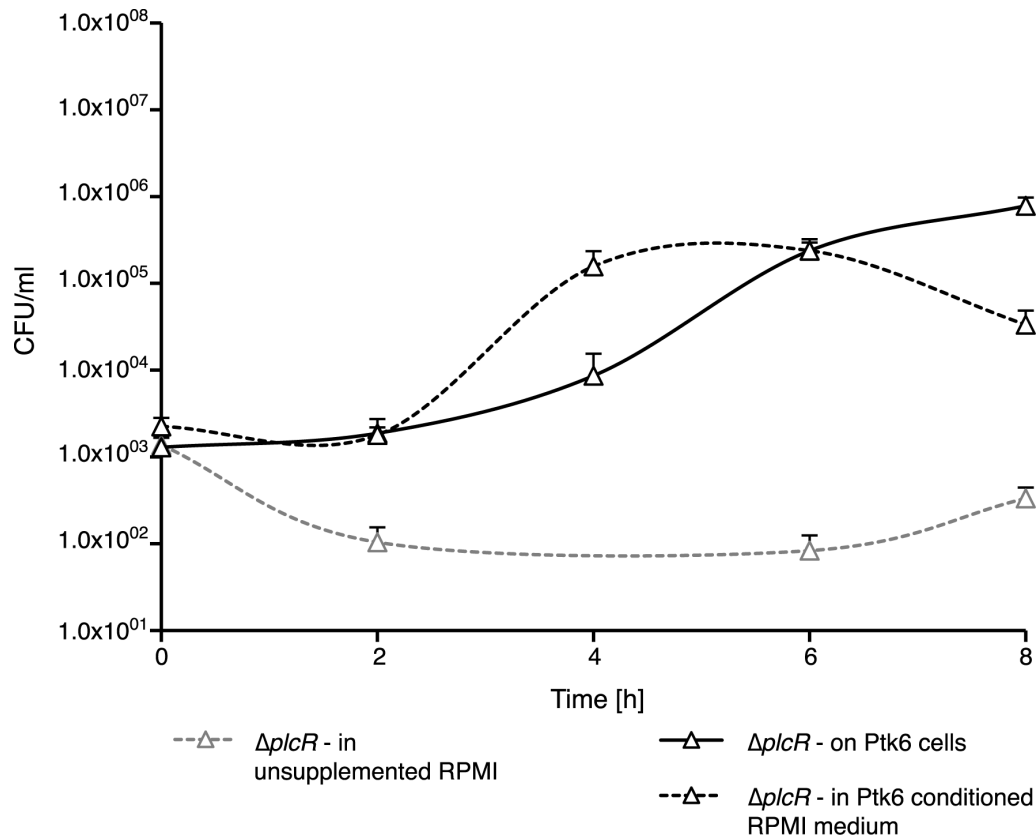


Figure 30: Growth rescue of *B. cereus* F4810/72 $\Delta plcR$ in unsupplemented cell culture medium by conditioning with IEC or co-cultivation. Ptk6 cells have been grown in unsuppl. RPMI 1640 for 24 h and conditioned medium was harvested by sterile filtration ($0.2 \mu\text{m}$). Growth of $\Delta plcR$ is significantly induced when using Ptk6 preconditioned medium (black dashed line) or growing on Ptk6 monolayers (black line) compared to unsupplemented cell culture medium (grey dashed line). Bacterial growth at 37°C without agitation was monitored by plating serial dilutions at time points indicated. Growth curves represent mean values + SEM ($n=3$).

In contrast, co-cultivation on Ptk6 resulted in higher maximal bacterial counts despite a delayed onset of growth (Figure 30), as growth stimulating compounds are not available right from the inoculation, but are secreted throughout the incubation period by viable intestinal cells. These results suggest that secreted factors of *B. cereus* as well as of IEC promote bacterial growth of *B. cereus* independent of direct cell-cell contact.

3.2.2 *InhA2* is involved in *B. cereus* growth regulation

3.2.2.1 Identification of *InhA* proteins as possible growth promoting factors

To identify PlcR-regulated extracellular factors promoting *B. cereus* growth under nutrient limiting conditions, supernatant of *B. cereus* F4810/72 *wild-type* grown in unsupplemented RPMI medium was harvested and sterile filtered ($0.2 \mu\text{m}$). FPLC size separation (Superdex-75 10/300 GL column) of concentrated extracellular proteins resulted in 19 fractions (7 – 23) containing 90% of the total secreted proteins (Figure 31).

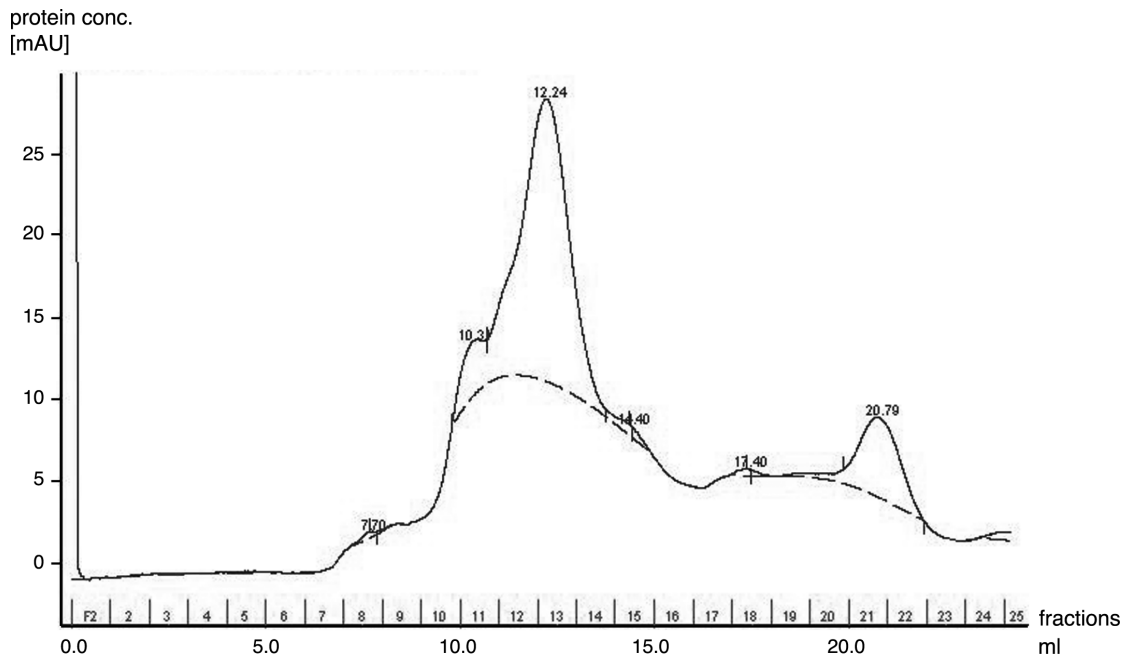


Figure 31: Protein separation of *B. cereus* F4810/72 supernatant via gel filtration. Secreted proteins were fractionated by size on a Superdex-75 10/300 GL gel filtration column and 1 ml fractions were obtained.

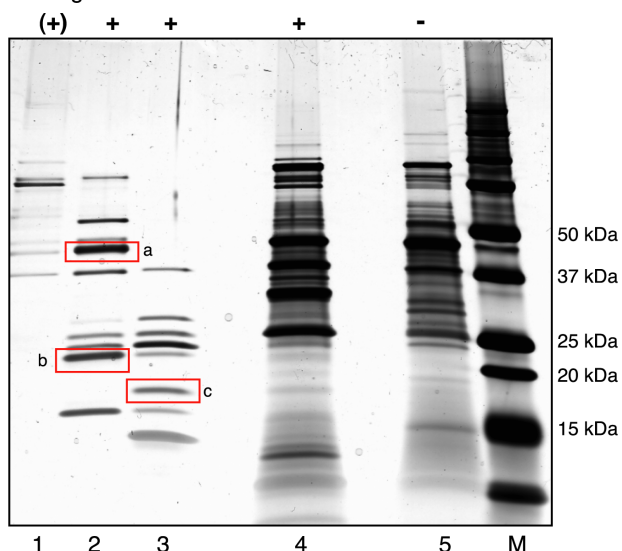
Six main protein peaks could be detected by their absorbance at 280 nm. These peaks eluted at 7.70, 10.31, 12.24, 14.40, 17.40 and 20.79 ml. All protein fractions were tested for their growth promoting capacity by inoculation with *B. cereus* $\Delta plcR$, incubation at 37 °C and CFU determination. Growth stimulating proteins were confined to fractions 11 and 12 corresponding to the second peak (10.31 ml).

Similar to chapter 3.1.3, SDS gel electrophoresis analysis of these two fractions was carried out. Comparison of proteins contained in growth promoting fractions of two independent gel filtration runs with total bacterial supernatant of *B. cereus* F4810/72 *wild-type* and $\Delta plcR$ identified three candidate protein bands (a, b, c in Figure 32) involved in growth promotion.

The three assigned protein bands at 45 kDa (a), 22 kDa (b) and 16 kDa (c) were sent to Proteome Factory AG (Berlin, Germany) as silver stained gel slices. NanoLC-ESI-MS/MS analysis did not provide significant hits for the two smaller protein bands (22 and 16 kDa). Only the 45 kDa protein was unambiguously identified as immune inhibitor A (InhA) of *B. cereus*. Database search with two unique peptide sequences, (K)LAVDPVAIEGTK(S) and (R)SKLAVDPVAIEGTK(S), revealed highest scores for the immune inhibitor A protein of *B. cereus* R309803 (gil229159747).

Growth promoting

activity



1: Fraction 10 (*wild-type* supernatant)
 2: Fraction 11 (*wild-type* supernatant)
 3: Fraction 12 (*wild-type* supernatant)
 4: *B. cereus* F4810/72 *wild-type* supernatant
 5: *B. cereus* F4810/72 Δ *plcR* supernatant
 M: prestained protein marker

Figure 32: SDS-PAGE analysis of growth promoting gel filtration fractions (+). Silver stained SDS gels demonstrated three distinct proteins at 45 kDa (a), 22 kDa (b) and 16 kDa (c) in the protein fractions, which were not expressed in the supernatant of the growth deficient Δ *plcR* strain. Protein bands a – c were identified via comparison of total extracellular proteins of *wild-type* and mutant *B. cereus* strains. Prestained protein marker (M).

B. cereus, like *B. thuringiensis* encodes for three immune inhibitor A proteins InhA1, InhA2 and InhA3. All three proteins exhibit metalloprotease activity and share more than 66% identity. BLASTN database search using the published gene sequences from the *B. cereus* type strain ATCC 14579 chromosome (NC_004722) (Guillemet *et al.* 2010) allowed the assignment of the sequences to the corresponding homologue genes and proteins in *B. cereus* F4810/72 (AH187) (NC_011658) (Table 10). The protein resulting from MS/MS identification was matched to InhA2 by BLASTP alignment of the two unique peptide sequences with the *B. cereus* F4810/72 InhA1, InhA2 or InhA3 protein sequence. Detailed sequence information about the InhA1, InhA2 and InhA3 proteins is provided in Table 10.

Table 10: Detailed gene and protein sequence information on the three immune inhibitor proteins A of *B. cereus* ATCC 14579 and *B. cereus* F4810/72.

<i>B. cereus</i> ATCC 14579			<i>B. cereus</i> F4810/72 (AH187)						
Gene locus tag ^a	Protein identification number (NCBI)	% ^b Identity	Gene locus tag	Protein identification numbers (NCBI) ^c	aa	% Identity ^d to InhA1	% Identity ^d to InhA2	% Identity ^d to InhA3	
InhA1	BC1284	gil30019435, NP_831066	94	BCAH187_A1437	gil217064622, ACJ78872	795	100	67	73
InhA2	BC0666	gil30018848, NP_830479	97	BCAH187_A0800	gil217067733, gil217958257, ACJ81983	799	67	100	70
InhA3	BC2984	gil30021099, NP_832730	96	BCAH187_A3035	gil217067441, ACJ81691	794	73	70	100

^a taken from Guillemet *et al.*, 2010

^b % amino acid sequence identity between proteins of *B. cereus* ATCC 14579 and F4810/72 as determined by BLASTP alignment

^c designated by BlastP database search using *B. cereus* ATCC 14579 protein sequences as query

^d % amino acid sequence identity between proteins of *B. cereus*

From all three immune inhibitor A metalloproteases only InhA2 (799 aa) is regulated by PlcR (Gohar *et al.* 2002) and has been characterised as a virulence factor in *B. cereus* pathogenicity in *G. mellonella* larvae (Guillemet *et al.* 2010). InhA2 protein sequence analysis on the SignalP 3.0 server identified a 32 aa signal peptide. Consequently, InhA2 is secreted as a protein of approximately 85 kDa that might be further processed to a smaller mature form such as the one detected after gel filtration with 45 kDa (a in Figure 32). Since bacterial growth and virulence are closely linked in many pathogens, InhA2 seemed to be an auspicious candidate for contributing to *B. cereus* growth regulation. The fact that InhA2 is secreted by *B. cereus* further fortified its possible involvement.

3.2.2.2 InhA2 stimulates *B. cereus* growth

To confirm a role for InhA2 in *B. cereus* growth stimulation by bacterial factors, the *inhA2* gene was cloned as transcriptional fusion with the xylose inducible promoter into the *B. megaterium* expression vector pWH1520 (Rygus and Hillen 1991; a kind gift of W. Hillen). The plasmid was introduced into *B. cereus* F4810/72 *wild-type* and $\Delta plcR$ via electroporation. *InhA2* expression was induced by the addition of D-xylose. Figure 33A and B show Coomassie stained SDS polyacrylamide gels of bacterial supernatants. Initially, three concentrations of D-xylose (0.05, 0.1, 0.5%) were tested for optimal induction of protein expression in LB medium (Figure 33A). InhA2 was detected as a protein of approximately 76 kDa in the supernatant of *B. cereus* F4810/72 $\Delta plcR$ pWHinhA2 induced with all three different D-xylose concentrations, but was absent from $\Delta plcR$ supernatant (Figure 33A). Subsequent experiments were carried out with 0.1% D-xylose, because protein induction was maximal at this concentration (Figure 33A). Comparison of *inhA2* expression levels between *wild-type* pWHinhA2 and $\Delta plcR$ pWHinhA2 revealed similar protein levels secreted, while endogenously expressed InhA2 was under detection limits in the *wild-type* supernatant (Figure 35B).

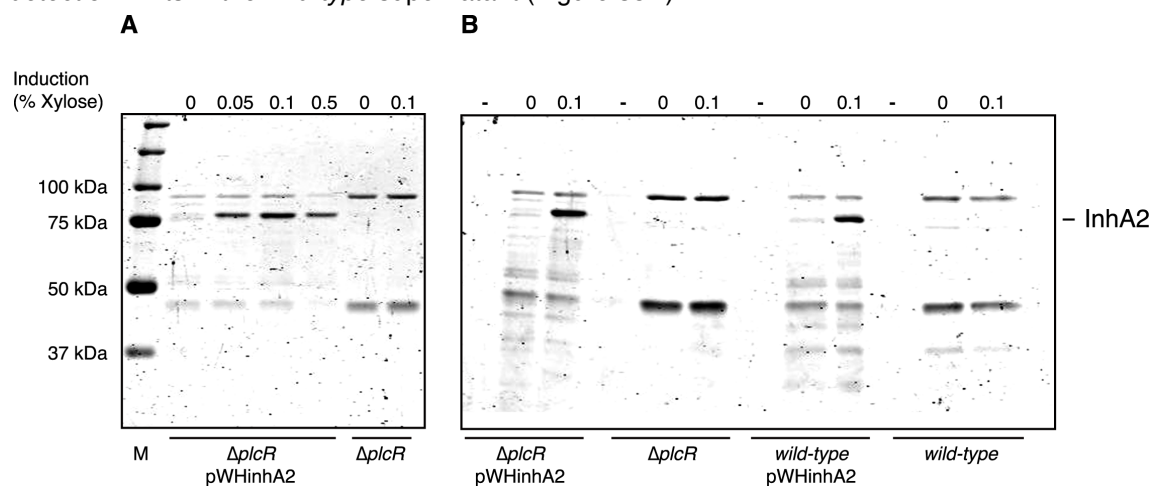


Figure 33: SDS-PAGE analysis of bacterial supernatant for InhA2 expression. **A:** InhA2 production and secretion by *B. cereus* F4810/72 $\Delta plcR$ pWHinhA2 was induced with different D-xylose concentrations (0.05, 0.1, 0.5%) in LB medium. $\Delta plcR$ served as a negative control. **B:** *B. cereus* F4810/72 *wild-type* pWHinhA2 and $\Delta plcR$ pWHinhA2 expressed and secreted InhA2 after xylose induction. Coomassie stained gels are shown. Samples prior to induction (-), without induction (0% xylose) (0), induced with different concentrations of D-xylose (0.05, 0.1, 0.5%), prestained protein marker (NEB) (M).

Weak protein bands in the supernatant of *wild-type* pWHinhA2 and $\Delta plcR$ pWHinhA2 without D-xylose induction (0%) indicate leakiness of the xylose inducible promoter.

After *inhA2* expression and protein secretion had been confirmed for *B. cereus* F4810/72 *wild-type* pWHinhA2 and $\Delta plcR$ pWHinhA2 (Figure 33), these genetically modified strains could be used to test, if *inhA2* expression can influence growth of *B. cereus* $\Delta plcR$ in un-suppl. medium. Therefore, *B. cereus* F4810/72 *wild-type*, *wild-type* pWHinhA2, $\Delta plcR$ and $\Delta plcR$ pWHinhA2 were precultivated in LB medium (15 h) at 37 °C. Subsequently, RPMI 1640 medium containing (+) or lacking (-) 0.1% D-xylose was inoculated with approximately 1×10^6 CFU/ml of each strain. Bacterial growth at 37 °C with continuous shaking was monitored by OD₆₀₀ measurement in 100-well plates (Bioscreen C system). Each experiment included 3-5 technical replicates of each condition and three independent experiments were carried out. Figure 34 illustrates bacterial growth curves of one representative experiment (mean values of 3 technical replicates). Generally, *B. cereus* growth in the nutrient-poor un-supplemented RPMI medium was reduced compared to growth in the full medium LB (see Ch. 3.1.5.3). As expected, similar growth kinetics were observed for *B. cereus* F4810/72 *wild-type* independent of D-xylose addition. However, *B. cereus* F4810/72 *wild-type* pWHinhA2 demonstrated retarded growth compared to *wild-type*. The lag phase was 4 h delayed for *wild-type* pWHinhA2 with D-xylose and 6 h without D-xylose, although maximal bacterial density was higher than for *wild-type* (Figure 34A). These data indicate that accessory *inhA2* expression in *B. cereus* *wild-type* has only a marginal growth promoting effect and is delayed probably due to additional antibiotic pressure (Tet) or increased energy expenditure for additive protein synthesis. In contrast, supplementation of the *plcR* deletion mutant with transiently expressed *inhA2* in $\Delta plcR$ pWHinhA2 resulted in significant growth stimulation 5 h after inoculation with a bacterial cell density maximum of OD₆₀₀ 0.7 similar to *wild-type* pWHinhA2 (Figure 34B). Even without D-xylose induction $\Delta plcR$ pWHinhA2 growth paralleled *wild-type* pWHinhA2, but was characterised by a delay of logarithmic growth phase onset of 8 h compared to xylose addition and larger standard deviations (Figure 34B).

This result suggests a second time that the xylose operon promoter is leaky and *B. cereus* growth regulation is an extremely complex process where minimal protein concentration changes can decide between growth initiation and dormancy. Deletion of *plcR* strongly attenuated *B. cereus* growth in un-suppl. RPMI medium (+/- D-xylose) also in 100-well plates as seen for cultivation in cell culture dishes and shaking flasks before. Although D-xylose cannot be metabolized as C-source by all *B. cereus* strains (e.g. not by the type strain ATCC 14579), there was a slight increase in optical density of $\Delta plcR$ when grown in RPMI medium with 0.1% D-xylose compared to un-suppl. medium (Figure 34B). Therefore, it is tempting to speculate that *B. cereus* F4810/72, like *B. cereus* ATCC 10987 might possess auxiliary genes that enable xylose utilization.

Taken together, InhA2 has been proven to play an essential role in *B. cereus* growth stimulation in nutrient-poor medium or conditions. It would be of great interest to focus further research on InhA2 and secreted metalloproteases in general to elucidate the detailed mechanism involved.

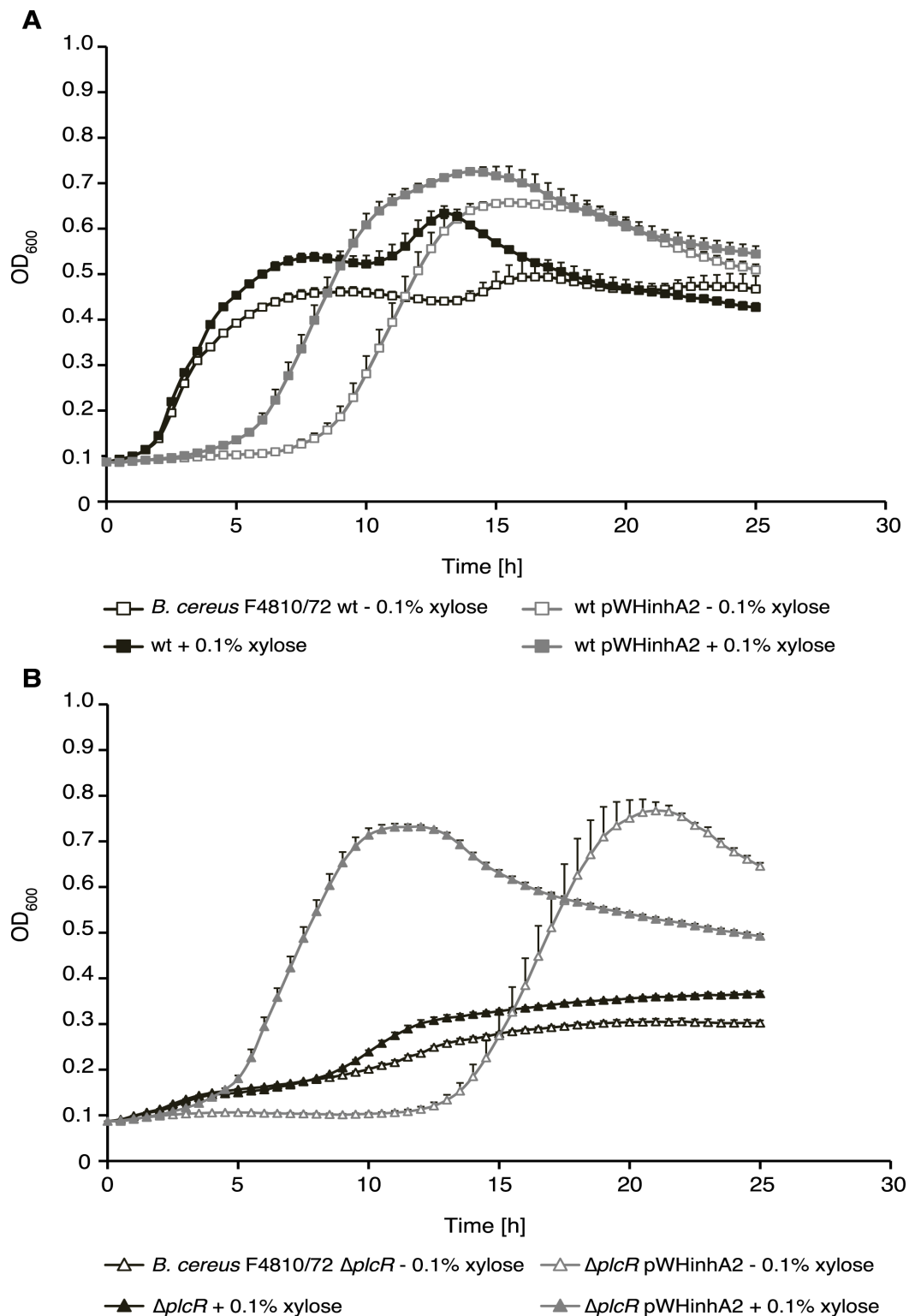


Figure 34: Rescue of *B. cereus* $\Delta plcR$ growth deficit by InhA2. Growth of **A:** *B. cereus* F4810/72 wild-type and pWHinhA2 and **B:** $\Delta plcR$ and $\Delta plcR$ pWHinhA2 in unsuppl. RPMI medium with (+) or without (-) 0.1% D-xylose was monitored. Strains were grown in 200 μ l respective medium at 37 °C and 60 rpm (100-well plate, Bioscreen C). Growth curves represent mean values + SEM of three technical replicates of one out of three representative experiments.

3.2.3 Identification of *B. cereus* proteome changes induced by host epithelial cells

The extracellular metalloprotease InhA2 has been identified as one of the secreted proteins under the control of PlcR that is involved *B. cereus* growth regulation (Ch. 3.2.2). InhA2 is produced by the pathogen itself probably dependent on cell density (as sensed via PapR/PlcR) and can then act in return on its producer by complex stimulation mechanisms.

As demonstrated in the previous chapter 3.2.1, *B. cereus* growth in nutrient-poor medium is also influenced to a great extent by host factors. To investigate the *B. cereus* growth rescue induced by IEC a different approach was chosen. The influence of compounds secreted by intestinal epithelial cells on *B. cereus* growth regulation was investigated on proteome level. Therefore, intracellular and extracellular proteomes of *B. cereus* F4810/72 *wild-type* and $\Delta plcR$ after 2 h incubation in unsupplemented RPMI medium or Ptk6 preconditioned RPMI (chRPMI) medium were obtained.

The *plcR* deletion mutant has been described previously to lack the majority of the *wild-type* secretome, since most of the PlcR regulated proteins are secreted (Gohar *et al.* 2008). Due to this characteristic of the *plcR* deletion mutant and additionally attributed to the relatively short incubation time (2 h) which limited growth and secretion it was not unexpected that the $\Delta plcR$ extracellular subproteomes only contained very low total protein concentrations (data not shown). Initial two-dimensional gel electrophoresis of the extracellular subproteome of $\Delta plcR$ revealed a strong reduction of secreted proteins in un-suppl. RPMI medium and the number of proteins within the secreted protein fraction was poorly increased after incubation in Ptk6 conditioned medium (data not shown). Therefore, it seemed unlikely that analysis of the secretome would gain valuable information about *B. cereus* growth regulation and subsequent experiments focused on the cytosolic protein fraction. Two-dimensional differential gel electrophoresis (2-D DIGE) was carried out to identify differentially expressed proteins of the cytosolic subproteome of *B. cereus* F4810/72 *wild-type* and $\Delta plcR$.

The experimental setup comprised four different conditions:

- A: *B. cereus* F4810/72 $\Delta plcR$ incubated in unsupplemented RPMI medium
- B: *B. cereus* F4810/72 $\Delta plcR$ incubated in Ptk6 conditioned medium
- D: *B. cereus* F4810/72 *wild-type* incubated in unsupplemented RPMI medium
- E: *B. cereus* F4810/72 *wild-type* incubated in Ptk6 conditioned medium.

The proteomic changes seen in the comparison of A/B and D/E together represent the treatment effect (un-suppl. RPMI medium vs. Ptk6 conditioned medium), while comparing A/D and B/E should show the genotypic differences between *wild-type* and $\Delta plcR$. The experiment included three biological replicates per condition (A, B, D, E) that were labelled and separated by 2-D DIGE according to the labelling scheme depicted in chapter 2.11.2 (Table 6). Figure 35 illustrates representative 2-D DIGE two-channel overlay images, the upper panel represents the

treatment effect (D/E and A/B), the lower panel the genotypic effect on protein expression (B/E and A/D).

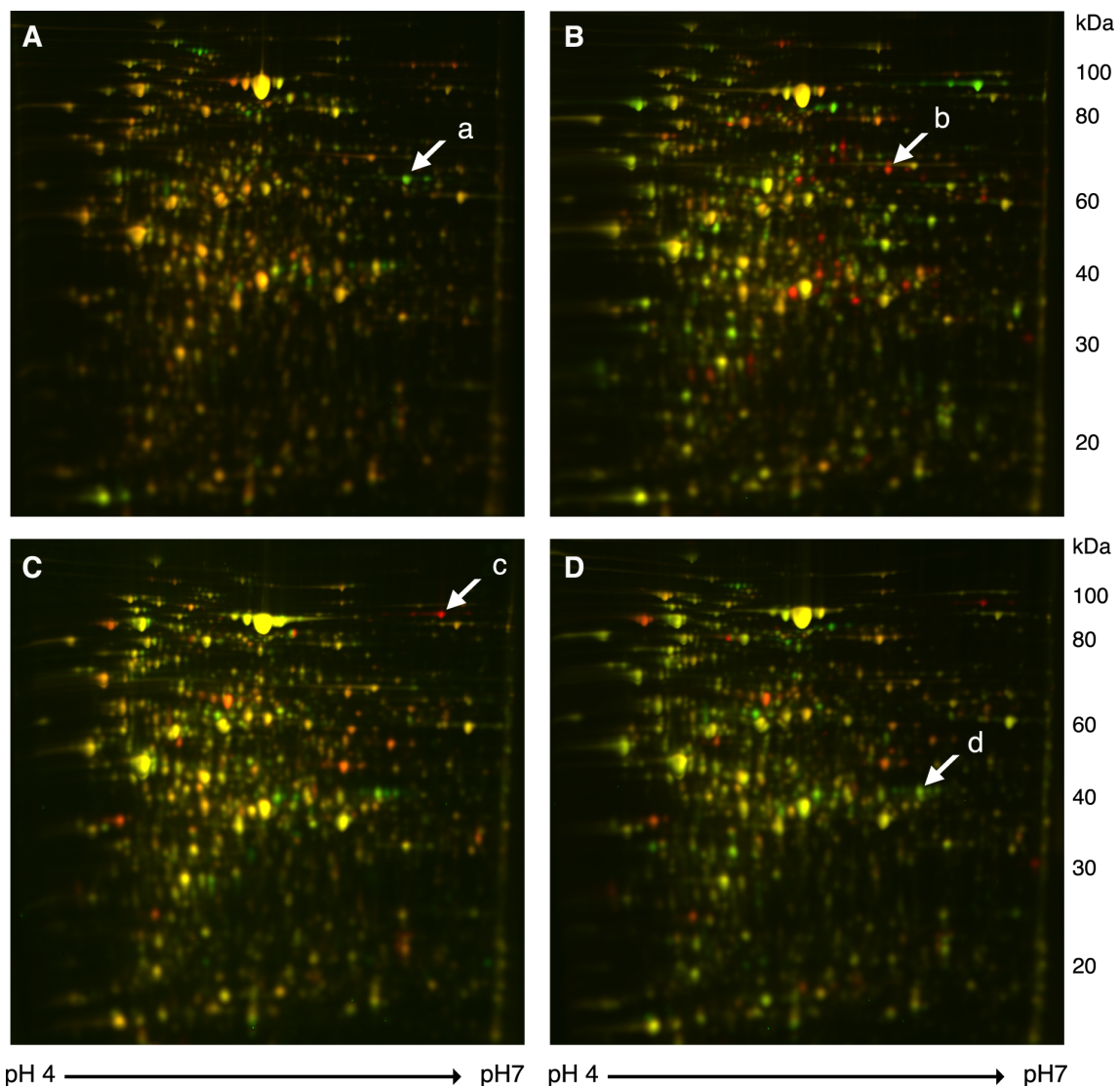


Figure 35: 2-D DIGE analysis of differentially expressed proteins in the cytosolic proteome of *B. cereus* F4810/72 *wild-type* or $\Delta plcR$. The effect of treatment with unsuppl. RPMI (Cy3, green) or Ptk6 conditioned medium (Cy5, red) on protein expression was assessed for *B. cereus* F4810/72 *wild-type* (A) and $\Delta plcR$ (B). Genotypic differences in protein expression between *wild-type* (Cy3, green) and $\Delta plcR$ (Cy5, red) were analysed after incubation in Ptk6 conditioned medium (C) or unsuppl. RPMI (D). Representative dual-channel overlay images are shown. Exemplary proteins regulated under the presented conditions are marked: a) *wild-type* protein upregulated in RPMI, b) $\Delta plcR$ protein upregulated in Ptk6 conditioned medium, c) higher abundant protein in $\Delta plcR$ when incubated in Ptk6 conditioned medium, d) higher abundant protein in *wild-type* when incubated in unsuppl. RPMI medium. Yellow spots indicate unchanged protein regulation.

To elucidate the influence of treatment of *B. cereus* with unsupplemented medium or secreted IEC factors on protein expression, differentially regulated proteins were detected in *wild-type* (Fig. 35A) or in $\Delta plcR$ cytosol (Fig. 35B). In addition, genotypic differences in protein expression between *wild-type* and $\Delta plcR$ were analysed after incubation in Ptk6 conditioned medium (Fig. 35C) or unsuppl. RPMI medium (Fig. 35D).

In the cytosolic proteome of *B. cereus* F4810/72 *wild-type* and/or $\Delta plcR$ a total number of 2358 protein spots was detected within the pH range of 4 – 7. Of these, 665 spots could be recovered in all 36 protein maps (all 2-D DIGE gels) analysed. Statistical analysis using the DeCyder software (GE Healthcare) revealed a large number of significantly regulated protein spots ($P < 0.05$) for each comparison of experimental conditions (treatment effect/genotypic effect) (Table 11). Incubation of *B. cereus* in IEC conditioned medium resulted in a ≥ 1.5 -fold up- or down-regulation of 39 and 33 proteins in *wild-type* and $\Delta plcR$ cytosol, respectively, compared to growth in unsupplemented medium. Applying a more stringent threshold of ≥ 3 -fold spot volume change still 10 and 7 proteins were found to be significantly regulated in *wild-type* and *plcR* deletion mutant when incubated in IEC conditioned medium. In addition, *plcR* gene deletion had pronounced influence on *B. cereus* protein expression so that a total of 90 or 74 proteins were differentially expressed in unsupplemented RPMI or IEC supernatant, respectively (Table 11).

Table 11: Number of total and differentially regulated protein spots in *B. cereus* F4810/72 *wild-type* and $\Delta plcR$ based on 2-D DIGE analysis.*

Spot selection				
Total number of spots	2358			
Number of spots in all protein spot maps (36)	665			
Differentially expressed spots ($p < 0.05$)	Treatment effect (unsuppl. RPMI vs. Ptk6 conditioned)		Genotypic effect (<i>wild-type</i> vs. $\Delta plcR$)	
	<i>wild-type</i>	$\Delta plcR$	unsuppl. RPMI	Ptk6 conditioned
minimal 1.3-fold change	52	49	106	129
≥ 1.5-fold change	39	33	90	74
≥ 2 -fold change	22	13	48	26
≥ 3 -fold change	10	7	22	9
Spot processing				
Spots selected for protein identification	-	33	-	-
Spots/proteins identified	-	22	-	-

* The DeCyder software (GE Healthcare) was used for image processing, spot detection and statistical analysis. Significant changes in spot volume ($P < 0.05$) were determined.

Since growth analysis in different media revealed the most profound growth differences between *B. cereus* $\Delta plcR$ incubated in unsupplemented medium and treatment with host (Ptk6)-conditioned medium (Ch. 3.2.1), especially $\Delta plcR$ proteins differentially regulated under these two conditions (A/B) were investigated. For detailed analysis of the effect of treatment with epithelial cell secreted factors on *B. cereus* $\Delta plcR$ protein patterns 33 significantly different regulated spots compared to incubation in unsuppl. medium were selected for protein identification by MALDI-TOF mass spectrometry. Thereof 22 protein spots were identified corresponding to 19 different proteins (Table 12). When comparing *B. cereus* *wild-type* and $\Delta plcR$ treatment specific proteomic changes it was apparent that 8 proteins identified from $\Delta plcR$ cytosol were regulated the same way in *wild-type*. Regulation of these proteins was

therefore assumed PlcR-independent. PlcR-specific treatment effect in the presence of host factors was detected for 11 proteins (spot #1-6, 8, 15-18 and 21,22) and these proteins were of greatest interest for growth induction due to their unique regulation in the *plcR* deletion mutant. A detailed list of all identified proteins, their regulation under the examined conditions and protein identification scores is provided in Table A4 in the Appendix (7.4). The identified proteins specifically regulated in the *B. cereus* $\Delta plcR$ mutant (and not in *wild-type*) in response to incubation medium, either epithelial cell supernatant (chRPMI) or un-suppl. RPMI were mainly involved in purine and protein biosynthesis.

In the presence of epithelial cell supernatant (chRPMI) 6 proteins were identified to be downregulated in *B. cereus* $\Delta plcR$ compared to incubation in the nutrient-poor un-supplemented medium. Among these, 4 proteins of the *pur* operon, PurL, PurD, PurM and PurC, involved in purine biosynthesis, the component E1 of a 2-Oxoglutarate dehydrogenase (OdhA/SucA) and an Isocitrate lyase (AceA) were detected (Table 12). The Phosphoribosylformylglycinamide synthase II (PurL) was identified in a spot-train with three different pI values (spot 1-3), each spot downregulated between 1.52 - 1.71-fold. This result suggests posttranslational modification of PurL.

In comparison, host derived factors in the Ptk6 conditioned medium induced the upregulation of several proteins in the $\Delta plcR$ cytosol. Most of the 13 identified upregulated proteins are involved in amino acid biosynthesis and in line with this in protein metabolism. A 2-isopropylmalate synthase (LeuA), two aminotransferases, the Phosphoserine aminotransferase (SerC) and the Branched-chain amino acid aminotransferase (IlvE 1) as well as two isoforms of the Ketol-acid reductoisomerase (IlvC1 and 2) were identified. Isoform 2 of IlvC was the most abundant upregulated protein identified in the cytosolic proteome of $\Delta plcR$ after incubation with IEC conditioned medium (Table 12). These conditions also favoured the expression of 5 tRNA synthetase genes (*ileS/ileS2*, *metS*, *thrS1* and *thrS2*).

Table 12: Differentially expressed proteins of *B. cereus* F4810/72 $\Delta plcR$ in Ptk6 conditioned medium compared to unsupplemented RPMI medium revealed by 2-D DIGE analysis.

Spot #	Protein name/activity (gene)	Swiss-Prot accession #	Av ratio ^a $\Delta plcR$ (Ptk6)/ $\Delta plcR$ (RPMI)	p-value $\Delta plcR$ (Ptk6)/ $\Delta plcR$ (RPMI)	MW (kDa) theor.	pH theor.	Signal peptide ^b
Purine biosynthesis							
1	Phosphoribosylformylglycinamide synthase II (<i>purL</i>)	B7HS32	-1.68	0.033	80.22	4.84	
2	Phosphoribosylformylglycinamide synthase II (<i>purL</i>)	B7HS32	-1.52	0.024	80.22	4.84	
3	Phosphoribosylformylglycinamide synthase II (<i>purL</i>)	B7HS32	-1.71	0.005	80.22	4.84	
4	Phosphoribosylamine-glycine ligase (<i>purD</i>)	B7HS37	-1.41	0.008	46.21	5.04	
5	Phosphoribosylaminoimidazole synthetase (<i>purM</i>)	B7HS34	-1.43	0.005	37.31	4.81	
6	Phosphoribosylaminoimidazole-succinocarboxamide synthase (<i>purC</i>)	B7HS29	-1.45	0.003	27.24	4.95	
Amino acid biosynthesis							
7	2-isopropylmalate synthase (<i>leuA</i>)	B7HKC4	1.82	0.034	54.70	5.32	
8	Ketol-acid reductoisomerase (<i>ilvC1</i>)	B7HKC3	1.66	0.009	36.75	5.3	
9	Ketol-acid reductoisomerase (<i>ilvC1</i>)	B7HKC3	1.89	0.008	36.75	5.3	
10	Phosphoserine aminotransferase (<i>serC</i>)	B7HXT1	1.47	0.024	40.29	5.57	
11	Ketol-acid reductoisomerase II (<i>ilvC2</i>)	B7HMM6	6.84	0.033	36.93	5.54	
12	Branched-chain amino acid aminotransferase (<i>ilvE1</i>)	B7HKC0	1.31	0.002	33.15	5.09	
Protein biosynthesis							
13	Isoleucyl-tRNA synthetase (<i>ileS</i>)	B7HQ07	4.77	0.042	118.49	5.29	
14	Isoleucyl-tRNA synthetase (<i>ileS2</i>)	B7HLM9	1.47	0.046	104.55	5.21	
15	Methionyl-tRNA synthetase (<i>metS</i>)	B7HPU9	1.51	0.015	68.83	5.17	
16	Threonyl-tRNA synthetase (<i>thrS1</i>)	B7HR64	2.44	0.002	73.50	5.36	
17	Threonyl-tRNA synthetase (<i>thrS2</i>)	B7HRL5	1.38	4,209E-05	74.02	5.37	
Other							
18	2-oxoglutarate dehydrogenase, E1 component (<i>odhA/sucA</i>)	B7I0H2	-1.31	0.049	106.50	5.66	
19	Putative oligopeptide ABC transporter, oligopeptide-binding protein	B7HNI4	1.5	0.004	62.94	8.02	+
20	Isocitrate lyase (<i>aceA</i>)	B7HZQ5	-1.82	0.003	46.80	5.7	
21	Neutral protease B (<i>nprB</i>)	B7HVW7	3.81	0.002	65.11	6.75	+ ^c
22	Immune inhibitor A (<i>inhA3</i>)	B7HVL4	5.69	3,728E-04	87.33	5.47	+

^a Av. ratio designates the average in-/decrease of $\Delta plcR$ protein spot abundance after incubation in Ptk6 conditioned medium compared to unsupplemented RPMI medium

^b Presence of a signal peptide was predicted on the SignalP 3.0 server;

^c unusual long signal peptide (71 aa) predicted

Two isoforms of the Isoleucyl- and the Threonyl-tRNA synthetase and one Methionyl-tRNA synthetase were detected to be upregulated up to 4.77-fold (IleS). Interestingly, the oligopeptide-binding component of a putative ABC-type oligopeptide transporter (OppA) was upregulated in $\Delta plcR$ when grown in IEC supernatant. Signal peptide analysis on the SignalP 3.0 server identified a distinct 28 aa signal peptide for the oligo-binding protein. OppA is a membrane-anchored protein that transports extracellular oligopeptides into the cell hence it is not surprising that it is secreted.

Moreover, a neutral protease B (NprB) and the metalloprotease immune inhibitor A3 (InhA3) were identified in $\Delta plcR$ cytosol after IEC supernatant treatment in contrast to unsupplemented medium (Table 12). Upregulation of both proteins was amongst the three most abundant with a 3.81- and 5.69-fold change in spot volume for NprB and InhA3, respectively. The chromosomally encoded NprB revealed 95-100% amino acid sequence identity to the neutral protease B proteins of *B. anthracis* str. Ames (BA_5282) and *B. cereus* group strains BDRD-ST26 (bcere0013_54270), Q1 (BCQ_4861) and ATCC 10987 (BCE_5183) based on BLASTP analysis. However, extracellular neutral protease B proteins of *B. cereus* 569 and *B. subtilis* (BSU11100), involved in processing of the quorum sensing peptide PapR, exhibited only 29% and 52% amino acid sequence similarity to the identified NprB of *B. cereus* F4810/72.

While for *B. cereus* F4810/72 InhA3 a signal peptide cleavage site is predicted between position 32 and 33 by SignalP 3.0 using both algorithms (see Ch. 2.13.), NprB seems to have an unusual long secretion signal (71 aa) that was only predicted by the hidden Markov model. Comparative genome analysis of *B. cereus* F4810/72 using the xBASE 2.0 database failed to predict a distinct PlcR-binding box upstream of *nprB* and *inhA3* genes in the first instance. Less stringent database query allowing 1 or 2 mismatches and using the two published consensus PlcR target sequences TATGnAnnnnTnCATA and ATGhAwwwTdCAT (Gohar *et al.* 2008) in the *B. cereus* F4810/72 genome yielded four potential PlcR-binding sites for NprB (-85, -236, -295, -662 bp upstream of the start codon) and three for InhA3 (-138, -602, -607). For an unambiguous assignment of *B. cereus* F4810/72 NprB and InhA3 to the list of PlcR controlled proteins comprehensive functional analysis is required. However, the identification of both proteins upregulated in the cytosol of a *plcR* deletion mutant hints to no or only partial/indirect PlcR regulation.

Both zinc dependent metalloproteases are potential candidates involved in growth induction under nutrient-limiting conditions.

Spot localisation on silver stained 2-D gel is indicated in Figure 36 for all identified proteins.

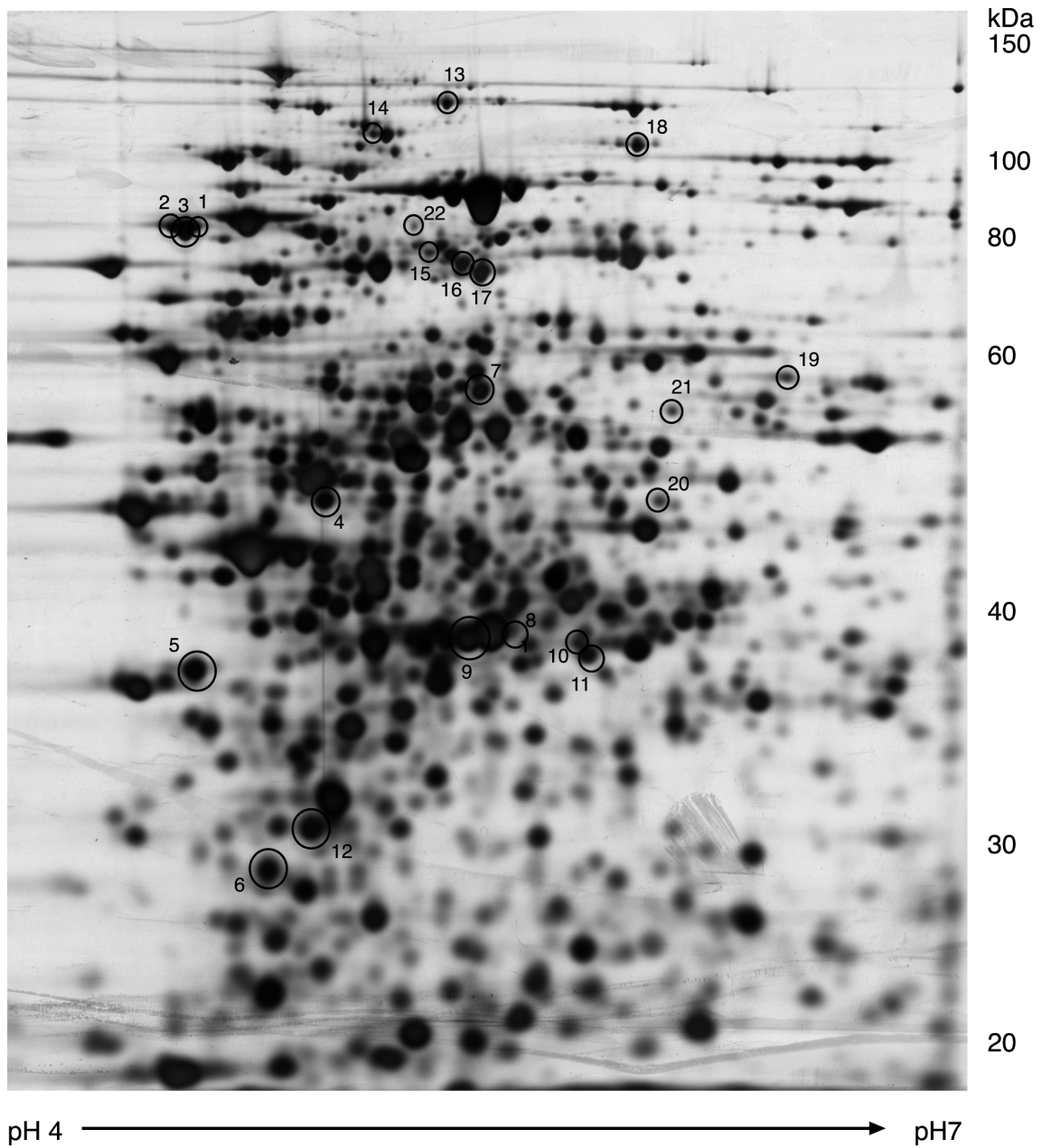


Figure 36: Representative silver stained 2-D gel. Cytosolic protein fraction of *B. cereus* F4810/72 $\Delta plcR$ was separated within the pH range of 4 - 7. Differentially regulated protein spots picked and identified by MALDI-TOF mass spectrometry are marked with black circles. Numbers indicated correspond to the respective spot # listed in Table 12.

4. DISCUSSION

4.1. *B. cereus* virulence mechanisms

4.1.1 *Toxin secretion upstages bacterial adhesion to host cells*

Bacillus cereus is a well established foodborne pathogen that causes emetic intoxication or diarrheal gastroenteritis by producing a broad set of virulence factors during exponential growth in the intestine. Ingestion of food contaminated with *B. cereus* spores is generally considered the route of infection, since only *B. cereus* spores and the emetic toxin cereulide are able to survive the stomach passage unscathed. Although some types of food may temporarily increase the pH preformed extracellular enterotoxins can not pass the stomach unaffected, while up to 26% of ingested vegetative *B. cereus* cells might reach the intestine (Clavel *et al.* 2004; Wijnands *et al.* 2009). Considering the infection route, *B. cereus* must have a mechanism that enables spores and vegetative cells to stay long enough in the small intestine to germinate, establish growth and produce enterotoxins causing disease. Adhesion of enteropathogens to the intestinal epithelium is believed to be such an essential pathogenic mechanism. Therefore, a preliminary screening for the adhesion capacity of *B. cereus* to two intestinal epithelial cell lines included seven *B. cereus* strains harbouring different toxin profiles. Immunofluorescence analysis detected very few *B. cereus* spores and vegetative cells attached to polarized intestinal epithelial cells (Ptk6)(Figure 5A and B). Initial comparison of *B. cereus* adherence to differentiated human colonic cancer Caco-2 cells and polarized Ptk6 cells derived from the colon mucosa of Ptk6 null mice revealed only minor differences between spores and vegetative cells and no reproducible influence of the epithelial cell line. Adhesion capacity was strain-dependent and with a mean adhesion efficiency of 0.8% for vegetative *B. cereus* cells and slightly higher 3.3% for spores comparable to previous studies that detected ~1% adhering spores for most of the tested strains (Andersson *et al.* 1998; Wijnands *et al.* 2007). However, detailed *B. cereus* adhesion characterisation using longer incubation times and higher MOIs was strongly hindered by the fact that all *B. cereus* strains included in the setting induced rapid host cell disruption probably due to enterotoxin expression. The destructive effect of *B. cereus* spores was only delayed for the germination process. Though these first results indicate a potential role of *B. cereus* adherence to intestinal epithelial cells as very first step in pathogenicity *in vivo*, the observed adhesion capacity was very low and became dominated by toxin secretion. As a consequence, subsequent experiments went one step further on deciphering of the observed cytotoxic effect towards epithelial cells.

Once the protective barrier of the mucosa or dermis is overcome, *B. cereus* causes serious and often-fatal non-gastrointestinal-tract infections characterised by extensive tissue destruction (Bottone 2010).

In this study the non-cancer cell line Ptk6 served as a model for the intestinal epithelial barrier

lining the intestine. When infected with 14 different *B. cereus* strains using a low MOI of 1, Ptk6 cell morphology was strongly affected (Figure 4) and cells started rounding and detaching within 2 – 4 h (Table 7). This cytotoxic effect was mediated by extracellular factors independent of direct bacteria-cell contact, since bacterial supernatants conferred almost immediate cell rounding and detachment (Table 8). Cytotoxicity of *B. cereus* vegetative cells and bacterial supernatant against a variety of eukaryotic cell types including epithelial cells and macrophages has been reported (Lindbäck *et al.* 1999; Ramarao and Lereclus 2005; Ramarao and Lereclus 2006). Minnaard *et al.* reported enterocyte disintegration due to F-actin disassembly and complete detachment of Caco-2 cells 3 h after infection with *B. cereus* cultures of 5 out of 15 tested strains (Minnaard *et al.* 2004). In contrast, all of the strains tested in the presented study caused massive epithelial cell damage (Table 7). The *B. cereus* strain set included also two strain used in probiotic formulas for human and piglet feeding, *B. cereus* var. *toyoi* and IP5832 (Duc *et al.* 2004; Hong *et al.* 2005). Interestingly, both strains caused epithelial cell disruption comparable to *B. cereus* NVH 0391- 98, the causative agent of a lethal foodborne outbreak (Lund *et al.* 2000). This finding emphasized the need of future detailed analysis of virulence gene regulation and expression levels for the safety risk assessment of individual strains, especially of those used as probiotics. Thereby, one has to keep in mind, that all *B. cereus* strains contained in probiotic formulas carry the genes for at least one of the diarrheal enterotoxins (Nhe) like disease-associated strains.

4.1.2 *PlcR*-mediated cytotoxicity towards intestinal epithelial cells

In the cytotoxicity screen only one mutant strain (*B. cereus* F4810/72 $\Delta plcR$), deleted for the major virulence regulator PlcR, was completely abolished in its cytotoxicity towards intestinal epithelial cells *in vitro* due to the lack of PlcR-dependent virulence gene expression (Table 7 and 8). These data confirmed the pivotal role of the PlcR regulon in *B. cereus* mediated virulence. The three enterotoxins CytK, Hbl and Nhe are part of the PlcR regulon and currently considered to be responsible for *B. cereus* diarrheal disease (Stenfors Arnesen *et al.* 2008). Of those three only the *nhe* operon is present in all currently known *B. cereus* strains (Guinebretière *et al.* 2002; Ngamwongsatit *et al.* 2008). In contrast, enterotoxin genes coding for Hbl and CytK are often absent even from *B. cereus* strains isolated from disease outbreaks, which argues against a prominent role in disease formation (Ehling-Schulz *et al.* 2005; Ehling-Schulz *et al.* 2006). For several further reasons Nhe is believed to be the major factor in *B. cereus* diarrheal disease: *in vitro* *B. cereus* cytotoxicity correlates well with Nhe concentration in the bacterial supernatant, neutralizing antibodies against Nhe abolish cytotoxicity almost completely and a *B. cereus* *nheBC* knockout mutant NVH 0075-95 $\Delta nheBC$ lost all cytotoxicity in cell culture based assays (Dietrich *et al.* 2005; Moravek *et al.* 2006; Fagerlund *et al.* 2008). So to clarify the distinct role of Nhe for Ptk6 cytotoxicity, the previously described *B. cereus* Nhe knockout mutant strain NVH 0075-95 $\Delta nheBC$ (Fagerlund *et al.* 2008) was included in the screening. The lack of NheB and NheC in the bacterial supernatant was validated by immunoblot (Figure 6) and absence of the *hbl* gene cluster as well as *cytK* and *hlyII* has been ensured (Table A1). Unexpectedly,

incubation of polarized colon epithelial cells (Ptk6) with *B. cereus* NVH 0075-95 $\Delta nheBC$ supernatant for 4 h resulted in nearly 90% of dead cells revealing that other cytotoxins contribute to epithelial cell cytotoxicity as well (Table 8 and Figure 25). Major differences to the previous study, in which the lack of Nhe in *B. cereus* NVH 0075-95 ($\Delta nheBC$) abolished the entire cytotoxicity of the *wild-type* strain, were the host cell type (Vero cells) and time of incubation (Fagerlund *et al.* 2008). It has been shown that HUVEC cells are extremely sensitive to Nhe-induced cytotoxicity (Didier *et al.* 2011). Primary HUVEC are endothelial cells isolated from human umbilical vein, while Vero cells are epithelial cells derived from kidneys of a green monkey and Caco-2 cells from well-differentiated colon cancer cells (Yasumura and Kawakita 1963; Fogh and Trempe 1975; Pinto *et al.* 1983). Due to varying origin all these cells may respond differently to cell cytotoxicity compared to Ptk6 cells derived from the colon mucosa of Ptk6 null mice as a model for polarized colon epithelial cells (Whitehead *et al.* 2008). Most importantly, Ptk6 is a non-cancer cell line that can form fully differentiated epithelial monolayers. Time of incubation is also maybe an important factor. Fagerlund *et al.* described that the uptake of propidium iodide into Vero and Caco-2 cells as an indicator for cell death was abolished in the absence of Nhe in the first 15-30 minutes after adding bacterial supernatant (Fagerlund *et al.* 2008). The presented observation that the onset of cell rounding and detachment was delayed in *B. cereus* NVH 0075-95 $\Delta nheBC$ compared to *wild-type* supports the finding that Nhe plays a significant role in the early phase of cell cytotoxicity. However, both strains caused cell death and complete detachment of epithelial cells 4 h after adding bacteria to the cells (Table 7) indicating additional PlcR-regulated virulence factors that cause IEC cytotoxicity.

4.1.3 *B. cereus* Sphingomyelinase – reassessment of a virulence factor

The presented work identified sphingomyelinase (SMase) from the supernatant of *B. cereus* NVH 0075-95 $\Delta nheBC$ as an important factor contributing to *B. cereus* cytotoxicity. SMase has been described before as a metal ion dependent phospholipase that enzymatically cleaves the membrane constituent sphingomyelin showing haemolytic activity against sheep erythrocytes (Ago *et al.* 2006). Furthermore, PCR amplification revealed the presence of *sph* gene in all *B. cereus* strains tested in this study (data not shown).

4.1.3.1 Co-transcription of *plc* and *sph*

Considering the *B. cereus* genomic organization, the *sph* gene is located directly 3' of the *plc* (PC-Plc) gene. Their close genetic localization and functional relationship conferring both phospholipase C activity has led to the assumption that *plc* and *sph* form a gene cluster or operon regulated by PlcR (Gohar *et al.* 2002). However, Yamada *et al.* (Yamada *et al.* 1988) and Pomerantsev *et al.* (Pomerantsev *et al.* 2003) described independent promoter regions for *plc* and *sph* including characteristic promoter structures such as a -35, -10 box and the RBS (Figure 17), that may suggest that *sph* transcription is driven from its own promoter directly upstream of the *sph* gene. But no *sph* transcription start has been determined by primer extension so far and it is unclear how *sph* transcription is regulated. Co-transcription analysis on

the basis of reverse transcriptase PCR confirmed the operon structure of the *plc-sph* gene cluster showing that *plc* and *sph* are transcribed from a common operon promoter region (P_{plc^*}) as one co-transcript (Figure 18). Furthermore, phenotypic analysis of *sph* deletion mutants and complemented strains revealed that a promoter region upstream of *plc* (P_{plc^*}) drives *sph* expression under the tested conditions, since only *B. cereus* Δsph complemented with pAD/*sph*/ P_{plc} reconstituted a haemolytic phenotype comparable to *wild-type*, while pAD/*sph*/ P_{sph} failed to induce haemolysis (Figure 19). Gohar *et al.* described only one PlcR binding box 124 bp upstream of the *plc* gene implying joint activation of *plc* and *sph* expression by PlcR (Gohar *et al.* 2008). Additionally by the absence of SMase protein in *B. cereus* $\Delta plcR$, this study confirmed PlcR regulation of *sph* gene, since deletion of *plcR* resulted in a lack of SMase protein expression (Figure 18 and 23), SMase activity (Figure 24), haemolysis and lecithinase activity of the *B. cereus* strain ($\Delta plcR$) (Figure 19 and 20), while *B. cereus* *wild-type* strains were positive for all assays. SMase protein and enzyme activity could be detected in 8 h bacterial culture supernatant, indicating a relatively high SMase protein stability in the supernatant, since *sph* transcript levels decrease towards the end of exponential growth phase (Figure 17). A study of SMase activity throughout the growth cycle of *B. cereus* F4810/72 confirmed highest SMase enzyme activity in mid-exponential growth phase and transition phase, while enzyme activity significantly decreased when cells entered stationary growth phase (Frenzel 2011, PhD Thesis). Pomerantsev *et al.* demonstrated a decrease of SMase activity during exponential phase despite increasing PlcR levels leading to the hypothesis that PlcR might have a dual role as activator and repressor of *sph* by binding to a complementary PlcR box overlapping the ribosome binding site upstream of the *sph* gene (Pomerantsev *et al.* 2003). The results presented in this study point in the same direction. They confirm activation of *sph* expression by PlcR, but also decreasing *plc-sph* co-transcript levels throughout late exponential growth. However, qRT-PCR analysis could further elucidate growth phase-dependent *sph* transcription activation.

4.1.3.2 SMase expression in $\Delta plcR$ rescued *B. cereus* virulence

Protein homologues of SMase in *S. aureus* (β -toxin) and *Cl. perfringens* (α -toxin) are well established virulence factors involved in cytotoxicity against host cells (McDonel 1980; Huseby *et al.* 2007). Walev *et al.* demonstrated cytotoxicity of *S. aureus* beta toxin, *Streptomyces* sp. SMase and *B. cereus* SMase against human monocytes (Walev *et al.* 1996). *B. cereus* SMase has been shown to inhibit neurite outgrowth in PC12 cells and to induce membrane damage in host neural cells (Tamura *et al.* 1994). The capacity of *B. cereus* to detach host cells *in vitro* correlated positively with the genomic presence of *sph* gene (Minnaard *et al.* 2007). However, the role of *B. cereus* SMase as a virulence factor is controversial, because SMase was nontoxic against Vero cells and in an *in vitro* retinal toxicity model (Granum and Nissen 1993; Beecher *et al.* 2000).

To elucidate the actual impact of SMase on *B. cereus* cytotoxicity towards Ptk6 cells *sph* gene expression driven from the cold shock protein (*cspA*) promoter was induced in the *plcR* deletion

mutant (Figure 9). The results demonstrate that SMase is a cytotoxic factor *in vitro*. Transient expression of *sph* in the non-cytotoxic *B. cereus* F4810/72 $\Delta plcR$ mutant was able to restore cytotoxicity to the level of the *wild-type* strain. Interestingly, cells infected with *wild-type* supernatant all “homogeneously” rounded and detached. Less cell rounding, but significant cell detachment was observed, when infecting cells with SMase in the $\Delta plcR$ supernatant (Figure 10). This could indicate the contribution of different toxins for different parts in the course of disintegration of epithelial cell morphology, e.g. a role for SMase in cell detachment and for Nhe in cell rounding.

4.1.3.3 SMase induced apoptosis in IEC

Applying the apoptotic marker Annexin V in immunofluorescence microscopy, it could be shown that the SMase cytotoxic effect was likely due to the induction of host cell apoptosis. While infection of IECs with wild-type *B. cereus* secretome resulted in plenty of SYTOX[®] Green-positive cells indicative for pore-formation and necrosis (Figure 14), SMase in the non-toxic $\Delta plcR$ secretome significantly induced apoptosis (Figure 15) as detected by exclusively Annexin V-stained cells. Single SYTOX[®] Green-positive cells after SMase treatment might represent late-apoptotic cells where leaky cell membranes allow entry of the dye.

Caspase-3 is an essential mediator of apoptosis that is activated in both, the receptor-mediated and the mitochondrial pathway, and subsequently cleaves downstream death substrates (Porter and Jänicke 1999; Salvesen 2002). Although caspase-3 is supposed to be crucial for almost all apoptotic processes, *Cl. difficile* toxin A (TcdA) showed a caspase-independent induction of apoptosis *in vitro* (Matte *et al.* 2009).

To test caspase-3 involvement, a second apoptosis assay measuring caspase-3 activity of SMase treated epithelial cells was carried out. The *in vitro* data provides evidence that *B. cereus* SMase-induced apoptosis is caspase-3 dependent. Epithelial cells incubated with supernatant of *B. cereus* F4810/72 $\Delta plcR$ expressing SMase demonstrated a 4-fold higher caspase-3 activity than cells treated with non-cytotoxic $\Delta plcR$ supernatant (Figure 16). Furthermore, similar caspase-3 activation could be induced by the addition of 1U/ml recombinant SMase (Sigma-Aldrich) in $\Delta plcR$ supernatant.

Induction of apoptosis in host cells is a commonly known virulence mechanism of many pathogenic bacteria. Recently, *B. cereus* haemolysin II (HlyII) has been identified as novel virulence factor inducing apoptosis to macrophages (Tran *et al.* 2011). Since *B. cereus* F4810/72 does not harbour the *hlyII* gene (Table A1, Appendix 7.1) it could be ruled out that the observed apoptosis induction was due to haemolysin II activity. Programmed cell death (apoptosis) of mammalian cells is a regular developmental process that can be initiated via three distinct pathways: a receptor-mediated event (involving e.g. CD95 or TNF), other non-receptor-mediated stress stimuli (UV irradiation, bacterial trigger) and deprivation of growth factors (for a review see (Gulbins and Li 2006)).

Also in eukaryotic cells several SMase proteins have been identified and differentiated according to their optimal pH range. Most of external death stimuli activate acid SMase

(aSMase) to cleave cell membrane sphingomyelin to ceramide, an important signalling molecule. Ceramide generation transforms the receptor spatial organisation in the cell membrane to lipid rafts, which seem to self-associate spontaneously to ceramide-enriched membrane platforms (Kolesnick *et al.* 2000). A critical involvement of these platforms in the induction of apoptosis has been supposed (Gulbins and Li 2006). Furthermore, Zundel and co-workers have demonstrated that the recruitment of caveolin 1 to ceramide leads to a sensitisation to apoptosis (Zundel *et al.* 2000). Besides aSMase, neutral SMases (nSMase) are considered to mediate stress-induced ceramide generation (Clarke *et al.* 2006). In addition to mammalian nSMases, neutral SMase activity has been found in yeast and bacteria, including *S. aureus* beta toxin, *Cl. perfringens* alpha toxin and the sphingomyelinase of the intracellular pathogen *Listeria ivanovii* (Gilmore *et al.* 1989; Huseby *et al.* 2007). Although levels of sequence identity between mammalian and bacterial SMase are low, approximately 20%, a common catalytic mechanism has been proposed, since several conserved residues, mainly in the active site, were found by inter-species sequence alignment (Clarke *et al.* 2006). Ago *et al.* suggested that *B. cereus* SMase might mimic the action of mammalian nSMase (Ago *et al.* 2006), however from preceding studies it was unclear, if *B. cereus* SMase can directly cause programmed cell death via ceramide generation when attacking the outer leaflet of the cell membrane. The release of ceramide from sphingomyelin by *B. cereus* SMase in B16 melanoma cells and apoptosis induction by SMase has been detected, when SMase was microinjected in *Xenopus* oocytes (Komori *et al.* 1999; Coll *et al.* 2007). In contrast, no cytotoxic effect could be observed when oocytes were incubated with extracellular SMase.

The presented study clearly confirmed the capacity of exogenously added *B. cereus* SMase to induce apoptosis in intestinal epithelial cells.

Differences in cytotoxicity and apoptosis induction observed between various cell lines may be attributed to variations in phospholipid composition and sphingomyelin content of host cell membranes as seen for red blood cells of different species varying in their sphingomyelin content ranging from 25 – 53.1% (human – sheep) (Crowell and Lutz 1989; Beecher and Wong 2000).

4.1.3.4 Influence of SMase to *B. cereus* virulence *in vitro*

In order to assess the contribution of SMase to overall *B. cereus* pathogenicity *sph* knockout mutants in *wild-type* and NVH 0075-95 $\Delta nheBC$ were generated. *In vitro*, *sph* deletion alone had little effect on epithelial cell cytotoxicity. But it added significantly to Nhe mediated cell cytotoxicity (Table 9). Deletion of *sph* in the NVH 0075-95 $\Delta nheBC$ mutant strain reduced the number of dead host cells nearly by the factor 3 suggesting a synergistic mode of action for Nhe and SMase (Figure 25). The phenomenon of haemolytic synergy of bacterial phospholipases C (SMase) and pore-forming toxins is well accepted (Bashford *et al.* 1986; Crowell and Lutz 1989; Beecher and Wong 2000). Comparison of haemolysis pattern of *B. cereus wild-type* and mutant strains revealed that in HbI⁻, HlyII⁻ *B. cereus* strains (F4810/72, NVH 0075-95) Nhe and SMase collaborate to induce lysis of sheep erythrocytes (Figure 19).

The pore-forming enterotoxin Nhe may act synergistically with SMase in *B. cereus* virulence *in vitro*.

4.1.3.5 Influence of SMase on *in vivo* pathogenicity

The importance of *B. cereus* SMase as a virulence factor is strongly supported by *in vivo* observations in various insects. *B. cereus* SMase caused significant mortality of German cockroaches, cut- and silkworms when applied as a purified enzyme expressed in *B. cereus* or *E. coli* (Nishiwaki *et al.* 2004; Usui *et al.* 2009). Recently, the lepidopteran larvae of the great wax moth *Galleria mellonella* have emerged as a popular insect model for the evaluation of microbial overall pathogenicity *in vivo* (Walters and Ratcliffe 1983; Fedhila *et al.* 2002; Fedhila *et al.* 2010; Guillemet *et al.* 2010; Mukherjee *et al.* 2010). *G. mellonella* larvae are well characterised and represent a cost-effective alternative to the time- and labour-intensive mouse or rabbit animal models the more as they resemble the vertebrate innate immune response (for a review see Ref. (Kavanagh and Reeves 2004)). Comparable virulence data has been obtained from very diverse species such as *G. mellonella* and mice (Salamitou *et al.* 2000). The *G. mellonella* insect model has commonly been used in experiments at temperatures ranging from 20 - 37 °C, however a very recent study also tested lower temperatures (15 °C) (Stenfors Arnesen *et al.* 2011). A comparison of infection routes (oral vs. intrahaemocoelic injection) and the virulence of different *B. cereus* and psychrotrophic *B. weihenstephanensis* strains at 15 °C and 37 °C revealed no significant virulence difference between infection routes applied and similar high insect virulence at 15 °C. *B. cereus* strains demonstrated equal high insect virulence at 15 and 37 °C, although high mortality was reached faster at 37 °C probably due to higher multiplication rates. An incubation temperature of 15 °C had to be applied to the insect injection experiments presented here in order to induce protein expression controlled by the *cspA* promoter. However, correlation of temperature and virulence had to be investigated first.

When testing the temperature dependency of SMase insecticidal activity, no difference could be observed between LD₅₀ values at 15 °C (0.711 ± 0.345 µg) and 37 °C (0.501 ± 0.185 µg) (Ch. 3.1.4.1). Although SMase enzyme activity is optimal at 37 °C, also *G. mellonella* larval immune response works efficiently at this temperature. When lowering temperature to 15 °C, efficiency of larval immune reaction might be influenced despite constant insect fitness as seen before (Stenfors Arnesen *et al.* 2011), but in return SMase activity should be decreased resulting in similar virulence degrees at 15 and 37 °C. Therefore, all *in vivo* experiments were carried out by direct injection into the haemocoel and incubation at 15 °C for better comparability.

In the *G. mellonella* insect model it was demonstrated that *sph* expression restored the pathogenic phenotype of the non-cytotoxic *B. cereus* F4810/72 $\Delta plcR$ mutant strain (Figure 12) suggesting that SMase is an important virulence factor *in vitro* and *in vivo*.

Furthermore, the contribution of SMase to overall *B. cereus* pathogenicity was evaluated using *sph* knockout mutants in the *G. mellonella* model. Given the strong role of Nhe for *in vitro* cell cytotoxicity, it was astonishing to see that the *B. cereus* NVH 0075-95 $\Delta nheBC$ mutant strain behaved similar to *wild-type* in *G. mellonella* larvae suggesting that Nhe does not contribute

much to pathogenicity in this *in vivo* model (Figure 26B). The mortality of *G. mellonella* larvae was significantly reduced in the *B. cereus sph* knockout mutant (Figure 26A), whereas the additional knockout of Nhe did not further reduce larvae mortality (Figure 26B). The differences in larvae mortality were not attributed to differences in growth of the *B. cereus* strains in the *G. mellonella* larvae (Figure 27).

The results are in line with results from studies with SMase homologues. Knockouts of SMase homologues in *L. ivanovii* and *S. aureus* significantly impacted bacterial virulence (Bramley *et al.* 1989; O'Callaghan *et al.* 1997). A *sph* knockout strain of *L. ivanovii* was less virulent in a mouse model compared to *wild-type* (González-Zorn *et al.* 1999).

Noteworthy, no difference in the pathogenic potential of emetic (F4810/72) and non-emetic/diarrheal (NVH 0075-95) *B. cereus wild-type* strains could be detected in the insect *G. mellonella* model (Fig. 26A and 26B) when larvae were infected *via* direct injection into the haemolymph. On basis of these results it is tempting to speculate about a minor role of emetic cereulide in the intermediate step of *B. cereus* infection represented by haemolymph injection. Establishment in the host and multiplication in the blood stream might require the secretion of proteases and degradation enzymes rather than the ionophoric activity of the emetic toxin.

However, deletion of the virulence regulator gene *plcR* delayed the time course of larval mortality compared to mortality of larvae injected with *wild-type*, but did not completely abolish *B. cereus* pathogenicity after intrahaemocoelic injection (Fig. 12 and 26A). This indicates that other non-PlcR regulated virulence factors such as cereulide contribute to pathogenesis, though to a less extent (Fig. 26A).

Deletion of *plcR* or inactivation by *papR* deletion strongly reduced virulence of *B. thuringiensis* and *B. cereus* against insect larvae and mice (Salamitou *et al.* 2000), indicating the tremendous importance of PlcR in transcriptional regulation of virulence factors. However, this was only the case for oral infection, while no difference in *B. cereus* virulence was observed when *wild-type* or $\Delta plcR$ spores were directly injected into the insect haemolymph. This strengthens the role of PlcR-regulated toxins in the initial step of infection when bacteria have to overcome the epithelial barrier and gain access to the blood stream.

Though an intrahaemocoelic infection route was applied, *plcR* deletion in the emetic *B. cereus* strain F4810/72 significantly reduced the virulence against *G. mellonella* larvae (Fig. 26A) and the PlcR-regulated protein SMase has been shown as important factor. Nevertheless, a strong dose-dependency was observed for all tested *B. cereus* strains. One order of magnitude increase of the infection dose (1×10^5 to 1×10^6 CFU/larva) strongly affected larvae mortality such as that the survival of larvae injected with 1×10^6 CFU $\Delta plcR$ dropped below 60% after 3 days in contrast to 6 days when 10-times less bacteria were applied (compare Fig. 26A and Fig. 12). Comparable results have been demonstrated in mouse models: the reduction of the intranasal infection dose of *B. cereus* $\Delta plcR$ or *B. thuringiensis* heavily decreased mortality of infected mice from 100% down to 22% or even abolished pathogenicity resulting in local inflammation and persistence (Hernandez *et al.* 1999; Salamitou *et al.* 2000). Considering the

remaining pathogenic activity of the *plcR* deletion mutant, there are two possible explanations that might intertwine: i) additional PlcR-independent factors such as HlyII (however showing low abundance) can contribute to *B. cereus* virulence *in vivo* and ii) global regulators other than PlcR might influence the expression of virulence factors normally driven by PlcR.

In vitro cytotoxicity may not always be a good predictor for *in vivo* pathogenicity as seen for the presented data here. *B. cereus* induced mortality in *G. mellonella* larvae is different from *B. cereus* induced diarrheal disease in the human gut. Intrahaemocoelic injection of microbes into an insect model rather mimics a non-gastrointestinal infection or the consequence of pathogens overcoming the intestinal epithelial barrier than diarrheal disease. Furthermore, differences in pathogenicity between the oral and the haemocoelic infection route have been detected for several human pathogens (Fedhila *et al.* 2010). Therefore, it could be interesting to investigate virulence of the *nheBC* and *sph* deletion mutants after oral infection. Pore-forming enterotoxins such as Hbl and Nhe that might directly act on the epithelial cells in the invertebrate midgut could be of great significance for *B. cereus* for getting access to the underlying tissue and the blood system. After disruption of the epithelial lining tissue degradative enzymes might gain importance for pathogenicity.

The contribution of SMase to *B. cereus* virulence has been underestimated in the past and this study shows for the first time that *B. cereus* SMase contributes significantly to *in vitro* cytotoxicity and *in vivo* pathogenicity. Secreted factors like SMase may contribute to the tissue destructive effects of *B. cereus* non-gastrointestinal-tract infections. And it is likely that more *B. cereus* secreted factors are involved, too.

4.2. Intrinsic and extrinsic factors influence *B. cereus* growth

4.2.1 The PlcR-dependent metalloprotease *InhA2* is involved in growth regulation

Colonization of the host gastrointestinal-tract or tissue and growth establishment in this environment are essential steps for successful disease initiation by microbial pathogens. As soil bacterium and opportunistic human pathogen, *B. cereus* is well adapted to growth in very different niches that comprise a wide spectrum of nutrient availability, ranging from protein rich human or insect host tissue to limited nutrient sources found in soil. Therefore, it was not surprising to detect bacterial growth of *B. cereus* F4810/72 *wild-type* in a relatively nutrient-poor RPMI medium both in cell culture plates without agitation (Fig. 28) and classically shaking in glass flasks (data not shown). Growth rate was slightly decreased compared to cultivation in nutrient-rich LB medium (Fig. 28, compare also Fig. 21) probably due to the lack of agitation and protein content. Despite of nutrient limitation to amino acids, vitamins, inorganic salts and 11.11 mM D-glucose in RPMI without FBS supplementation significant growth of *wild-type* *B. cereus* could be detected (Fig. 28). This is in sharp contrast to a *plcR* deletion mutant. Growth of *B. cereus* F4810/72 Δ *plcR* was completely inhibited in the nutrient-poor RPMI medium

suggesting that PlcR-regulated proteins are involved in growth initiation and/or nutrient supply or processing. Interestingly, the growth deficit as a result of *plcR* deletion could be rescued in sterile RPMI medium conditioned with *wild-type B. cereus* (Fig. 29). This is indicative for the secretion of PlcR-regulated proteins by *B. cereus* that directly or indirectly mediate bacterial growth under nutrient-limiting conditions.

A *B. cereus* immune inhibitor A (InhA) was identified as potential growth promoting protein in the supernatant of *B. cereus* F4810/72 *wild-type* (Ch. 3.2.2). Immune inhibitor A is a zinc dependent metalloprotease that belongs to the M6 peptidase family and was firstly identified in *B. thuringiensis* (Dalhammar and Steiner 1984). In recent years, several homologous proteins have been identified in the *B. thuringiensis* relatives *B. cereus* and *B. anthracis* (Charlton *et al.* 1999; Chung *et al.* 2006). BLASTP search for homologous proteins also revealed similar proteases in *B. mycooides* and *B. weihenstephanensis*. The pathogenic species *B. cereus*, *B. thuringiensis* and *B. anthracis* even possess more than one chromosomal gene encoding immune inhibitor A proteins. The genome of *B. cereus* for example, comprises the genes *inhA1*, *inhA2* and *inhA3* (Gohar *et al.* 2005; Wang *et al.* 2006). This redundancy of immune inhibitor A genes in *Bacillus* is most likely attributed to a successful adaptation and specialization to environmental niches and host species. Expression of the three metalloproteases might be sequentially and inactivation of one protein might be compensated by its homologue. However, complex differential transcriptional regulation is necessary to enable perfect adaptation to environmental changes such as nutrient availability without excessive energy expenditure for redundant protein expression.

Bacillus immune inhibitor A proteins are both secreted and associated with the spore exosporium and have been mainly associated with virulence in several *B. cereus* group members (Fedhila *et al.* 2002; Chung *et al.* 2008; Chung *et al.* 2009; Guillemet *et al.* 2010; Chung *et al.* 2011; Mukherjee *et al.* 2011). Guillemet *et al.* demonstrated that InhA metalloproteases of *B. cereus* counteract the host immune system. They concomitantly contribute to virulence since deletion of all three *inhA* genes resulted in a decrease of insect pathogenicity (Guillemet *et al.* 2010). However, the individual activity of the three immune inhibitor A proteins is poorly understood.

InhA1 was first identified from *B. thuringiensis* due to its hydrolyzing activity against two insect antimicrobial proteins, cecropin and attacin (Dalhammar and Steiner 1984). *B. cereus* InhA1 shares 91% identity with InhA1 of *B. anthracis*. It represents one of the major proteases found in the supernatant of *B. anthracis* and is responsible for host barrier impairment due to massive degradation of host tissue components (Chitlaru *et al.* 2006). Furthermore, spore-associated InhA1 is involved in the intracellular survival and escape from host macrophages (Ramarao and Lereclus 2005). In *B. thuringiensis*, InhA1 transcription is activated at the onset of sporulation in a complex regulation circuit involving the global regulators Spo0A, AbrB, SinR/I as well as a bacterial metalloprotease camelysin (Grandvalet *et al.* 2001). Genomic localization of *inhA1*,

sinI, *sinR* and *camelysin* is highly conserved in *B. cereus* F4810/72 (data not shown), suggesting similar regulation patterns compared to *B. thuringiensis*.

In contrast, almost nothing is known about the function and regulation of InhA3. Only low amounts of InhA3 have been detected in *B. cereus* (Gilois *et al.* 2007).

Since no assignment to InhA1, InhA2 and InhA3 was made when annotating the genes of *B. cereus* strain F4810/72, gene and protein sequences were compared to published sequences of InhA1, InhA2 and InhA3 of the *B. cereus* type strain ATCC14579 (Guillemet *et al.* 2010) for corresponding annotation in F4810/72 (Table 10). Sequence alignment of two unique peptides, obtained from mass spectrometry, with the three InhA sequences enabled the unambiguous identification of immune inhibitor A2 from *B. cereus* F4810/72 as putative growth promoting extracellular protein (Ch. 3.2.2.1).

Immune inhibitor A2 protein shares 67% sequence identity with InhA1 and 70% identity with InhA3 (Table 10). Unlike InhA1 and InhA3, InhA2 is part of the PlcR virulence regulon. Hence, protein expression is activated during post-exponential and transition phase by direct binding of PlcR to an atypical (one mismatch) DNA consensus sequence in the *inhA2* promoter region (Fedhila *et al.* 2003). Although InhA2 is not sufficient to cause full virulence in the absence of other PlcR-regulated proteins, a distinct role in *B. cereus* virulence during oral infection of *Galleria mellonella* has been demonstrated (Fedhila *et al.* 2002; Fedhila *et al.* 2003).

The fact that the identified putative growth promoting protein InhA2 is the only InhA that is PlcR-activated fits perfectly to the growth deficiency observed for the *plcR* deletion mutant in RPMI medium.

To confirm the importance of InhA2 for *B. cereus* $\Delta plcR$ growth in nutrient-poor medium, *inhA2* was expressed in *B. cereus* $\Delta plcR$ under the control of a xylose inducible promoter. InhA2 is encoded as a 799 aa protein that is secreted as a 85 kDa protein after cleavage of a 32 aa signal peptide (VYA-ET), as predicted on the SignalP 2.0 server using both neuronal network and hidden Markov models trained on Gram-positive bacteria. Subsequent (auto-) proteolytic processing, such as N-terminal and C-terminal propeptide cleavage has been reported for many zinc metalloproteases of pathogenic bacteria (Miyoshi and Shinoda 2000; Vaitkevicius *et al.* 2008). Overexpressed InhA2 migrated on a denaturing SDS gel as a protein of about 76 kDa (Fig. 33), indicating that the secreted protein might undergo at least one proteolytic processing step cleaving off an N-terminal propeptide. Additional degradation might occur extracellular, resulting in smaller protein fragments (45 kDa), like this detected by gel filtration and subsequent SDS-PAGE (Figure 32). Extensive protein processing/degradation has been observed for *B. thuringiensis*, *B. cereus* and *B. anthracis* InhA, as well as for other microbial zinc metalloproteases such as *V. cholerae* PrtV (Lövgren *et al.* 1990; Charlton *et al.* 1999; Chung *et al.* 2006; Vaitkevicius *et al.* 2008). After SDS-PAGE, fragments of InhA were detected migrating at molecular weights of 70-75 kDa, 46 kDa and 18 kDa. Chung *et al.* (2006) detected a 70-75 kDa pro-InhA, while the major active form of InhA was found as a 46 kDa protein after chromatographic purification (Chung *et al.* 2006).

Xylose-driven *inhA2* expression was sufficient to induce growth of *plcR* deletion mutant in RPMI medium. Since addition of xylose to the medium did not enable growth of $\Delta plcR$ without *inhA2* expression (Fig. 34B), growth rescue is clearly attributed to the presence of InhA2 and not due to utilization of xylose. When $\Delta plcR$ pWH $inhA2$ was incubated without the addition of xylose, onset of exponential growth was strongly delayed and highly variable (represented by high SEM). This confirms the leakiness of the xylose inducible promoter used as observed on SDS gel (Fig. 33) and highlights the strong dependency of growth initiation on a critical concentration of growth mediator. Growth onset of *wild-type B. cereus* F4810/72 was delayed upon *inhA2* expression induction. A possible explanation could be the higher energy expenditure necessary for additional protein expression and antibiotic resistance (Fig. 34A).

Many human pathogenic microorganisms produce zinc-binding metalloproteases that exhibit proteolytic activity towards a broad spectrum of host proteins and are therefore regarded as virulence factors (Miyoshi and Shinoda 2000). *B. cereus* InhA proteins are highly similar to the metalloprotease PrtV of *Vibrio cholerae* and the thermolysin family of metalloproteases including *Bacillus thermoproteolyticus* thermolysin, *Pseudomonas aeruginosa* elastase and a *Vibrio vulnificus* protease (Ogierman *et al.* 1997). They are members of the zincin superfamily and share a highly conserved catalytic site as well as the consensus motif HEXXH for zinc binding (Miyoshi and Shinoda 2000). Unlike proteases of the thermolysin family (M4 peptidases), *B. cereus* InhA2 and *V. cholerae* PrtV belong to the protease clan M6. A role for M6 metalloproteases has been suggested in environmental persistence and survival, since this type of proteases is produced by a variety of environmental bacteria including *Bacillus*, *Vibrio*, *Clostridium* and *Geobacillus* (Rawlings *et al.* 2006; Vaitkevicius *et al.* 2008). Although survival and growth of a pathogen might be closely linked to its virulence, poor information on growth regulatory contribution of bacterial metalloproteases is available in contrast to their well established pathophysiological importance. An InhA protein expressed by the Gram-positive bacterium *Mycobacterium tuberculosis* has been implicated in bacterial fatty acid metabolism and growth. However, this protein is a 2-trans-enoyl-acyl carrier protein reductase that does not share any sequence similarity or common enzyme activity with *B. cereus* immune inhibitor A (Marrakchi *et al.* 2000; Molle *et al.* 2010).

Due to its extracellular and/or cell wall-associated localization (Gohar *et al.* 2008) and the proteolytic activity one could speculate of two scenarios how InhA2 can initiate or promote *B. cereus* growth: i) InhA2 cleaves secreted bacterial proteins or peptides, that might in turn function as additional peptide or amino acid source or ii) InhA2 targets transmembrane proteins on the bacterial cell surface. After shedding of the extracellular domain the cleaved peptide could either be internalized and provide a nutrient source as indicated above or initiate a signalling cascade into the bacterial cell to influence protein expression.

The highly similar metalloprotease PrtV of the Gram-negative human pathogen *V. cholerae* was suggested to be involved in nutrient acquisition (Ogierman *et al.* 1997). The *prtV* gene is part of a pathogenicity island of *V. cholerae* comprising a haemolysin, lecithinase, lipase (*lipA*) and

other accessory proteins (*hylB*, *lipB*) needed for the degradation of nutritional macromolecules such as phospholipids, proteins and lipids released after host tissue damage (see Fig. 37). In the *B. cereus* chromosomal genome *inhA2* is also encoded in close vicinity to degradative enzymes namely *plc* and *sph* (Fig. 37). Similar to *V. cholerae* *inhA2* is separated from the haemolysin and lecithinase genes by three other open reading frames, however these genes encode a putative multidrug resistance protein (A0801), a zinc-binding dehydrogenase family oxidoreductase (A0802) and one hypothetical protein (A0803) instead of lipases. Although the proteins of *B. cereus* and *V. cholerae* encoded in the presented locus share only functional similarity instead of sequence identity it is tempting to speculate that the *inhA2* locus is also involved in nutrient acquisition of *B. cereus*.

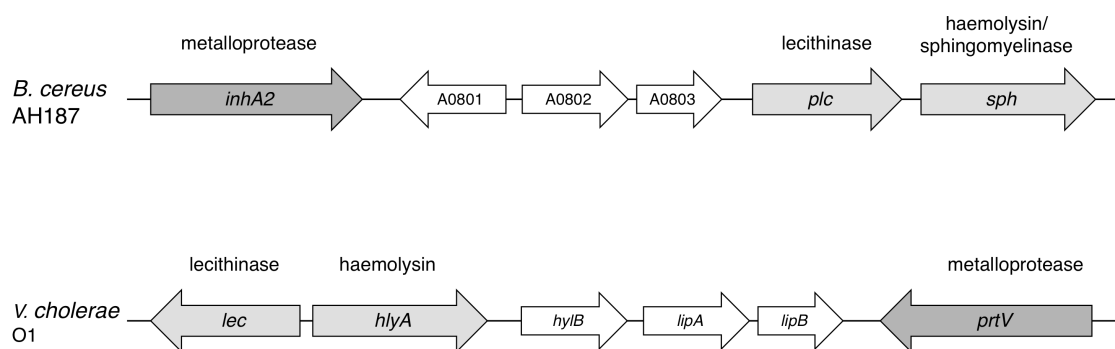


Figure 37: Genetic organization of the metalloprotease and haemolysin gene cluster of *B. cereus* AH187 (F4810/72) in comparison to *V. cholerae* O1. *B. cereus* *inhA2* and *V. cholerae* *prtV* encode highly similar zinc metalloproteases and are both in close vicinity to two phospholipase genes encoding a lecithinase and haemolysin activity. Arrow orientation indicates the direction of gene transcription.

The close genomic localisation of genes encoding immune inhibitor A2 and two other PlcR-regulated enzymes might indicate a cooperative activity not only for host tissue degradation but also for providing additional nutrients in a cell-density dependent manner.

In the experiments using unsupplemented RPMI, growth limitation of $\Delta plcR$ was most likely a consequence of nutrient limitation and the lack of proteins that help to make additional nutrients accessible. Interestingly, data of Wang *et al.* indicate that the expression of a *Bacillus megaterium* immune inhibitor A homologous protein Bmg1465 is stress-related and its expression is highly induced under limitation of nutrients during stationary growth phase (Wang *et al.* 2006). Especially, high amounts of cell-associated InhA were found to be degraded by *B. megaterium* and degradation products might serve as amino acid source for the cells. *B. megaterium* InhA is highly similar to *B. cereus* InhA, sharing 58% identity to InhA1, 55% identity to InhA2 and 60% identity to InhA3. Secreted InhA2 might also be subject to proteolytic degradation and proteomic approaches identified several degradation fragments of InhA2 in the supernatant of *B. cereus* (Gohar *et al.* 2002; Gohar *et al.* 2005). This suggests that InhA2 itself could represent a nutrient source that is missing in a *plcR* deletion mutant.

On the other hand, InhA has been identified as a major protease in *B. anthracis* secretome that can induce and mediate massive shedding of the mammalian membrane proteoglycan syndecan-1 ectodomain that is involved in barrier permeability (Chung *et al.* 2006). One could speculate that in the absence of host cells and sufficient nutritional peptides, immune inhibitor A could be secreted by *B. cereus* and act on bacterial surface proteins in return to make additional peptides and amino acids available and activate signal cascades. Several proteinaceous structures such as surface layer proteins, flagellin, cell wall anchor domain proteins and glycoproteins have been described not only to be attached to the exosporium but also on the cell surface of vegetative growing *B. cereus* cells (Fox *et al.* 2003; Karunakaran and Biggs 2011). These could be targets to InhA2 degradation, especially when the *B. cereus* population is already partially sporulated, the spore surface proteins might serve as nutrient source for still growing vegetative cells.

The exact mechanism how immune inhibitor A metalloproteases can induce bacterial growth could not be addressed in this study and has to be subjected to further investigations. Nevertheless, the findings support the hypothesis that many microbial proteins, well established as virulence factors, might have multiple functions. In conclusion, the results of this study indicate a close link between microbial growth, metabolism and disease initiation. Many established virulence factors are likely even more important for general bacterial fitness and adaptation to adverse environmental conditions.

4.2.2 Influence of IEC-derived factors on B. cereus $\Delta plcR$ proteome and growth

As described in chapter 3.2.1, the growth defect observed for a *B. cereus* F4810/72 *plcR* deletion mutant in nutrient-poor RPMI medium could not only be rescued by the expression of the bacterial protein InhA2 (Ch. 3.2.2.2), but also in the presence of host-derived factors. To analyze the effect of IEC secreted factors on *B. cereus* $\Delta plcR$ growth, the proteome of the *plcR* deletion mutant in unsupplemented RPMI medium was compared to protein expression in RPMI preconditioned with epithelial cells (IEC). Changes in *B. cereus* secretome resulting from *plcR* inactivation have been studied in rich medium (Gohar *et al.* 2002), where the amount of extracellular proteins decreased by 50% upon *plcR* disruption. Here the secretome of a *plcR* deletion mutant incubated in nutrient-poor medium showed further decrease in the amount of secreted proteins, that was not significantly affected by the treatment with host cell conditioned medium (data not shown). Although it cannot be excluded that variations in incubation time could bring to light distinct changes in the secretome induced by IEC factors, this study focused on the cytosolic proteome where significant differential protein expression could be observed in response to host-derived factors already after 2 h incubation (Ch. 3.2.3, Tab. 11). Comparison of $\Delta plcR$ proteins expressed in un-suppl. RPMI and IEC preconditioned RPMI revealed 49 differentially regulated (≥ 1.3 -fold) protein spots. Of these 33 spots were selected for MALDI-TOF mass spectrometry and 22 spots could be identified belonging to 19 different proteins (Tab. 12). 74% of these specifically regulated proteins can be assigned to three core metabolic

pathways including purine biosynthesis (PurC, PurD, PurL, PurM), amino acid biosynthesis (LeuA, SerC, IlvE, IlvC1/2) and protein metabolism (IleS1/2, MetS, ThrS1/2). Additionally, the single proteins OppA, AceA, OdhA and the two proteases InhA3 and NprB were identified. Interestingly, 8 proteins, namely the 2-isopropylmalate synthase (LeuA), Ketol-acid reductoisomerase (IlvC1), Ketol-acid reductoisomerase II (IlvC2), Branched-chain amino acid aminotransferase (IlvE1), Isoleucyl-tRNA synthetase (IleS), Isoleucyl-tRNA synthetase (IleS2), oligopeptide-binding protein (OppA) and Isocitrate lyase (AceA), are generally regulated in response to treatment, indicated by a parallel regulation in *wild-type B. cereus* (Tab. A4, Appendix 7.4). In contrast, the regulation of the residual 11 proteins is PlcR-specific making them exceptionally interesting in the light of PlcR-dependent growth regulation.

4.2.2.1 Regulation of proteins involved in amino acid and protein biosynthesis

Upregulation of proteins involved in amino acid synthesis and protein biosynthesis (aminoacyl-tRNA synthetases) was partially PlcR-specific and treatment-effected and is therefore assumed to represent a very general response mechanism upon amino acid starvation. Although RPMI medium provides several essential amino acids, one could speculate that during preincubation with IEC, the amino acids could have been consumed by the epithelial cells leading to amino acid starvation during subsequent *Bacillus* incubation. Except for IlvC2 (6.84-fold) and IleS (4.77-fold), expression of the respective proteins was only slightly increased, ranging from 1.31- to 2.44-fold (Tab. 12). This indicates that IEC conditioned RPMI medium mainly lacks branched-chain amino acid isoleucine. The genes encoding amino acid biosynthetic enzymes 2-isopropylmalate synthase (*leuA*) and Ketol-acid reductoisomerase (*ilvC1/2*) are members of the *ilv-leu* operon that comprises the seven genes *ilvBHC-leuABCD*. In *B. subtilis* the *ilv-leu* operon together with the three monocistronic transcription units (*ilvA*, *ilvD* and *ybgE*) encode the enzymes needed for BCAA biosynthesis (Fink 1993). An additional enzyme, IlvE1, catalyzes the transamination of the branched-chain amino acids to their respective alpha-keto acids. Growth of *E. coli* is essentially dependent on IlvE-controlled valine production (Zhang *et al.* 2010).

Gram-positive bacteria commonly use conserved mechanisms to regulate core metabolic processes. Induction of several aminoacyl-tRNA synthetase genes (Grundy and Henkin 1993; Pelchat and Lapointe 1999) and the *ile-leu* operon (Grandoni *et al.* 1992) has been shown to be regulated by a common antitermination mechanism that involves uncharged tRNAs and a conserved T-box sequence in the 5' untranslated region of the mRNA transcript (Green *et al.* 2010). Aminoacyl-tRNA synthetases play an essential role for protein biosynthesis as they catalyze the charging of tRNAs with their cognate amino acids. It has been demonstrated for the threonyl-tRNA synthetase gene *thrS* in *B. subtilis* that starvation of the corresponding amino acid threonine specifically induced expression in direct proportion to growth rate (Putzer *et al.* 1995).

Although an incubation time of 2 h was chosen to limit proteomic differences due to differential growth initiation, it cannot be fully excluded that increase in aminoacyl-tRNA synthetase expression is due to growth induction in IEC conditioned medium. However, it is more likely that

other additional regulatory mechanisms contribute to their upregulation in IEC conditioned medium. Recently, several groups have independently identified a regulatory circuit for branched-chain amino acid biosynthesis involving the global regulator CodY and the two response regulators CcpA and TnrA (Shivers and Sonenshein 2005; Tojo *et al.* 2005). While CodY acts as negative regulator and TnrA represses *ilv-leu* operon expression under nitrogen-limiting conditions, CcpA induces gene expression in response to glucose availability. This represents a complex balanced regulatory network linking carbon, nitrogen and amino acid metabolism (for a review see (Sonenshein 2007)). Bacterial proteomic changes observed in the presented study might represent an adaptation of core metabolic pathways to the nutritional status found in the host as reflected by IEC conditioned medium.

4.2.2.2 Downregulation of proteins involved in TCA cycle and purine biosynthesis

In contrast to most of the identified proteins which are upregulated in IEC conditioned medium, six proteins including four members of the *pur* operon, one Isocitrate lyase (AceA) and the E1 component of the 2-oxoglutarate dehydrogenase (SucA/OdhA) were found to be less abundant in conditioned medium compared to unsupplemented RPMI. The latter both enzymes also belong to core metabolic pathways. The 2-oxoglutarate dehydrogenase complex (ODHC) consists of three enzyme components and is involved in the tricarboxylic acid (TCA) cycle to generate energy through oxidation of acetate (Carlsson and Hederstedt 1989). Expression of ODHC is repressed by glucose in the medium (Resnekov *et al.* 1992). Obviously, the IEC conditioned medium contains sufficient amounts of glucose to downregulate *odhA* expression and on the other hand upregulated amino acid biosynthesis via CcpA. Noteworthy, this study could only detect the E1 component of the 2-oxoglutarate dehydrogenase complex to be downregulated, although in *B. subtilis* data indicate that *odhA* and *odhB* form an operon and are therefore likely to be cotranscribed (Resnekov *et al.* 1992). The Isocitrate lyase (AceA) is required for conservation and utilization of C₂-compounds such as ethanol and acetate in the glyoxylate pathway. This pathway bypasses the TCA cycle and AceA cleaves isocitrate to glyoxylate thereby releasing succinate. Glyoxylate can then be further metabolized to malat and finally to oxaloacetate, itself an intermediate of the TCA cycle (Cozzone 1998). It has been shown that AceA is essential for *Salmonella* persistence in the host (Fang *et al.* 2005) and *Pseudomonas aeruginosa* repressed *aceA* transcription in ethanol-glucose containing media until readily utilizable glucose was exhausted (Kretzschmar *et al.* 2008). Based on these findings it is tempting to speculate about a higher content of easily consumable substrates in the RPMI medium after preconditioning with epithelial cells than without conditioning.

In addition to the two single enzymes described above, also four members of the *Bacillus pur* operon were downregulated in IEC conditioned medium particularly in the *plcR* mutant, indicating that the observed effect was specific and no artefact. Similar to *B. subtilis*, the operon for purine biosynthetic enzymes in *B. cereus* F4810/72 comprises a 12 gene-cluster, *purEKB-purC(ORF)QLF-purMNH-purD* that is mapped in Figure 38A (Ebbole and Zalkin 1989). The *pur* operon encodes the enzymes of inosine monophosphate (IMP) biosynthesis that is a precursor

of the purine compounds adenosine monophosphate (AMP) and guanosine monophosphate (GMP) (Fig. 38B) (Saxild and Nygaard 1991).

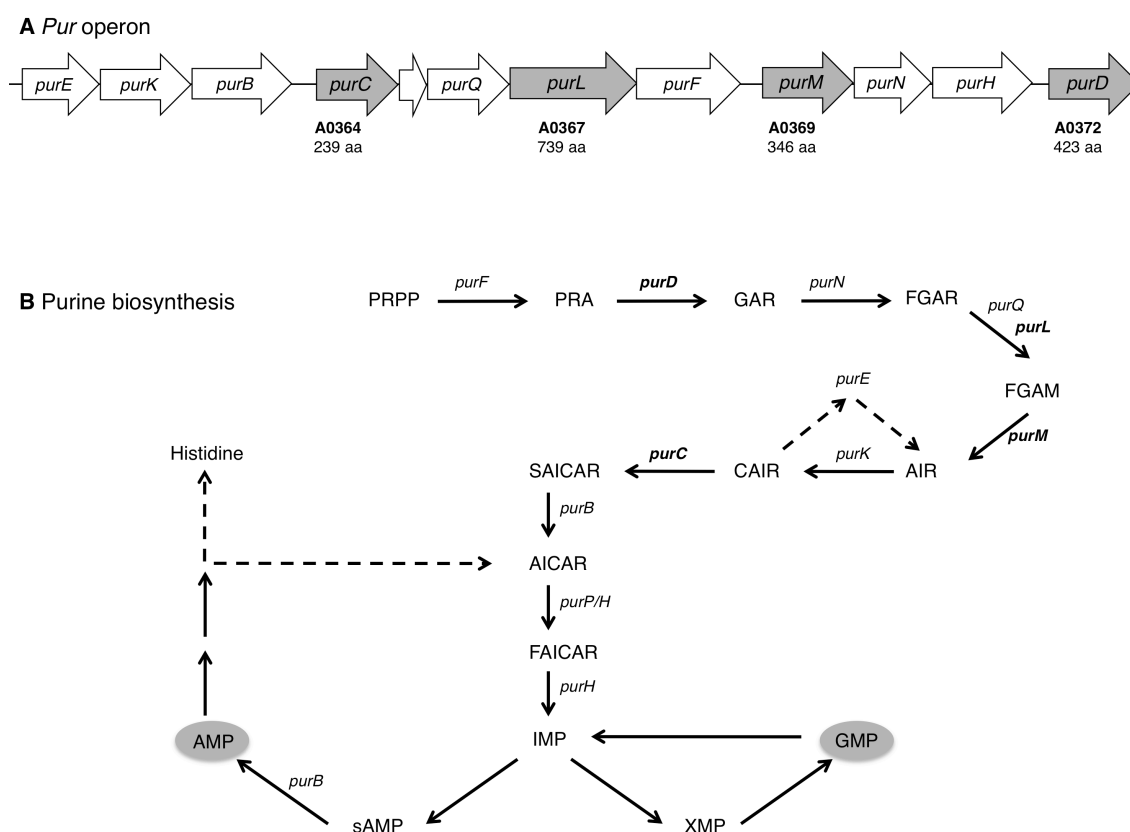


Figure 38: Genetic organization of the *pur* operon of *B. cereus* F4810/72 encoding genes involved in purine biosynthesis. **A:** *Pur* operon organization, genes encoding for proteins identified by MALDI-TOF mass spectrometry are marked in grey, respective locus_tags and aa length are indicated. Arrow orientation indicates direction of gene transcription. **B:** Pathway of purine biosynthesis in *B. subtilis* as adapted from Saxild *et al.* (Saxild and Nygaard 1991). Enzymes encoded by the *pur* operon are identified by their gene symbols, genes encoding for proteins identified by MALDI-TOF mass spectrometry are marked in bold. PRPP, phosphoribosylpyrophosphate; PRA, phosphoribosylamine; GAR, glycinamide ribonucleotide; FGAR, formylglycinamide ribonucleotide; FGAM, formylglycinamide ribonucleotide; AIR, aminoimidazole ribonucleotide; CAIR, carboxyaminoimidazole ribonucleotide; SAICAR, aminoimidazolesuccino-carboxamide ribonucleotide; AICAR, aminoimidazolecarboxamide ribonucleotide; FAICAR, formamido-imidazolecarboxamide ribonucleotide; IMP, inosine monophosphate; sAMP adenylosuccinate; AMP, adenosine monophosphate; XMP, xanthosine monophosphate; GMP, guanosine monophosphate.

The purines adenine and guanine are not only crucial constituents of DNA and RNA, but also components of essential biomolecules such as NADH, coenzyme A, ATP and GTP. Therefore, tight regulation of purine biosynthesis is very important for the bacterial cell in order to avoid excess energy expenditure. In the well-characterised *Bacillus subtilis*, transcription repression of the *pur* operon genes has been demonstrated as a result of the addition of purines (adenine, adenosine, guanine and guanosine) to the growth medium (Nishikawa *et al.* 1967; Ebbola and Zalkin 1989; Saxild and Nygaard 1991). Transcriptional repression of the purine biosynthesis is mediated by direct DNA-binding of the PurR repressor (Bera *et al.* 2003). I observed the downregulation of four members of the *pur* operon, namely *purC*, *purD*, *purL* and *purM* upon

incubation with IEC conditioned medium suggesting the secretion or release of purines or purine containing compounds (DNA, RNA) by epithelial host cells into the medium. On the 2-D gels, PurL was detected in a three spot train (spot #1-3, Fig. 36) indicative for posttranslational modification. Except for PurL (-1.52-, -1.68, -1.71-fold), very similar regulation patterns were calculated for PurC (-1.45-fold), PurD (-1.41-fold) and PurM (-1.43-fold) confirming the simultaneous downregulation of *pur* operon genes in response to IEC conditioned medium. This is in contrast to previous results with *B. subtilis*, where *purC* gene expression was found to be 3.0- to 6.8-fold higher than other *pur* genes probably because of enhanced translational efficiency (Ebole and Zalkin 1989). The reason why I could not detect all of the *pur* operon genes to be regulated in *B. cereus* F4810/72 $\Delta plcR$ under the given conditions, could be i) that not all significantly regulated protein spots could be identified unambiguously by mass spectrometry and ii) the not very abundant downregulation of these genes. Therefore, some *pur* operon members may be missed due to their only weak regulation below the 1.3 threshold as seen for *purK*, which was identified although it was only 1.24-fold downregulated (hence not included in Tab. 12 and Fig. 36).

4.2.2.3 Regulation of secreted proteins

All proteins identified so far were clearly located in the cytosol of *B. cereus*. However, three proteins could be detected in the cytosolic subproteome of *B. cereus* $\Delta plcR$ that harbour secretion signal peptides as predicted on the SignalP 3.0 server (Ch. 2.13.). One of these is the oligopeptide-binding protein OppA of a putative oligopeptide ABC transporter, that was upregulated in response to host-conditioned medium in *B. cereus* $\Delta plcR$, but also in *wild-type*. OppA is the extracellular located membrane-bound unit of the oligopeptide transporter that serves as peptide-ligand, while the subunits OppB, OppC, OppD and OppF build up the transmembrane pore including two cytoplasmic ATPases (Perego *et al.* 1991). The ATP-binding cassette (ABC) transporter is responsible for the uptake of small peptides (Detmers *et al.* 2001) and is widely distributed among bacteria (Guyer *et al.* 1986; Hiles *et al.* 1987; Pearce *et al.* 1992). In *Bacillus* the oligopeptide permease transporter is an essential contributor to environmental sensing via several two-component quorum sensing systems, such as PlcR/PapR and RapA/PhrA (Perego and Hoch 1996; Perego 1997; Slamti and Lereclus 2002). Recently, Gominet *et al.* demonstrated that in *B. thuringiensis* Opp is necessary for *plcR* expression independently of Spo0A as it reimports the processed PapR peptide and so enables PlcR activation (Gominet *et al.* 2001; Slamti and Lereclus 2002) (compare Figure 3). The *B. thuringiensis opp* genes constitute an operon and are co-transcribed throughout exponential and stationary growth phase (Gominet *et al.* 2001) similar to the *B. subtilis opp* operon (Koide *et al.* 1999). By contrast, little is known about *opp* transcriptional regulation in *B. cereus*. Although I could only identify the peptide-binding subunit OppA among the differentially regulated proteins, the data provide a first hint that the main function of bacterial oligopeptide permease could be the import of extracellular peptides for their use as carbon and nitrogen source. In response to host environment and/or limitation of proteinaceous/amino acid nutrients *B. cereus* might

upregulate the peptide transporter or at least the peptide-ligand OppA to facilitate nutrient acquisition.

From the data it is not clear if OppA was found in the cytosolic fraction as a remnant of membrane proteins after cell disruption, if OppA is accumulated both extra- and intracellular or if accumulation is a consequence of a secretion defect in the *plcR* deletion mutant. The same questions remain for the two most interesting proteins identified by 2-D DIGE.

4.2.2.4 Upregulation of the metalloproteases *InhA3* and *NprB*

Upon treatment with IEC conditioned medium the two zinc dependent metalloproteases immune inhibitor A3 (*InhA3*) and neutral protease B (*NprB*) were amongst the four most abundant *PlcR*-specific upregulated proteins with a 5.69- and 3.81-fold upregulation, respectively. Homologous proteins of *B. anthracis*, namely *InhA1* (BA1295) and *Npr599* (BA0599), misleadingly also termed *NprB*, have been found secreted at high levels. In minimal medium containing O₂ *InhA1* and *Npr599* represented more than 90% of total *B. anthracis* secretome proteins (Chitlaru *et al.* 2006). Also high stress-induced expression of two related proteins was detected in *B. megaterium*. While *B. megaterium* neutral protease *NprM* was secreted at high levels, the immune inhibitor A similar protein was found accumulated in the cytosol upon glucose limitation (Wang *et al.* 2006). Since this study focussed on the *B. cereus* F4810/72 cytosolic subproteome, no clear evidence can be provided for additional extracellular accumulation of the metalloproteases *InhA3* and *NprB*, however a secretion defect cannot be excluded likewise. Protein spots on 2-D gels were detected at molecular weights of unprocessed (pre)propeptide forms of *InhA3* (spot #22, 81 kDa) and *NprB* (spot #21, 62 kDa) such as normally found intracellular prior to secretion and processing (Fig. 36). Analysis of amino acid sequences of both metalloproteases on the SignalP 3.0 server ((Bendtsen *et al.* 2004); <http://www.cbs.dtu.dk/services/SignalP-3.0/>) revealed a signal peptide cleavage site between aa 29 and 30 (SHA-AY) for *InhA3* similar to the 32 aa signal peptide found in *InhA3* (Bc2984) of *B. cereus* ATCC14579 (Guillemet *et al.* 2010). In contrast to other members of the neutral protease family (Miyoshi and Shinoda 2000), prediction for *NprB* defined an unusually long (71 aa) non-canonical signal peptide, which could suggest an alternative secretion pathway or the entire cytosolic localization of *NprB*.

The genomes of the three pathogenic members of the *B. cereus* group *B. anthracis*, *B. thuringiensis* and *B. cereus* harbour numerous genes encoding for protein/peptide degradation, peptide and amino acid transport as well as their metabolism (Mols *et al.* 2007). This redundancy might reflect an adaptation to the mainly proteinaceous nutrients available in the host (Ivanova *et al.* 2003; Gohar *et al.* 2005). As emphasized before, secreted proteases play important roles in bacterial virulence. *B. anthracis* *NprB*/599 and *InhA1* are strongly involved in the clinical manifestation of anthrax by the induction of the host fibrinolytic system, degradation of host matrix and tissue components, disruption of host barrier and counteracting the immune system (Chung *et al.* 2006; Chung *et al.* 2011) (Ch. 4.2.1). The additionally

contribution of microbial metalloproteases to nutrient acquisition and growth has long been proposed and could be confirmed in this study for InhA2.

As discussed above (Ch. 4.2.1) very few information is available from literature about transcriptional regulation and physiological function of the third homologous protein of the immune inhibitor family InhA3. *InhA3* expression was highly induced in sporulation (HCT) medium and the immune inhibitor A3 protein was found to be secreted and reabsorbed to the bacterial surface (Gominet *et al.* 2001). My data confirmed the expression of *inhA3* under nutrient-limiting conditions (in preconditioned RPMI medium) and indicate that after *plcR* inactivation InhA3, most likely in combination with other factors like NprB, might compensate the lack of InhA2 and other essential PlcR-regulated proteins. In the presence of host-derived factors (found in IEC conditioned medium) InhA3 expression might be triggered, the protease is secreted and can induce bacterial growth *via* a yet unknown mechanism.

Other members of the zinc metalloprotease family, the neutral proteases have been identified in the genomes of almost all *B. cereus* group members. 2-D DIGE analysis accompanied by mass spectrometric protein identification detected *B. cereus* NprB (BCAH187_A5197) as one of the most highly abundant proteins expressed by *B. cereus* F4810/72 $\Delta plcR$ when incubated in IEC conditioned medium. Based on the data presented here one could speculate that NprB contributes to growth rescue in $\Delta plcR$.

Genome-wide BLASTP analysis revealed the presence of at least two other genes in the *B. cereus* F4810/72 genome that encode for neutral proteases similar to the identified NprB (BCAH187_A5197), namely Npr599 (BCAH187_A0727) and a truncated form of bacillolysin (BCAH187_A5530; commonly termed NprB in other *B. cereus* strains). In spite of their common enzymatic activity, the three *B. cereus* neutral proteases share only low amino acid sequence identity and are likely to be members of different transcriptional regulation circuits. However, it is unclear which regulators control the redundant neutral protease expression, especially of NprB, in *B. cereus* F4810/72.

For bacteria it is of essential importance to sense their environment and control their protein expression accordingly. The *B. cereus* group members have evolved several two-component systems to scan environmental changes in a quorum-sensing manner. The PlcR-PapR regulation system has been discussed in detail for its involvement in *B. cereus* virulence. Homologues of the bacillolysin (BCAH187_A5530), the truncated *nprB*, have been found located directly upstream of the *plcR* gene in *B. thuringiensis* (Lereclus *et al.* 2000), *B. cereus* strains ATCC 14579 (Gohar *et al.* 2005) and 569 (Pomerantsev *et al.* 2009) sharing one PlcR-box, however being transcribed in the opposite direction (Økstad *et al.* 1999). This neutral protease is expressed as prepropeptide (Pomerantsev *et al.* 2009). After secretion the neutral protease propeptide is processed to the mature protease in a common mechanism for secreted metalloproteases (either autocatalytic or by other proteases) (Miyoshi and Shinoda 2000; Park *et al.* 2004). *B. cereus* 569 NprB is PlcR-regulated and is in turn involved in maturation of the PapR signalling peptide of the PlcR quorum-sensing system (Pomerantsev *et al.* 2009). *PlcR*

deletion completely abolished *nprB* expression in *B. cereus* ATCC14579 (Gohar *et al.* 2002). Interestingly, *B. cereus* ATCC 10987 and *B. anthracis* strains completely lack the PlcR-PapR associated *nprB* (Pomerantsev *et al.* 2009). Although genomic localization of the *nprB^{tr}-plcR-papR* gene is conserved in the emetic *B. cereus* F4810/72 strain, *nprB^{tr}* is functionally inactive due to truncation (Fig. 39). This arises the question how signalling peptide processing is performed in those strains. It is tempting to speculate that other chromosomally encoded neutral proteases such as the identified NprB (BCAH187_A5197) and Npr599 or plasmid-derived proteases can take over this function. In line with this, Frenzel (2011) recently identified a neutral protease, termed NprC38 that is encoded on the pXO1-like megaplasmid pBCE in the emetic *B. cereus* F4810/72 (Frenzel 2011, PhD Thesis).

NprB (BCAH187_A5197) expression in *B. cereus* F4810/72 $\Delta plcR$ (Ch. 3.2.3) clearly indicates a regulation mechanism independent of PlcR. In *B. thuringiensis* the NprR-NprX regulon has been demonstrated to activate neutral protease A transcription at the beginning of sporulation to increase secreted protease and provide nutrients that might allow a delay of sporulation (Perchat *et al.* 2011). Analysis of the genomic regions flanking *nprB* could not identify genes homologous to *nprR-nprX*. In contrast, two genes directly upstream of the *B. cereus* F4810/72 neutral protease gene *npr599* (BCAH187_A0727) were highly similar to *B. thuringiensis nprR* and *nprX* (Fig. 39).

NprR is a transcriptional regulator of the RNPP family like PlcR (Declerck *et al.* 2007) and together with its signalling peptide NprX constitutes a two-component quorum-sensing system. While *B. cereus* F4810/72 Npr599 is highly similar to *B. thuringiensis* NprA (97% identity, 100% sequence coverage), the identified NprB (BCAH187_A5197) shares only 41% identity with Npr599 and NprA. This could explain the found regulation analogy for NprA and Npr599, while a third, different regulation mechanism might control *nprB* expression in the emetic *B. cereus* F4810/72.

Since transcriptional regulator genes are often located adjacent to the genes they control, further genomic analysis was performed and revealed, that *B. cereus* F4810/72 *nprB* is in fact located in close vicinity to a gene (BCAH187_A5199) annotated as a MarR family transcriptional regulator (Fig. 39). Comparable genetic organization could be found for *B. cereus* ATCC10987 *nprB* (ATCC10987) and *B. anthracis* Sterne *nprB* (GBAA_5282), two genes whose protein products share highest sequence similarity with *B. cereus* F4810/72 NprB (97% and 95% identity).

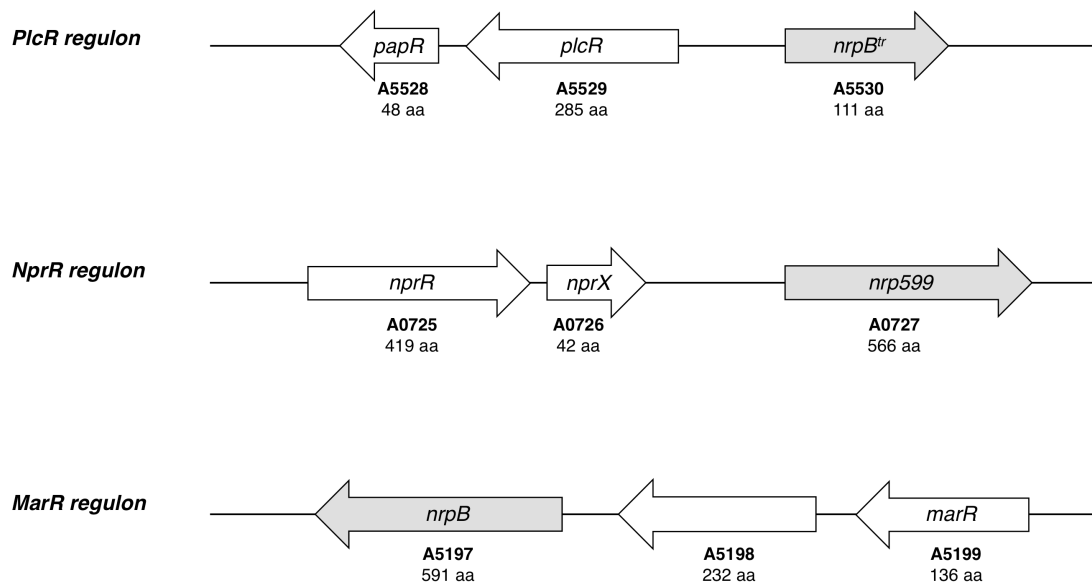


Figure 39: Organization of the genomic regions directly upstream of three different *B. cereus* F4810/72 neutral protease genes. A truncated bacillolysin/*nprB* gene (*nprB^{tr}*) is part of the PlcR virulence regulon, while *npr599* seems to be controlled by the NprR-NprX quorum-sensing system. A MarR family transcriptional regulator gene *marR* was found in close vicinity to the intact neutral protease B gene (*nprB*), indicating a potential involvement of a MarR-like regulator in *nprB* expression (as discussed in the text). Respective locus_tags and aa length of the corresponding proteins are indicated.

Homologous proteins of the MarR (**M**ultiple **a**ntibiotic **r**esistance **r**egulator) family are distributed throughout Achaea, Gram-negative (MarR, *E. coli*; SlyA, *Salmonella typhimurium*) and Gram-positive bacteria (OhrR, *B. subtilis*) (Sulavik *et al.* 1995; Sulavik *et al.* 1997; Fuangthong *et al.* 2001; Pérez-Rueda and Collado-Vides 2001; Stapleton *et al.* 2002). They exhibit regulatory physiological functions in the response to environmental stress, control of virulence factors and regulation of aromatic catabolic pathways (Wilkinson and Grove 2006).

Commonly, MarR acts as a repressor of target gene transcription by direct binding to the promoter sequence of its target genes (Wilkinson and Grove 2006). Though to the best of the authors knowledge nothing is known about an involvement of MarR in the regulation of *B. cereus* neutral protease expression.

Therefore, one could only speculate that host secreted factors in the IEC conditioned medium could directly or indirectly act on MarR to release the regulator from its target DNA resulting in derepression of *nprB* transcription.

In summary, several aspects of the observed proteomic changes in *B. cereus* F4810/72 Δ *plcR* need to be further investigated in more detail to allow a final conclusion, if differential protein expression patterns simply result from an altered repertoire of nutritional molecules provided by host cells or if epithelial cell factors can per se act as growth regulators.

4.3. Conclusion and perspectives

In conclusion, this study provides evidence, that the long known *B. cereus* haemolytic enzyme sphingomyelinase (SMase) has been underestimated for its contribution to *B. cereus* overall pathogenicity. In a screen for novel cytotoxic factors other than the well-known enterotoxin Nhe, SMase was identified as a strong inducer of epithelial cell death via apoptosis in a caspase-3 dependent pathway. By the use of single and double deletion mutants of *sph* and *nheBC* in *B. cereus* F4810/72 and NVH 0075-95, it was shown that SMase is a key player in *B. cereus* cytotoxicity *in vitro* and pathogenicity *in vivo*, both in emetic and diarrheal strains. While SMase and Nhe synergistically induced *B. cereus* cytotoxicity *in vitro*, only SMase but not Nhe contributed significantly to the mortality rate of *Galleria mellonella* larvae after intrahaemocoelic injection as an *in vivo* model for *B. cereus* non-gastrointestinal-tract infection. It is expected that these results might help to improve our limited understanding of *B. cereus* pathogenesis in systemic infections. Since antibiotic treatment may not be sufficient to prevent extensive tissue destruction conveyed by secreted bacterial toxins and degradative enzymes, SMase could be a promising target for antidote development. Thus, continuative work will be necessary to elucidate the complex mechanism how the pore-forming toxin Nhe and the phospholipase SMase cooperate to mediate epithelial barrier disintegration. Oral infection of the insect or mammalian host with bacterial mutant strains might provide insights into the role of SMase (and Nhe) for bacterial establishment and conquering host barriers as initial steps for disease initiation. An in-depths analysis of *sph* gene expression under various host-simulating conditions, for instance by qPCR, promoter-fusion constructs and *in vivo* imaging would yield important information about bacteria-host interaction and virulence gene regulation in response to host environment. Furthermore, this could help to identify and differentiate between low and high toxin producer *B. cereus* strains, which is of high importance with respect to food safety issues and human pathogenicity.

A second focus of this work was the characterization of the impact of intrinsic bacterial and host-derived factors on bacterial proliferation under nutrient-limiting conditions. Obviously, PlcR-regulated proteins play a pivotal role for bacterial growth, since *plcR* deletion resulted in a severe growth defect of *B. cereus* F4810/72 in nutrient-poor RPMI medium. Reconstitution of growth by a *wild-type* PlcR-dependent protease, immune inhibitor A2 and in the presence of epithelial cell-derived factors was observed. Two independent approaches identified members of the extracellular zinc metalloprotease family (InhA2, InhA3 and NprB) as strong candidates that might mediate nutrient acquisition or cell signalling essential for growth stimulation. These results may promote investigations to decipher the biological role of protease gene redundancy in *B. cereus* and the highly complex network of their differential transcriptional activation. For instance, deletion of protease genes, characterization of inhibitor and substrate specificity and detailed confocal microscopic imaging of protease localization could help to fully define the mechanistic action of *B. cereus* F4810/72 proteases. In a global analysis of $\Delta plcR$ proteins expressed differentially in unsupplemented RPMI medium and IEC-conditioned medium the

importance of host-bacteria interaction was emphasized as intestinal epithelial cell secretome was shown to enhance bacterial multiplication and significantly altered the cytosolic proteome of *B. cereus* F4810/72. Evidence is provided that in nutrient-poor medium the lack of PlcR regulator can only be rescued by external stimulation signals originating from host cells or bacterial competitors. However, substantial future work is necessary to uncover the exact mechanism how intestinal epithelial cells or their secreted factors can directly influence *B. cereus* core metabolic pathways resulting in growth stimulation.

5. REFERENCES

- Abee, T., M. N. Groot, M. Tempelaars, M. Zwietering, R. Moezelaar and M. van der Voort (2011).** Germination and outgrowth of spores of *Bacillus cereus* group members: diversity and role of germinant receptors. *Food Microbiol* **28**(2): 199-208.
- Agaisse, H., M. Gominet, O. A. Okstad, A. B. Kolstø and D. Lereclus (1999).** PlcR is a pleiotropic regulator of extracellular virulence factor gene expression in *Bacillus thuringiensis*. *Mol Microbiol* **32**(5): 1043-1053.
- Agata, N., M. Mori, M. Ohta, S. Suwan, I. Ohtani and M. Isobe (1994).** A novel dodecadepsipeptide, cereulide, isolated from *Bacillus cereus* causes vacuole formation in HEp-2 cells. *FEMS Microbiol Lett* **121**(1): 31-34.
- Agata, N., M. Ohta, Y. Arakawa and M. Mori (1995).** The *bceT* gene of *Bacillus cereus* encodes an enterotoxic protein. *Microbiology* **141**(4): 983-988.
- Agata, N., M. Ohta, M. Mori and M. Isobe (1995).** A novel dodecadepsipeptide, cereulide, is an emetic toxin of *Bacillus cereus*. *FEMS Microbiol Lett* **129**(1): 17-20.
- Ago, H., M. Oda, M. Takahashi, H. Tsuge, S. Ochi, N. Katunuma, M. Miyano and J. Sakurai (2006).** Structural basis of the sphingomyelin phosphodiesterase activity in neutral sphingomyelinase from *Bacillus cereus*. *J Biol Chem* **281**(23): 16157-16167.
- Andersson, A., P. E. Granum and U. Rønner (1998).** The adhesion of *Bacillus cereus* spores to epithelial cells might be an additional virulence mechanism. *Int J Food Microbiol* **39**(1-2): 93-99.
- Andersson, M. A., P. Hakulinen, U. Honkalampi-Hämäläinen, D. Hoornstra, J. C. Lhuguenot, J. Mäki-Paakkanen, M. Savolainen, I. Severin, A. L. Stamatii, L. Turco, A. Weber, A. von Wright, F. Zucco and M. Salkinoja-Salonen (2007).** Toxicological profile of cereulide, the *Bacillus cereus* emetic toxin, in functional assays with human, animal and bacterial cells. *Toxicon* **49**(3): 351-367.
- Andree, H. A., C. P. Reutelingsperger, R. Hauptmann, H. C. Hemker, W. T. Hermens and G. M. Willems (1990).** Binding of vascular anticoagulant alpha (VAC alpha) to planar phospholipid bilayers. *J Biol Chem* **265**(9): 4923-4928.
- Anonymous (2009).** The Community Summary Report on Food-borne Outbreaks in the European Union in 2007. *The EFSA Journal* **271**: 1-128.
- Anonymous (2010).** The Community Summary Report on Trends and Sources of Zoonoses, Zoonotic Agents and Food-borne Outbreaks in the European Union in 2008. *The EFSA Journal* **8**(1): 1496-1865
- Arantes, O. and D. Lereclus (1991).** Construction of cloning vectors for *Bacillus thuringiensis*. *Gene* **108**(1): 115-119.
- Aronson, A. I. and Y. Shai (2001).** Why *Bacillus thuringiensis* insecticidal toxins are so effective: unique features of their mode of action. *FEMS Microbiol Lett* **195**(1): 1-8.
- Asano, S. I., Y. Nukumizu, H. Bando, T. Iizuka and T. Yamamoto (1997).** Cloning of novel enterotoxin genes from *Bacillus cereus* and *Bacillus thuringiensis*. *Appl Environ Microbiol* **63**(3): 1054-1057.
- Ash, C., J. A. Farrow, M. Dorsch, E. Stackebrandt and M. D. Collins (1991).** Comparative analysis of *Bacillus anthracis*, *Bacillus cereus*, and related species on the basis of reverse transcriptase sequencing of 16S rRNA. *Int J Syst Bacteriol* **41**(3): 343-346.
- Auger, S., N. Ramarao, C. Faille, A. Fouet, S. Aymerich and M. Gohar (2009).** Biofilm formation and cell surface properties among pathogenic and nonpathogenic strains of the *Bacillus cereus* group. *Appl Environ Microbiol* **75**(20): 6616-6618.

- Avashia, S. B., W. S. Riggins, C. Lindley, A. Hoffmaster, R. Drumgoole, T. Nekomoto, P. J. Jackson, K. K. Hill, K. Williams, L. Lehman, M. C. Libal, P. P. Wilkins, J. Alexander, A. Tvaryanas and T. Betz (2007).** Fatal pneumonia among metalworkers due to inhalation exposure to *Bacillus cereus* Containing *Bacillus anthracis* toxin genes. *Clin Infect Dis* **44**(3): 414-416.
- Baida, G., Z. I. Budarina, N. P. Kuzmin and A. S. Solonin (1999).** Complete nucleotide sequence and molecular characterization of hemolysin II gene from *Bacillus cereus*. *FEMS MicrobiolLett* **180**(1): 7-14.
- Baida, G. E. and N. P. Kuzmin (1995).** Cloning and primary structure of a new hemolysin gene from *Bacillus cereus*. *Biochim Biophys Acta* **1264**(2): 151-154.
- Barrie, D., J. A. Wilson, P. N. Hoffman and J. M. Kramer (1992).** *Bacillus cereus* meningitis in two neurosurgical patients: an investigation into the source of the organism. *J Infect* **25**(3): 291-297.
- Bashford, C. L., G. M. Alder, G. Menestrina, K. J. Micklem, J. J. Murphy and C. A. Pasternak (1986).** Membrane damage by hemolytic viruses, toxins, complement, and other cytotoxic agents. A common mechanism blocked by divalent cations. *J Biol Chem* **261**(20): 9300-9308.
- Beecher, D. J. and J. D. Macmillan (1990).** A novel bicomponent hemolysin from *Bacillus cereus*. *Infect Immun* **58**(7): 2220-2227.
- Beecher, D. J. and J. D. Macmillan (1991).** Characterization of the components of hemolysin BL from *Bacillus cereus*. *Infect Immun* **59**(5): 1778-1784.
- Beecher, D. J., T. W. Olsen, E. B. Somers and A. C. Wong (2000).** Evidence for contribution of tripartite hemolysin BL, phosphatidylcholine-preferring phospholipase C, and collagenase to virulence of *Bacillus cereus* endophthalmitis. *Infect Immun* **68**(9): 5269-5276.
- Beecher, D. J., J. L. Schoeni and A. C. Wong (1995).** Enterotoxigenic activity of hemolysin BL from *Bacillus cereus*. *Infect Immun* **63**(11): 4423-4428.
- Beecher, D. J. and A. C. Wong (1994).** Improved purification and characterization of hemolysin BL, a hemolytic dermonecrotic vascular permeability factor from *Bacillus cereus*. *Infect Immun* **62**(3): 980-986.
- Beecher, D. J. and A. C. Wong (1997).** Tripartite hemolysin BL from *Bacillus cereus*. Hemolytic analysis of component interactions and a model for its characteristic paradoxical zone phenomenon. *J Biol Chem* **272**(1): 233-239.
- Beecher, D. J. and A. C. Wong (2000).** Cooperative, synergistic and antagonistic haemolytic interactions between haemolysin BL, phosphatidylcholine phospholipase C and sphingomyelinase from *Bacillus cereus*. *Microbiology* **146**(12): 3033-3039.
- Bendtsen, J. D., H. Nielsen, G. von Heijne and S. Brunak (2004).** Improved prediction of signal peptides: SignalP 3.0. *J Mol Biol* **340**(4): 783-795.
- Bennett, H. J., D. M. Pearce, S. Glenn, C. M. Taylor, M. Kuhn, A. L. Sonenshein, P. W. Andrew and I. S. Roberts (2007).** Characterization of *relA* and *codY* mutants of *Listeria monocytogenes*: identification of the CodY regulon and its role in virulence. *Mol Microbiol* **63**(5): 1453-1467.
- Bera, A. K., J. Zhu, H. Zalkin and J. L. Smith (2003).** Functional dissection of the *Bacillus subtilis* pur operator site. *J Bacteriol* **185**(14): 4099-4109.
- Berry, C., S. O'Neil, E. Ben-Dov, A. F. Jones, L. Murphy, M. A. Quail, M. T. Holden, D. Harris, A. Zaritsky and J. Parkhill (2002).** Complete sequence and organization of pBtoxis, the toxin-coding plasmid of *Bacillus thuringiensis* subsp. israelensis. *Appl Environ Microbiol* **68**(10): 5082-5095.

- Betz, F. S., B. G. Hammond and R. L. Fuchs (2000).** Safety and advantages of *Bacillus thuringiensis*-protected plants to control insect pests. *Regul Toxicol Pharmacol* **32**(2): 156-173.
- Blum, H., H. Beier and H. J. Gross (1987).** Improved silver staining of plant proteins, RNA and DNA in polyacrylamide gels. *Electrophoresis* **8**: 93-99.
- Bottone, E. J. (2010).** *Bacillus cereus*, a volatile human pathogen. *Clin Microbiol Rev* **23**(2): 382-398.
- Bramley, A. J., A. H. Patel, M. O'Reilly, R. Foster and T. J. Foster (1989).** Roles of alpha-toxin and beta-toxin in virulence of *Staphylococcus aureus* for the mouse mammary gland. *Infect Immun* **57**(8): 2489-2494.
- Britton, R. A., P. Eichenberger, J. E. Gonzalez-Pastor, P. Fawcett, R. Monson, R. Losick and A. D. Grossman (2002).** Genome-wide analysis of the stationary-phase sigma factor (sigma-H) regulon of *Bacillus subtilis*. *J Bacteriol* **184**(17): 4881-4890.
- Budarina, Z. I., D. V. Nikitin, N. Zenkin, M. Zakharova, E. Semenova, M. G. Shlyapnikov, E. A. Rodikova, S. Masyukova, O. Ogarkov, G. E. Baida, A. Solonin and K. Severinov (2004).** A new *Bacillus cereus* DNA-binding protein, HlyIIR, negatively regulates expression of *B. cereus* haemolysin II. *Microbiology* **150**(11): 3691-3701.
- Cadot, C., S. L. Tran, M. L. Vignaud, M. L. De Buyser, A. B. Kolstø, A. Brisabois, C. Nguyen-Thé, D. Lereclus, M. H. Guinebretière and N. Ramarao (2010).** InhA1, NprA, and HlyII as candidates for markers to differentiate pathogenic from nonpathogenic *Bacillus cereus* strains. *J Clin Microbiol* **48**(4): 1358-1365.
- Callegan, M. C., M. S. Gilmore, M. Gregory, R. T. Ramadan, B. J. Wiskur, A. L. Moyer, J. J. Hunt and B. D. Novosad (2007).** Bacterial endophthalmitis: therapeutic challenges and host-pathogen interactions. *Prog Retin Eye Res* **26**(2): 189-203.
- Callegan, M. C., S. T. Kane, D. C. Cochran and M. S. Gilmore (2002).** Molecular mechanisms of *Bacillus* endophthalmitis pathogenesis. *DNA Cell Biol* **21**(5-6): 367-373.
- Callegan, M. C., S. T. Kane, D. C. Cochran, M. S. Gilmore, M. Gominet and D. Lereclus (2003).** Relationship of plcR-regulated factors to *Bacillus* endophthalmitis virulence. *Infect Immun* **71**(6): 3116-3124.
- Carlsson, P. and L. Hederstedt (1989).** Genetic characterization of *Bacillus subtilis* odhA and odhB, encoding 2-oxoglutarate dehydrogenase and dihydrolipoamide transsuccinylase, respectively. *J Bacteriol* **171**(7): 3667-3672.
- Charlton, S., A. J. Moir, L. Baillie and A. Moir (1999).** Characterization of the exosporium of *Bacillus cereus*. *J Appl Microbiol* **87**(2): 241-245.
- Chaudhuri, R. R., N. J. Loman, L. A. Snyder, C. M. Bailey, D. J. Stekel and M. J. Pallen (2008).** xBASE2: a comprehensive resource for comparative bacterial genomics. *Nucleic Acids Res* **36**((Database issue)): D543-546.
- Chitlaru, T., O. Gat, Y. Gozlan, N. Ariel and A. Shafferman (2006).** Differential proteomic analysis of the *Bacillus anthracis* secretome: distinct plasmid and chromosome CO₂-dependent cross talk mechanisms modulate extracellular proteolytic activities. *J Bacteriol* **188**(10): 3551-3571.
- Chung, M. C., S. C. Jorgensen, T. G. Popova, J. H. Tonry, C. L. Bailey and S. G. Popov (2009).** Activation of plasminogen activator inhibitor implicates protease InhA in the acute-phase response to *Bacillus anthracis* infection. *J Med Microbiol* **58**(6): 737-744.
- Chung, M. C., S. C. Jorgensen, J. H. Tonry, F. Kashanchi, C. Bailey and S. Popov (2011).** Secreted *Bacillus anthracis* proteases target the host fibrinolytic system. *FEMS Immunol Med Microbiol* **62**(2): 173 - 181.
- Chung, M. C., T. G. Popova, S. C. Jorgensen, L. Dong, V. Chandhoke, C. L. Bailey and S. G. Popov (2008).** Degradation of circulating von Willebrand factor and its regulator

- ADAMTS13 implicates secreted *Bacillus anthracis* metalloproteases in anthrax consumptive coagulopathy. *J Biol Chem* **283**(15): 9531-9542.
- Chung, M. C., T. G. Popova, B. A. Millis, D. V. Mukherjee, W. Zhou, L. A. Liotta, E. F. Petricoin, V. Chandhoke, C. Bailey and S. G. Popov (2006).** Secreted neutral metalloproteases of *Bacillus anthracis* as candidate pathogenic factors. *J Biol Chem* **281**(42): 31408-31418.
- Clarke, C. J., C. F. Snook, M. Tani, N. Matmati, N. Marchesini and Y. A. Hannun (2006).** The extended family of neutral sphingomyelinases. *Biochemistry* **45**(38): 11247-11256.
- Clavel, T., F. Carlin, D. Lairon, C. Nguyen-The and P. Schmitt (2004).** Survival of *Bacillus cereus* spores and vegetative cells in acid media simulating human stomach. *J Appl Microbiol* **97**(1): 214-219.
- Coll, O., A. Morales, J. C. Fernández-Checa and C. Garcia-Ruiz (2007).** Neutral sphingomyelinase-induced ceramide triggers germinal vesicle breakdown and oxidant-dependent apoptosis in *Xenopus laevis* oocytes. *J Lipid Res* **48**(9): 1924-1935.
- Cozzone, A. J. (1998).** Regulation of acetate metabolism by protein phosphorylation in enteric bacteria. *Annu Rev Microbiol* **52**: 127-164.
- Craig, C. P., W. S. Lee and M. Ho (1974).** Letter: *Bacillus cereus* endocarditis in an addict. *Ann Intern Med* **80**(3): 418-419.
- Crowell, K. M. and F. Lutz (1989).** *Pseudomonas aeruginosa* cytotoxin: the influence of sphingomyelin on binding and cation permeability increase in mammalian erythrocytes. *Toxicon* **27**(5): 531-540.
- Dalhammar, G. and H. Steiner (1984).** Characterization of inhibitor A, a protease from *Bacillus thuringiensis* which degrades attacins and cecropins, two classes of antibacterial proteins in insects. *Eur J Biochem* **139**(2): 247-252.
- de Vries, Y. P. (2006, PhD Thesis).** *Bacillus cereus* Spore Formation, Structure, and Germination. Wageningen Wageningen University.
- Declerck, N., L. Bouillaut, D. Chaix, N. Rugani, L. Slamti, F. Hoh, D. Lereclus and S. T. Arold (2007).** Structure of PlcR: Insights into virulence regulation and evolution of quorum sensing in Gram-positive bacteria. *Proc Natl Acad Sci USA* **104**(47): 18490-18495.
- Detmers, F. J., F. C. Lanfermeijer and B. Poolman (2001).** Peptides and ATP binding cassette peptide transporters. *Res Microbiol* **152**(3-4): 245-258.
- Di Franco, C., E. Beccari, T. Santini, G. Pisaneschi and G. Tecce (2002).** Colony shape as a genetic trait in the pattern-forming *Bacillus mycoides*. *BMC Microbiol* **2**: 33-47.
- Didier, A., R. Dietrich, S. Gruber, S. Bock, M. Moravek, T. Nakamura, T. Lindbäck, P. Granum and E. Märtilbauer (2011).** Monoclonal Antibodies Neutralize *Bacillus cereus* Nhe Enterotoxin by Inhibiting Ordered Binding of Its Three Exoprotein Components. *Infect Immun* ahead of print
- Dierick, K., E. Van Coillie, I. Swiecicka, G. Meyfroidt, H. Devlieger, A. Meulemans, G. Hoedemaekers, L. Fourie, M. Heyndrickx and J. Mahillon (2005).** Fatal family outbreak of *Bacillus cereus*-associated food poisoning. *J Clin Microbiol* **43**(8): 4277-4279.
- Dietrich, R., M. Moravek, C. Bürk, P. Granum and E. Märtilbauer (2005).** Production and characterization of antibodies against each of the three subunits of the *Bacillus cereus* nonhemolytic enterotoxin complex. *Appl Environ Microbiol* **71**(12): 8214-8220.
- Dineen, S. S., A. C. Villapakkam, J. T. Nordman and A. L. Sonenshein (2007).** Repression of *Clostridium difficile* toxin gene expression by CodY. *Mol Microbiol* **66**(1): 206-219.
- Dommel, M. K., (2008, PhD Thesis).** Molecular characterization of the genetic locus responsible for cereulide toxin production in emetic *Bacillus cereus*. Freising, Technische Universität München.

- Dommel, M. K., G. Lücking, S. Scherer and M. Ehling-Schulz (2011).** Transcriptional kinetic analyses of cereulide synthetase genes with respect to growth, sporulation and emetic toxin production in *Bacillus cereus*. *Food Microbiol* **28**(2): 284-290.
- Doyle, R. J. (2000).** Contribution of the hydrophobic effect to microbial infection. *Microbes Infect* **2**(4): 391-400.
- Drobniewski, F. A. (1993).** *Bacillus cereus* and Related Species. *Clin Microbiol Rev* **6**(4): 324-338.
- Duc, I., H. A. Hong, T. M. Barbosa, A. O. Henriques and S. M. Cutting (2004).** Characterization of *Bacillus* probiotics available for human use. *Appl Environ Microbiol* **70**(4): 2161-2171.
- Dunn, A. K. and J. Handelsman (1999).** A vector for promoter trapping in *Bacillus cereus*. *Gene* **226**(2): 297-305.
- Duport, C., S. Thomassin, G. Bourel and P. Schmitt (2004).** Anaerobiosis and low specific growth rates enhance hemolysin BL production by *Bacillus cereus* F4430/73. *Arch Microbiol* **182**(1): 90-95.
- Duport, C., A. Zigha, E. Rosenfeld and P. Schmitt (2006).** Control of enterotoxin gene expression in *Bacillus cereus* F4430/73 involves the redox-sensitive ResDE signal transduction system. *J Bacteriol* **188**(18): 6640-6651.
- Durfee, T., Nelson, R., Baldwin, S., Plunkett, G., 3rd, Burland, V., Mau, B., Petrosino, J. F., Qin, X., Muzny, D. M., Ayele, M., Gibbs, R. A., Csorgo, B., Posfai, G., Weinstock, G. M. and Blattner, F. R. (2008).** The complete genome sequence of *Escherichia coli* DH10B: insights into the biology of a laboratory workhorse. *J Bacteriol* **190**(7): 2597-606.
- Ebbole, D. J. and H. Zalkin (1989).** *Bacillus subtilis* pur operon expression and regulation. *J Bacteriol* **171**(4): 2136-2141.
- Ehling-Schulz, M., M. Fricker, H. Grallert, P. Rieck, M. Wagner and S. Scherer (2006a).** Cereulide synthetase gene cluster from emetic *Bacillus cereus*: structure and location on a mega virulence plasmid related to *Bacillus anthracis* toxin plasmid pXO1. *BMC Microbiol* **6**: 20.
- Ehling-Schulz, M., M. Fricker and S. Scherer (2004).** *Bacillus cereus*, the causative agent of an emetic type of food-borne illness. *Mol Nutr Food Res* **48**(7): 479-487.
- Ehling-Schulz, M., M. Fricker and S. Scherer (2004).** Identification of emetic toxin producing *Bacillus cereus* strains by a novel molecular assay. *FEMS Microbiol Lett* **232**(2): 189-195.
- Ehling-Schulz, M., M. H. Guinebretiére, A. Monthán, O. Berge, M. Fricker and B. Svensson (2006b).** Toxin gene profiling of enterotoxic and emetic *Bacillus cereus*. *FEMS Microbiol Lett* **260**(2): 232-240.
- Ehling-Schulz, M., Knutsson, R., Scherer, S. . (2011).** *Bacillus cereus*. In Y. L. P. Fratamico, and S. Kathariou (Ed.), *Genomes of Foodborne and Waterborne Pathogens* (pp. 147-164). Washington, D.C.: ASM Press
- Ehling-Schulz, M., U. Messelhäusser and P. E. Granum. (2011).** *Bacillus cereus* in milk and dairy production. In J. Hoorfar (Ed.), *Rapid Detection, Identification, and Quantification of Foodborne Pathogens* (pp. 275-289). Washington, D.C.: ASM Press
- Ehling-Schulz, M., B. Svensson, M. H. Guinebretiére, T. Lindbäck, M. Andersson, A. Schulz, M. Fricker, A. Christiansson, P. Granum, E. Märtilbauer, C. Nguyen-The, M. Salkinoja-Salonen and S. Scherer (2005).** Emetic toxin formation of *Bacillus cereus* is restricted to a single evolutionary lineage of closely related strains. *Microbiology* **151**(1): 183-197.
- Ehling-Schulz, M., N. Vukov, A. Schulz, R. Shaheen, M. Andersson, E. Märtilbauer and S. Scherer (2005).** Identification and partial characterization of the nonribosomal peptide

- synthetase gene responsible for cereulide production in emetic *Bacillus cereus*. *Appl Environ Microbiol* **71**(1): 105-113.
- Fagerlund, A., J. Brillard, R. Fürst, M. H. Guinebretière and P. Granum (2007)**. Toxin production in a rare and genetically remote cluster of strains of the *Bacillus cereus* group. *BMC Microbiol* **7**: 43.
- Fagerlund, A., T. Lindbäck and P. Granum (2010)**. *Bacillus cereus* cytotoxins Hbl, Nhe and CytK are secreted via the Sec translocation pathway. *BMC Microbiol* **10**(304): 304.
- Fagerlund, A., T. Lindbäck, A. K. Storset, P. Granum and S. P. Hardy (2008)**. *Bacillus cereus* Nhe is a pore-forming toxin with structural and functional properties similar to the ClyA (HlyE, SheA) family of haemolysins, able to induce osmotic lysis in epithelia. *Microbiology* **154**(3): 693-704.
- Faille, C., Y. Lequette, A. Ronse, C. Slomianny, E. Garénaux and Y. Guerardel (2010)**. Morphology and physico-chemical properties of *Bacillus* spores surrounded or not with an exosporium. Consequences on their ability to adhere to stainless steel. *Int J Food Microbiol* **143**(3): 125-135.
- Fang, F. C., S. J. Libby, M. E. Castor and A. M. Fung (2005)**. Isocitrate lyase (AceA) is required for *Salmonella* persistence but not for acute lethal infection in mice. *Infect Immun* **73**(4): 2547-2549.
- Fedhila, S., C. Buisson, O. Dussurget, P. Serror, I. Glomski, P. Liehl, D. Lereclus and C. Nielsen-Leroux (2010)**. Comparative analysis of the virulence of invertebrate and mammalian pathogenic bacteria in the oral insect infection model *Galleria mellonella*. *J Invertebr Pathol* **103**(1): 24-29.
- Fedhila, S., M. Gohar, L. Slamti, P. Nel and D. Lereclus (2003)**. The *Bacillus thuringiensis* PlcR-regulated gene *inhA2* is necessary, but not sufficient, for virulence. *J Bacteriol* **185**(9): 2820-2825.
- Fedhila, S., P. Nel and D. Lereclus (2002)**. The *InhA2* metalloprotease of *Bacillus thuringiensis* strain 407 is required for pathogenicity in insects infected via the oral route. *J Bacteriol* **184**(12): 3296-3304.
- Fink, P. S. (1993)**. Biosynthesis of the branched-chain amino acids. In A. L. Sonenshein, Hoch, J.A., Losick, R. (Ed.), *Bacillus Subtilis and Other Gram-Positive Bacteria*. Washington, DC: American Society for Microbiology Press
- Finlay, B. B. and S. Falkow (1997)**. Common themes in microbial pathogenicity revisited. *Microbiol Mol Biol Rev* **61**(2): 136-169.
- Fogh, J. and G. Trempe. (1975)**. New human tumor cell lines. In J. Fogh (Ed.), *Human Tumor Cells in vitro* New York: Plenum Publishing Corp.
- Fox, A., G. C. Stewart, L. N. Waller, K. F. Fox, W. M. Harley and R. L. Price (2003)**. Carbohydrates and glycoproteins of *Bacillus anthracis* and related bacilli: targets for biodetection. *J Microbiol Methods* **54**(2): 143-152.
- Frenzel, E. (2011, PhD Thesis)**. Regulation of the biosynthesis of the food-borne *Bacillus cereus* toxin cereulide. Freising, Technische Universität München.
- Fricker, M., U. Messelhäusser, U. Busch, S. Scherer and M. Ehling-Schulz (2007)**. Diagnostic real-time PCR assays for the detection of emetic *Bacillus cereus* strains in foods and recent food-borne outbreaks. *Appl Environ Microbiol* **73**(6): 1892-1898.
- Fuangthong, M., S. Atichartpongkul, S. Mongkolsuk and J. D. Helmann (2001)**. OhrR is a repressor of ohrA, a key organic hydroperoxide resistance determinant in *Bacillus subtilis*. *J Bacteriol* **183**(14): 4134-4141.
- Gavrilenko, I. V., G. E. Baïda, A. V. Karpov and N. P. Kuz'min (1993)**. Nucleotide sequence of phospholipase C and sphingomyelinase genes from *Bacillus cereus* BKM-B164. *Bioorg Khim* **19**(1): 133-138.

- Gharahdaghi, F., C. R. Weinberg, D. A. Meagher, B. S. Imai and S. M. Mische (1999).** Mass spectrometric identification of proteins from silver-stained polyacrylamide gel: a method for the removal of silver ions to enhance sensitivity. *Electrophoresis* **20**(3): 601-605.
- Ghelardi, E., F. Celandroni, S. Salvetti, M. Ceragioli, D. J. Beecher, S. Senesi and A. C. Wong (2007).** Swarming behavior of and hemolysin BL secretion by *Bacillus cereus*. *Appl Environ Microbiol* **73**(12): 4089-4093.
- Ghosh, A. C. (1978).** Prevalence of *Bacillus cereus* in the faeces of healthy adults. *J Hyg (Lond)* **80**(2): 233-236.
- Gilmore, M. S., A. L. Cruz-Rodz, M. Leimeister-Wächter, J. Kreft and W. Goebel (1989).** A *Bacillus cereus* cytolytic determinant, cereolysin AB, which comprises the phospholipase C and sphingomyelinase genes: nucleotide sequence and genetic linkage. *J Bacteriol* **171**(2): 744-753.
- Gilois, N., N. Ramarao, L. Bouillaut, S. Perchat, S. Aymerich, C. Nielsen-Leroux, D. Lereclus and M. Gohar (2007).** Growth-related variations in the *Bacillus cereus* secretome. *Proteomics* **7**(10): 1719-1728.
- Glatz, B. A. and J. M. Goepfert (1976).** Defined conditions for synthesis of *Bacillus cereus* enterotoxin by fermenter-grown cultures. *Appl Environ Microbiol* **32**(3): 400-404.
- Gohar, M., K. Faegri, S. Perchat, S. Ravnum, O. A. Økstad, M. Gominet, A. B. Kolstø and D. Lereclus (2008).** The PlcR virulence regulon of *Bacillus cereus*. *PLoS one* **3**(7): e2793.
- Gohar, M., N. Gilois, R. Graveline, C. Garreau, V. Sanchis and D. Lereclus (2005).** A comparative study of *Bacillus cereus*, *Bacillus thuringiensis* and *Bacillus anthracis* extracellular proteomes. *Proteomics* **5**(14): 3696-3711.
- Gohar, M., O. A. Økstad, N. Gilois, V. Sanchis, A. B. Kolstø and D. Lereclus (2002).** Two-dimensional electrophoresis analysis of the extracellular proteome of *Bacillus cereus* reveals the importance of the PlcR regulon. *Proteomics* **2**(6): 784-791.
- Gominet, M., L. Slamti, N. Gilois, M. Rose and D. Lereclus (2001).** Oligopeptide permease is required for expression of the *Bacillus thuringiensis* plcR regulon and for virulence. *MolMicrobiol* **40**(4): 963-975.
- González-Zorn, B., G. Domínguez-Bernal, M. Suárez, M. T. Ripio, Y. Vega, S. Novella and J. A. Vázquez-Boland (1999).** The *smcL* gene of *Listeria ivanovii* encodes a sphingomyelinase C that mediates bacterial escape from the phagocytic vacuole. *Mol Microbiol* **33**(3): 510-523.
- Gordon, R. E., W. C. Haynes and C. Hor-Nay. (1973).** The Genus *Bacillus*. In U. Agricultural Research Service (Ed.), *Agricultural handbook* (Vol. 427). Washington, D.C.: US Government Printing Office
- Gouaux, E. (1998).** alpha-Hemolysin from *Staphylococcus aureus*: an archetype of beta-barrel, channel-forming toxins. *J Struct Biol* **121**(2): 110-122.
- Grandoni, J. A., S. A. Zahler and J. M. Calvo (1992).** Transcriptional regulation of the *ilv-leu* operon of *Bacillus subtilis*. *J Bacteriol* **174**(10): 3212-3219.
- Grandvalet, C., M. Gominet and D. Lereclus (2001).** Identification of genes involved in the activation of the *Bacillus thuringiensis inhA* metalloprotease gene at the onset of sporulation. *Microbiology* **147**(7): 1805-1813.
- Granum, P. E. and T. Lund (1997).** *Bacillus cereus* and its food poisoning toxins. *FEMS Microbiol Lett* **157**(2): 223-228.
- Granum, P. E. and H. Nissen (1993).** Sphingomyelinase is part of the 'enterotoxin complex' produced by *Bacillus cereus*. *FEMS Microbiol Lett* **110**(1): 97-100.
- Granum, P. E., K. O'Sullivan and T. Lund (1999).** The sequence of the non-haemolytic enterotoxin operon from *Bacillus cereus*. *FEMS Microbiol Lett* **177**(2): 225-229.

- Green, N. J., F. J. Grundy and T. M. Henkin (2010).** The T box mechanism: tRNA as a regulatory molecule. *FEBS Lett* **584**(2): 318-324.
- Grundy, F. J. and T. M. Henkin (1993).** tRNA as a positive regulator of transcription antitermination in *B. subtilis*. *Cell* **74**(3): 475-482.
- Grunert, T., N. R. Leitner, M. Marchetti-Deschmann, I. Miller, B. Wallner, M. Radwan, C. Vogl, T. Kolbe, D. Kratky, M. Gemeiner, G. Allmaier, M. Müller and B. Strobl (2011).** A comparative proteome analysis links tyrosine kinase 2 (Tyk2) to the regulation of cellular glucose and lipid metabolism in response to poly(I:C). *J Prot.*
- Guillemet, E., C. Cadot, S. L. Tran, M. H. Guinebretière, D. Lereclus and N. Ramarao (2010).** The InhA metalloproteases of *Bacillus cereus* contribute concomitantly to virulence. *J Bacteriol* **192**(1): 286-294.
- Guinebretière, M. H., V. Broussolle and C. Nguyen-The (2002).** Enterotoxigenic profiles of food-poisoning and food-borne *Bacillus cereus* strains. *J Clin Microbiol* **40**(8): 3053-3056.
- Gulbins, E. and P. L. Li (2006).** Physiological and pathophysiological aspects of ceramide. *Am J Physiol Regul Integr Comp Physiol* **290**(1): R11-26.
- Guyer, C. A., D. G. Morgan and J. V. Staros (1986).** Binding specificity of the periplasmic oligopeptide-binding protein from *Escherichia coli*. *J Bacteriol* **168**(2): 775-779.
- Hardy, S. P., T. Lund and P. E. Granum (2001).** CytK toxin of *Bacillus cereus* forms pores in planar lipid bilayers and is cytotoxic to intestinal epithelia. *FEMS Microbiol Lett* **197**(1): 47-51.
- Harrington, H. A., K. L. Ho, S. Ghosh and K. C. Tung (2008).** Construction and analysis of a modular model of caspase activation in apoptosis. *Theor Biol Med Model* **5**: 26.
- Harvie, D. R., S. Vilchez, J. R. Steggles and D. J. Ellar (2005).** *Bacillus cereus* Fur regulates iron metabolism and is required for full virulence. *Microbiology* **151**(2): 569-577.
- Hauge, S. (1955).** Food poisoning caused by aerobic spore forming bacilli. *J Appl Bacteriol* **18**.
- Heinrichs, J. H., D. J. Beecher, J. D. Macmillan and B. A. Zilinskas (1993).** Molecular cloning and characterization of the hblA gene encoding the B component of hemolysin BL from *Bacillus cereus*. *J Bacteriol* **175**(21): 6760-6766.
- Helgason, E., O. A. Okstad, D. A. Caugant, H. A. Johansen, A. Fouet, M. Mock, I. Hegna and A. B. Kolstø (2000).** *Bacillus anthracis*, *Bacillus cereus*, and *Bacillus thuringiensis*-one species on the basis of genetic evidence. *Appl Environ Microbiol* **66**(6): 2627-2630.
- Hernaiz, C., A. Picardo, J. I. Alos and J. L. Gomez-Garces (2003).** Nosocomial bacteremia and catheter infection by *Bacillus cereus* in an immunocompetent patient. *Clin Microbiol Infect* **9**(9): 973-975.
- Hernandez, E., F. Ramiisse, T. Cruel, R. le Vagueresse and J. D. Cavallo (1999).** *Bacillus thuringiensis* serotype H34 isolated from human and insecticidal strains serotypes 3a3b and H14 can lead to death of immunocompetent mice after pulmonary infection. *FEMS Immunol Med Microbiol* **24**(1): 43-47.
- Hiles, I. D., L. M. Powell and C. F. Higgins (1987).** Peptide transport in *Salmonella typhimurium*: molecular cloning and characterization of the oligopeptide permease genes. *Mol Gen Genet* **206**(1): 101-109.
- Hilliard, N. J., R. L. Schelonka and K. B. Waites (2003).** *Bacillus cereus* bacteremia in a preterm neonate. *J Clin Microbiol* **41**(7): 3441-3444.
- Ho, N. T., L. Baccigalupi, A. Huxham, A. Smertenko, P. H. Van, S. Ammendola, E. Ricca and A. S. Cutting (2000).** Characterization of *Bacillus* species used for oral bacteriotherapy and bacterioprophyllaxis of gastrointestinal disorders. *Appl Environ Microbiol* **66**(12): 5241-5247.

- Hoffmaster, A. R., J. Ravel, D. A. Rasko, G. D. Chapman, M. D. Chute, C. K. Marston, B. K. De, C. T. Sacchi, C. Fitzgerald, L. W. Mayer, M. C. Maiden, F. G. Priest, M. Barker, L. Jiang, R. Z. Cer, J. Rilstone, S. N. Peterson, R. S. Weyant, D. R. Galloway, T. D. Read, T. Popovic and C. M. Fraser (2004). Identification of anthrax toxin genes in a *Bacillus cereus* associated with an illness resembling inhalation anthrax. *Proc Natl Acad Sci USA* **101**(22): 8449-8454.
- Hong, H. A., I. Duc and S. M. Cutting (2005). The use of bacterial spore formers as probiotics. *FEMS Microbiol Rev* **29**(4): 813-835.
- Huang, C. J., T. K. Wang, S. C. Chung and C. Y. Chen (2005). Identification of an antifungal chitinase from a potential biocontrol agent, *Bacillus cereus* 28-9. *J Biochem Mol Biol* **38**(1): 82-88.
- Huseby, M., K. Shi, C. Brown, J. Digre, F. Mengistu, K. Seo, G. Bohach, P. Schlievert, D. Ohlendorf and C. Earhart (2007). Structure and Biological Activities of Beta Toxin from *Staphylococcus aureus*. *J Bacteriol* **189**(23): 8719-8726.
- Ivanova, N., A. Sorokin, I. Anderson, N. Galleron, B. Candelon, V. Kapatral, A. Bhattacharyya, G. Reznik, N. Mikhailova, A. Lapidus, L. Chu, M. Mazur, E. Goltsman, N. Larsen, M. D'Souza, T. Walunas, Y. Grechkin, G. Pusch, R. Haselkorn, M. Fonstein, S. D. Ehrlich, R. Overbeek and N. Kyrpides (2003). Genome sequence of *Bacillus cereus* and comparative analysis with *Bacillus anthracis*. *Nature* **423**(6935): 87-91.
- Jensen, G. B., B. M. Hansen, J. Eilenberg and J. Mahillon (2003). The hidden lifestyles of *Bacillus cereus* and relatives. *Environ Microbiol* **5**(8): 631-640.
- Jernigan, D. B., P. L. Raghunathan, B. P. Bell, R. Brechner, E. A. Bresnitz, J. C. Butler, M. Cetron, M. Cohen, T. Doyle, M. Fischer, C. Greene, K. S. Griffith, J. Guarner, J. L. Hadler, J. A. Hayslett, R. Meyer, L. R. Petersen, M. Phillips, R. Pinner, T. Popovic, C. P. Quinn, J. Reefhuis, D. Reissman, N. Rosenstein, A. Schuchat, W. J. Shieh, L. Siegal, D. L. Swerdlow, F. C. Tenover, M. Traeger, J. W. Ward, I. Weisfuse, S. Wiersma, K. Yeskey, S. Zaki, D. A. Ashford, B. A. Perkins, S. Ostroff, J. Hughes, D. Fleming, J. P. Koplan, J. L. Gerberding and T. National Anthrax Epidemiologic Investigation (2002). Investigation of bioterrorism-related anthrax, United States, 2001: epidemiologic findings. *Emerging Infect Dis* **8**(10): 1019-1028.
- Jiang, M., W. Shao, M. Perego and J. A. Hoch (2000). Multiple histidine kinases regulate entry into stationary phase and sporulation in *Bacillus subtilis*. *Mol Microbiol* **38**(3): 535-542.
- Johnson, K. M. (1984). *Bacillus cereus* food-borne illness. An update. *J Food Prot* **47**: 145-153.
- Karunakaran, E. and C. A. Biggs (2011). Mechanisms of *Bacillus cereus* biofilm formation: an investigation of the physicochemical characteristics of cell surfaces and extracellular proteins. *Appl Microbiol Biotechnol* **89**(4): 1161-1175.
- Kavanagh, K. and E. P. Reeves (2004). Exploiting the potential of insects for in vivo pathogenicity testing of microbial pathogens. *FEMS Microbiol Rev* **28**(1): 101-112.
- Kawamura-Sato, K., Y. Hirama, N. Agata, H. Ito, K. Torii, A. Takeno, T. Hasegawa, Y. Shimomura and M. Ohta (2005). Quantitative analysis of cereulide, an emetic toxin of *Bacillus cereus*, by using rat liver mitochondria. *Microbiol Immunol* **49**(1): 25-30.
- Klee, S. R., M. Ozel, B. Appel, C. Boesch, H. Ellerbrok, D. Jacob, G. Holland, F. H. Leendertz, G. Pauli, R. Grunow and H. Nattermann (2006). Characterization of *Bacillus anthracis*-like bacteria isolated from wild great apes from Cote d'Ivoire and Cameroon. *J Bacteriol* **188**(15): 5333-5344.
- Klein, G. (2011). Molecular characterization of the probiotic strain *Bacillus cereus* var. *toyoi* NCIMB 40112 and differentiation from food poisoning strains. *J Food Prot* **74**(7): 1189-1193.
- Koide, A., M. Perego and J. A. Hoch (1999). ScoC regulates peptide transport and sporulation initiation in *Bacillus subtilis*. *J Bacteriol* **181**(13): 4114-4117.

- Kolesnick, R. N., F. M. Goñi and A. Alonso (2000). Compartmentalization of ceramide signaling: physical foundations and biological effects. *J Cell Physiol* **184**(3): 285-300.
- Kolstø, A. B., N. J. Tourasse and O. A. Økstad (2009). What sets *Bacillus anthracis* apart from other *Bacillus* species? *Annu Rev Microbiol* **63**: 451-476.
- Komori, H., S. Ichikawa, Y. Hirabayashi and M. Ito (1999). Regulation of intracellular ceramide content in B16 melanoma cells. Biological implications of ceramide glycosylation. *J Biol Chem* **274**(13): 8981-8987.
- Kotiranta, A., M. Haapasalo, K. Kari, E. Kerosuo, I. Olsen, T. Sorsa, J. H. Meurman and K. Lounatmaa (1998). Surface structure, hydrophobicity, phagocytosis, and adherence to matrix proteins of *Bacillus cereus* cells with and without the crystalline surface protein layer. *Infect Immun* **66**(10): 4895-4902.
- Kotiranta, A., K. Lounatmaa and M. Haapasalo (2000). Epidemiology and pathogenesis of *Bacillus cereus* infections. *Microbes Infect* **2**(2): 189-198.
- Kramer, J. M. and R. J. Gilbert. (1989). *Bacillus cereus* and other *Bacillus* species. In M. P. Doyle (Ed.), *Foodborne Bacterial Pathogens* (pp. 21-70). New York: Marcel Dekker Inc.
- Kreft, J., H. Berger, M. Härtle, B. Müller, G. Weidinger and W. Goebel (1983). Cloning and expression in *Escherichia coli* and *Bacillus subtilis* of the hemolysin (cereolysin) determinant from *Bacillus cereus*. *J Bacteriol* **155**(2): 681-689.
- Kretschmar, U., V. Khodaverdi, J. H. Jeoung and H. Görisch (2008). Function and transcriptional regulation of the isocitrate lyase in *Pseudomonas aeruginosa*. *Arch Microbiol* **190**(2): 151-158.
- Kuppe, A., L. M. Evans, D. A. McMillen and O. H. Griffith (1989). Phosphatidylinositol-specific phospholipase C of *Bacillus cereus*: cloning, sequencing, and relationship to other phospholipases. *J Bacteriol* **171**(11): 6077-6083.
- Kuroki, R., K. Kawakami, L. Qin, C. Kaji, K. Watanabe, Y. Kimura, C. Ishiguro, S. Tanimura, Y. Tsuchiya, I. Hamaguchi, M. Sakakura, S. Sakabe, K. Tsuji, M. Inoue and H. Watanabe (2009). Nosocomial bacteremia caused by biofilm-forming *Bacillus cereus* and *Bacillus thuringiensis*. *Intern Med (Tokyo, Japan)* **48**(10): 791-796.
- Laemmli, U. K. (1970). Cleavage of structural proteins during the assembly of the head of bacteriophage T4. *Nature* **227**(5259): 680-685.
- Lazazzera, B. A. (2000). Quorum sensing and starvation: signals for entry into stationary phase. *Curr Opin Microbiol* **3**(2): 177-182.
- Lebessi, E., H. D. Dellagrammaticas, G. Antonaki, M. Foustoukou and N. Iacovidou (2009). *Bacillus cereus* meningitis in a term neonate. *J Matern Fetal Neonatal Med* **22**(5): 458-461.
- Lechner, S., R. Mayr, K. P. Francis, B. M. Prüss, T. Kaplan, E. Wiessner-Gunkel, G. S. Stewart and S. Scherer (1998). *Bacillus weihenstephanensis* sp. nov. is a new psychrotolerant species of the *Bacillus cereus* group. *Int J Syst Bacteriol* **48 Pt 4**: 1373-1382.
- Lereclus, D., H. Agaisse, M. Gominet, S. Salamitou and V. Sanchis (1996). Identification of a *Bacillus thuringiensis* gene that positively regulates transcription of the phosphatidylinositol-specific phospholipase C gene at the onset of the stationary phase. *J Bacteriol* **178**(10): 2749-2756.
- Lereclus, D., H. Agaisse, C. Grandvalet, S. Salamitou and M. Gominet (2000). Regulation of toxin and virulence gene transcription in *Bacillus thuringiensis*. *Int J Med Microbiol* **290**(4-5): 295-299.
- Lindbäck, T., A. Fagerlund, M. S. Rødland and P. Granum (2004). Characterization of the *Bacillus cereus* Nhe enterotoxin. *Microbiology* **150**(12): 3959-3967.
- Lindbäck, T., S. P. Hardy, R. Dietrich, M. Sødring, A. Didier, M. Moravek, A. Fagerlund, S. Bock, C. Nielsen, M. Casteel, P. Granum and E. Märklbauer (2010). Cytotoxicity of

- the *Bacillus cereus* Nhe enterotoxin requires specific binding order of its three exoprotein components. *Infect Immun* **78**(9): 3813-3821.
- Lindbäck, T., O. A. Økstad, A. L. Rishovd and A. B. Kolstø (1999).** Insertional inactivation of hblC encoding the L2 component of *Bacillus cereus* ATCC 14579 haemolysin BL strongly reduces enterotoxigenic activity, but not the haemolytic activity against human erythrocytes. *Microbiology* **145** (11): 3139-3146.
- Lövgren, A., M. Zhang, A. Engström, G. Dalhammar and R. Landén (1990).** Molecular characterization of immune inhibitor A, a secreted virulence protease from *Bacillus thuringiensis*. *Mol Microbiol* **4**(12): 2137-2146.
- Lücking, G. (2009, PhD Thesis).** Molecular characterization of cereulide synthesis in emetic *Bacillus cereus*. Freising, Technische Universität München.
- Lücking, G., M. K. Dommel, S. Scherer, A. Fouet and M. Ehling-Schulz (2009).** Cereulide synthesis in emetic *Bacillus cereus* is controlled by the transition state regulator AbrB, but not by the virulence regulator PlcR. *Microbiology* **155**(3): 922-931.
- Lund, T., M. L. De Buyser and P. E. Granum (2000).** A new cytotoxin from *Bacillus cereus* that may cause necrotic enteritis. *Mol Microbiol* **38**(2): 254-261.
- Lund, T. and P. E. Granum (1996).** Characterisation of a non-haemolytic enterotoxin complex from *Bacillus cereus* isolated after a foodborne outbreak. *FEMS Microbiol Lett* **141**(2-3): 151-156.
- Lund, T. and P. E. Granum (1997).** Comparison of biological effect of the two different enterotoxin complexes isolated from three different strains of *Bacillus cereus*. *Microbiology* **143**(10): 3329-3336.
- Mahler, H., A. Pasi, J. M. Kramer, P. Schulte, A. C. Scoging, W. Bär and S. Krähenbühl (1997).** Fulminant liver failure in association with the emetic toxin of *Bacillus cereus*. *N Engl J Med* **336**(16): 1142-1148.
- Majerczyk, C. D., P. M. Dunman, T. T. Luong, C. Y. Lee, M. R. Sadykov, G. A. Somerville, K. Bodi and A. L. Sonenshein (2010).** Direct targets of CodY in *Staphylococcus aureus*. *J Bacteriol* **192**(11): 2861-2877.
- Majerczyk, C. D., M. R. Sadykov, T. T. Luong, C. Lee, G. A. Somerville and A. L. Sonenshein (2008).** *Staphylococcus aureus* CodY negatively regulates virulence gene expression. *J Bacteriol* **190**(7): 2257-2265.
- Marrakchi, H., G. Lanéelle and A. Quémard (2000).** InhA, a target of the antituberculous drug isoniazid, is involved in a mycobacterial fatty acid elongation system, FAS-II. *Microbiology* **146**(2): 289-296.
- Martineau, F., F. J. Picard, P. H. Roy, M. Ouellette and M. G. Bergeron (1996).** Species-specific and ubiquitous DNA-based assays for rapid identification of *Staphylococcus epidermidis*. *J Clin Microbiol* **34**(12): 2888-2893.
- Matte, I., D. Lane, E. Côté, A. E. Asselin, L. C. Fortier, C. Asselin and A. Piché (2009).** Antiapoptotic proteins Bcl-2 and Bcl-XL inhibit *Clostridium difficile* toxin A-induced cell death in human epithelial cells. *Infect Immun* **77**(12): 5400-5410.
- McDonel, J. L. (1980).** *Clostridium perfringens* toxins (type A, B, C, D, E). *Pharmacol Ther* **10**(3): 617-655.
- Meer, R. R., J. Baker, F. W. Bodyfelt and M. W. Griffiths (1991).** Psychrotrophic *Bacillus* spp. in fluid milk products: a review. *J Food Prot* **54**: 969-979.
- Merrell, D. S. and S. Falkow (2004).** Frontal and stealth attack strategies in microbial pathogenesis. *Nature* **430**(6996): 250-256.
- Mignot, T., M. Mock, D. Robichon, A. Landier, D. Lereclus and A. Fouet (2001).** The incompatibility between the PlcR- and AtxA-controlled regulons may have selected a nonsense mutation in *Bacillus anthracis*. *Mol Microbiol* **42**(5): 1189-1198.

- Mikkola, R., N. E. Saris, P. A. Grigoriev, M. A. Andersson and M. S. Salkinoja-Salonen (1999). Ionophoretic properties and mitochondrial effects of cereulide: the emetic toxin of *B. cereus*. *Eur J Biochem* **263**(1): 112-117.
- Miller, I. and M. Gemeiner (1992). Two-dimensional electrophoresis of cat sera: protein identification by cross reacting antibodies against human serum proteins. *Electrophoresis* **13**(7): 450-453.
- Minnaard, J., L. Delfederico, V. Vasseur, A. Hollmann, I. Rolny, L. Semorile and P. F. Pérez (2007). Virulence of *Bacillus cereus*: a multivariate analysis. *Int J Food Microbiol* **116**(2): 197-206.
- Minnaard, J., V. Lievin-Le Moal, M. H. Coconnier, A. L. Servin and P. F. Pérez (2004). Disassembly of F-actin cytoskeleton after interaction of *Bacillus cereus* with fully differentiated human intestinal Caco-2 cells. *Infect Immun* **72**(6): 3106-3112.
- Miyoshi, S. and S. Shinoda (2000). Microbial metalloproteases and pathogenesis. *Microbes Infect* **2**(1): 91-98.
- Mock, M. and A. Fouet (2001). Anthrax. *Annu Rev Microbiol* **55**: 647-671.
- Molle, V., G. Gulten, C. Vilchèze, R. Veyron-Churlet, I. Zanella-Cléon, J. C. Sacchettini, W. R. Jacobs and L. Kremer (2010). Phosphorylation of InhA inhibits mycolic acid biosynthesis and growth of *Mycobacterium tuberculosis*. *Mol Microbiol* **78**(6): 1591-1605.
- Mols, M. (2009, PhD Thesis). *Bacillus cereus* Acid Stress Responses. Wageningen Wageningen University.
- Mols, M. and T. Abee (2011). *Bacillus cereus* responses to acid stress. *Environ Microbiol* **13**(11): 2835-2843.
- Mols, M., M. de Been, M. H. Zwietering, R. Moezelaar and T. Abee (2007). Metabolic capacity of *Bacillus cereus* strains ATCC 14579 and ATCC 10987 interlinked with comparative genomics. *Environ Microbiol* **9**(12): 2933-2944.
- Moravek, M., R. Dietrich, C. Buerk, V. Broussolle, M. H. Guinebretière, P. Granum, C. Nguyen-The and E. Märklbauer (2006). Determination of the toxic potential of *Bacillus cereus* isolates by quantitative enterotoxin analyses. *FEMS Microbiol Lett* **257**(2): 293-298.
- Moriarty-Craige, S. E. and D. P. Jones (2004). Extracellular thiols and thiol/disulfide redox in metabolism. *Annu Rev Nutr* **24**: 481-509.
- Mossel, D. A., M. J. Koopman and E. Jongerijs (1967). Enumeration of *Bacillus cereus* in foods. *Appl Microbiol* **15**(3): 650-653.
- Moyer, A., R. Ramadan, J. Thurman, A. Burroughs and M. Callegan (2008). *Bacillus cereus* Induces Permeability of an In Vitro Blood-Retina Barrier. *Infect Immun* **76**(4): 1358-1367.
- Mukherjee, D. V., J. H. Tonry, K. S. Kim, N. Ramarao, T. G. Popova, C. Bailey, S. Popov and M. C. Chung (2011). *Bacillus anthracis* Protease InhA Increases Blood-Brain Barrier Permeability and Contributes to Cerebral Hemorrhages. *PLoS ONE* **6**(3): e17921.
- Mukherjee, K., B. Altincicek, T. Hain, E. Domann, A. Vilcinskis and T. Chakraborty (2010). *Galleria mellonella* as a model system for studying *Listeria* pathogenesis. *Appl Environ Microbiol* **76**(1): 310-317.
- Nakamura, L. K. (1998). *Bacillus pseudomycooides* sp. nov. *Int J Syst Bacteriol* **48** (Pt 3): 1031-1035.
- Nesbitt, W. E., R. J. Doyle and K. G. Taylor (1982). Hydrophobic interactions and the adherence of *Streptococcus sanguis* to hydroxylapatite. *Infect Immun* **38**(2): 637-644.

- Nesvizhskii, A. I., A. Keller, E. Kolker and R. Aebersold (2003). A statistical model for identifying proteins by tandem mass spectrometry. *Anal Chem* **75**(17): 4646-4658.
- Ngamwongsatit, P., W. Buasri, P. Pianariyanon, C. Pulsrikarn, M. Ohba, A. Assavanig and W. Panbangred (2008). Broad distribution of enterotoxin genes (*hblCDA*, *nheABC*, *cytK*, and *entFM*) among *Bacillus thuringiensis* and *Bacillus cereus* as shown by novel primers. *Int J Food Microbiol* **121**(3): 352-356.
- Niessen, C. M. (2007). Tight junctions/adherens junctions: basic structure and function. *J Invest Dermatol* **127**(11): 2525-2532.
- Nishikawa, H., H. Momose and I. Shio (1967). Regulation of purine nucleotide synthesis in *Bacillus subtilis*. II. Specificity of purine derivatives for enzyme repression. *J Biochem* **62**(1): 92-98.
- Nishiwaki, H., K. Ito, K. Otsuki, H. Yamamoto, K. Komai and K. Matsuda (2004). Purification and functional characterization of insecticidal sphingomyelinase C produced by *Bacillus cereus*. *Eur J Biochem* **271**(3): 601-606.
- O'Callaghan, R. J., M. C. Callegan, J. M. Moreau, L. C. Green, T. J. Foster, O. M. Hartford, L. S. Engel and J. M. Hill (1997). Specific roles of alpha-toxin and beta-toxin during *Staphylococcus aureus* corneal infection. *Infect Immun* **65**(5): 1571-1578.
- Oda, M., M. Takahashi, T. Matsuno, K. Uoo, M. Nagahama and J. Sakurai (2010). Hemolysis induced by *Bacillus cereus* sphingomyelinase. *Biochim Biophys Acta* **1798**(6): 1073-1080.
- Ogierman, M. A., A. Fallarino, T. Riess, S. G. Williams, S. R. Attridge and P. A. Manning (1997). Characterization of the *Vibrio cholerae* El Tor lipase operon lipAB and a protease gene downstream of the hly region. *J Bacteriol* **179**(22): 7072-7080.
- Økstad, O. A., M. Gominet, B. Purnelle, M. Rose, D. Lereclus and A. B. Kolstø (1999). Sequence analysis of three *Bacillus cereus* loci carrying PlcR-regulated genes encoding degradative enzymes and enterotoxin. *Microbiology* **145**(11): 3129-3138.
- Ouhib, O., T. Clavel and P. Schmitt (2006). The production of *Bacillus cereus* enterotoxins is influenced by carbohydrate and growth rate. *Curr Microbiol* **53**(3): 222-226.
- Park, C. H., S. J. Lee, S. G. Lee, W. S. Lee and S. M. Byun (2004). Hetero- and autoprocessing of the extracellular metalloprotease (Mpr) in *Bacillus subtilis*. *Bacteriol* **186**(19): 6457-6464.
- Pearce, S. R., M. L. Mimmack, M. P. Gallagher, U. Gileadi, S. C. Hyde and C. F. Higgins (1992). Membrane topology of the integral membrane components, OppB and OppC, of the oligopeptide permease of *Salmonella typhimurium*. *Mol Microbiol* **6**(1): 47-57.
- Pelchat, M. and J. Lapointe (1999). Aminoacyl-tRNA synthetase genes of *Bacillus subtilis*: organization and regulation. *Biochem Cell Biol* **77**(4): 343-347.
- Perchat, S., T. Dubois, S. Zouhir, M. Gominet, S. Poncet, C. Lemy, M. Aumont-Nicaise, J. Deutscher, M. Gohar, S. Nessler and D. Lereclus (2011). A cell-cell communication system regulates protease production during sporulation in bacteria of the *Bacillus cereus* group. *Mol Microbiol* **82**(3): 619-633.
- Perego, M. (1997). A peptide export-import control circuit modulating bacterial development regulates protein phosphatases of the phosphorelay. *Proc Natl Acad Sci USA* **94**(16): 8612-8617.
- Perego, M., C. F. Higgins, S. R. Pearce, M. P. Gallagher and J. A. Hoch (1991). The oligopeptide transport system of *Bacillus subtilis* plays a role in the initiation of sporulation. *Mol Microbiol* **5**(1): 173-185.
- Perego, M. and J. A. Hoch (1996). Cell-cell communication regulates the effects of protein aspartate phosphatases on the phosphorelay controlling development in *Bacillus subtilis*. *Proc Natl Acad Sci USA* **93**(4): 1549-1553.

- Pérez-Rueda, E. and J. Collado-Vides (2001).** Common history at the origin of the position-function correlation in transcriptional regulators in archaea and bacteria. *J Mol Evol* **53**(3): 172-179.
- Perkins, D. N., D. J. Pappin, D. M. Creasy and J. S. Cottrell (1999).** Probability-based protein identification by searching sequence databases using mass spectrometry data. *Electrophoresis* **20**(18): 3551-3567.
- Phillips, Z. E. and M. A. Strauch (2002).** *Bacillus subtilis* sporulation and stationary phase gene expression. *Cell Mol Life Sci* **59**(3): 392-402.
- Pinto, M., S. Rabine-Leon, M. Appay, M. Kedingler, N. Triadou, E. Dussaulx, B. Louroix, P. Simon-Assmann and K. Haffeb (1983).** Enterocyte-like differentiation and polarization of the human colon carcinoma cell line Caco-2 in culture. *Biol Cell* **47**: 323-330.
- Pomerantsev, A. P., K. V. Kalnin, M. Osorio and S. H. Leppla (2003).** Phosphatidylcholine-specific phospholipase C and sphingomyelinase activities in bacteria of the *Bacillus cereus* group. *Infect Immun* **71**(11): 6591-6606.
- Pomerantsev, A. P., O. M. Pomerantseva, A. S. Camp, R. Mukkamala, S. Goldman and S. H. Leppla (2009).** PapR peptide maturation: role of the NprB protease in *Bacillus cereus* 569 PlcR/PapR global gene regulation. *FEMS Immunol Med Microbiol* **55**(3): 361-377.
- Porter, A. G. and R. U. Jänicke (1999).** Emerging roles of caspase-3 in apoptosis. *Cell Death Differ* **6**(2): 99-104.
- Priest, F. G. and B. Alexander (1988).** A frequency matrix for probabilistic identification of some bacilli. *J Gen Microbiol* **134**(11): 3011-3018.
- Prüss, B. M., R. Dietrich, B. Nibler, E. Märtilbauer and S. Scherer (1999).** The hemolytic enterotoxin HBL is broadly distributed among species of the *Bacillus cereus* group. *Appl Environ Microbiol* **65**(12): 5436-5442.
- Putzer, H., S. Laalami, A. A. Brakhage, C. Condon and M. Grunberg-Manago (1995).** Aminoacyl-tRNA synthetase gene regulation in *Bacillus subtilis*: induction, repression and growth-rate regulation. *Mol Microbiol* **16**(4): 709-718.
- Radwan, M., I. Miller, T. Grunert, M. Marchetti-Deschmann, C. Vogl, N. O'Donoghue, M. J. Dunn, T. Kolbe, G. Allmaier, M. Gemeiner, M. Müller and B. Strobl (2008).** The impact of tyrosine kinase 2 (Tyk2) on the proteome of murine macrophages and their response to lipopolysaccharide (LPS). *Proteomics* **8**(17): 3469-3485.
- Rajkovic, A., M. Uyttendaele, A. Vermeulen, M. Andjelkovic, I. Fitz-James, P. in 't Veld, Q. Denon, R. Vérhe and J. Debevere (2008).** Heat resistance of *Bacillus cereus* emetic toxin, cereulide. *Lett Appl Microbiol* **46**(5): 536-541.
- Ramarao, N. and D. Lereclus (2005).** The InhA1 metalloprotease allows spores of the *B. cereus* group to escape macrophages. *Cell Microbiol* **7**(9): 1357-1364.
- Ramarao, N. and D. Lereclus (2006).** Adhesion and cytotoxicity of *Bacillus cereus* and *Bacillus thuringiensis* to epithelial cells are FlhA and PlcR dependent, respectively. *Microbes Infect* **8**(6): 1483-1491.
- Randhawa, M. A. (2009).** Calculation of LD50 values from the method of Miller and Tainter, 1944. *J Ayub Med Coll Abbottabad* **21**(3): 184-185.
- Ratnayake-Lecamwasam, M., P. Serror, K. W. Wong and A. L. Sonenshein (2001).** *Bacillus subtilis* CodY represses early-stationary-phase genes by sensing GTP levels. *Genes Dev* **15**(9): 1093-1103.
- Rawlings, N. D., F. R. Morton and A. J. Barrett (2006).** MEROPS: the peptidase database. *Nucleic Acids Res* **34**(Database issue): D270-272.
- Read, T. D., S. N. Peterson, N. Tourasse, L. W. Baillie, I. T. Paulsen, K. E. Nelson, H. Tettelin, D. E. Fouts, J. A. Eisen, S. R. Gill, E. K. Holtzapple, O. A. Okstad, E. Helgason, J. Rillstone, M. Wu, J. F. Kolonay, M. J. Beanan, R. J. Dodson, L. M.**

- Brinkac, M. Gwinn, R. T. DeBoy, R. Madpu, S. C. Daugherty, A. S. Durkin, D. H. Haft, W. C. Nelson, J. D. Peterson, M. Pop, H. M. Khouri, D. Radune, J. L. Benton, Y. Mahamoud, L. Jiang, I. R. Hance, J. F. Weidman, K. J. Berry, R. D. Plaut, A. M. Wolf, K. L. Watkins, W. C. Nierman, A. Hazen, R. Cline, C. Redmond, J. E. Thwaite, O. White, S. L. Salzberg, B. Thomason, A. M. Friedlander, T. M. Koehler, P. C. Hanna, A. B. Kolstø and C. M. Fraser (2003). The genome sequence of *Bacillus anthracis* Ames and comparison to closely related bacteria. *Nature* **423**(6935): 81-86.
- Resnekov, O., L. Melin, P. Carlsson, M. Mannerlöv, A. von Gabain and L. Hederstedt (1992). Organization and regulation of the *Bacillus subtilis* odhAB operon, which encodes two of the subenzymes of the 2-oxoglutarate dehydrogenase complex. *Mol Gen Genet* **234**(2): 285-296.
- Ryan, P. A., J. D. Macmillan and B. A. Zilinskas (1997). Molecular cloning and characterization of the genes encoding the L1 and L2 components of hemolysin BL from *Bacillus cereus*. *J Bacteriol* **179**(8): 2551-2556.
- Ryguis, T. and W. Hillen (1991). Inducible high-level expression of heterologous genes in *Bacillus megaterium* using the regulatory elements of the xylose-utilization operon. *Appl Microbiol Biotechnol* **35**(5): 594-599.
- Salamitou, S., F. Ramière, M. Brehélin, D. Bourguet, N. Gilois, M. Gominet, E. Hernandez and D. Lereclus (2000). The plcR regulon is involved in the opportunistic properties of *Bacillus thuringiensis* and *Bacillus cereus* in mice and insects. *Microbiology* **146**(11): 2825-2832.
- Salvesen, G. S. (2002). Caspases: opening the boxes and interpreting the arrows. *Cell Death Differ* **9**(1): 3-5.
- Sambrook, J. and Russell, D. W. (2001). *Molecular Cloning: a Laboratory Manual*, 3rd Edn., Cold Spring Harbor, NY: Cold Spring Harbor Laboratory Press.
- Sánchez, B., S. Arias, S. Chaignepain, M. Denayrolles, J. M. Schmitter, P. Bressollier and M. C. Urdaci (2009). Identification of surface proteins involved in the adhesion of a probiotic *Bacillus cereus* strain to mucin and fibronectin. *Microbiology* **155**(5): 1708-1716.
- Sartor, R. B. (2008). Microbial influences in inflammatory bowel diseases. *Gastroenterology* **134**(2): 577-594.
- Sasahara, T., S. Hayashi, Y. Morisawa, T. Sakihama, A. Yoshimura and Y. Hirai (2011). *Bacillus cereus* bacteremia outbreak due to contaminated hospital linens. *Eur J Clin Microbiol Infect Dis* **30**(2): 219-226.
- Saxild, H. H. and P. Nygaard (1991). Regulation of levels of purine biosynthetic enzymes in *Bacillus subtilis*: effects of changing purine nucleotide pools. *J Gen Microbiol* **137**(10): 2387-2394.
- Scallan, E., R. M. Hoekstra, F. J. Angulo, R. V. Tauxe, M. A. Widdowson, S. L. Roy, J. L. Jones and P. M. Griffin (2011). Foodborne illness acquired in the United States--major pathogens. *Emerging infectious diseases* **17**(1): 7-15.
- Schoeni, J. L. and A. C. Wong (2005). *Bacillus cereus* food poisoning and its toxins. *J Food Prot* **68**(3): 636-648.
- Setlow, P. (2006). Spores of *Bacillus subtilis*: their resistance to and killing by radiation, heat and chemicals. *J Appl Microbiol* **101**(3): 514-525.
- Shevchenko, A., M. Wilm, O. Vorm and M. Mann (1996). Mass spectrometric sequencing of proteins silver-stained polyacrylamide gels. *Anal Chem* **68**(5): 850-858.
- Shinagawa, K., Y. Ueno, D. Hu, S. Ueda and S. Sugii (1996). Mouse lethal activity of a HEp-2 vacuolation factor, cereulide, produced by *Bacillus cereus* isolated from vomiting-type food poisoning. *J Vet Med Sci* **58**(10): 1027-1029.

- Shiota, M., K. Saitou, H. Mizumoto, M. Matsusaka, N. Agata, M. Nakayama, M. Kage, S. Tatsumi, A. Okamoto, S. Yamaguchi, M. Ohta and D. Hata (2010). Rapid detoxification of cereulide in *Bacillus cereus* food poisoning. *Pediatrics* **125**(4): e951-955.
- Shivers, R. P. and A. L. Sonenshein (2004). Activation of the *Bacillus subtilis* global regulator CodY by direct interaction with branched-chain amino acids. *Mol Microbiol* **53**(2): 599-611.
- Shivers, R. P. and A. L. Sonenshein (2005). *Bacillus subtilis* *ilvB* operon: an intersection of global regulons. *Mol Microbiol* **56**(6): 1549-1559.
- Slamti, L. and D. Lereclus (2002). A cell-cell signaling peptide activates the PlcR virulence regulon in bacteria of the *Bacillus cereus* group. *EMBO J* **21**(17): 4550-4559.
- Slamti, L. and D. Lereclus (2002). A cell-cell signaling peptide activates the PlcR virulence regulon in bacteria of the *Bacillus cereus* group. *EMBO J* **21**(17): 4550-4559.
- Sonenshein, A. L. (2007). Control of key metabolic intersections in *Bacillus subtilis*. *Nat Rev Microbiol* **5**(12): 917-927.
- Spira, W. M. and G. J. Silverman (1979). Effects of glucose, pH, and dissolved-oxygen tension on *Bacillus cereus* growth and permeability factor production in batch culture. *Appl Environ Microbiol* **37**(1): 109-116.
- Stapleton, M. R., V. A. Norte, R. C. Read and J. Green (2002). Interaction of the *Salmonella typhimurium* transcription and virulence factor SlyA with target DNA and identification of members of the SlyA regulon. *J Biol Chem* **277**(20): 17630-17637.
- Stenfors Arnesen, L., A. Fagerlund and P. Granum (2008). From soil to gut: *Bacillus cereus* and its food poisoning toxins. *FEMS Microbiol Rev* **32**(4): 579-606.
- Stenfors Arnesen, L., P. Granum, C. Buisson, J. Bohlin and C. Nielsen-Leroux (2011). Using an insect model to assess correlation between temperature and virulence in *Bacillus weihenstephanensis* and *Bacillus cereus*. *FEMS Microbiol Lett* **317**(2): 196-202.
- Strauch, M. A. (1995). Delineation of AbrB-binding sites on the *Bacillus subtilis* *spo0H*, *kinB*, *ftsAZ*, and *pbpE* promoters and use of a derived homology to identify a previously unsuspected binding site in the *bsuB1* methylase promoter. *J Bacteriol* **177**(23): 6999-7002.
- Strauch, M. A. and J. A. Hoch (1993). Transition-state regulators: sentinels of *Bacillus subtilis* post-exponential gene expression. *Mol Microbiol* **7**(3): 337-342.
- Strauch, M. A., M. Perego, D. Burbulys and J. A. Hoch (1989). The transition state transcription regulator AbrB of *Bacillus subtilis* is autoregulated during vegetative growth. *Mol Microbiol* **3**(9): 1203-1209.
- Sulavik, M. C., M. Dazer and P. F. Miller (1997). The *Salmonella typhimurium* mar locus: molecular and genetic analyses and assessment of its role in virulence. *J Bacteriol* **179**(6): 1857-1866.
- Sulavik, M. C., L. F. Gambino and P. F. Miller (1995). The MarR repressor of the multiple antibiotic resistance (*mar*) operon in *Escherichia coli*: prototypic member of a family of bacterial regulatory proteins involved in sensing phenolic compounds. *Mol Med* **1**(4): 436-446.
- Sutherland, A. D. and A. M. Limond (1993). Influence of pH and sugars on the growth and production of diarrhoeagenic toxin by *Bacillus cereus*. *J Dairy Res* **60**(4): 575-580.
- Tamura, H., M. Noto, K. Kinoshita, S. Ohkuma and H. Ikezawa (1994). Inhibition of NGF-induced neurite outgrowth of PC12 cells by *Bacillus cereus* sphingomyelinase, a bacterial hemolysin. *Toxicon* **32**(5): 629-633.
- Thomas, C. M. and C. A. Smith (1987). Incompatibility group P plasmids: genetics, evolution, and use in genetic manipulation. *Ann Rev Microbiol* **41**: 77-101.

- Thwaite, J., T. Laws, T. Atkins and H. Atkins (2009).** Differential cell surface properties of vegetative *Bacillus*. *Lett Appl Microbiol* **48**(3): 373-378.
- Titball, R. W. (1993).** Bacterial phospholipases C. *Microbiol Rev* **57**(2): 347-366.
- Tojo, S., T. Satomura, K. Morisaki, J. Deutscher, K. Hirooka and Y. Fujita (2005).** Elaborate transcription regulation of the *Bacillus subtilis* *ilv-leu* operon involved in the biosynthesis of branched-chain amino acids through global regulators of CcpA, CodY and TnrA. *Mol Microbiol* **56**(6): 1560-1573.
- Tran, S. L., E. Guillemet, M. Gohar, D. Lereclus and N. Ramarao (2010).** CwpFM (EntFM) is a *Bacillus cereus* potential cell wall peptidase implicated in adhesion, biofilm formation, and virulence. *J Bacteriol* **192**(10): 2638-2642.
- Tran, S. L., E. Guillemet, M. Ngo-Camus, C. Clybouw, A. Puhar, A. Moris, M. Gohar, D. Lereclus and N. Ramarao (2011).** Hemolysin II is a *Bacillus cereus* virulence factor that induces apoptosis of macrophages. *Cell Microbiol* **13**(1): 92-108.
- Trieu-Cuot, P., C. Carlier, P. Martin and P. Courvalin (1987).** Plasmid transfer by conjugation from *Escherichia coli* to Gram-positive bacteria. *FEMS Microbiol Lett* **48**(1-2): 289-294.
- Trieu-Cuot, P., C. Carlier, C. Poyart-Salmeron and P. Courvalin (1991).** An integrative vector exploiting the transposition properties of Tn1545 for insertional mutagenesis and cloning of genes from gram-positive bacteria. *Gene* **106**(1): 21-27.
- Turnbull, P. C., K. Jørgensen, J. M. Kramer, R. J. Gilbert and J. M. Parry (1979).** Severe clinical conditions associated with *Bacillus cereus* and the apparent involvement of exotoxins. *J Clin Pathol* **32**(3): 289-293.
- Usui, K., S. Miyazaki, C. Kaito and K. Sekimizu (2009).** Purification of a soil bacteria exotoxin using silkworm toxicity to measure specific activity. *Microb Pathogenesis* **46**(2): 59-62.
- Vaitkevicius, K., P. K. Rompikuntal, B. Lindmark, R. Vaitkevicius, T. Song and S. N. Wai (2008).** The metalloprotease PrtV from *Vibrio cholerae*. *FEBS J* **275**(12): 3167-3177.
- van der Voort, M., O. P. Kuipers, G. Buist, W. M. de Vos and T. Abee (2008).** Assessment of CcpA-mediated catabolite control of gene expression in *Bacillus cereus* ATCC 14579. *BMC Microbiol* **8**: 62.
- van Engeland, M., L. J. Nieland, F. C. Ramaekers, B. Schutte and C. P. Reutelingsperger (1998).** Annexin V-affinity assay: a review on an apoptosis detection system based on phosphatidylserine exposure. *Cytometry* **31**(1): 1-9.
- van Schaik, W., A. Château, M. A. Dillies, J. Y. Coppée, A. L. Sonenshein and A. Fouet (2009).** The global regulator CodY regulates toxin gene expression in *Bacillus anthracis* and is required for full virulence. *Infect Immun* **77**(10): 4437-4445.
- Vilain, S., Y. Luo, M. B. Hildreth and V. S. Brözel (2006).** Analysis of the life cycle of the soil saprophyte *Bacillus cereus* in liquid soil extract and in soil. *Appl Environ Microbiol* **72**(7): 4970-4977.
- Vogelmann, R., M. R. Amieva, S. Falkow and W. J. Nelson (2004).** Breaking into the epithelial apical-junctional complex--news from pathogen hackers. *Curr Opin Cell Biol* **16**(1): 86-93.
- Walev, I., U. Weller, S. Strauch, T. Foster and S. Bhakdi (1996).** Selective killing of human monocytes and cytokine release provoked by sphingomyelinase (beta-toxin) of *Staphylococcus aureus*. *Infect Immun* **64**(8): 2974-2979.
- Walters, J. B. and N. A. Ratcliffe (1983).** Studies on the in vivo cellular reactions of insects: fate of pathogenic and non-pathogenic bacteria in *Galleria mellonella* nodules. *Journal of Insect Physiology* **29**(5): 417-424.
- Wang, W., J. Sun, R. Hollmann, A. P. Zeng and W. D. Deckwer (2006).** Proteomic characterization of transient expression and secretion of a stress-related metalloprotease in high cell density culture of *Bacillus megaterium*. *J Biotechnol* **126**(3): 313-324.

- Wazny, T. K., N. Mummaw and B. Styrt (1990).** Degranulation of human neutrophils after exposure to bacterial phospholipase C. *Eur J Clin Microbiol Infect Dis* **9**(11): 830-832.
- Westerlund, B. and T. K. Korhonen (1993).** Bacterial proteins binding to the mammalian extracellular matrix. *Mol Microbiol* **9**(4): 687-694.
- Whitehead, R. H., P. S. Robinson, J. A. Williams, W. Bie, A. L. Tyner and J. L. Franklin (2008).** Conditionally immortalized colonic epithelial cell line from a Ptk6 null mouse that polarizes and differentiates *in vitro*. *J Gastroenterol Hepatol* **23**(7 Pt 1): 1119-1124.
- Wibawan, I. T., C. Lämmler and F. H. Pasaribu (1992).** Role of hydrophobic surface proteins in mediating adherence of group B streptococci to epithelial cells. *J Gen Microbiol* **138**(6): 1237-1242.
- Widdowson, M. A., A. Sulka, S. N. Bulens, R. S. Beard, S. S. Chaves, R. Hammond, E. D. Salehi, E. Swanson, J. Totaro, R. Woron, P. S. Mead, J. S. Bresee, S. S. Monroe and R. I. Glass (2005).** Norovirus and foodborne disease, United States, 1991-2000. *Emerg Infect Dis [serial on the Internet]* **11**(1): 95-102.
- Wijnands, L. M., J. B. Dufrenne, F. M. van Leusden and T. Abee (2007).** Germination of *Bacillus cereus* spores is induced by germinants from differentiated Caco-2 Cells, a human cell line mimicking the epithelial cells of the small intestine. *Appl Environ Microbiol* **73**(15): 5052-5054.
- Wijnands, L. M., A. Pielaat, J. B. Dufrenne, M. H. Zwietering and F. M. van Leusden (2009).** Modelling the number of viable vegetative cells of *Bacillus cereus* passing through the stomach. *J Appl Microbiol* **106**(1): 258-267.
- Wilkinson, S. P. and A. Grove (2006).** Ligand-responsive transcriptional regulation by members of the MarR family of winged helix proteins. *Curr Issues Mol Biol* **8**(1): 51-62.
- Yamada, A., N. Tsukagoshi, S. Udaka, T. Sasaki, S. Makino, S. Nakamura, C. Little, M. Tomita and H. Ikezawa (1988).** Nucleotide sequence and expression in *Escherichia coli* of the gene coding for sphingomyelinase of *Bacillus cereus*. *Eur J Biochem* **175**(2): 213-220.
- Yasumura, Y. and M. Kawakita (1963).** The research for the SV40 by means of tissue culture technique. *Nippon Rinsho* **21**(6): 1201-1219.
- Zhang, K., H. Li, K. M. Cho and J. C. Liao (2010).** Expanding metabolism for total biosynthesis of the nonnatural amino acid L-homoalanine. *Proc Natl Acad Sci USA* **107**(14): 6234-6239.
- Zigha, A., E. Rosenfeld, P. Schmitt and C. Duport (2006).** Anaerobic cells of *Bacillus cereus* F4430/73 respond to low oxidoreduction potential by metabolic readjustments and activation of enterotoxin expression. *Arch Microbiol* **185**(3): 222-233.
- Zigha, A., E. Rosenfeld, P. Schmitt and C. Duport (2007).** The redox regulator Fnr is required for fermentative growth and enterotoxin synthesis in *Bacillus cereus* F4430/73. *J Bacteriol* **189**(7): 2813-2824.
- Zundel, W., L. M. Swiersz and A. Giaccia (2000).** Caveolin 1-mediated regulation of receptor tyrosine kinase-associated phosphatidylinositol 3-kinase activity by ceramide. *Mol Cell Biol* **20**(5): 1507-1514.

6. PUBLICATIONS

Publications in peer-reviewed journals resulting from this work:

Doll, V. M., Frenzel, E., Schmid, R.M., Scherer, S., Ehling-Schulz, M. and Vogelmann, R., InhA2 and InhA3 promote *Bacillus cereus* growth under nutrient limiting conditions. in preparation.

Frenzel, E., Doll, V. M., Pauthner, M., Lücking, G., Scherer, S., Ehling-Schulz, M. (2012). CodY orchestrates the expression of virulence determinants in emetic *Bacillus cereus* by impacting key regulatory circuits. *Mol Microbiol*, submitted 02/2012.

Doll, V. M., Schmid, R.M., Ehling-Schulz, M. and Vogelmann, R. (2012). *Bacillus cereus* Sphingomyelinase is Important in Non-Gastrointestinal-Tract Infectious Disease. *PLoS Pathogens*, submitted 12/2011.

OTHER PUBLICATIONS:

Waldherr, F. W., Doll, V. M., Meissner, D. and Vogel, R.F. (2010). Identification and characterization of a glucan-producing enzyme from *Lactobacillus hilgardii* TMW 1.828 involved in granule formation of water kefir. *Food Microbiol* **27** (5): 672-678

Abstracts & Proceedings:

Doll Viktoria, Lücking Genia, Ehling-Schulz Monika and Vogelmann Roger. *Bacillus cereus* Sphingomyelinase Induces Cytotoxicity in Intestinal Epithelial Cells. 50th ASCB Annual Meeting. Philadelphia, USA. (11.12.-15.12.2010) 747

Doll Viktoria, Ehling-Schulz Monika and Vogelmann Roger. *Bacillus cereus* Sphingomyelinase Induces Cytotoxicity in Ptk6 Intestinal Epithelial Cells. 3rd Seeon Conference: Microbiota, Probiota and Host. Kloster Seeon/Chiemsee, Germany. (18.6.-20.6.2010)

Doll Viktoria, Ehling-Schulz Monika and Vogelmann Roger. *Bacillus cereus* Sphingomyelinase Induces Cytotoxicity in Ptk6 Intestinal Epithelial Cells. 5. Treffen des wissenschaftlichen Nachwuchts der GBM-Studiengruppe "Biochemische Pharmakologie und Toxikologie". Schloss Reisenburg/Günzburg, Germany. (14.5.-15.5.2010)

Doll Viktoria, Ehling-Schulz Monika and Vogelmann Roger. Dramatic Damaging Effects of *Bacillus cereus* on Barrier Function of Intestinal Epithelial Cells. 2nd Seeon Conference: Microbiota, Probiota and Host. Kloster Seeon/Chiemsee, Germany. (23.4.-25.4.2009)

7. APPENDIX

7.1. *B. cereus* strains used in cytotoxicity screening

Table A1: *B. cereus* strains used in cytotoxicity and adhesion screening including their toxin profiles.

<i>B. cereus</i> strain ^a	Description/source	Toxin gene profile			Reference of toxin profile
		<i>nhe</i>	<i>hbl</i>	<i>cytK</i>	
* F4810/72	emetic reference strain, isolated from vomit from cooked rice (UK)	+	-	-	Ehling-Schulz <i>et al.</i> , 2005
* F4810/72 Δ <i>plcR</i>	emetic reference strain harbouring <i>plcR</i> deletion (Germany)	(+) ^b	-	-	Lücking <i>et al.</i> , 2009
* NVH 0075-95	<i>nhe</i> reference strain, diarrhoeal food poisoning (Norway)	+	-	-	Lund and Granum, 1996
* NVH 0075-95 Δ <i>nheBC</i> (NVH 1173)	<i>nhe</i> reference strain with <i>nheB</i> truncation and <i>nheC</i> deletion (Norway)	(+) ^c	-	-	Fagerlund <i>et al.</i> , 2008
NVH 0230-00	diarrhoeal food poisoning (Norway)	+	+	+	Guinebretiere <i>et al.</i> , 2002
NVH 0861-00	diarrhoeal food poisoning (Norway)	+	-	-	Guinebretiere <i>et al.</i> , 2002
NVH 0391-98	<i>cytK</i> reference strain, diarrhoeal food poisoning (France)	(+) ^d	-	+	Guinebretiere <i>et al.</i> , 2002; Fagerlund <i>et al.</i> , 2007
* F837/76	<i>hbl</i> reference strain, isolate from surgical wound (UK)	+	+	-	Beecher and Macmillan, 1990, Guinebretiere <i>et al.</i> , 2002
F3605/73	emetic food poisoning (UK)	+	-	-	Ehling-Schulz <i>et al.</i> , 2005
F4430/73	diarrhoeal food poisoning (Belgium)	+	+	+	Guinebretiere <i>et al.</i> , 2002
INRA I21	cooked food (France)	+	+	-	Ehling-Schulz <i>et al.</i> , 2005; Guinebretiere <i>et al.</i> , 2002
* RIVM BC67	human faeces, emetic food poisoning	+	-	+	Ehling-Schulz <i>et al.</i> , 2005
WSBC 10030	pasteurized milk (Germany)	+	-	-	Prüss <i>et al.</i> , 1999; Ehling-Schulz <i>et al.</i> , 2005
WSBC 10035	pasteurized milk (Germany)	+	-	-	Prüss <i>et al.</i> , 1999; Ehling-Schulz <i>et al.</i> , 2005
* var. <i>toyoi</i>	probiotic used in piglet feeding (Germany)	+	+	-	This study
IP 5832	probiotic used in human (France)	+	+	-	Duc <i>et al.</i> , 2004

^a Source of strains: F, Central Public Health Laboratory Service, London, united Kingdom; INRA, Institut National de Recherche Agronomique, Avignon, France; NVH, The Norwegian School of Veterinary Science, Oslo, Norway; RIVM, Rijksinstituut voor Volksgezondheid en Milieu, Bilthoven, Netherlands; WSBC, Weihenstephan *Bacillus cereus* Collection, Weihenstephan, Germany

^b no enterotoxin gene expression

^c no *nheB*, *nheC* expression

^d novel gene variant encoding *Nhe*, Fagerlund *et al.*, 2007

* *B. cereus* strains used for adhesion assay

7.2. Vectors and Plasmids

Table A2: Vectors and recombinant plasmids used in this study

Vector/Plasmid	Description	Reference or source
TOPO pCR 2.1	PCR cloning vector; Amp ^r Kan ^r	Invitrogen
pCR 2.1/cm	pCR 2.1 derivative containing the chloramphenicol resistance cassette; Amp ^r Kan ^r Cm ^r	This study
pCR 2.1 $\Delta sph/cm$	pCR 2.1 derivative containing ~1.2 kb up- and downstream flanking regions of <i>sph</i> and the chloramphenicol resistance cassette; Amp ^r Kan ^r Cm ^r	This study
pAD123	shuttle vector for Gram positive hosts, containing a promoter-less <i>gfpmut3a</i> ; Amp ^r Cm ^r	Dunn and Handelsman, 1999
pAD/P <i>cspA</i>	pAD123 derivative containing the promoter region of the cold shock protein CspA in front of <i>gfp</i> ; Amp ^r Cm ^r	Dommel, 2008
pAD/ <i>sph</i> /P <i>cspA</i>	pAD123 derivative containing the <i>cspA</i> promoter region in front of the <i>sph</i> gene (lacking <i>gfp</i>); Amp ^r Cm ^r	This study
pAD/ <i>sph</i> /P <i>cspA</i> /tet	pAD123 derivative containing the <i>cspA</i> promoter region in front of the <i>sph</i> gene and an additional Tet resistance cassette; Amp ^r Cm ^r Tet ^r	This study
pAD/ <i>sph</i> /P <i>plc</i> /tet	pAD123 derivative containing the <i>plc</i> promoter region in front of the <i>sph</i> gene (lacking <i>gfp</i>) and an additional Tet resistance cassette; Amp ^r Cm ^r Tet ^r	This study
pAD/ <i>sph</i> /P <i>sph</i> /tet	pAD123 derivative containing the <i>sph</i> promoter region in front of the <i>sph</i> gene (lacking <i>gfp</i>) and an additional Tet resistance cassette; Amp ^r Cm ^r Tet ^r	This study
pAT113	conjugative suicide vector for <i>Bacillus</i> ; Kan ^r Erm ^r	Trieu-Cuot <i>et al.</i> , 1991
pAT113 $\Delta sph/cm$	pAT113 derivative containing ~1.2 kb up- and downstream flanking regions of <i>sph</i> and the Cm resistance cassette; Cm ^r Erm ^r Kan ^r	This study
pHT315	gram-negative/gram-positive shuttle vector for <i>Bacillus</i> containing a promoterless <i>gfp</i> gene, Amp ^r , Erm ^r	Arantes and Lereclus, 1991
pHT315/ <i>gfp</i> /P <i>aph3A</i>	pHT315 derivative containing the <i>aph3A</i> promoter region in front of the <i>gfp</i> gene; Amp ^r Erm ^r	Arantes and Lereclus, 1991
pWH1520	shuttle vector for protein expression in <i>B. megaterium</i> utilizing a xylose inducible promoter; Amp ^r Tet ^r	A kind gift of W. Hillen, University of Erlangen; Rygus and Hillen, 1991
pWHinhA2	pWH1520 derivative carrying the <i>inhA2</i> gene of <i>B. cereus</i> F4810/72 under xylose operon control; Amp ^r Tet ^r	Frenzel, unpublished

7.3. Oligonucleotide primers

Table A3: Oligonucleotide primers used in this study

Primer	Sequence (5' - 3') ^a	Description	Reference ^b
Primer for deletion mutagenesis			
sph_up_Sac_F	GAGGAGCTCAGATGAAAAAGAAAG	854 bp upstream flanking region of <i>sph</i> gene, ending 73 bp before start codon, <i>SacI</i> restriction site	This study
sph_up_Spe_R	TTTACTAGTTTAACGATCTCCGTAC		This study
sph_down_Xho_F	ACTCTCGAGCCAATATGTATAAGAC	1476 bp downstream flanking region of <i>sph</i> gene, starting 69 bp after stop codon, <i>XhoI</i> restriction site	This study
sph_down_Xba_R	AGCTCTAGAACTTTGTTCTCTGC		This study
Cm_F	CTCGAATTCATCAAGATAAGAAAG	942 bp fragment including the chloramphenicol resistance sequence	(1)
Cm_R_Not	ATAGCGGCCGCATTATCTCATATTA TAAAAG		(1)
Primer for cotranscription test			
inplc_for	GTACAAATCCAGAAGAGTGG	537 bp fragment including 3' end of <i>plc</i> , intergenic region and 5' end of <i>sph</i>	This study
insph_rev	GCGATCTGAAGCACTATTATC		This study
16SA1	GGAGGAAGGTGGGGATGACG	amplification of the 16S rDNA reference gene <i>rnm</i>	(2)
16SA2	ATGGTGTGACGGGCGGTGTG		(2)
Primer for gene complementation			
Pplc_for	ACGAATTC AACATTAACATCCGGT ACG	538 bp upstream region of <i>plc</i> , including the operon promoter	This study
Pplc_rev	ATGAGCTCGTAATAGCTGCTGCT AAAG		This study
Psph1_for	CGCGAATTCGATATGAAACAAGC ATTC	<i>sph</i> gene plus 499 bp upstream region, including the putative <i>sph</i> promoter	This study
sph_Hind_R	AAAAGCTTTAGGACTACTTCATAG AAATAGTTGC		This study
TetR_for_Nsi	CGAATGCATCGATGAAGATGGATT TTCTATTATTG	1776 bp fragment including the tetracycline resistance sequence	(3)
TetR_rev_Nsi	ATCATGCATCGATTTAGAAATCCC TTTGAGAATGT		(3)
Primer for protein overexpression			
sph_Sac_F	TTAGAGCTCGGAGGGATGGAACG TGAAAG	complete <i>sph</i> gene, starting 11 bp before start codon, <i>SacI</i> and <i>HindIII</i> restriction site	This study
sph_Hind_R	AAAAGCTTTAGGACTACTTCATAG AAATAGTTGC		This study

Table A3 – *continued*

Primer	Sequence (5' - 3') ^a	Description	Reference ^b
Primer for protein overexpression			
inhA2_Sma_F2	AT ACCCGGG AATGAGAAGAAAAG CGCCATTT	complete <i>inhA2</i> gene, starting 1 bp before start codon, <i>SmaI</i> and <i>KpnI</i> restriction site	(3)
inhA2_Kpn_R	GT GGTAC CTTAACGTTTAATCCA AACAGCG		(3)
Primer for sequencing and test PCR			
pAD_F	GCACATTTCCCCGAAAAGTGC	sequencing and test primer for pAD123	(4)
pAD_R	CCATTGGGATATATCAACG		(4)
pAT113_for	ATG ACC ATG ATT ACG CCA AGC	sequencing and test primer for pAT113	(1)
pAT113_rev	AGA TCC GCG CGA GCT GTA		(1)
pCR2_1_for	GTGAGTTAGCTCACTCATTAGGC	sequencing and test primer for TOPO pCR2.1	(1)
pCR2_1_rev	CTCTTCGCTATTACGCCAGCTG		(1)
pWH1520_for	GTTCACTTAAATCAAAGGGGGA	sequencing and test primer for pWH1520	(3)
pWH1520_rev	CAGCCTAGTTAAGTAGCTAT		This study

^a Restriction sites are indicated in bold.

^b (1) Lücking, 2009; (2) Martineau *et al.*, 1996; (3) Frenzel, unpublished, (4) Dommel, unpublished.

7.4. MALDI-TOF mass spectrometric protein identification

Table A4: Detailed statistical analysis of differentially expressed proteins of *B. cereus* F4810/72 Δ plcR in Ptk6 conditioned medium compared to unsupplemented RPMI medium. Listed proteins were identified by MALDI-TOF mass spectrometry.

Spot #	Spot # DeCyder ^a	Accession number (NCBI)	Designation	Av ratio ^a Δ plcR (Ptk6)/ Δ plcR (RPMI) wt (RPMI)	Av ratio wt (Ptk6)/ wt (RPMI)	Av ratio Δ plcR (RPMI)/ wt (RPMI)	Av ratio Δ plcR (Ptk6)/ wt (Ptk6)	Peptide mass fingerprint			MS/MS
								Probability based MASCOT significant score	Sequ. cov. %	Matched/ unmatched peptides	
1	700	BCAH187_A0367	PurL	-1.68	n.s.	3.03	2.42	44	6	3(3)	42
2	704	BCAH187_A0367	PurL	-1.52	n.s.	3.04	2.57	40	6	4(8)	70
3	718	BCAH187_A0367	PurL	-1.71	n.s.	3.54	2.88	137	30	15(36)	80
4	1383	BCAH187_A0372	PurD	-1.41	n.s.	3.47	3.02	149	31	11(14)	159
5	1710	BCAH187_A0369	PurM	-1.43	-1.29	3.92	3.56	121	33	8(12)	68
6	2044	BCAH187_A0364	PurC	-1.45	n.s.	3.66	3.13	181	48	10(15)	35
7	1139	BCAH187_A1559	LeuA	1.82	2.16	2.57	2.16	168	38	11(13)	201
8	1658	BCAH187_A1558	IivC1	1.66	n.s.	n.s.	n.s.	93	20	6(8)	95
9	1663	BCAH187_A1558	IivC1	1.89	1.98	1.88	1.8	192	41	11(12)	166
10	1676	BCAH187_A3294	SerC	1.47	n.s.	-1.26	n.s.	101	22	7(10)	107
11	1693	BCAH187_A1968	IivC2	6.84	6.82	n.s.	n.s.	163	35	9(9)	91
12	1955	BCAH187_A1555	IivE1	1.31	1.60	1.55	1.27	258	64	15(17)	221
13	317	BCAH187_A2323	IleS	4.77	2.79	n.s.	n.s.	51	8	5(8)	86
14	397	BCAH187_A3947	IleS2	1.47	1.33	-1.24	n.s.	50	5	4(4)	122
15	770	BCAH187_A0047	MetS	1.51	n.s.	n.s.	1.33	87	10	9(12)	48
16	798	BCAH187_A2489	ThrS1	2.44	-2.86	-4.23	n.s.	120	26	12(23)	114
17	804	BCAH187_A4701	ThrS2	1.38	-1.25	-1.62	n.s.	72	12	6(10)	203
18	455	BCAH187_A1418	OdhA/SucA	-1.31	n.s.	1.1	n.s.	119	16	9(10)	92

Table A4 - continued

Spot #	Spot # DeCyder ^a	Accession number (NCBI)	Designation	Av ratio ^a $\Delta p/cR$ (Ptk6)/ $\Delta p/cR$ (RPMI)	Av ratio wt (Ptk6)/ wt (RPMI)	Av ratio $\Delta p/cR$ (RPMI)/ wt (RPMI)	Av ratio $\Delta p/cR$ (Ptk6)/ wt (Ptk6)	Peptide mass fingerprint			MS/MS Probability based MOWSE score
								Probability based MASCOT significant score	Sequ. cov. %	Matched/ unmatched peptides	
19	1124	BCAH187_A2142	Putative oligopeptide ABC transporter, oligopeptide-binding protein	1.5	2.76	2.46	n.s.	37	-	3	87
20	1413	BCAH187_A1287	AceA	-1.82	-2.22	1.87	2.28	95	20	6(7)	131
21	1213	BCAH187_A5197	NprB	3.81	n.s.	n.s.	1.46	28	-	2(3)	33
22	691	BCAH187_A3035	InhA3	5.69	n.s.	2.57	11.57	34	5	4(12)	29

^a Original spot number as assigned by the DeCyder software

^b Av. Ratio (X/y) designates the average change of spot abundance of condition x-proteins compared to control y-proteins. n.s., statistical analysis revealed no significant differences in protein expression.

8. DANKSAGUNG

Mein Dank gilt Herrn Prof. Dr. Siegfried Scherer und Herrn Prof. Dr. Roland Schmid für die Möglichkeit, meine Doktorarbeit im Rahmen einer Kooperation zwischen der Abteilung Mikrobiologie des ZIEL und dem Klinikum rechts der Isar, TU München durchführen zu dürfen.

Des Weiteren bedanke ich mich außerordentlich bei Herrn PD Dr. Roger Vogelmann und Frau Prof. Dr. Monika Ehling-Schulz für die Stellung des Themas, ihre engagierte Betreuung und Unterstützung durch fachlichen Rat, sowie die beständige Motivation.

Herrn Dr. Tom Grunert danke ich für die gute, engagierte Kooperation so wie meine Einweisung in die 2-D DIGE Analyse und Proteinidentifizierung.

Großer Dank gilt auch Christian Bolz für die Ermöglichung der FPLC Protein Auftrennung und seine Hilfe dabei, sowie Andreas Schlitzer für die Unterstützung bei den Durchflusszytometrie Analysen.

Frau Dr. Elrike Frenzel danke ich, dass ich die von ihr konstruierten *B. cereus*-Mutanten (F4810/72 wt pWHinhA2 und $\Delta plcR$ pWHinhA2) und Plasmide nutzen durfte.

Besonders danke ich Frau Dr. Genia Lücking, für die vielen hilfreichen Ratschläge und die großzügige Bereitstellung der von ihr konstruierten Plasmide und der *B. cereus*-Mutante $\Delta plcR$.

Mein ganz spezieller Dank gilt Frau Dr. Sylvia Steininger für Ihre kompetente und konstruktive Beratung, die vielen wissenschaftlichen und privaten Gespräche, ihre fachliche (auch tatkräftige) Unterstützung und das Proof-reading meiner Arbeit.

Die angenehme Arbeitsatmosphäre der AG Vogelmann und der AG *Bacillus cereus* haben wesentlich zum Gelingen dieser Arbeit beigetragen. Deshalb danke ich meinen Kollegen, Christiane Pelz, Katrin Mayr, Martin Kullik, Martina Fricker, Tobias Bauer und Andrea Rütschle für die vielen hilfreichen und motivierenden Gespräche, die fachlichen Diskussionen und die gute gemeinsame Zeit. Ein ganz besonderer Dank gilt Romy Wecko, Laura Tschernek, Sarah Franke und Claudia Weiss für ihre hervorragende technische Assistenz und Fabian Coscia, Christopher Huptas und Jana Tretter, die in Forschungspraktika zu Teilen dieser Arbeit beigetragen haben.

Frau Dorothea Wörner danke ich für die exzellente Koordination des GRK1482 und ihre unermüdliche Hilfe.

Der größte Dank gebührt meiner Familie, meinen Eltern, Großeltern und meinem Bruder für ihr Interesse, ihr Vertrauen in mich und die vielen Ermutigungen.

Von ganzem Herzen danke ich Florian für seine Geduld und die uneingeschränkte Unterstützung. Danke, dass du immer an mich geglaubt hast.

~ Nicht das Beginnen wird belohnt, sondern einzig und allein das Durchhalten. ~
(Katharina von Siena)

CURRICULUM VITAEViktoria Magdalena Doll

PERSONAL DETAILS

Date of Birth 19.07.1983, München, Germany
Nationality German

EDUCATION

08/2008 – 01/2012 **PhD (Dr. rer. nat.)**
Department of Microbiology, ZIEL &
2nd Department of Internal Medicine, Klinikum rechts der Isar,
Technische Universität München
Advisor: Prof. Dr. S. Scherer & Prof. Dr. M. Ehling-Schulz
Co-Advisor: Prof. Dr. R. Schmid & PD Dr. R. Vogelmann

10/2006 – 07/2008 **Master of Science in Molecular Biotechnology**
Chair of Technical Microbiology,
Department of Nutrition and Food Science,
Technische Universität München
Master thesis: „Isolation and characterisation of a
glycosyltransferase of *Lactobacillus hilgardii*“
Advisor: Prof. Dr. R. Vogel

RESEARCH AND WORKING EXPERIENCE

08/2007 – 10/2007 **International internship**
NNE Pharmaplan, Kopenhagen, Denmark

08/2006 – 06/2007 **Student assistant**
Adolf Butenandt Institute, Chair of Biochemistry -
Neurobiochemistry - Ludwig-Maximilians-Universität München,
Advisor: Prof. Dr. J. Tatzelt

GRANTS

08/2008 – 07/2011 **Scholarship of the German Research Foundation (DFG)**
(GRK1482)